

Tsunami Impacts and Mitigation Plans for the Khoa Lak (Andaman Sea), Coastal Areas of Thailand.

Somsak Wathanaprida

A Thesis submitted to
the School of Environmental Sciences
at the University of East Anglia, Norwich
in partial fulfilment of the requirements for the degree of
Doctor of Philosophy

September 2010

ABSTRACT

Tsunami Impacts and Mitigation Plans for the Khao Lak (Andaman Sea) Coastal Areas of Thailand.

Somsak Wathanaprida

School of Environmental Sciences, University of East Anglia, Norwich, NR4 7TJ, UK

To build a tsunami-resilient coastal community it is fundamental to understand the characteristics of past tsunami patterns and likely impact of possible future events. The MOST model (Method of Splitting Tsunami) and ComMIT (Community Model Interface for Tsunami) were used to model patterns of water levels, wave speed and direction, and inundation distances resulting from the 2004 Indian Ocean tsunami on the Khao Lak coast of Thailand. The model of the 2004 tsunami was calibrated against estimates of water depths made along the coast in early 2005; an $M_w = 9.3$ earthquake in the model was found to best match observations. The model was verified against a variety of other evidence, including digital photographs and video clips taken on the day of the tsunami, mainly from two sites along the Khao Lak coast at Nang Thong and Bang Niang beaches, together with aerial surveys and a tide-gauge record. The timing and extent of water recession prior to the arrival of the first wave, the heights and number of the subsequent waves, and the inundation distances corresponded well providing confidence in the application of the MOST model to this coastal region.

Historical evidence suggest that tsunami of the magnitude of 2004 are rare (200-700 y) so for mitigation planning in the Khao Lak area a smaller tsunamigenic-earthquake ($M_w = 8.4$) was chosen (100-500 y). Sensitivity to the choice of M_w was also considered. The tsunami from such an event is similar in its character to the 2004 event, less extreme but still highly destructive, reaching the Khao Lak coast in ~ 2 h 20 min, and preceded by receding water levels. The third waves which arrives at 4 h 0 min after the earthquake is predicted to be the most destructive, resulting in inundation of 4.5-5.5 m depth and wave speeds of 6-8 m/s at the coastline. The mitigation plan and measures for Bang Niang and Nang Thong Beaches were developed based on the occurrence of such a $M_w = 8.4$ event.

*This dissertation is dedicated to the memory of my father,
Somkiat Wathanaprida.*

*His words of inspiration and encouragement still think over.
To my mother Pensri Wathanaprida who has not only raised and nurtured me,
but also supported me all the way since the beginning of my studies.*

Acknowledgement

I am heartily thankful to my supervisor, Professor Chris E. Vincent, whose encouragement, supervision and support enabled me to build up an understanding of the issue. His knowledgeable advice, insightful criticisms, and patient encouragement assisted the writing of this dissertation in many ways.

Any attempt at any level can not be satisfactorily completed without the support and guidance of these academic people. I would like to express my immense gratitude to Dr. Paul Burton for his helpful comments on this dissertation. I gratefully thank Dr. Tony Dolphin for his support and guidance. Moreover, I wish to thank all staff of the School of Environmental Sciences, University of East Anglia for their constant support that has encouraged me to come up with this dissertation.

I would like to thank my colleagues at the Department of Mineral Resources of Thailand, who helped me a lot in gathering information, collecting data and guiding me from time to time in conducting this research. I also would like to make a special reference to Mr. Wichien Intasen who is a Senior Geologist of the Department of Mineral Resources. Without their support, I could not have gotten such relevant data.

I would also thank Assoc. Prof. Absornsuda Siripong and all staff of the UNESCO-IOC International Training Course on Tsunami Numerical Modelling Course II: Tsunami inundation modelling, which was held on 29 June – 6 July 2007 at Chulalongkorn University.

It is a pleasure to thank those who made this thesis possible, Dr. Peter Wilson and Dr. Tom Greaves for editing this dissertation. I am also thankful to my brother who always believed in me, and my friends who have provided their whole support at all times for the successful completion of this dissertation.

Lastly, I present my regards and blessings to all of those who supported me in any respect during the completion of my study.

TABLE OF CONTENTS

| | |
|---|-----------|
| ABSTRACT..... | ii |
| Acknowledgement..... | iv |
| CHAPTER 1 INTRODUCTION | 1 |
| CHAPTER 2 TSUNAMI WAVES IN THE INDIAN OCEAN..... | 3 |
| 2-1 Tsunami Definition and General Characteristics..... | 3 |
| 2-2 Geological Settings Relating to Earthquakes and Tsunamis in the Indian Ocean Region..... | 4 |
| 2-2.1 Geomorphologic Features of the Indian Ocean..... | 4 |
| 2-2.2 Plate Tectonics in the Indian Ocean..... | 5 |
| 2-2.3 Subduction and Seafloor Spreading at the Andaman and Sunda Trenches..... | 7 |
| 2-3 The History of Tsunamis in the Region of the Indian Ocean | 9 |
| 2-4 The 2004 Indian Ocean Earthquake and Tsunami..... | 15 |
| 2-4.1 Rupture zone of the 2004 Earthquake | 15 |
| 2-4.2 Characteristics of the 2004 Earthquake..... | 18 |
| 2-4.2.1 Rupture and Rupture Velocity..... | 18 |
| 2-4.2.2 Slow Slip..... | 18 |
| 2-4.2.3 Seafloor Displacement Heights..... | 21 |
| 2-4.3 Horizontal Movement and Vertical Movement Resulting from the 2004 Earthquake | 25 |
| 2-4.4 The Energy Released by the 2004 Indian Ocean Earthquake. | 27 |
| 2-5 Future Earthquake Generated Tsunami in the Indian Ocean Region. 28 | |
| 2-5.1 The Arakan Section..... | 29 |

| | | |
|--|--|-----------|
| 2-5.2 | The Sumatra Section | 30 |
| 2-5.3 | The Andaman-Nicobar Section | 33 |
| CHAPTER 3 THE 2004 INDIAN OCEAN TSUNAMI INCIDENT AND ITS CONSEQUENCES IN THAILAND | | 35 |
| 3-1 | Topography and Tsunami Characteristics..... | 35 |
| 3-2 | Tsunami Wave Height and Speed..... | 36 |
| 3-3 | Tsunami Effects and Devastation | 37 |
| 3-3.1 | Natural Geomorphologic Changes | 37 |
| 3-3.2 | Loss of Life and Physical Damage to Property | 39 |
| CHAPTER 4 NUMERICAL MODELLING OF TSUNAMI PROPAGATION AND INUNDATION FORECASTING. | | 42 |
| 4-1 | Wave Propagation Modelling | 43 |
| 4-2 | Wave Inundation Modelling..... | 44 |
| 4-3 | MOST (Method Of Splitting Tsunami) Numerical Model..... | 45 |
| 4-4 | ComMIT (Community Model Interface for Tsunami)..... | 46 |
| 4-5 | Numerical Tsunami Forecasts for the Indian Ocean and the Thai Coast | 46 |
| CHAPTER 5 REGIONAL SETTING& METHODOLOGY..... | | 50 |
| 5-1 | Regional Setting..... | 50 |
| 5-1.1 | General Location of Khao Lak, Phang-nga Province..... | 50 |
| 5-1.2 | Geological Setting | 52 |
| 5-1.3 | Coastal Geomorphology of Khao Lak..... | 52 |
| 5-1.4 | Climate | 54 |

| | | |
|--|--|-----------|
| 5-1.5 | Economic Development and Land Use..... | 54 |
| 5-2 | Acquisition& Preparation of Detailed Data..... | 55 |
| 5-2.1 | Data Acquisition..... | 55 |
| 5-1.1.1 | Preparation of data..... | 60 |
| 5-2.2 | The Study Area..... | 62 |
| 5-3 | Methodology | 65 |
| 5-3.1 | The MOST/ComMIT Model..... | 65 |
| 5-1.1.2 | Model Setup..... | 65 |
| 5-1.1.2.1 | Rupture sources (vertical seafloor displacement heights)..... | 67 |
| 5-3.2 | Simulation of the 2004 Tsunami | 68 |
| 5-1.1.3 | Scenario 1 and 2..... | 69 |
| 5-1.1.4 | Scenario 3, 4, 5 and 6..... | 69 |
| 5-1.1.5 | Scenario 7, 8, 9 and 10 | 71 |
| 5-1.1.6 | Scenario 11, 12 and 13..... | 72 |
| 5-1.1.7 | Scenario 14 | 72 |
| 5-1.1.8 | Scenario 15 and 16 | 73 |
| CHAPTER 6 COMPARISON OF MODEL OUTCOMES AND THE 2004 TSUNAMI SURVEYED DATA | | 78 |
| 6-1 | Comparison of Maximum Tsunami Wave Heights from Modelling and Surveyed Data | 78 |
| 6-2 | Comparison of Modelled Tsunami Profiles of Scenario 11 with Surveyed Data | 88 |
| 6-3 | Comparison of Tsunami Inundation Area from the Model with Surveyed Inundation Area of the 2004 Indian Ocean Tsunami. | 91 |
| 6-4 | Effects of Tide on Tsunami Wave Height and Inundation Distance | 95 |

| | |
|--|------------|
| 6-5 Comparison of Tsunami Arrival Time from the Model and Tide Gauge Records of Kuraburi..... | 98 |
| CHAPTER 7 THE 2004 INDIAN OCEAN TSUNAMI WAVE PATTERN AT KHAO LAK: MODEL SIMULATION | 100 |
| 7-1 The 2004 Indian Ocean tsunami wave propagation from the model | 100 |
| 7-2 Nearshore Tsunami Propagation and Inundation along Khao Lak's Coast. 102 | |
| 7-2.1 The first wave trough and crest | 102 |
| 7-2.2 The Second and Subsequent Waves | 107 |
| 7-3 Detail of Tsunami Wave Behaviour of the Model at Nang Thong and Bang Niang Beaches and Comparison with the Tsunami Observations. | 111 |
| 7-3.1 First wave recession along Nang Thong and Bang Niang Beaches | 111 |
| 7-3.2 The behaviour of the first wave crest. | 114 |
| 7-3.3 Comparing tsunami wave pattern at Sunset Beach and south of Nang Thong Beach | 120 |
| 7-3.4 Comparing Tsunami Wave Pattern at Nang Thong Beach. | 129 |
| 7-3.5 Comparing Tsunami Wave Pattern at Bang Niang Beach. | 142 |
| 7-4 Vulnerability of the Khao Lak Area to Tsunami Generated by Earthquakes in the Future..... | 156 |
| CHAPTER 8 TSUNAMI MITIGATION..... | 161 |
| 8-1 Tsunami Mitigation at Policy Level | 162 |
| 8-2 The Concept of Tsunami Community Resilience | 164 |
| 8-2.1 Tsunami Warning Systems and Emergency Planning..... | 167 |
| 8-2.2 Coastal Zoning and Land Use Planning. | 170 |
| 8-2.3 Standards for Building Regulations | 173 |

| | | |
|-----------|--|-----|
| 8-2.4 | Tsunami Protection | 176 |
| 8-2.4.1 | Natural Protection..... | 176 |
| 8-2.4.1.1 | Beach Forests and Mangrove Forests. | 176 |
| 8-2.4.1.2 | Sand dunes | 178 |
| 8-2.4.1.3 | Sea grass beds..... | 179 |
| 8-2.4.1.4 | Coral reefs..... | 179 |
| 8-2.4.2 | Man-made Protection..... | 180 |
| 8-2.5 | Public Knowledge | 182 |

CHAPTER 9 TSUNAMI IMPACT REDUCTION SCHEMES FOR BANG NIANG AND NANG THONG BEACHES, KHAO LAK. 185

9-1 Component 1: Understanding the Pattern of Tsunami waves at Bang Niang and Nang Thong Beaches..... 185

| | | |
|---------|---|-----|
| 9-1.1 | Tool 1: Tsunami Modelling for Prediction of Tsunami Pattern at Bang Niang and Nang Thong Beaches..... | 186 |
| 9-1.1.1 | Selected source of potential earthquake eruption that might cause tsunami impact to Khao Lak. | 186 |
| 9-1.1.2 | Tsunami pattern at Bang Niang and Nang Thong Beaches. | 187 |
| 9-1.2 | Tool 2: Classification of the Tsunami-Affected Zones. | 192 |

9-2 Component 2: Building Resilience of the Bang Niang and Nang Thong Beach Communities..... 195

| | | |
|----------|---|-----|
| 9-2.1 | Tool 3: Tsunami Warning Systems and Evacuation Plans..... | 195 |
| 9-2.2 | Tool 4: Coastal Zoning and Land Use Planning for Tsunami Mitigation. | 198 |
| 5-1.1.9 | Tsunami Affected Zone and Tsunami Safe Zone..... | 198 |
| 5-1.1.10 | Set Back Policy..... | 200 |
| 5-1.1.11 | Breakwaters and Seawalls to Reduce Tsunami Impact..... | 200 |
| 5-1.1.12 | Evacuation Shelters..... | 200 |
| 9-2.3 | Tool 5: Recommendation for Building Code of Construction. | 201 |

| | | |
|-------------|--|------------|
| 9-3 | Component 3: Conservation of the Natural Environment | 203 |
| 9-3.1 | Tool 6 Restoring Beach Forest and Sand Dunes along Bang Niang and Nang Thong Beaches..... | 203 |
| 9-4 | Component 4: Strengthening Local Administrator and Community Responsibility and Cooperation among stakeholders..... | 204 |
| 9-4.1 | Tool 7: Policy Formulation and Enforcement. | 204 |
| 9-4.2 | Tool 8: Tsunami Knowledge Distribution for the Community. | 206 |
| 9-4.3 | Tool 9: Encouraging More Research and Technology Development for Tsunami Impact Alleviation..... | 208 |
| | CHAPTER 10 DISCUSSION AND CONCLUSIONS..... | 210 |
| 10-1 | Limitation of the Study..... | 215 |
| 10-2 | Future Research | 216 |
| | References | 218 |

LIST OF FIGURES

| | |
|--|----|
| FIGURE 2-1 OCEANIC PLATES WHICH SUPPORT THE INDIAN OCEAN BASIN AND TECTONIC ELEMENTS. | 5 |
| FIGURE 2-2 GEOGRAPHICAL AND GEOLOGICAL FEATURES OF THE NORTH EAST INDIAN OCEAN SHOWING THE EPICENTRE OF THE 2004 EARTHQUAKE (RED STAR), RAPID SLIP ZONE (RED BOX) AND SLOW SLIP AREA (BLUE BOX). FROM SHAPIRO ET AL. (2008). | 7 |
| FIGURE 2-3 EARTHQUAKE HISTORY IN THE NORTH EAST INDIAN OCEAN. FROM CHLIEH ET AL. (2007). | 12 |
| FIGURE 2-4 THE SUMATRA SUBDUCTION ZONE, WHERE THE INDO-AUSTRALIAN PLATE SUBDUCTS BENEATH THE EURASIAN PLATE. AREA OF SUBDUCTION IS SHOWN BY WAVY LINES AND DOTS. [HTTP://TODAY.CALTECH.EDU/GPS/SIEH/SUMATRA_05JAN2005_02.JPG] | 13 |
| FIGURE 2-5 THE 2004 RUPTURE ZONE FROM SUMATRA TO THE ANDAMAN ISLAND REGION WHICH CAUSED THE 2004 TSUNAMI. FROM MENKE ET AL. (2006)). | 17 |
| FIGURE 2-6 THE 2004 EARTHQUAKE UPLIFT AND SUBDUCTION AREAS. ARROWS SHOW THE HORIZONTAL MOVEMENT OF THE SEAFLOOR WHILE THE COLOUR CONTOURS SHOW SUBSIDENCE ON THE EAST AND UPLIFT ON THE WEST SIDE OF SUBDUCTION ZONE (SONG ET AL., 2008). | 26 |
| FIGURE 5-1 STUDY AREA OF KHAO LAK (RED BOX ON INSET MAP) SHOWING THE MAIN BEACHES AND COASTAL FEATURES. | 51 |
| FIGURE 5-2 CONDUCTING THE BATHYMETRIC SURVEY ALONG THE ANDAMAN COAST. | 55 |
| FIGURE 5-3 THE INNOVAR SES-2000 LIGHT DIGITAL PARAMETRIC ECHO-SOUNDER USED FOR MEASURING THE WATER DEPTH OF THE STUDY AREA. | 56 |
| FIGURE 5-4 LEICA SYSTEM 1200, REAL TIME KINEMATIC GPS SURVEYS FOR TOPOGRAPHIC DATA. ROVER RECEIVER, BASE UNIT AND BASE STATION. | 58 |
| FIGURE 5-5 BATHYMETRIC SURVEY LINES AND TOPOGRAPHIC SURVEY POINTS OF KHAO LAK AREA. | 59 |
| FIGURE 5-6 BATHYMETRIC SURVEY LINES AND TOPOGRAPHIC SURVEY POINTS OF BANG NIANG AND NANG THONG BEACHES. | 60 |
| FIGURE 5-7 DEPTH AND HEIGHT OF KHAO LAK AREA. | 63 |
| FIGURE 5-8 DETAILED BATHYMETRY AND TOPOGRAPHY OF BANG NIANG AND NANG THONG BEACHES. | 64 |
| FIGURE 5-9 THREE NESTED GRIDS USED FOR STUDYING TSUNAMI GENERATION, PROPAGATION AND INUNDATION OF KHAO LAK: GRID A; GREEN RECTANGULAR, GRID B; YELLOW | |

| | |
|---|----|
| RECTANGULAR AND GRID C; RED RECTANGULAR. (ALSO SHOWN IN GREEN IS THE RUPTURE ZONE)..... | 67 |
| FIGURE 5-10 SUBDUCTION ZONE SHOWING SUB-UNITS USED FOR SIMULATING THE 2004 INDIAN OCEAN EARTHQUAKE-GENERATED TSUNAMI BY MOST/COMMIT MODEL..... | 68 |
| FIGURE 5-11 VERTICAL SEAFLOOR DISPLACEMENT HEIGHTS OF SCENARIO2 | 69 |
| FIGURE 6-1 COMPARISON OF TSUNAMI WAVE MAXIMUM HEIGHT OF SCENARIOS 1 AND 2 WITH SURVEYED DATA. | 80 |
| FIGURE 6-2 COMPARISON OF TSUNAMI MAXIMUM WAVE HEIGHT FROM SCENARIOS 3, 4, 5 AND 6 WITH SURVEYED DATA. | 81 |
| FIGURE 6-3 COMPARISON OF TSUNAMI MAXIMUM WAVE HEIGHT FROM SCENARIOS 7, 8, 9 AND 10 WITH SURVEYED DATA. | 82 |
| FIGURE 6-4 COMPARISON OF TSUNAMI MAXIMUM WAVE HEIGHT FROM SCENARIOS 11, 12, AND 13 WITH SURVEYED DATA. | 83 |
| FIGURE 6-5 COMPARISON OF TSUNAMI MAXIMUM WAVE HEIGHT FROM SCENARIOS 14, 15, AND 16 WITH SURVEYED DATA. | 84 |
| FIGURE 6-6 LINEAR REGRESSION LINES OF MODELLED MAXIMUM TSUNAMI WAVE HEIGHTS OF 14 SCENARIOS AGAINST THE SURVEYED DATA BY SIRIPONG, ET AL. (2005). ALSO SHOWN IS THE ONE-TO-ONE LINE (BLACK). | 86 |
| FIGURE 6-7 LINEAR REGRESSION LINES OF MODELLED MAXIMUM TSUNAMI WAVE HEIGHTS OF 14 SCENARIOS AGAINST THE SURVEYED DATA BY MATSUTOMI (2005). ALSO SHOWN IS THE ONE-TO-ONE LINE (BLACK). | 86 |
| FIGURE 6-10 COMPARISON OF TSUNAMI WAVE HEIGHTS AT NANG THONG BEACH ALONG THE SAME CROSS SECTION LINE AS SIRIPONG, ET AL. (2005) AND JARUSIRI AND CHOOWONG (2005)..... | 90 |
| FIGURE 6-11 COMPARISON OF TSUNAMI WAVE HEIGHTS ACROSS BANG NIANG BEACH THROUGH THE SPECIFIC POINTS SURVEYED BY HORI ET AL. (2007) | 90 |
| FIGURE 6-12 COMPARISON OF TSUNAMI INUNDATION AREA OF KHAO LAK FROM MODEL WITH REAL INUNDATION FROM THE SURVEYED DATA OF THE 2004 TSUNAMI..... | 93 |
| FIGURE 6-13 COMPARISON OF TSUNAMI INUNDATION AREA SIMULATED BY MODEL VS. REAL INUNDATION AREA FROM SURVEYED DATA OF BANG NIANG AND NANG THONG BEACHES. | 94 |
| FIGURE 6-14 INUNDATION AREA AND MAXIMUM WAVE HEIGHT OF TSUNAMI WAVE ALONG THE BANG NIANG BEACH AND NANG THONG BEACH WITH 1.0 M TIDE..... | 96 |
| FIGURE 6-15 INUNDATION AREA AND MAXIMUM WAVE HEIGHT OF TSUNAMI WAVE ALONG THE BANG NIANG BEACH AND NANG THONG BEACH WITHOUT TIDAL EFFECTS. | 97 |
| FIGURE 6-16 TIDE GAUGE DATA FROM KURABURI NAVAL STATION, PHANG-NGA PROVINCE, NORTH OF THE STUDY AREA..... | 99 |

- FIGURE 6-17 TSUNAMI WAVE HEIGHT VS. ARRIVAL TIME AT BANG NIANG BEACH COMPUTED FROM THE MOST MODEL AND THE COMMIT INTERFACE OF THE 2004 INDIAN OCEAN TSUNAMI..... 99
- FIGURE 7-2 (TOP) VIEW OF KHAO LAK AREA. THIS PICTURE WAS TAKEN FROM THE KHAO LAK NATIONAL PARK, IN THE SOUTH OF THE STUDY AREA; IT SHOWS THE DRAWDOWN OF SEAWATER DUE TO THE FIRST TSUNAMI WAVE TROUGH THAT REACHED THE AREA AT 10.11 AM (+ 2 H 13 MIN). SUBMERGED ROCK OUTCROPS WHICH ARE NEVER NORMALLY EXPOSED COME INTO VIEW (CAPTURED FROM VIDEO: [HTTP://WWW.RADARHEINRICH.DE/TSUNAMIARCHIV/VIDEOS14/THAILAND/SUNSET-BEACH-TSUNAMI-ORIGINAL.WMV](http://www.radarheinrich.de/tsunamiarchiv/videos14/thailand/sunset-beach-tsunami-original.wmv))..... 104
- FIGURE 7-3 KHAO LAK AREA IN ‘NORMAL CONDITIONS, NOVEMBER 2008 DURING A LOW TIDE. 104
- FIGURE 7-4 THE FIRST WAVE TROUGH REACHED THE KHAO LAK AT AROUND 10.11 AM OF 26 DECEMBER 2004. ON THE HORIZON THE FIRST OF THE SERIES OF BREAKING WAVES (FIGURE 7-1) CAN BE SEEN APPROACHING THE COAST. 105
- FIGURE 7-5 (+ 2 H 30 MIN) FIRST TSUNAMI CREST HAS STARTED TO INUNDATE THE SOUTHERN PART OF KHAO LAK , FROM THE NATIONAL PARK HEADQUARTERS TO PAKARANG CAPE WHILE THE NORTHERN PART OF THE KHAO LAK COAST IS STILL EXPOSED IN THE INITIAL TROUGH. 106
- FIGURE 7-6 (+ 2 H 47 MIN) THE WHOLE OF THE KHAO LAK COAST IS TOTALLY FLOODED BY FIRST TSUNAMI WAVE INCLUDING PAKARANG CAPE WHERE WAVES INUNDATE FROM BOTH THE NORTH-WEST AND SOUTH-WEST. 107
- FIGURE 7-7 (+ 2H 55 MIN) SECOND TSUNAMI CREST ATTACKING KHAO LAK..... 108
- FIGURE 7-8 (+ 3 H 13 MIN) SECOND TSUNAMI WAVE CREST ATTACKS KHAO LAK AT 3 H 13 MIN. 109
- FIGURE 7-9 (+ 3 H 18 MIN) TWO SECOND TSUNAMI WAVE CREST, APPROACHING FROM DIFFERENT DIRECTIONS COLLIDE AT NANG THONG BEACH AND CAUSE THE HIGH MAGNITUDE OF RUN UP LEVEL. 110
- FIGURE 7-10 3-D DIAGRAM OF THE SIMULATED 2004 INDIAN OCEAN FIRST TSUNAMI WAVE TROUGH WHICH APPROACHES THE COASTAL AREA OF BANG NIANG AND NANG THONG BEACHES VIEWED FROM THE SOUTHWEST, COVERING THE SAME AREA AS FIGURE 7-11. THE LOWER (BLUE SHADES) SURFACE IS THE OFFSHORE BATHYMETRY (COLOUR CONTOURS EVERY 2 M) AND THE UPPER (PARTIALLY TRANSPARENT) SURFACE IS THE INSTANTANEOUS WATER LEVEL WITH CURRENT VECTORS SUPERIMPOSED. BRIGHTER COLOURS ARE THE ONSHORE TOPOGRAPHY..... 111
- FIGURE 7-11 (+ 2 H 12 MIN) SEA LEVEL RECESSION AND THE DEPTH-AVERAGED WATER CURRENT SPEEDS CAUSED BY THE ARRIVAL OF THE FIRST TSUNAMI WAVE TROUGH AT BANG NIANG AND NANG THONG BEACHES. THE ALONGSHORE DISTANCE IS ~ 6 KM, ON-OFFSHORE ~ 6 KM..... 112
- FIGURE 7-12 WATER LEVEL RECESSION RESULTING FROM THE FIRST TSUNAMI WAVE TROUGH THAT IMPACTED THE KHAO LAK AREA. THIS IMAGE WAS TAKEN FROM THE SCENIC VIEW POINT NEAR THE NATIONAL PARK HEADQUARTERS SHOWING THE EXPOSED ROCKS AND

| | |
|--|-----|
| SEABED RESULTING FROM THE SEAWATER DRAWN DOWN ON 26 DECEMBER 2004 (TIME UNKNOWN) (HTTP://WWW.RADARHEINRICH.DE). | 113 |
| FIGURE 7-13 KHAO LAK AREA IN NOVEMBER 2008 DURING A NORMAL LOW TIDE. THIS IMAGE IS OF THE SAME AREA AS FIGURE 7-12..... | 113 |
| FIGURE 7-14 (+ 2 H 20 MIN) 3-D DIAGRAM OF THE SIMULATED 2004 INDIAN OCEAN FIRST TSUNAMI WAVE CREST APPROACHING THE COASTAL AREA OF BANG NIANG AND NANG THONG BEACHES AND VIEWED FROM THE SOUTH. ALONGSHORE DISTANCE IS ~6 KM, CROSS-SHORE ~6 KM. THE LOWER SURFACE (BLUE SHADES) IS THE OFFSHORE BATHYMETRY (COLOUR CONTOURS EVERY 2 M). THE UPPER SURFACE (PARTIALLY TRANSPARENT) IS THE INSTANTANEOUS WATER LEVEL WITH CURRENT VECTORS SUPERIMPOSED; PINKS AND REDS ARE THE HIGHEST WATER LEVELS. BRIGHTER COLOURS ARE THE ONSHORE TOPOGRAPHY..... | 115 |
| FIGURE 7-15 (+2 H 20 MIN) THE WAVE TROUGH CONTINUES TO CAUSE WATER REGRESSION CLOSE TO THE SHORE. AT THE SAME TIME THE WAVE CREST IS APPROACHING THE COASTLINE AS A WALL OF WATER WITH MULTIPLE BREAKING CRESTS. THE WHITE PATCH IN THE CENTRE OF THE IMAGE IS AN EXPOSED ROCK OUTCROP. | 115 |
| FIGURE 7-16 CROSS SECTION DIAGRAM OF THE FIRST WAVE TROUGH AND WAVE CREST AT BANG NIANG BEACH +2H 20 MIN. THE WAVE IS MOVING FROM RIGHT TO LEFT. | 116 |
| FIGURE 7-17 CROSS SECTION DIAGRAM OF THE FIRST WAVE TROUGH AND WAVE CREST AT NANG THONG BEACH +2H 20 MIN. THE WAVE IS MOVING FROM RIGHT TO LEFT. | 116 |
| FIGURE 7-18 TSUNAMI RECESSION AT NANG THONG BEACH 10.20 AM (+2H 22 MIN) (HTTP://WWW.RADARHEINRICH.DE/WBBLITE/THREAD.PHP?THREADID=2844) | 117 |
| FIGURE 7-19 (+2 H 25 MIN) 3-D DIAGRAM OF SIMULATED FIRST TSUNAMI WAVE CREST TO ATTACK THE COASTAL AREA OF BANG NIANG AND NANG THONG BEACHES LOOKING NORTH. AREA, SCALE AND COLOUR CONTOURS ARE THE SAME AS FIGURE 7-10 AND FIGURE 7-14. THE TSUNAMI WAVE APPROACHES FROM TWO DIRECTIONS (WEST AND SOUTHWEST) PRODUCING VERY HIGH WATER LEVELS WHERE THEY INTERACT – SEE THE RED AREAS TO THE SOUTH ALONG NANG THONG BEACH. | 119 |
| FIGURE 7-20 (+2 H 25 MIN) SIMULATED TSUNAMI FIRST WAVE CRESTS REACHING BANG NIANG AND NANG THONG BEACHES FROM THE WEST AND FROM THE SOUTHWEST AROUND THE PAKARANG CAPE HEADLAND, COMBINING TO PRODUCED THE HIGHEST AND FASTEST WAVE CRESTS ALONG THE SOUTHERN PART OF NANG THONG BEACH. | 119 |
| FIGURE 7-21 3-D DIAGRAM OF THE FIRST TSUNAMI CREST ATTACKS BANG NIANG BEACH AND NANG THONG BEACH AT +2 H 27 MIN AFTER THE QUAKE..... | 121 |
| FIGURE 7-22 SIMULATED FIRST 2004 INDIAN OCEAN TSUNAMI WAVE CRESTS ATTACKS BANG NIANG BEACH AND NANG THONG BEACH AT +2 H 27 MIN, WHILE THE SECOND TSUNAMI WAVE CLOSELY FOLLOWS THE FIRST ONE..... | 122 |
| FIGURE 7-23 CROSS SECTION DIAGRAM OF FIRST WAVE TROUGH AND WAVE CREST AT NANG THONG BEACH +2H 27 MIN..... | 122 |
| FIGURE 7-24 THE FIRST WAVE CREST ARRIVING AT SUNSET BEACH (A SMALL POCKET BEACH, AND CONSIDERED TO BE PART OF NANG THONG BEACH)..... | 123 |

| | |
|---|-----|
| FIGURE 7-25 TOP VIEW OF FIRST WAVE CREST THAT REACHED SUNSET BEACH, A SMALL BEACH CLOSE TO THE KHAO LAK NATIONAL PARK TAKEN FROM A HEADLAND (SEEN TO THE LEFT IN FIGURE 7-24; HTTP://WWW.RADARHEINRICH.DE/WBBLITE/THREAD.PHP?THREADID=322)..... | 124 |
| FIGURE 7-26 FIRST TSUNAMI WAVE CREST REACHED NANG THONG BEACH AFTER 10.25 AM (+2H 27 MIN) (HTTP://WWW.RADARHEINRICH.DE/WBBLITE/THREAD.PHP?THREADID=2844). | 124 |
| FIGURE 7-27 BREAKING OF THE TSUNAMI WAVE AROUND ROCKS OUTCROPS AT SUNSET BEACH (RIGHT), AND WAVE RECEDING FOLLOWING BY THE FIRST TSUNAMI WAVE CREST WAS GOING TO REACH BANG NIANG BEACH (ON TOP LEFT) (HTTP://WWW.RADARHEINRICH.DE/TSUNAMIARCHIV/VIDEOS14/PC-DVD-UI/VIDEOS/THAILAND-TSUNAMI.HTML). | 125 |
| FIGURE 7-28 TYPICAL SUNSET BEACH, NANG THONG BEACH AND BANG NIANG BEACH IN NOVEMBER 2008 DURING LOW TIDE (COMPARE TO THE TSUNAMI EVENT WHICH ATTACKED THE SAME AREA ON 26 DECEMBER 2004 IN PREVIOUS FIGURE). | 125 |
| FIGURE 7-29 HIGH TSUNAMI CREST REACHED SUNSET BEACH, KHAO LAK ON 26 DECEMBER 2004 AT 10.29 AM (+2 H 31 MIN) (HTTP://NEWS.BBC.CO.UK/2/HI/IN_PICTURES/4293123.STM). | 126 |
| FIGURE 7-30 SUNSET BEACH IN NOVEMBER 2008 DURING LOW TIDE (LEFT), SHOWING FLAT BEACH WITH FEW ROCK OUTCROP COMPARED TO THE DAY TSUNAMI ATTACKED THIS BEACH IN DECEMBER 2004 (RIGHT: (HTTP://WWW.RADARHEINRICH.DE/WBBLITE/THREAD.PHP?THREADID=1689)). | 126 |
| FIGURE 7-31 BREAKING OF TSUNAMI WAVE ON THE SHORE OF SUNSET BEACH (HTTP://NEWS.BBC.CO.UK/2/HI/IN_PICTURES/4293123.STM). | 127 |
| FIGURE 7-32 FIRST TSUNAMI WAVE RECESSION IN FRONT OF PALM BEACH RESORT, SUNSET BEACH, KHAO LAK. FIRST SMALL WAVE CREST FOLLOWED BY THE SECOND HUGE WAVE CAN BE SEEN FROM THIS VIEW (HTTP://OURWORLD.WORLDFEARNING.ORG) | 128 |
| FIGURE 7-33 SURGING OF TSUNAMI WAVES CAUSED HIGH WAVE CREST REACHED THE AREA IN FRONT OF PALM BEACH RESORT (HTTP://OURWORLD.WORLDFEARNING.ORG). | 128 |
| FIGURE 7-34 INUNDATION DUE TO THE TSUNAMI WAVE WHICH ATTACKED PALM BEACH RESORT ON 26 DECEMBER 2004 (HTTP://OURWORLD.WORLDFEARNING.ORG). | 129 |
| FIGURE 7-35 THE FIRST WAVE CREST APPROACHING THE COASTAL OF KHAO LAK. | 130 |
| FIGURE 7-36 THE FIRST WAVE CREST SHOALING AS IT APPROACHES LAND AFTER THE FIRST RECESSION (HTTP://WWW.RADARHEINRICH.DE/WBBLITE/THREAD.PHP?THREADID=364). | 131 |
| FIGURE 7-37 DETAILED DIAGRAM OF WAVE SPEED AND DIRECTION THAT ATTACKS NANG THONG BEACH AT +2 H 27 MIN. | 131 |
| FIGURE 7-38 TSUNAMI WAVE FROM THE MODEL ATTACKS BANG NIANG AND NANG THONG BEACHES AT +2H 30 MIN (10.32 AM). | 133 |

| | |
|---|-----|
| FIGURE 7-39 CROSS SECTION DIAGRAM OF TSUNAMI WAVE AT NANG THONG BEACH +2H 30 MIN | 133 |
| FIGURE 7-40 TSUNAMI WAVES FROM THE MODEL ATTACKS BANG NIANG AND NANG THONG BEACHES AT +2H 35 MIN (10.33 AM). | 134 |
| FIGURE 7-41 CROSS SECTION DIAGRAM OF TSUNAMI WAVE AT BANG NIANG BEACH +2H 35 MIN | 134 |
| FIGURE 7-42 +2H 46 MIN, THE MAXIMUM INUNDATION DISTANCE AND AREA WERE DUE THE COMBINED EFFECTS OF THE SECOND WAVE RUN DOWN AND THE THIRD WAVE RUN UP. | 136 |
| FIGURE 7-43 CROSS SECTION DIAGRAM OF TSUNAMI WAVE AT BANG NIANG BEACH +2H 46 MIN | 136 |
| FIGURE 7-44 PATH OF POLICE PATROL BOAT TRANSPORTED BY THE TSUNAMI ON 26 DECEMBER 2004 AT OFFSHORE NANG THONG BEACH. | 138 |
| FIGURE 7-45 COMPARISON OF WAVE DIRECTION IN FRONT OF NANG THONG BEACH AND MAP SHOWING THE DIRECTION MOVED OF THE POLICE PATROL BOAT BY THE TSUNAMI WAVE (WWW.KHAOLAKMAP.COM). | 138 |
| FIGURE 7-46 FIRST WAVE CREST APPROACHING NEARSHORE NANG THONG BEACH BEFORE REACHING THE TWO POLICE PATROL BOATS. | 139 |
| FIGURE 7-47 FIRST TSUNAMI WAVE AT NEARSHORE NANG THONG BEACH WAS AS HIGH AS POLICE PATROL BOATS HEIGHTS (HTTP://WWW.RADARHEINRICH.DE/WBBLITE/THREAD.PHP?THREADID=321). | 139 |
| FIGURE 7-48 FIRST TSUNAMI WAVE TROUGH REACHED OFFSHORE NANG THONG BEACH CAUSING WATER DRAWN DOWN, WHILE THE FIRST WAVE CREST BROKE AT THE UNDERWATER ROCK OUTCROPS RESULTING IN HIGH BREAKING WAVES (HTTP://WWW.RADARHEINRICH.DE/WBBLITE/THREAD.PHP?THREADID=321). | 140 |
| FIGURE 7-49 FIRST TSUNAMI WAVE CREST REACHING NANG THONG BEACH AND ATTACKING THE TWO POLICE PATROL BOATS, CAUSING ONE TO SINK; THE OTHER WAS TRANSPORTED 2.6 KM AWAY (HTTP://WWW.RADARHEINRICH.DE/WBBLITE/THREAD.PHP?THREADID=321). | 140 |
| FIGURE 7-50 ESTIMATED HEIGHT OF FIRST TSUNAMI WAVE CREST WHICH REACHED AND BROKE AT NEARSHORE NANG THONG BEACH (HTTP://WWW.RADARHEINRICH.DE/ WBBLITE/ THREAD. PHP?THREADID=2844). | 141 |
| FIGURE 7-51 POLICE PATROL BOAT NUMBER 813 WAS TRANSPORTED BY TSUNAMI WAVE. THIS IMAGE WAS TAKEN 1 WEEK AFTER THE 2004 TSUNAMI EVENT..... | 141 |
| FIGURE 7-52 POLICE PATROL BOAT WAS MOVED 2.6 KM FROM ITS MOORING AND STRANDED 1.25 KM FROM THE COASTLINE DUE TO THE HIGH ENERGY TSUNAMI WAVE THAT ATTACKED KHAO LAK ON 26 DECEMBER 2004. THE HEIGHT OF POLICE PATROL BOAT IS ABOUT 5 M..... | 142 |
| FIGURE 7-53 DIAGRAM OF WAVE SPEED AND DIRECTION OF THE FIRST TSUNAMI WAVE TO ATTACH BANG NIANG BEACH AT +2 H 27 MIN. THE BLUE OVAL SHOWS THE LOCATION OF MUKDARA BEACH RESORT | 144 |

| | |
|--|-----|
| FIGURE 7-54 DETAILED DIAGRAM OF WAVE PATTERN AROUND MUKDARA BEACH RESORT AT +2 H 27 MIN. WAVE SPEEDS ARE ~4-6 M/S, HEIGHTS ARE 4-6 M ABOVE MSL AND THE WAVE APPROACHES MUKDARA BEACH RESORT FROM THE SOUTHWEST. | 144 |
| FIGURE 7-55 FIRST WAVE REACHED MUKDARA BEACH RESORT AT +2H 31 MIN (10:29 AM) (HTTP://WWW.RADARHEINRICH.DE/WBBLITE/THREAD.PHP?THREADID=3178). | 145 |
| FIGURE 7-56 THE FLOODED BUILDINGS AND SMALL ROAD HAS NOW BEEN REPLACED BY THE CORRIDOR TO THE CONFERENCE HALL BUT THE GREEN WATER TOWER STILL REMAINS AND APPEARS IN THE BOTH PICTURES. | 145 |
| FIGURE 7-57 DETAILED DIAGRAM OF TSUNAMI WAVE WHICH INUNDATES THE MUKDARA BEACH RESORT AREA, BANG NIANG BEACH AT +2 H 35 MIN. | 146 |
| FIGURE 7-58 PHOTOGRAPH TAKEN AT 10.32 AM ON 24 DECEMBER 2004 (+2H 34 MIN) OF THE FIRST WAVE OVERWHELMING MUKDARA BEACH RESORT. WATER DEPTH FROM THE KNOWN HEIGHT OF BUILDINGS IS ESTIMATED TO BE 3.7 M (HTTP://WWW.RADARHEINRICH.DE/WBBLITE/THREAD.PHP?THREADID=3178). | 146 |
| FIGURE 7-59 THIS BUILDING IS APPROXIMATELY 5 M HIGH AND WAS ALMOST SUBMERGED BY THE FIRST TSUNAMI WAVE THAT ATTACKED NANG THONG BEACH..... | 147 |
| FIGURE 7-60 WATER DEPTH DUE TO THE TSUNAMI WAVE WAS APPROXIMATELY 3 M ABOVE THE GROUND FLOOR AT 10.37 AM ON 26 DECEMBER 2004 AND RISING RAPIDLY (HTTP://WWW.RADARHEINRICH.DE/WBBLITE/THREAD.PHP?THREADID=3178). | 147 |
| FIGURE 7-61 THIS WALL WAS UNDERWATER DURING THE FIRST TSUNAMI WAVE ATTACKED ON 10.37 AM OF 26 DECEMBER 2004..... | 148 |
| FIGURE 7-62 INUNDATION DUE TO THE WAVE FROM THE SOUTHWEST MERGING WITH THE WAVE FROM THE WEST AT BANG NIANG BEACH AND NANG THONG BEACH AT +2 H 46 MIN. | 149 |
| FIGURE 7-63 THE WAVE THAT TOTALLY FLOODED MUKDARA BEACH RESORT (BANG NIANG BEACH) STARTS TO DRAW BACK (+2 H 46 MIN). | 149 |
| FIGURE 7-64 WAVE RETREATING AT +3 H 00 MIN (10:58 AM). | 150 |
| FIGURE 7-66 MUKDARA BEACH RESORT LOOKING SEAWARD AT 10.59 AM 3) H 01MIN) (HTTP://WWW.RADARHEINRICH.DE/WBBLITE/THREAD.PHP?THREADID=3178). | 152 |
| FIGURE 7-67 MUKDARA BEACH RESORT IN NOVEMBER 2008 TAKEN FROM THE SAME LOCATION AS FIGURE ABOVE. | 152 |
| FIGURE 7-68 FIRST WAVE CREST REACHES BEYOND THE SWIMMING POOL AND THE BUILDINGS OF KHAO LAK ORCHID HOTEL TO THE CANAL BEHIND THE HOTEL..... | 154 |
| FIGURE 7-69 SWIMMING POOL IN FRONT OF THE KHAO LAK ORCHID HOTEL | 154 |
| FIGURE 7-71 KHAO LAK ORCHID RESORT WAS FLOODED BY THE TSUNAMI TO THE FLOOR OF THE 2 ND STORY BUILDINGS WHICH IS APPROXIMATELY 6-7 M HIGH. | 155 |
| FIGURE 7-72 THE RELATIONSHIP BETWEEN RUPTURE LENGTH AND SEISMIC MOMENT M_0 FOR DIP-SLIP EARTHQUAKES WITH $M_w > 7.5$ TAKEN FROM HENRY AND DAS (2001) WITH THE | |

| | |
|---|-----|
| ADDITION OF THE 2004 INDIAN OCEAN AND THE 2005 NIAS EVENTS. THE SOLID LINE IS THE BEST-FIT CORRELATION FROM HENRY AND DAS (2001); THE DASHED LINE IS FROM WELLS AND COPPERSMITH (1994). THE SOLID DOT IS THE MW = 8.4 EVENT SELECTED FOR THE MITIGATION SCENARIO..... | 158 |
| FIGURE 7-73 SECTIONS ALONG THE NICOBAR SECTION OF THE FAULT USED TO GENERATE THE MW = 8.4 TSUNAMI, SHADED GREEN, USING THE MOST MODEL; EACH BOX IS 100 KM X 50 KM. THE GREEN BOX IS GRID B, AND THE BLUE BOX, CENTRED ON KHAO LAK IS GRID C. | 160 |
| FIGURE 9-2 THE WAVE CREST REACHES BANG NIANG AND NANG THONG BEACHES AT +4 H 0 MIN. | 188 |
| FIGURE 9-3 CROSS-SECTION PROFILE OF WAVE INUNDATION BETWEEN A AND A' (SEE FIGURE 9-2) AT NORTH OF BANG NIANG BEACH +4H 0 MIN..... | 189 |
| FIGURE 9-4 CROSS-SECTION PROFILE OF WAVE INUNDATION BETWEEN B AND B' AT BANG NIANG BEACH (ACROSS PONG CANAL) +4H 0 MIN. | 189 |
| FIGURE 9-5 CROSS-SECTION PROFILE OF WAVE INUNDATION BETWEEN C AND C' AT BANG NIANG BEACH +4H 0 MIN..... | 190 |
| FIGURE 9-6 CROSS-SECTION PROFILE OF WAVE INUNDATION BETWEEN D AND D' AT NANG THONG BEACH +4H 0 MIN. | 191 |
| FIGURE 9-7 ESTIMATED WAVE SPEEDS AND WAVE DIRECTIONS FOR THE SIMULATED TSUNAMI THAT WOULD REACH BANG NIANG AND NANG THONG BEACHES AT +4H 0 MIN AFTER THE EARTHQUAKE. THE MOST VULNERABLE AREA WOULD BE AT BANG NIANG BEACH, BETWEEN THE BANG NIANG AND PONG CANALS, WHERE THE HIGHEST WAVE SPEEDS AND WAVE HEIGHTS WOULD BE ENCOUNTERED. | 193 |
| FIGURE 9-8 BUILDING DAMAGE FROM THE 2004 TSUNAMI WAVES THAT ATTACKED NANG THONG BEACH. (MODIFIED FROM (SILPAKORN UNIVERSITY, 2006)). | 194 |
| FIGURE 9-9 LOCATION OF DART BUOY (8.905 N 88.540 E) AND DIGITAL TIDE GAUGE AT MIANG ISLAND RELATIVE TO THE SUNDA SUBDUCTION ZONE AND THE COAST OF KHAO LAK, WITH ESTIMATED DISTANCES AND TSUNAMI TRAVEL TIMES. | 197 |
| FIGURE 9-10 ELEVATED AND FLOW THROUGH FIRST FLOORED BUILDING DESIGNS FOR KHAO LAK BY ARCHITECTS AT SILPAKORN UNIVERSITY. THE TOP FLOOR IS ALSO DESIGNED FOR USE AS A VERTICAL SHELTER. (SILPAKORN UNIVERSITY, 2006). | 203 |

LIST OF TABLES

| | |
|---|-------------------------------------|
| TABLE 2-1 TSUNAMI HISTORY IN THE INDIAN OCEAN REGION. FROM DOMINEY-HOWES ET AL. (2007)..... | 14 |
| TABLE 2-2 SUMMARY OF SOURCES AND THE CHARACTERISTICS DEDUCED FOR THE DECEMBER 2004 EARTHQUAKE. | 24 |
| TABLE 2-3 ESTIMATED RETURN PERIODS OF EARTHQUAKE ALONG THE ANDAMAN-NICOBAR SECTION OF THE SUNDA SUBDUCTION FROM VARIOUS DOCUMENTS. | 34 |
| TABLE 5-1 SLIP HEIGHT DETAIL ACCORDING TO VARIOUS DOCUMENTS USED FOR SIMULATION OF TSUNAMI WAVE BY USING MOST/COMMIT MODEL IN 16 SCENARIOS. | 76 |
| TABLE 5-2 ERUPTION SOURCES FOR MODEL CALCULATION FOR THE 16 DIFFERENT SCENARIOS. | 77 |
| TABLE 6-1 R^2 VALUES FOR THE LINEAR REGRESSION OF PREDICTED AGAINST OBSERVED (MATSUTOMI ET AL. (2005) AND SIRIPONG ET AL. (2005) TSUNAMI WAVE HEIGHTS FOR 14 RUPTURE SCENARIOS..... | 87 |
| TABLE 9-1 ESTIMATED TSUNAMI WARNING PERIOD AT KHAO LAK FROM VARIOUS METHODS | ERROR! BOOKMARK NOT DEFINED. |

Chapter 1 Introduction

The 2004 Indian Ocean tsunami caused many casualties and led to the loss of numerous properties in different countries located around the Indian Ocean. The Andaman coast of Thailand was severely damaged and lives were lost there, partially due to the lack of public awareness of the phenomenon of the tsunami. As a result, it is necessary to supply local people and tourists with information on tsunamis and the action to be taken at the time, to ensure the security of the population in the future. Mitigation plans have proved to be one of the most effective ways to reduce the destruction and loss of life from most natural hazards, and this includes tsunamis and earthquakes. To create an effective mitigation plan and protective measures for each natural hazard, it is vital to understand the causes and effects of that specific hazard first. To plan against tsunamis it is necessary to recognize the cause (usually a submarine earthquake) and understand the variable effects for different locations. Though many researchers have studied the 2004 submarine earthquake which caused the 2004 Indian Ocean tsunami, the direct effects of that earthquake which caused the severe destruction along the Andaman coast of Thailand have not been investigated in detail.

Numerical modelling is the best-known technique at present to simulate tsunami propagation and inundation following an underwater tectonic event. It can also be used to study the pattern of the wave that attacks any particular area. Numerical models have been developed to study tsunami propagation patterns and to devise proper mitigation plans and protective measures for tsunami-prone countries such as the USA, Australia and Japan, but adequate modelling has not been done for Thailand. In order to simulate the precise outcome that represents the actual tsunami, an accurate source position of the submarine earthquake, as well as detailed bathymetry and topography of the areas concerned, are needed as inputs to the numerical model. The resulting model output can then be analysed to generate mitigation plans, evacuation procedures and other protective measures.

The objectives of this research are a) to simulate the 2004 tsunami from its source at the point of the earthquake, b) validate the model using the limited evidence available from

Khao Lak, on the Andaman coast of Thailand, and c) to create a mitigation plan and propose protective measures for the Khao Lak area, using the results from the predictive model to prepare for any future destructive tsunami event in the Khao Lak area.

Chapter 2 Tsunami Waves in the Indian Ocean.

2-1 Tsunami Definition and General Characteristics.

Tsunami is a Japanese word meaning “harbour wave”. This word consists of two Japanese characters, “tsu” (harbour) and “nami” (wave). It refers to giant waves which attack coastlines. A tsunami comprises not a single wave but a series of ocean waves, usually generated by submarine earthquakes. Tsunami waves have long periods and wavelengths. In the deep ocean, their heights may reach only a few metres above the sea surface. By contrast, when the waves reach shallow waters, the heights increase significantly, resulting in a rapid rise in sea level and flooding of low-lying coastal areas.

The majority of tsunamis are the consequence of submarine earthquakes generated by seafloor displacement. However, a tsunami might occur as the result of volcanic activity, landslip occurring above or below the sea surface, underwater explosions, or meteorite impacts. A tsunami can be generated when the sea floor suddenly deforms and shifts the overlying water vertically. At the epicentre a magnitude of 7.5 or more on the Richter scale is enough to distort the seafloor causing the overlying water mass to shift upward, resulting in a long wave-length tsunami wave which may then travel for thousands of kilometres.

In general, an earthquake generating tsunami occurs at a thrust fault, where an oceanic plate subducts under a continental plate. The oceanic plate moves down until the fault line cracks, causing an earthquake that lifts the seafloor. Consequently, the water mass above the earthquake zone is instantaneously displaced, moving upwards from its previous position and waves are formed which propagate on the sea surface as the mass of water is displaced. Only earthquakes that cause a tsunami larger than the result of the expected seismic waves and have larger amplitudes than the seismic waves that generate it are classified as tsunami earthquakes.

2-2 Geological Settings Relating to Earthquakes and Tsunamis in the Indian Ocean Region.

2-2.1 Geomorphologic Features of the Indian Ocean

The Indian Ocean is the third largest Ocean of the world (after the Pacific Ocean and Atlantic Ocean). The total area of the water body of the Indian Ocean is 68.556 million sq km, and it includes the Andaman Sea, the Arabian Sea, the Bay of Bengal, the Flores Sea, the Great Australian Bight, the Gulf of Aden, the Gulf of Oman, the Java Sea, the Mozambique Channel, the Persian Gulf, the Red Sea, the Savu Sea, the Strait of Malacca, the Timor Sea, and other tributary water bodies. It is fringed by Africa, Asia, Australia and the Southern Ocean. The coastline of the Indian Ocean stretches for 66,526 km (Central Intelligence Agency, 2008). The Indian Ocean basin is supported by 2 main plates and 2 microplates: the Indian (India) Plate, the Australian (Australia) Plate, the Sunda Microplate and the Burma Microplate (Figure 2-1) (Berman, 2005). The Indian Plate was a part of the ancient Gondwanaland continent before it separated and became itself a major tectonic plate. The Indian Plate and the Australian Plate were separated by the Wharton ridge spreading centre (Figure 2-2). Approximately 40 million years ago (Ma), the Indian Plate combined with the neighbouring Australian Plate to become the Indo-Australian Plate which supports the larger parts of the Indian Ocean basin (Shapiro et al., 2008).

The Sunda Microplate and the Burma Microplate are situated in Southeast Asia and are part of the massive Eurasian Plate which stretches across Europe and Asia (Berman, 2005). The Sunda Microplate (Figure 2-1) underlies the South China Sea, the Andaman Sea, southern parts of Vietnam and Thailand along with Malaysia, the Indonesian islands of Borneo, Sumatra, Java, and part of the Celebes, plus the southwestern Philippines islands of Palawan and the Sulu Archipelago. The Burma Microplate is a small tectonic plate located between the Indo-Australian Plate and the Sunda Microplate, covering the Andaman Islands, the Nicobar Islands, and north-western Sumatra (Figure 2-1 and Figure 2-3) (Bird, 2003). Moreover, the Andaman Sea is divided from the main Indian Ocean by this Island Arc.

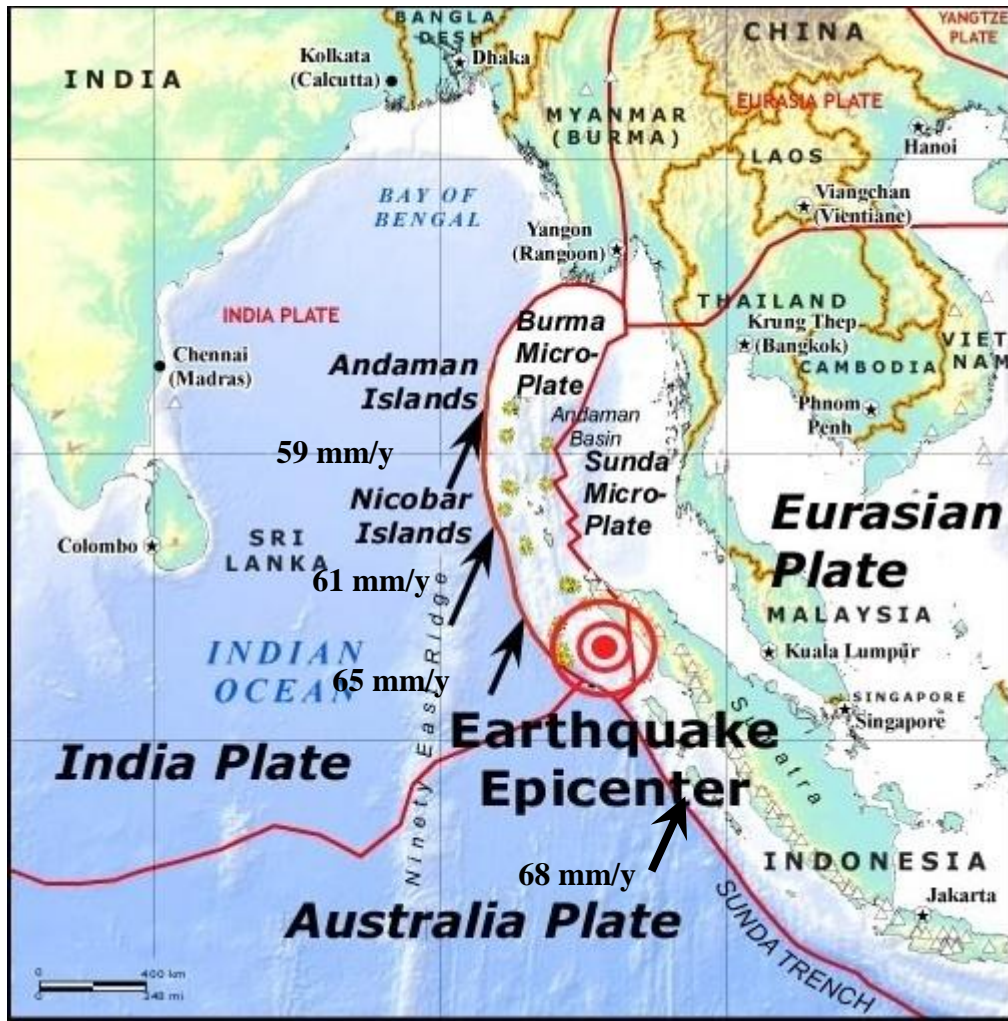


Figure 2-1 Oceanic plates which support the Indian Ocean basin and tectonic elements.

[[http://www.hgs.org/attachments/files/1015/The%20Great%20Sumatra-Andaman%20Earthquake%20of%20December%2026,%202004%20Figure 1.jpg](http://www.hgs.org/attachments/files/1015/The%20Great%20Sumatra-Andaman%20Earthquake%20of%20December%2026,%202004%20Figure%201.jpg)]

2-2.2 Plate Tectonics in the Indian Ocean

The Indian Plate, which underlies the Indian Ocean and the Bay of Bengal, and the Australian Plate started to merge 50-55 Ma, creating the Indo-Australian Plate. The Indo-Australian Plate is drifting north-east at an average speed of 6 cm/year and slides under the Burma Microplate which is part of the Eurasian Plate (Aitchison, 2005; Berman, 2005). The oblique motion between plates has resulted in microplates, for example the Burma Microplate and the Sunda Microplate which underlie significant portions of Southeast Asia (Banerjee et al., 2007; Engdahl et al., 2007; Gahalaut and Catherine, 2006; Karlsrude et al., 2005; Shapiro et al., 2008).

There are 3 main trenches where the Indo-Australian Plate is subducting beneath the Eurasian Plate: the Andaman Trench in the north, the Sunda Trench and the Java Trench in the south. The Sunda Trench is located in the north eastern part of the [Indian Ocean](#). It stretches from the [Lesser Sunda Islands](#) past [Java](#), around the southern coast of [Sumatra](#), and on to the [Andaman Islands](#). The trench is bordered by the [Burma](#) and [Sunda](#) Microplates on the east, and the [Indian Plate](#) on the west (Figure 2-2) (Shapiro et al., 2008). The Sunda Trench and Java Trench also form the boundary between the [Indian and Australian Plates](#) and the [Eurasian Plate](#). Subduction along these plate boundaries resulted in the [2004 Indian Ocean earthquake](#) and the ensuing deadly [tsunami](#) of December 26, 2004 (Harinarayana and Hirata, 2005). The Sunda Trench is a very active fault zone. [Earthquakes](#) in this region are either caused by thrust-faulting, where the [fault line](#) slips at right angles to the trench; or by strike-slip faulting, where material to the east of the fault line slips along the direction of the trench.

The Andaman Trench serves as a boundary between the Indian Plate and the Burma Microplate. It stretches from the Bay of Bengal to the west of the Sunda archipelago, covering the basin supporting the Andaman and Nicobar Islands (Figure 2-2). Moreover, the Andaman fault is a strike-slip fault and lies in the Andaman Sea, to the east of the Andaman and Nicobar Islands. The Andaman Sea is being broadened by sea floor spreading, occurring along undersea ridges. Engdahl et al. (2007) explained that the Sumatra fault system is transitioned by the Andaman back arc spreading centre fault complex and the west Andaman Fault (Figure 2-2). The Burma Microplate is known been seismically active across its whole area for the period from 1918 to 2005. Along the Andaman Trench, relative plate motion is parallel to the trench. Trench-normal convergence occurs at the Northern Andaman Island at a rate of around 14 mm/y.

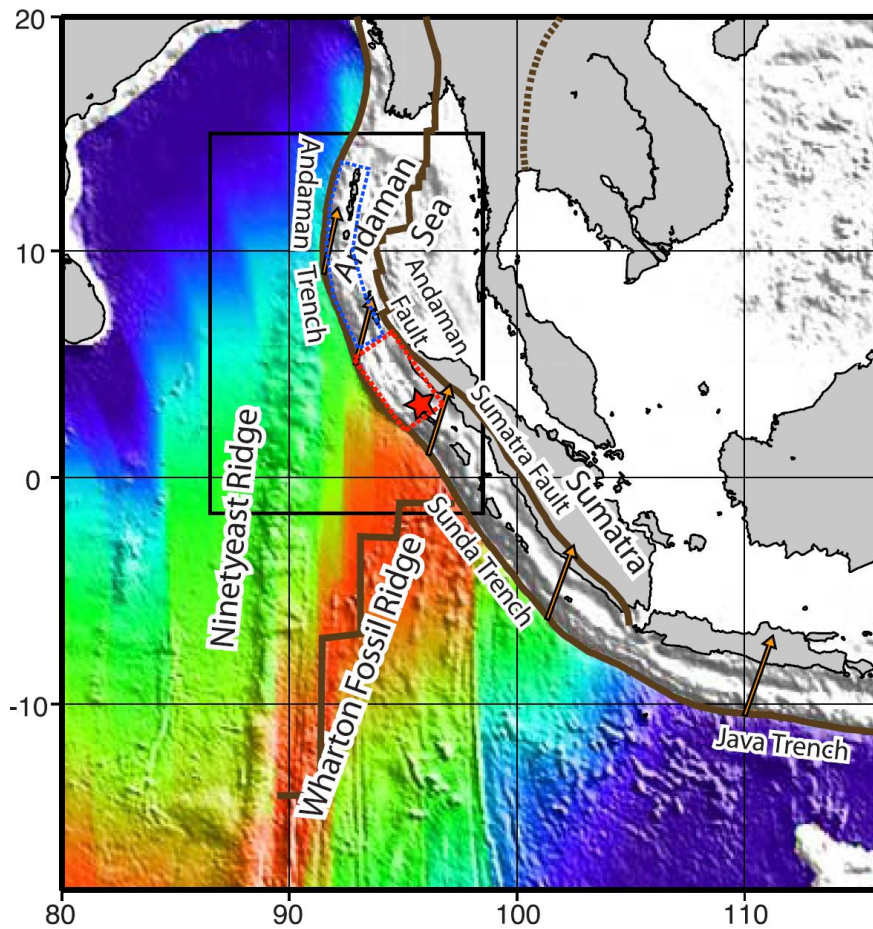


Figure 2-2 Geographical and geological features of the North East Indian Ocean showing the epicentre of the 2004 earthquake (red star), rapid slip zone (red box) and slow slip area (blue box). From Shapiro et al. (2008).

2-2.3 Subduction and Seafloor Spreading at the Andaman and Sunda Trenches

Strain built up at the subduction zone culminated in the 2004 submarine earthquake in the Indian Ocean. Ioualalen et al. (2007) reported that the relative movement between the Indian Plate and the Sunda Microplate is about 40 mm/y in a 20° N direction. The movement between the Indian Plate and the Australian Plate is around 50 mm/y at an azimuth of 8° N. The oblique subduction of the Indian Plate (part of the Indo-Australian Plate) under the Eurasian Plate causes westwardly decreasing trench-normal convergence at a rate of 74 mm/y along the central portion of the Java Trench. This is significantly faster than the 15 mm/y at the Andaman Trench plate boundary of the Burma Microplate, where it trends southward toward the Andaman Islands and the

Nicobar Islands. These faults formed in response to the relative oblique convergence between the Indian Plate and the Sunda Microplate. The Andaman Trench has an oblique thrust motion with a convergence rate of 14 mm/y. The subduction rate of the Nicobar-Andaman subduction zone decreases from 48 mm/y in the south (the tip of the Sumatra Island) to 14 mm/y in the north (Grevemeyer and Tiwari, 2006; Shapiro et al., 2008). Radha Krishna and Sanu (2002) reports that the rates of seismic deformation velocities for the Sunda subduction zone decrease northward from 5.2 to 0.65 mm/y near Nias island, off Sumatra, to 1.12 to 0.13 mm/y near the Great Nicobar Islands and to as little as 0.4 to 0.04 mm/y north of 8° N along the Andaman–Nicobar Islands section.

Karlsrude et al. (2005) reported that displacement occurs when the stress is released from the subduction zone. While the subducting plate is moving down and dragging the overlying plate in the locked fault mode, the stress is increasing until it reaches a point beyond the frictional strength. The overlying plate then bounces back, causing vertical displacement of the sea floor and thereby generating a tsunami along the subduction zone. The starting point of the 2004 rupture was the Sunda Trench where the warmest and thinnest lithosphere is to be found; the rupture then continued to the north towards the Andaman Trench.

Shapiro et al. (2008) reported that active spreading in the back-arc beneath the Andaman Sea and anomalously strong strain partitioning along the oblique Sumatra-Andaman subduction, is accommodated by strike-slip motion released along the transform Sumatra and Andaman faults that run parallel to the trench. Like all similarly large earthquakes, the December 26, 2004 event was caused by thrust-faulting. A 100 km instantaneous rupture subsequently caused about 1,600 km of the interface to rupture, which moved the fault 15 m and lifted the sea floor several metres, thereby creating the great [tsunami](#). Shapiro et al. (2008) reported that previous large earthquakes (magnitude > 9) have normally occurred at the highly active plate boundary where subduction is perpendicular to the trench. Oblique incidence of the Indian Plate and the Burma Microplate is found west of the Andaman Sea and thrust earthquakes are observed frequently along the Andaman-Nicobar Section of the Sunda Subduction.

2-3 The History of Tsunamis in the Region of the Indian Ocean

The history of Indian Ocean tsunamis presented here is divided into 2 main sections, related to the main seismic zones: the Sumatra Section and the Andaman-Nicobar Section (Figure 2-1). Dominey-Howes et al. (2007) present a table summarizing the history of those tsunamis that occurred in the Indian Ocean from 326 B.C. until the Nias earthquake and tsunami of 28 March 2005 (Table 2-1). The Richter magnitude scale or Local Magnitude scale (M_L), which was used before the '70, has been replaced by the Moment Magnitude scale (M or M_w); both M and M_w symbols are used in this Chapter depending on that used in the original documents. Although the first known tsunami occurred in 326 B.C., the first scientifically-documented tsunami in this region occurred in the Sumatra section in 1797 (Figure 2-3). Following this, two more tsunamis are recorded for the 18th century and eleven in the 19th century, of which the 1881 tsunami was the highest following an earthquake of > 8.7 on the Richter scale. In the 20th century there were 6 large magnitude earthquakes and tsunamis of which the 1974 event was the most serious. So far, two tsunamis have occurred in the 21st century.

The Sumatra section has been the most vulnerable to earthquakes, followed by the Andaman-Nicobar section and then the Arakan (Figure 2-3) (Harry et al., 2007). The Sumatra subduction zone is one of the most active tectonic plate boundaries in the world (Figure 2-4). In the past 36 years, prior to the 2004 event, earthquakes with $M > 5$ occurred 237 times along the Sumatra subduction zone. Seismic potential along the Java segment is low and only smaller earthquakes ($M < 8.0$) take place in this segment; Stein and Okal (Stein and Okal, 2005b) reported that prior to the 2004 Indian Ocean earthquake, the junction between the Indian Plate and the Sunda Microplate had not experienced a large earthquake in the past 150 years. Grevemeyer and Tiwari (2006) state that there was no historical record for any earthquake with magnitude (M) greater than 9.0 in either the Sumatra Section or the Andaman-Nicobar Section before the 2004 earthquake. However, the historic earthquake record for the Sunda–Andaman Subduction zone suggests that the potential for great destructive megathrust earthquakes is much larger for the Sumatra Section than along the Java Section, especially for that part of the Sumatra Section situated north of the Sunda Subduction

along the Sumatra Fault. Major earthquakes occurred in southern Sumatra in 1797 ($M \sim 8.4$), 1833 ($M \sim 9.0$), and in 1861 ($M \sim 8.5$) in Northern Sumatra (Figure 2-3). The 2005 Nias earthquake ruptured in the same area as the 1861 event, and a smaller earthquake ($M \sim 7.8$) in 1907 (Figure 2-3).

Borrero et al. (2006) reported that the 1797 earthquake had a magnitude between 8.4 - 8.6 from 0.5°S - 3.2°S ($\sim 300 \text{ km}$) and an average slip of 6 m. The 1833 quake extended for $\sim 320 \text{ km}$, from 2.1°S - 5.0°S ; its slip was as high as 18 m and its magnitude between 8.6-8.9 (Borrero et al. 2006). However, data from uplifted coral data suggest that the 1833 earthquake ruptured for $\sim 1000 \text{ km}$ (Geist et al., 2006; Sinadinovski, 2006) and numerical modelling by Dominey-Howes et al. (2007), suggest that the slip was 9.8 m (based on the uplift of coral atolls off Sumatra and a subduction width 200 km). Chlieh et al. (2007) reported that the Nias segment of the Sunda subduction zone, situated between Simeulue Island and Batu Island, cracked in 1861. The earthquakes in 1833 and 1861 are estimated to have generated tsunami waves 5-10 m high and to have caused massive damage to the populated areas along the southern coast of Indonesia. They might have had some effect on Sri Lanka and the Maldives, but would have had little impact on Thailand and the Bay of Bengal because the origins are located further southeast and most of the energy was dissipated into the open Indian Ocean (Bilham, 2005; Sinadinovski, 2006). Consistent with the study of the uplift of coral atolls by Dominey-Howes et al. (2007) is that the 1833 earthquake produced a tsunami wave that attacked the west coast of Sumatra, southern India, Sri Lanka and the coast of Western Australia. Dominey-Howes et al. (2007) numerical model for the 1861 earthquake and tsunami and proposed that the 3.9 m slip generated only a local small tsunami that resulted in run-ups of several metres locally and damaged only the coast nearby. It is similar in magnitude to the 2005 Nias Islands tsunami.

Although, the Sumatra Section has seen the most intense activity, it is the Andaman-Nicobar Section which is the main focus of this research. Three major tsunamis occurred near the Andaman-Nicobar Section, two in 1881 and one in 1945 (Table 2-1). The first recorded earthquake for the Andaman Section was on 28 January 1679. This earthquake occurred near the middle and the Northern Andaman Islands. Its rupture area and magnitude were equal to those of the 1941 event ($M \sim 7.7$) (Table 2-1 and

Figure 2-3). However, Rajendran et al. (2007) indicate that the 1679 earthquake did not generate a tsunami because of its small vertical displacement.

In 1881, an earthquake of magnitude 7.9 occurred near the Island of Car Nicobar in the Sumatra Section and the Andaman-Nicobar Section and generated a tsunami which affected the Andaman and Nicobar Islands, the coasts of India and Sri Lanka (Figure 2-3) (Bilham, 2005; Ortiz and Bilham, 2003; Rajendran et al., 2007; Seno and Hirata, 2007). Rajendran et al. (2007), citing Rogers (1883), state that the 1881 earthquake generated a tsunami with a height < 0.75 m at Car Nicobar Island, and that the tide gauge stations at Madras recorded a 0.25 m high wave. The small tsunami generated by an earthquake of $M_w = 7.7$ hit the west coast of the Andaman Islands on 26 June 1941 (Figure 2-3) (Bilham, 2005) causing an uplift of ~ 1.50 m along the western part of the middle Andaman Island. Chlieh et al. (2007) reported that there is no historical record of any earthquake with $M_w > 8.0$ occurring in the subduction zone between Sumatra and Myanmar.

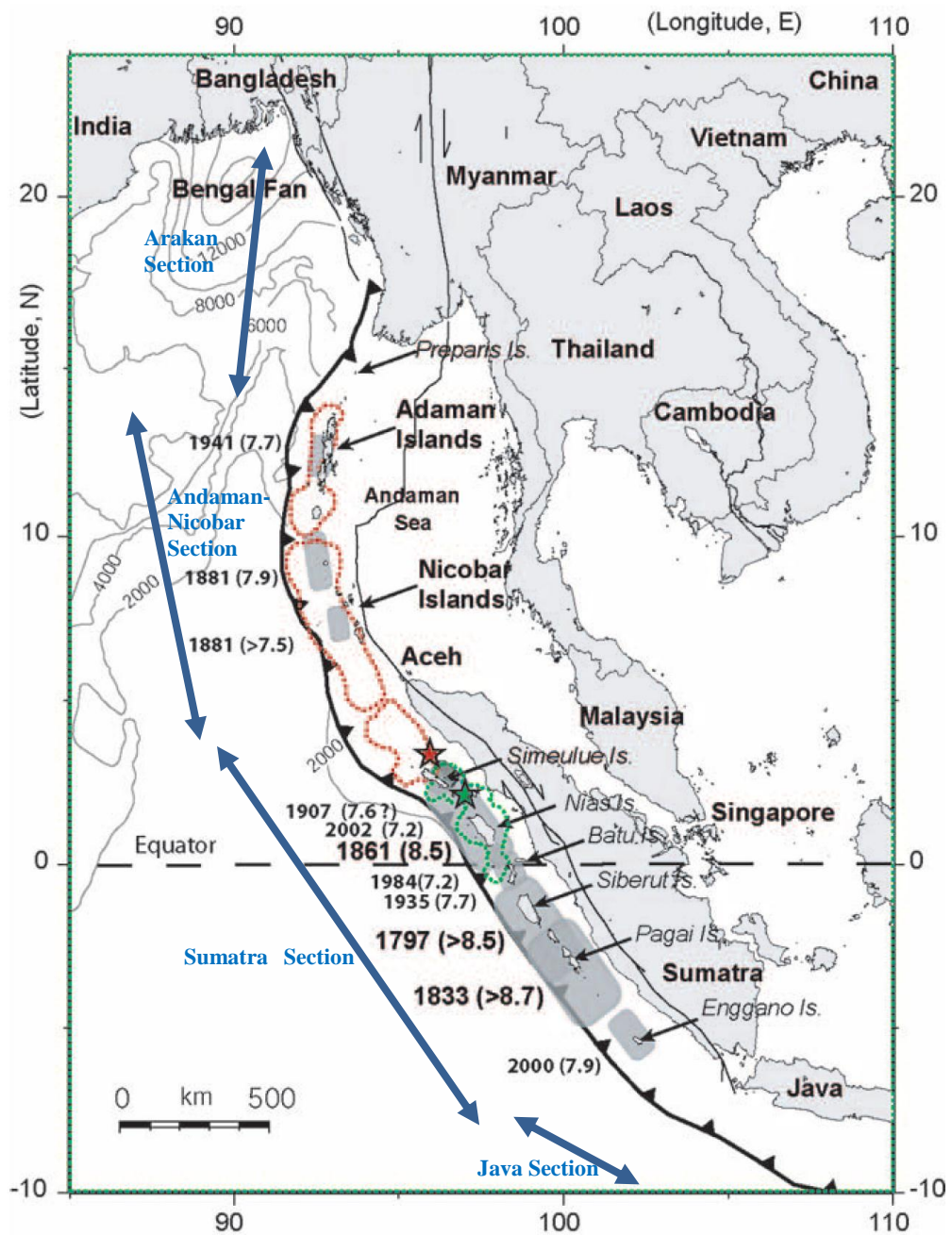


Figure 2-3 Earthquake history in the North East Indian Ocean. From Chlieh et al. (2007).

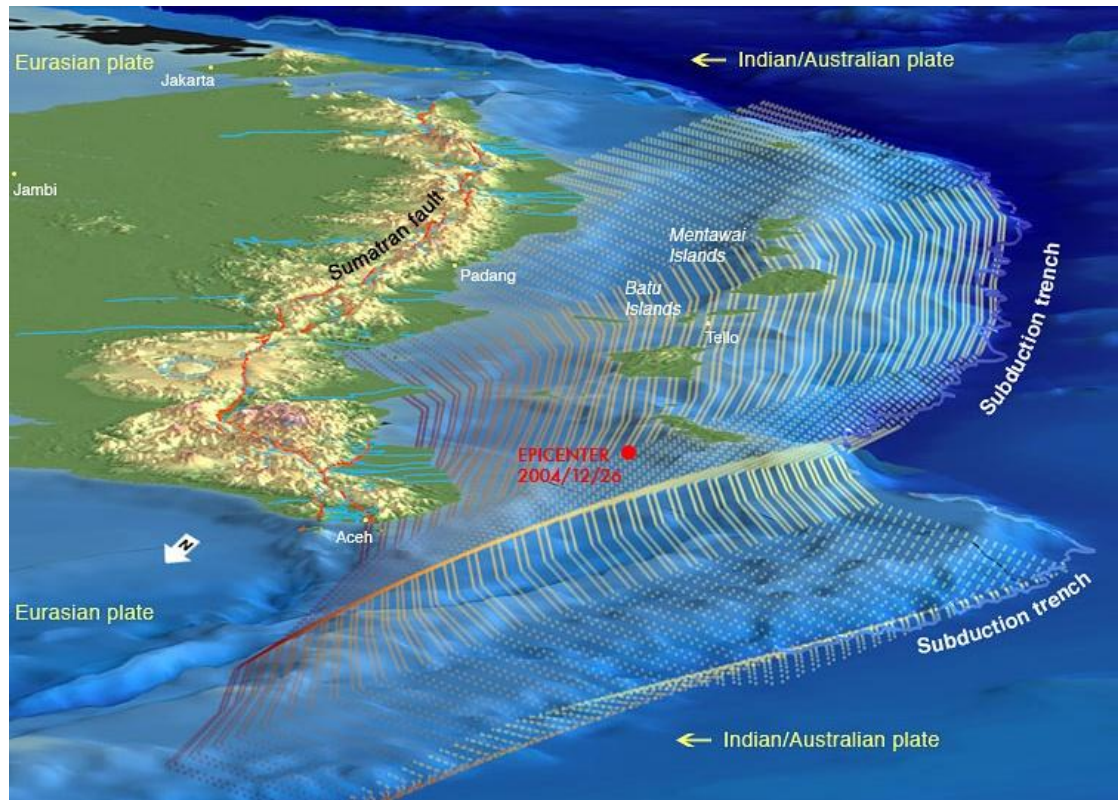


Figure 2-4 The Sumatra Subduction Zone, where the Indo-Australian Plate subducts beneath the Eurasian Plate. Area of Subduction is shown by wavy lines and dots.
 [http://today.caltech.edu/gps/sieh/sumatra_05jan2005_02.jpg]

| Event number | Year | Date | Tsunami source (trigger mechanism and area—if known) | Mag. (where tsunami generated by an earthquake) | Max. run-up (metres) | Deaths / effects / comments | References | | Confidence Index (CI) |
|--------------|--------|-----------|--|---|------------------------------------|-----------------------------------|------------|-----------|-----------------------|
| | | | | | | | Primary | Secondary | |
| 1 | 326 BC | ? | Unknown source: mouth of River Indus | | | Macedonian fleet destroyed | 5 | 3 | 0 |
| 2 | 1008 | ? | Earthquake on Persian Gulf coast (Iran) | | | | | 4, 25 | 0 |
| 3 | 1524 | ? | Unknown source: Gulf of Cambay | | | Reported by Vasco Da Gama's fleet | 9 | 26 | 2 |
| 4 | 1737 | 11 Oct | Cyclone impact in Hoogly Delta | | | 3000 deaths ⁸ | 7 | 4, 5, 8 | 0 |
| 5 | 1762 | 2 Apr | Earthquake on Arakan coast (Myanmar) | | | Many deaths (?) ¹⁰ | 27 | 3, 4, 10 | 3 |
| 6 | 1770 | ? | Earthquake S Sumatra | | | | 14 | 1 | 2 |
| 7 | 1797 | 10–11 Feb | Earthquake W Sumatra | 8.5–8.7 ³⁰ | | | 14 | 1, 30 | 3 |
| 8 | 1819 | 18 Mar | Earthquake S Sumatra | | | | 14 | 1 | 2 |
| 9 | 1833 | 24 Nov | Earthquake W Sumatra | 8.7 ¹³⁰ –9.2 ¹⁸ | | | 14, 19 | 1, 18, 30 | 3 |
| 10 | 1842 | 11 Nov | Bay of Bengal | | | | | 4 | 1 |
| 11 | 1843 | 5–6 Jan | Earthquake N Sumatra | | | | 10 | 1 | 3 |
| 12 | 1847 | 31 Oct | Earthquake Nicobar Is. | | | | | 4 | 1 |
| 13 | 1861 | 16 Feb | Earthquake N Sumatra | 8.3–8.5 ¹ | 7 ¹ | | 15, 10 | 1 | 3 |
| 14 | 1868 | 19 Aug | Earthquake? Andaman Is. | | 4 ⁴ | | | 4 | 1 |
| 15 | 1881 | 31 Dec | Earthquake Nicobar Is. | 7.1 ¹² | 1 ¹² | | 13 | 12 | 4 |
| 16 | 1882 | ? Jan | Unknown: Sri Lanka | | | | | 4 | 1 |
| 17 | 1883 | 27 Aug | Krakatoa eruption: Sunda Strait | | 35 | 3,600 deaths | 21 | 20 | 4 |
| 18 | 1886 | ? | Unkown: Bay of Bengal | | | | | 4 | 1 |
| 19 | 1907 | 4 Jan | Earthquake NW Sumatra | 7.6 ² | | | | 1 | 4 |
| 20 | 1921 | 11 Sep | Earthquake Java | 7.5 ² | | | | 1 | 4 |
| 21 | 1941 | 26 Jun | Earthquake Andaman Is. | 7.7 | | (5000?) deaths ⁵ | 16 | 4, 12 | 3 |
| 22 | 1945 | 27 Nov | Earthquake Makran coast (Pakistan) | 8.1 ²⁴ | 15 | | 11 | 4, 23, 24 | 4 |
| 23 | 1977 | 19 Aug | Earthquake Java | 8.3 | 30 | | 22 | | 4 |
| 24 | 1994 | 2 Jun | Earthquake Java | 7.6 ¹⁷ | 13 | 200 deaths | | 17 | 4 |
| 25 | 2004 | 26 Dec | Earthquake NW Sumatra-Andaman Is. | 9.0–9.3 ²⁸ | 31 ²⁹ –49 ³¹ | 20,000 plus deaths | | 28 | 4 |
| 26 | 2005 | 28 Mar | Earthquake NW Sumatra | 8.7 | 3 | | | | 4 |

Primary and secondary sources listed in Table 1:

1. Newcomb and McCann (1987), 2. Gutenberg and Richter (1954), 3. Lisitzin (1974), 4. Murty and Bapat (1999), 5. Murty and Rafiq (1991), 6. Nandy (1994), 7. Baird-Smith (1843a), 8. Bilham (1994), 9. Logan (1887), 10. Oldham (1869), 11. Pendse (1946), 12. Ortiz and Bilham (2003), 13. Oldham (1884), 14. Wichmann (1918a), 15. Wichmann (1918b), 16. Jhingran (1952), 17. Abercrombie et al. (2001), 18. Zachariasen et al. (1999), 19. Estridge (1883), 20. Simkin and Fiske (1983), 21. Warton and Evans (1888), 22. Pararas-Carayannis (1977), 23. Page et al. (1979), 24. Byrne et al. (1992), 25. Ambraseys and Melville (1982), 26. Bilham (1998), 27. Hirst (1763), 28. Lay et al. (2005), 29. Borrero (2005), 30. Natawidjaja et al. (2006), and 31. Shibayama et al. (2005)

Table 2-1 Tsunami history in the Indian Ocean region. From Dominey-Howes et al. (2007).

2-4 The 2004 Indian Ocean Earthquake and Tsunami

On Sunday 26 December 2004, at 07:58:53 local time (00:58:53 UTC), a very strong earthquake of $M_w = 9.3$ occurred off the west coast of Northern Sumatra. The 2004 earthquake was the first major earthquake recorded with the modern instruments developed during the sixties (Intergovernmental Oceanographic Commission, 2005). Ghobarah et al. (2006) stated that the 2004 earthquake is the second largest earthquake recorded instrumentally, the largest being the 1960 Chilean earthquake ($M_w = 9.5$). The epicentre of the earthquake (3.30° N, 95.78° E) was 155 km from the west coast of Northern Sumatra, Indonesia, approximately 255 km south west of Banda Aceh, the capital city of the Aceh province, and about 640 km from Phuket Island on the Andaman coast of Thailand. The 2004 earthquake was uncommonly strong in the extent of its geographical deformation. Its rupture length along the [subduction zone](#) was extensive, with an estimated length of 1,200 - 1300 km, and an uplift of ~15 m. It is the longest rupture ever known to have been caused by one earthquake (Banerjee et al., 2007; Chlieh et al., 2007). The slip distribution, rupture area and magnitude of the 2004 Andaman-Sumatra earthquake has been estimated using different methods such as seismic waves, static offsets and a combination between seismic and geodetic data (Banerjee et al., 2007). Both seismic and geodetic data yield the same magnitude of the 2004 earthquake. Purnachandra (2007) reported from Harvard University data that the 2004 earthquake has a strike of 329° , dip 8° and a rake of 110° degrees, indicating a thrust fault mechanism with a northwest-southeast trend. It was an event of 'surprising complexity' (Bilham, 2005).

2-4.1 Rupture zone of the 2004 Earthquake

The 2004 earthquake was associated with the subduction of the Indian Plate beneath the Burma Microplate (part of the Eurasian Plate). The quake was caused by the release of tectonic strain built up by the subduction of both plates at the rate of between 59-68 mm/y (Figure 2-1) (Gahalaut and Catherine, 2006; Liu, 2005; Subarya et al., 2006). Rupture resulting from the 2004 earthquake can be divided into 3 segments: the Andaman, the Nicobar and the Sumatran Segments (Ammon et al., 2005; Banerjee et al., 2007; Lay et al., 2005). It also involved the rupture of multiple segments running

from Myanmar to Northern Sumatra Island (Rajendran et al., 2007). Figure 2-5, Menke et al. (2006) shows a sketch of the Sumatra-Andaman island area of the 2004 rupture zone.

Different authors describe the 2004 rupture in different ways. According to Subarya et al. (2006) the seismic moment for the earthquake was released between latitudes 2° - 10° N which agrees with Neetu et al. (2005) who reported that the rupture extended up to 600 km to the north-northwest of the epicentre ($\sim 9^{\circ}$ N). Chlieh et al. (2007) reported that there were 3 distinct peaks of released moment, viz. at 4° N, 7° N and 9° N. Ishii et al. (2005) also reported that the release of energy occurred at 3° N, 5° N and 8° - 10° N with a minimum at 7° N; the energy release ceased at 12° N. Ammon et al. (2005) reported that energy was released from 3 segments: at 4° - 6° N, 8° - 10° N and 12° - 13.75° N. Pietrzak et al. (2007) used a numerical model to test which segments created the 2004 tsunami waves, in comparison to images of the tsunami wave propagation in the open ocean measured by the Jason-1 satellite; this implied that the rupture extended from 2.5° to 13° N, but with a minimum occurring at 5° to 6° N; the simulation suggested that the source of the 2004 tsunami might have originated from as far south as 2° N but should not have extended beyond 14° N, and correlated to offshore uplift of the Andaman Islands. Chlieh et al. (2007) reported that the rupture must have propagated as far as 15° N.

The section of largest slip occurred between 3° and 5° N (inverted from co-seismic GPS data) (Ishii et al., 2005; Pietrzak et al., 2007). The high tsunami amplitude experienced in Sri Lanka and India, which are perpendicular to the fault, supports the conclusion that rupture occurred on the north and north-trending segments (Bilek, 2007; Bilham, 2005; Sinadinovski, 2006; Stein and Okal, 2005b; Stein and Okal, 2007; Vigny et al., 2005) and is consistent with the large horizontal displacement observed in Thailand (8 cm in Bangkok) and along the Malaysian peninsular (2 cm in Singapore to 17 cm in Langkawi Island). The rupture extended as far north as the Andaman sea; Jason-1 satellite images show the tsunami propagating outwards from the northern length of slip between 8° to 10° N (from Katchell Island in the Nicobar to the Little Andaman Islands, centred at Car Nicobar Island).

Piatanesi and Lorito (2007) used tsunami waveforms, recorded by many tide gauges, to estimate the rupture process of the 2004 Indian Ocean earthquake. These results revealed that displacement was concentrated in 3 main sections: the southern part of the fault from the hypocenter to about 5° N (slip ~ 10 -30 m), the main slip located between 6° - 11° N (slip ~ 10 m) and the northernmost and deep part of the fault (slip ~ 20 m). This matches up with Ammon et al. (2005), Tanioka et al. (2006) and Hirata et al. (2006) with the exception of the northernmost section, for which they conclude that there is no evidence of any movement north of 12° N. All assumptions show very large slip off Banda Aceh, and major slip between 7° N - 11° N. Furthermore, it is evident that the northern segment of the rupture between 9° - 14° N, around the Andaman Islands, demonstrates a slow slip mechanism. It is also possible that slow slip occurred for the first 50s at the epicentre of the Sumatra segment, located between 2° - 6° N, but it was large rapid slip that still dominated in this portion. On the other hand, the Nicobar island segment showed moderately rapid slip followed by slower slip for about 1 h (see Slow Slip section).

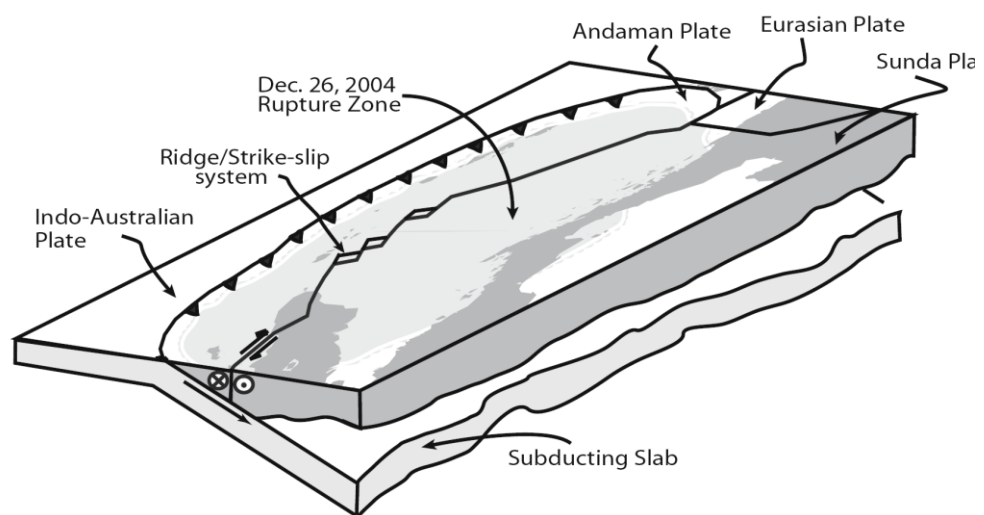


Figure 2-5 The 2004 rupture zone from Sumatra to the Andaman Island region which caused the 2004 tsunami. From Menke et al. (2006).

2-4.2 Characteristics of the 2004 Earthquake

The Sumatra-Andaman earthquake of 26 December 2004 started near a sharp bend in the trench Geist et al. (2007). Its hypocenter was situated north of Simeulue Island at a depth of 30 km (Figure 2-1, Figure 2-2 and Figure 2-4).

The 2004 earthquake did not constitute a simple event but was surprisingly complex (Bilham, 2005). It occurred in two phases over an extended period of time, and included periods of both rapid slip and slow slip (Figure 2-2). The duration of high frequency energy radiation was approximately 500 s (Ni et al. (2005), and translated into a rupture zone length of 1,200 -1,300 km, the longest ever recorded, with average rupture speed ~ 2.5 km/s.

2-4.2.1 *Rupture and Rupture Velocity*

Kruger and Ohrnberger (2005) reported that the total rupture length was 1,150 km, and ruptured with an average rupture speed of 2.3-2.7 km/s, and had a total rupture period of at least 430 s (probably 450-480 s); the location of the seismic energy maximum did not move during the first 60 s. Later however, the rupture ran in the north-northwest direction for 600 km, before changing to the north direction for roughly 550 km and ending at the northern end of the Andaman Islands. Lay et al. (2005) state that low energy and slow rupture initially happened for the first 50 s, before rapid rupture of ~ 2.5 km/s velocity occurred towards the Andaman Islands for 1300 km. The rapid rupture of the 2004 earthquake began on the southeast Sumatra section and caused 20 m of vertical displacement there during the first 230 s. Generally, longer-duration earthquakes may be indicative of slow rupture as it propagates in the low-rigidity materials found in shallow fault zones; this results in interference between the direct and reflected waves, and makes it complicated to confine the source mechanism using classical inversion methods (Bilek, 2007; Chlieh et al., 2007; Piatanesi and Lorito, 2007).

2-4.2.2 *Slow Slip*

In the context of the 2004 earthquake ‘slow slip’ is mainly used by authors to describe the slip that occurred in the period of up to one hour following the rupture (and initial rapid slip), rather than the after-slip, slow or silent slip that associated with large

earthquakes with timescales of days to a year. Slow slip is not included in the conventional estimations of seismic moment. For example, the 2004 earthquake was underestimated by the conventional method based on surface waves; the conventional method omitted slow slip as that is not detectable from the surface waves. Schwartz and Rokosky (2007) state that slow slip mechanisms can be observed in numerical simulations of the earthquake cycle. Bilham (2005) reported that the slow slip experienced in the 2004 earthquake is different from previous earthquakes and has changed the way seismologists assess past conservative seismic hazards and suggests that such conservative seismic forecasts may not suit future needs.

Ammon et al. (2005) reported that fault sliding began slowly for the first 40-60 s but then grew rapidly as large amounts of slip occurred off the west coast of Sumatra (3°N – 4°N) before spreading north-northwest at a speed of about 2.5 km/s along the 1200-1300 km of the Andaman trough. The slip models they used, obtained from inversions of body and surface waves, show that slip gradually decreased to the north “*suggesting a relationship between megathrust coupling and rupture velocity and/or slip rate. The results indicate that the fault was well-coupled in the south, somewhat less coupled in the central portion, and weakly coupled in the north of the rupture zone. The sub-ducting slab dip angle, age, and plate motion obliquity all increase from the southern (Sumatra) segment to northern (Andaman) segments of the rupture, perhaps contributing to reduction of interplate coupling as a function of distance northward. The reduction of slip just north of the Great Nicobar Island coincides with a northward rotation of the trench, and the rupture terminated in a region where the trench is parallel with the interplate motion (or even extensional)*” Ammon et al (2005).

The slip in the models used by Ammon et al (2005) north of 8°N is too small to explain GPS displacements observed in the Nicobar Island (1-2 m vertical, 5 m horizontal) and the Andaman Island (1-2 m vertical, 3 m horizontal). They state that they need to increase the slip in the section north of 8°N by a factor of 2 to 3 but adding rapid slip of this magnitude considerably reduces the fit to the normal-mode amplitudes so they conclude most of this additional slip was probably slow and occurred at a time scale beyond the seismic band.

Slow slip is supported by Lay et al (2005) and agrees with Stein and Okal (2005b), who also report that slow slip occurred over the northern part of the rupture zone, and that split modes are better fitted by a source with centroid at 7° N rather than at the epicentre

at 3° N where rupture started (Bilham, 2005; Liu, 2005; Stein and Okal, 2005b; Stein and Okal, 2007; Subarya et al., 2006; Synolakis et al., 2005). Lay et al (2005) state that the northern portion of the fault appears to have slipped 3 to 7 m more than accounted for by the seismic model, with a time scale of ~1 hour or longer. This slow slip occurred only along the Nicobar and Andaman Islands segments of the rupture zone, where the plate convergence is increasingly oblique and slip is strongly partitioned. They note that, with the low convergence rate of 14 mm/year in the region, it would take 700 years to accumulate 10 m of slip potential in the region, which is consistent with the lack of historical great events in the northern part of the subduction zone.

Lay et al (2005) present a useful summary rupture diagram (their Figure 8) showing fast slip (seismic moment 6.5×10^{22} Nm) and slow slip (seismic moment 3.0×10^{22} Nm) components showing that slow slip contributed nearly one third of the seismic moment.

After the main shock, 31 earthquakes with magnitudes between 5.5-7.3 occurred in the following 48 h, with the seismicity shifting northward along the 1200 km long rupture zone (Sinadinovski (2006). Moreover, 125 aftershocks of $M > 5.0$ were triggered around the edge of the rupture over the following 3 week period but these aftershocks did not cause any further tsunamis. Vallee (2007) states that aftershock locations for the 2004 earthquake were spread along 1300 km, and were the evidence of long and ‘slow’ slip.

Although there is agreement on the occurrence of slow slip there is disagreement as to its importance for the generation of the tsunami. Lay et al 2005 state that the northern third of the aftershock zone appears not to have produced rapid vertical ocean-bottom displacements capable of generating large tsunami waves and is consistent with satellite altimetry observations of the deep-water waves obtained from the fortuitous passage of two satellites over the Indian Ocean 2 to 3 hours after the rupture occurred. Bilham (2005) also believes that slip occurred too slowly in the last 5 min (rupture along the Andaman section) to generate either tsunamis or sizable 20-s surface waves, the amplitudes of which are used to assign a Richter magnitude for an earthquake.

Stein and Okal (2005), on the other hand believe that the slow slip helped to excite the tsunami, as suggested by successful modelling of the wave from sea levels detected by

the Jason satellite, using a source that included the northern segment. Large tsunami amplitudes in Sri Lanka and India also support rupture on the northern, north-trending segment, because tsunami amplitudes are largest when perpendicular to the fault. (Seno and Hirata, 2007) also state the 2004 earthquake was characterised by slow slip and caused “unexpected tsunami waves larger than the seismic slip result alone would explain”. Geist et al. (2007) indicated that the generation of a tsunami depends on longer source process times than those provided by seismic excitation. A tsunami can thus be generated from a small magnitude earthquake with long duration, for example the 1992 Nicaragua earthquake. Moreover, shallow earthquakes have longer-scale source intervals than deeper ones. Seno and Hirata (2007) suggested that the 2004 event is a hybrid event with longer source duration.

2-4.2.3 *Seafloor Displacement Heights*

Several methods have been used to estimate the uplift over the earthquake’s rupture area. Vigny et al. (2005) pointed out from the seismic inversion and GPS records that the displacement of the 2004 earthquake was not homogeneous along the whole subduction zone but varies between 15-25 m, decreasing northward from the epicentre. Rhie et al. (2007) calculated the slip allocation of the 2004 Indian Ocean earthquake by joint inversion of tele-seismic and regional geodetic datasets and found that the large slip patch of the 2004 Indian Ocean earthquake was located at the 4° N and that high slip region (> 10 m) did not extend beyond 10° N. Chlieh et al. (2007) reported that high displacement occurred at 4° N, 7° N, 9° N with a total seismic moment of $6.7-7.0 * 10^{22}$ N m ($M_w = 9.15$). Banerjee et al. (2007) reported that the rupture distribution ($M_w = 9.22$) was estimated to be 15m along the southern Andaman Section, the Nicobar Section and the Northern Sumatra Section. Fujii and Satake (2007) developed a tsunami source model and used it to calculate the rupture distribution, based on tide gauge data and satellite images. They conclude that uplifts of up to 13-25 m occurred offshore of Sumatra Island and around 7 m for the Nicobar Island Section. The 2004 Indian Ocean Earthquake characteristics, including rupture length, rupture width, seafloor displacement height, seismic period and rupture velocity, are presented in Table 2-2. These factors were applied for simulating the 2004 tsunami modelling which affected the Andaman Coast of Thailand.

The 2004 Indian Ocean earthquake displacement shows that seafloor uplift occurred on the west side with large horizontal displacement in the southwest direction along the Sumatra Section, a lower horizontal displacement for the Nicobar Section and the smallest at the Andaman Section while sea bottom subsidence took place along the east side of the eruption area (Figure 2-6) (Pietrzak et al., 2007; Song et al., 2008). Kowalik, Knight et al. (2007) indicated that the fault plane is broken into 2 segments with maximum uplift of ~5.1 m and maximum subsidence of ~4.7 m (Bilham, 2005) also indicates that the 2004 earthquake generated up to 10 m of uplift and subsidence from the earthquake elastic rebound.

| Sources | Methodology Used | Rupture length (km) | Rupture width (km) | Seafloor displacement height (m) | Seismic period (s) | Rupture velocity (km/s) | Apply for Scenario # in Table 5-1 |
|---|--|-------------------------------------|--------------------|--|----------------------|----------------------------|-----------------------------------|
| (Ammon et al., 2005) | Broadband seismic waveforms (Seismic data from Global Seismic Network (inversion of body and surface wave)), Use short-period S wave and P wave. | 1200-1300 | 200 | 15-20 | 480-600 | 2.5-3.0 | 3, 4, 5 and 6 |
| (Banerjee et al., 2005) | Far-field GPS data | | | 5 | | | |
| (Bilham, 2005) | GPS data (field measurements of uplifted or subsided coral heads) | 1200-1500 | 150 | - | 515-1320 | - | |
| (Ishii et al. 2005) | Hi-Net seismic array (from Japan as an antenna to map the progression of slip by monitoring the direction of high-frequency radiation). | 1200 | - | - | 480 | 2.8 | |
| (Kruger and Ohrmberger, 2005) | Seismological data from broadband seismic stations of the German Regional Seismic Network. | 1150 (600+550) | - | - | 430 (450-480) | 2.3-2.7 | |
| (Lay et al., 2005) | Seismological analyses of the extensive, openly available seismogram data set from the international Federation of Digital Seismic Networks (FDSN) backbone network. | 1200 | 160-170 | 20 (Sumatra) <2 (Nicobar& Andaman) | 500 | 2.5 (2.0-3.0) | 3,4,13, |
| (Liu, 2005) | Seismological data. | - | - | 20 | 200 | 2.0 | 5-12 |
| (Ni et al., 2005) (Kanamori and Eeri, 2006) | Seismological data (High-frequency seismic records obtained from the Global Seismic Network) | 1200-1300 | | | 500 | 2.5 | |
| (Stein and Okal, 2005b), (Stein and Okal, 2007) | Seismological data (an analysis of the Earth's normal modes 0S2 , 0S3 and 0S4.) | 1200 | 200 | 12-15 | - | 2.5-3.0 | 1,2,3,4,15, 16 |
| (Vigny et al., 2005) | Geodetic data (Far-field GPS data (60 Global Positioning System (GPS) sites in southeast Asia)). (Geodetic Space Techniques) Divided rupture into 2 sections | >1000 650 (south) 450 (north) | - | - | > 600 (240for north) | 3.7 (south) 2.0 (north) | |
| (Gahalaut and Catherine, 2006) | Global Positioning System (GPS) measurements of near - field coseismic displacements (13 sites located in Andaman–Nicobar islands) | 1500 | 120-160 | 3.8-7.9 (Andaman) 11-15 (Nicobar) | - | | 4,5,6,7,8,9, 10,12 |
| (Menke et al., 2006) | Review | - | - | Average=5 Max > 30 | - | 2.8 (south) 2.1 (north) | |
| (Sinadinovski, 2006) | Seismological data | 1200 | 50 | 15 | | 2.1 | 3 |
| (Tanioka et al., 2006) | Rupture process was estimated using tsunami waveforms observed at 5 tide gauges and the co-seismic vertical deformation observed along the coast | 1200 | - | 23 m at Aceh coast 21 m at Simeulue | - | Average = 1.7 | 5,6,7,8,9,10 ,11,12,14 |

| | | | | | | | |
|------------------------------|---|-----------|-------|---|---------|----------|--------------------|
| | | | | 10-15 m at Little Andaman and Car Nicobar | | | |
| (Chlieh et al., 2007) | Geodetic data (Near-field Global Positioning System (GPS)) estimation of vertical displacement derived from remote sensing using optical images (ASTER, SPOT, and IKONOS 3 peaks : 4N, 7N, and 9 N, | 1500 | < 150 | - | - | 2.2-2.6 | |
| (Seno and Hirata, 2007) | Back projecting the wave front recorded on the sea surface height (SSH) by the satellite altimetry | - | - | 20-40 Max = 40 | - | - | |
| (Vallee, 2007) | Seismological data (Empirical green's function (EGF)) | 1150-1200 | - | 20 m at Sumatra 10 m at Nicobar | 580+-20 | 2.0-2.5 | 1,2,3,4,8,9, 10 |
| (Piatanesi and Lorito, 2007) | Tide gauge data (nonlinear inversion method is used for retrieving slip distribution and the rupture velocity) | 1500 | - | South 5° N= 10 Max=30 (Aceh) 6.5-11 ° N=10 Northernmost 11-14 ° N =20 | - | 2.0-2.25 | 1,2,14 |

Table 2-2 Summary of sources and the characteristics deduced for the December 2004 earthquake.

2-4.3 Horizontal Movement and Vertical Movement Resulting from the 2004 Earthquake

Song et al. (2008) disputes the tuned displacement of the Titov et al. (2005) model on the grounds that it is overestimated by the GPS measurement and seismic inversion data. They use the horizontal impulse momentum for tsunami mechanism to achieve clarification. Song et al. (2008) state that it is not only the vertical dislocation of the seafloor in relation to the submarine earthquake that is the main source of tsunami generation, but that the horizontal impulse of the rupture was responsible for up to two thirds of the height of the tsunami detected from the satellite imagery over the open sea. A numerical model taking into account the additional horizontal effect yields a tsunami amplitude equal to that recorded by the Jason-1 satellite and the tide gauge data. Additionally, the kinetic energy of the tsunami was made up of approximately 30% from the vertically-forced tsunami height and 70% from the horizontally-forced tsunami. Vertical deformation alone is not enough to have generated the enormous 2004 Indian Ocean tsunami. The horizontal impulse of the faulting along the continental slope generated kinetic energy 5 times larger than the energy derived from the vertical dislocation. The asymmetrical tsunami pattern of leading-elevation waves towards Sri Lanka as opposed to the leading-depression wave pattern toward the Andaman Sea coast of Thailand is further evidence of a horizontally forced mechanism.

Because of the horizontal and vertical displacements, 2D shallow water theory is probably inadequate to represent the tsunami generation mechanism. Instead, the tsunami formation mechanism developed for 3D fault motions along continental slopes seems to be appropriate. Earthquake-tsunami models based on the seismically-inverted earthquake displacements and a 3D ocean model have been developed to cope with this horizontal component of displacement. Vertical and horizontal forcing induced by the quake can also be incorporated by treating the faulting along the continental slope as object movement in a fluid; the horizontal motion can, in fact, create greater tsunami heights and longer wavelengths than those induced by vertical uplift alone. The results of these analyses correlate very well with the leading wave heights recorded by Jason and Envisat satellites (Song et al., 2008).

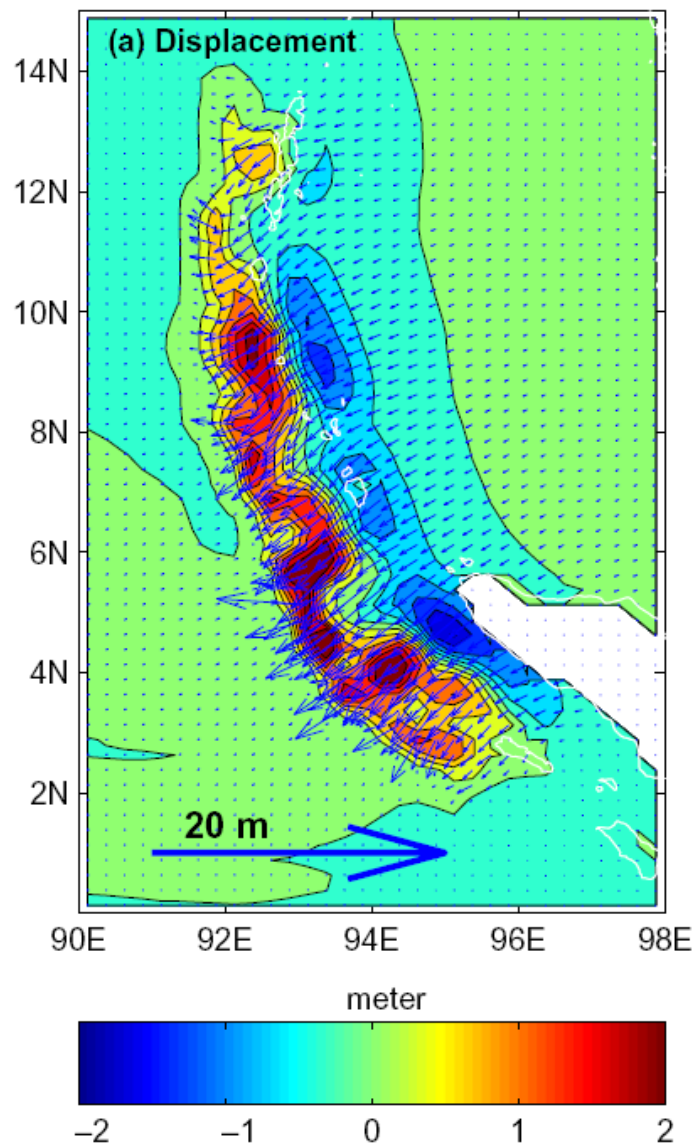


Figure 2-6 The 2004 earthquake uplift and subduction areas. Arrows show the horizontal movement of the seafloor while the colour contours show subsidence on the east and uplift on the west side of subduction zone (Song et al., 2008).

More evidence also shown by Vigny et al. (2005) estimated that Phuket Island had moved 34 m in 50 days following the Boxing Day earthquake, and Rajendran et al. (2007) reported that the South Indian Shield shifted eastward by 10-16 m; Car Nicobar Island was estimated to have moved 6.5 m in the southwest direction.

Rajendran et al. (2007) reported that the 2004 earthquake caused a 0.5-1 m uplift of North Andaman Island. The western margin of South Andaman Island rose approximately 1-1.5 m above its pre-earthquake level, while the eastern part of the

island sank by more than 1 m. The Nicobar and Car Nicobar Islands, south of 10° N, subsided by 1 - 3 m. Gahalaut and Catherine (2006) estimated that the co-seismic slip of the Andaman section was 3.8-7.9 m and 11-15 m for the Nicobar section, with vertical subsidence of approximately 0.5-2.8 m for the Andaman-Nicobar Islands. The overall horizontal displacement along the Andaman-Nicobar Islands is computed to be between 1.5-6.5m.

2-4.4 The Energy Released by the 2004 Indian Ocean Earthquake.

The Seismic Moment (M_0) and the Moment Magnitude Scale (M_w) are used here to compare earthquake intensity. The seismic moment is a measure of the size of an earthquake based on the area of fault rupture, the average [slip](#), and the force that was required to overcome the friction holding the rocks offset by faulting together [<http://earthquake.usgs.gov/learning/glossary.php?term=seismic%20momen>]. The scalar seismic moment M_0 is defined by the equation $M_0 = \mu Au$, where

- μ is the [shear modulus](#) of the rocks involved in the earthquake, typically 30 [gigaPascals](#)
- A is the area of the rupture along the [geologic fault](#) where the earthquake occurred, and
- u is the average displacement.

The 26 December 2004 Sumatra earthquake had a magnitude of 9.3 on the Richter scale and a Seismic Moment M_0 of $> 2 * 10^{23}$ N m (Ghobarah et al., 2006). Bilek et al. (2007) indicated that the spectral amplitudes for the Sumatra-Andaman earthquake are smaller than those of the 1960 Chilean earthquake by a factor of 1.5 to 3.0.

Initially, the M_0 of the 2004 earthquake was estimated to be $3.57 * 10^{22}$ N m ($M_w = 9.0$) based on the surface wave in the first 300 s only (Liu, 2005) cited in (Ji, 2005). Subsequently Stein and Okal (2005b) and Stein and Okal (2007) reported that M_0 was 2.5 times bigger than previously reported, as large as $1.3 * 10^{23}$ N m ($M_w = 9.3$) because the previous calculation had not accounted for the slow slip effect that was not initially observable from the surface waves. The 2004 Sumatra earthquake released energy of

4.3×10^8 J, equivalent to the total energy used by the US population over a period of 6 months.

2-5 Future Earthquake Generated Tsunami in the Indian Ocean Region.

The 2004 Indian Ocean earthquake caused the mega-tsunami which devastated several countries around the Indian Ocean region, including the Andaman coast of Thailand. This raises the question as to when such a strong earthquake and mega-tsunami will impact the region again. If these events are going to happen, when and how they are going to occur? What significant subsequent effects will they have on the coast of Thailand?

Though earthquake forecasting is not presently feasible, the potential for future earthquakes can be assessed from the seismic data and historical records of preceding earthquakes. Subarya et al. (2006) stated that the magnitude of an earthquake on a particular thrust increases linearly with the convergence rate and decreases linearly with the age of the subducting plate. Furthermore, the return period for an earthquake of a given magnitude is inversely related to the slip rate of the fault. Karlsrude et al. (2005) suggested that the recurrence period of the earthquake can be estimated from 1) the magnitude-frequency regression obtainable from available seismicity catalogues and 2) tectonic considerations. However, the tectonically-derived estimate is more accurate than that can be derived from the 36 years of earthquake records. From the 1964-1999 seismological data of the Sumatra Trench, it can be inferred that the return period of the earthquake of $M_w = 8.5$ is 195 years, and for the $M_w = 9.3$ is 1140 years. The seismicity is quite low for the Java Trench, for which the return period is approximately 260 years for the $M_w = 8.5$ event. Peterson et al. (2007) suggest from their models that a large earthquake with $M_w > 9.2$ occurs every 256 years along the Sumatra Subduction Zone.

Some parts of the active zone between the Indian Plate and the Sunda Microplate have not experienced a large earthquake in the past 150 years (Ioualalen et al., 2007; Stein and Okal, 2005b). Moreover, McCloskey et al. (2005) reported that the northern section of the Sumatra Section of the zone has not experienced a large earthquake in the past 100 years.

The 2004 Indian Ocean earthquake was the result of the accretion of strain. The stresses caused by the 2004 Indian Ocean earthquake and the 2005 Nias earthquakes may spread further south, enhancing the earthquake hazard for the nearby fault segments in the near future (McCloskey et al., 2005). Moreover, Vigny et al. (2005) believe that the 2004 earthquake shook only some of the Sunda Subduction Zone, causing stress increase on the adjacent segments further south on the Sumatra Trench and further north on the Arakan Trench in Myanmar.

Subarya et al. (2006) suggested that the total seismic slip released by the 2004 earthquake would result in a repetition of the event and that a tsunami would happen again in the next 230 to 600 years. However if 50% of the slip is aseismic, or taken up by smaller events, the return period would range from 460 to 1,200 years. Chlieh et al. (2007) estimated the return period of the earthquake equivalent to the 2004 event, if the stress of the 2004 earthquake was totally released, between 140-420 years. In addition, Borrero et al. (2006) studied paleo-seismic data for this region and concluded that great earthquakes recur approximately every 200 to 240 years along the Sunda Subduction Zone.

The 2004 earthquake is considered to have increased the chance of seismic hazard on the nearby segments of the subduction zone, especially at the north end of the rupture. This research will focus on the north end of the 2004 rupture including the Arakan Section, the Andaman-Nicobar Section and the northern part of the Sumatra Section.

2-5.1 The Arakan Section

Prior to the 2004 event, there had been little concern about the subduction in the Northern Bay of Bengal and along the Myanmar coast (Figure 2-3) although the tectonic environment, the stress, the strain and the historical earthquake activity of the area are indicators of a high seismic risk: a large mega-thrust earthquake and the succeeding tsunami wave generated off the coast of Myanmar would threaten a large population (Cummins, 2007). For example, the 1762 tsunami following from a magnitude 8.5 earthquake on the Arakan fault was modelled using 10 m of uplift and subsidence, a 700 km length rupture (from Chittagong to Foul island) and a width of 125 km where the seismogenic zone is extended offshore beneath the Bengal fan. A

recurrent earthquake of this magnitude would have severe effects on the population of Chittagong and the Northern Bay of Bengal (currently 60 million).

Cummins (2007) also reported that the deformation front of the Arakan Section (Arakan Fault) is located at the Ramree islands ($\sim 20^\circ \text{N}$), whilst the Chittagong-Tripura fold belt is an active feature related to the subduction of the India Plate beneath the Burma Microplate. For the Arakan Section, the extension of the seismogenic zone beneath the Bengal fan, about 200-300 km westward of this boundary, has major implications for earthquake and tsunami risk. Compared to the north of the Andaman-Nicobar Section (Andaman Trench), the convergence of the Bay of Bengal rupture is less oblique and might yield shorter recurrent times (a few hundred years) for large thrust earthquakes.

Moreover, much of the Bay of Bengal has 2-10 km of sediment covering the upper surface and is the world's largest submarine fan system. The Bengal fan insulates the underlying rocks; the thick sediments create thermal conditions that cause significant up-dip extension of the thermal regime required for seismogenesis. In addition, the entire 900 km length of this area, stretching from the northern end of the Andaman-Nicobar Section to the northern tip of the Bay of Bengal, has the potential for generating tsunami earthquakes. The southern rupture extends to Foul Island ($\sim 17^\circ \text{N}$), and reaches Ramree Island ($\sim 20^\circ \text{N}$) and may extend to Chittagong at the northern end, where evidence was reported of 60 sq miles of submerged land. By locking the Arakan Section, the subduction zone could generate $M_w = 8.5$ earthquakes every 100 years, and an $M_w = 9.0$ event every 500 years. Moreover, due to the rapid rate of sedimentation in the Bay of Bengal, submarine landslides could also cause tsunamis in this part of the Indian Ocean (Cummins, 2007).

2-5.2 The Sumatra Section

Chlieh et al. (2007) reported that the subduction zone beneath the Sumatra Section has generated several major earthquakes in the past two hundred years, including the M_w 8.5-9.0 tremor in 1797, the $M_w \sim 8.5$ event in 1861 at the Nias Segment, and the M_w 8.7 earthquake on 28 March 2005 (Figure 2-3 and Table 2-1). Nalbant et al. (2005) reported that an earthquake similar to that in 1833 might happen every 230 years; however, there is no historical record of any strong earthquake in the section further

south. So, the chance of a great earthquake along the southern part of the 2004 rupture zone that could cause a great and dangerous tsunami still remains.

For the southern end of the Sumatra Section, the $M_w = 8.7$ Nias earthquake in March 2005 was triggered by the 2004 earthquake. Strain has been added on the transform faults behind the subduction, both along the Sumatra Fault and on the Sagiang Fault in Myanmar. The risk of significant earthquakes in the near future is therefore very high, as seismic strain has been released as a consequence of the major earthquakes recorded on both the Sumatra and the Sagiang Faults. Stress transfer has possibly been recognised as the activating factor for earthquakes on adjacent faults (Vigny et al., 2005).

The 2004 earthquake rupture did not progress immediately to the south-southeast along the Sumatra Fault, due to a barrier that blocked the rupture front, but the stress was transferred to the south increasing the stress on that section. This barrier broke 3 months later with the $M_w = 8.7$ earthquake of 28 March 2005 and arouses fears that a domino effect of highly-stressed plate boundaries to the south and east may follow (Bilham, 2005; Kruger and Ohrnberger, 2005; Stein and Okal, 2005b). This could take place as a megathrust event which may affect the northwest coast of Australia. Borrero et al. (2006) agrees with this conclusion when reporting that the section of Sumatra coast southeast of the 2004 subduction event is one of the most dangerous regions where a tsunami may strike in the near future. It is a densely populated region, with more than 1 million people, so that the risk of any future tsunami poses a great danger.

Engdahl et al. (2007) reported that increased seismicity occurred at the northern end of the rupture limit of the 1797 and 1833 earthquake (around Siberut and Mentawai Islands) earthquakes as well as at the southern end of the 1861 event around Nias Island (Figure 2-3, Figure 2-4 and Table 2-1). Nalbant et al. (2005) suggests that the paleo-seismological data gives an indication that the Mentawai segment of the boundary is a good candidate for triggering failure (Figure 2-3 and Figure 2-4). McCloskey et al. (2008) indicates that paleo-geodetic evidence reveals that the rupture beneath Siberut Island may give rise to a mega-earthquake for the Sumatra Section, as it has been locked since 1797 and is thus well advanced in its seismic cycle; no mega-earthquake has been generated beneath Siberut Island since 1797 (Figure 2-3). (Figure 2-3) Dewey

et al. (2007) states that the 1833 rupture of the Sumatra Segment has remained dormant after the 2004 earthquake; this segment is seen as a candidate for a future great underthrust earthquake. According to the model simulations by McCloskey et al. (2008), the future rupture of the Mentawai segment (Figure 2-3 and Figure 2-4) may have less effect on the coast of Thailand, and the Indian coast than that of the 2004 event, as the orientation of this segment will propagate most of the energy towards the southwest. Moreover, Sumatra and the adjacent Islands will obstruct tsunami waves propagating to the north and east.

Karlsruhe et al. (2005) suggest that it is possible that an $M_w < 8.5$ earthquake might occur along the Sunda Subduction in the next 50-100 years causing a tsunami to hit the Andaman coast of Thailand. An earthquake of this magnitude would produce a tsunami with run-up of 1.5-2.0 m above mean sea level along the Thai coasts (2.5-3.0 m wave height during high tide). An $M_w > 9.0$ earthquake similar to the 2004 event on the Sumatra Subduction Zone and a resulting mega-tsunami that damages the Thai Andaman coasts is not likely to happen within 400 years of the 2004 Indian Ocean earthquake and mega-tsunami, since the 2004 rupture covered the whole subduction area up to the Andaman Islands, and released the entire accumulated energy and stress. However, should it occur, it would be at high and undesirable risk to human life and property.

Stein and Okal (2007) conclude that the real 2004 earthquake magnitude either $M_w = 9.3$ or $M_w = 9.0$ is not the most important issue. The important point is that the entire aftershock zone ruptured. Sinadinovski (2006) questions whether the entire stress on the plate boundary north of the Sumatra Section has been released or whether it is still accumulating, in which case it will be released at some future date by a megathrust earthquake, causing a subsequent significant tsunami. It can therefore be assumed that Thailand, Sri Lanka and the Bay of Bengal will be the main targets of future direct tsunami impact.

This research is directed towards tsunamis that might affect the coast of Thailand. On the basis of the foregoing, the Andaman-Nicobar Section and the northern part of the Sumatra Section of the Sunda Subduction Zone are used in the model simulations.

2-5.3 The Andaman-Nicobar Section

The 2004 Sumatra-Andaman earthquake is considered to have increased the chance of seismic hazard on the nearby segments of the 2004 subduction zone, especially at the north end of the rupture (Rajendran et al., 2007). They suggested from the historical data that the return period for large earthquakes in the Andaman Segment is at least 250 years. If all the strain built up on the northern part of the Andaman-Nicobar Section has been released during the 2004 rupture, this section might be free of earthquakes and tsunamis for the next 400 years (Stein and Okal (2005b). On the other hand, the southern part of the 2004 rupture (the Sumatra Section) may be at risk of a significant earthquake and tsunami since the southern part of the rupture only partially slipped. Karlsrude et al. (2005) indicated that the likely source for a future tsunami on the Andaman coast of Thailand is a major shallow earthquake on the Andaman-Nicobar Section; they also concluded that a mega-thrust earthquake and tsunami are not likely to occur in the next few hundred years. As a result, the tsunami risk along the Thai coast in the next 50-100 years is likely to come from a $M_w = 8.5$ event occurring along a critical area of the Andaman-Nicobar Section.

With the movement between the Indian Plate and the Sunda Microplate of about 40 mm/y in a 20° N direction and the movement between the Indian Plate and the Australian Plate of around 50 m/y in an 8° N direction, the combined return period for a $M_w > 8.5$ is estimated to be 200 years for the Nicobar segment and 270 years for the Andaman segment of the Andaman-Nicobar Section of the plate boundary (Ioualalen et al., 2007). For an average subduction rate of 30 mm/y the return period of $M_w = 8.5$ would be 200 years for the Nicobar segment and 430 years for the Andaman segment (Karlsrude et al., 2005). This is in agreement with Pietrzak et al. (2007), where it is stated that for the north end of the 2004 rupture (the Andaman-Nicobar and Arakan Sections; offshore Myanmar and the Arakan Trench), elastic build up constitutes a significant component of the relative motion between the Indian Plate and the Sunda Microplate, so that it is likely that a $M_w = 8.5$ quake will be generated over the period of 100 years and may result in a $M_w = 9.0$ every 500 years. For $M_w = 8.0$, the return period is estimated to be 95 and 150 years for the Nicobar and Andaman segments of the Andaman-Nicobar Section, respectively, with a combined return period calculated to be 60 years (Karlsrude et al., 2005).

| Document | Return Period of the Andaman-Nicobar Section (years) | | |
|-------------------------|--|--|---|
| | Overall Section | Andaman Segment | Nicobar Segment |
| Rajendran et al. (2007) | - | 250 | - |
| Stein and Okal (2005) | > 400 | - | - |
| Ioualalen et al. 2007 | - | 270 ($M_w > 8.5$) | 200 ($M_w > 8.5$) |
| Karlsruhe et al. (2005) | - 60 ($M_w = 8.0$) | 430 ($M_w = 8.5$) 150 ($M_w = 8.0$) | 200 ($M_w = 8.5$) 95 ($M_w = 8.0$) |
| Pietrzak et al. (2007) | - | > 100 ($M_w = 8.5$) > 500 ($M_w = 9.0$) | - |

Table 2-3 Estimated Return Periods of Earthquake along the Andaman-Nicobar Section of the Sunda Subduction from various documents.

Chapter 3 The 2004 Indian Ocean Tsunami Incident and its Consequences in Thailand

The 2004 earthquake resulted in a rise in sea surface on the west side of the rupture, and a lowering of the sea surface on the east side (bipolar geometry). The wave crest radiated outwards to the west, whilst a wave trough (depression) spread out to the east. Along the eastern side of the rupture, the large depressions of the propagating tsunami wave travelled directly towards the Andaman coast of Thailand (Pietrzak et al., 2007) followed by crest which hit the Andaman coast of Thailand ~2 h after the earthquake, causing severe geomorphologic changes and destruction (Ghobarah et al., 2006; Kruger and Ohrnberger, 2005; Liu, 2005; Purnachandra, 2007; Subarya et al., 2006).

3-1 Topography and Tsunami Characteristics

Tsunami run-up heights along the coastal area of Thailand varied by almost a factor of three; the waves which hit Patong Beach broke very close to the shore in the form of a plunging breaker due to the steep offshore bathymetry and then broke into tongues of water which ran through the community after hitting the beach (Chatenoux and Peduzzi, 2007). Tsunami prone areas are far more likely to suffer damage where the waves can attack from two sides (Synolakis et al., 2005). In Thailand, the Namkhem Fishing Village was one of the most severely destroyed areas, as it was attacked by waves from the Pak Ko Canal to the north-northeast and from the beach to the west. The Pakarang Cape, situated south of Namkhem, was also attacked by waves from two directions; directly from the south and by the refraction wave from the north. At Phi Phi Island, a popular tourist spot, the tsunami struck twice due to the local geography. The island comprises two pocket beaches separated by a tombolo. The tsunami waves first hit the west side, then refracted and diffracted into the north-facing side before reaching the south-facing beaches (Ghobarah et al., 2006). Most of the fatalities resulted from the debris removed by the first wave and carried back by the second. From this, it is clear that it is vital to relate both the topography and the nearshore bathymetry of each coastal area to the consequences of the tsunami.

It was very difficult to escape the tsunami waves that penetrated 3 km inland over the flat plain at Banda Aceh. In the Khao Lak coastal area of Thailand, the tsunami wave

penetrated 1.0-1.5 km inland, where it was held at the foot of the hill (Synolakis et al., 2005). Ghobarah et al. (2006) pointed out that the surrounding topography of elevated ground and hills in the Khao Lak area, restrained the water level. This resulted in a tsunami-safe zone beyond 1.5 km inland. Before the 2004 tsunami, channels and stream openings along the coastline at Khao Lak were narrow and blocked by deposits of beach sand. After the tsunami the river channels and streams changed their planar form to a wedge shape. Stream openings also opened up to widths of 50–200 m.

3-2 Tsunami Wave Height and Speed

The tsunami waves, generated on 26 December 2004, arrived at high tide on the southwest coast of Thailand 1 h 30 min to 2 h after the initial earthquake. Ioualalen et al. (2007) reported that the first tsunami wave arrived at the coast of Thailand as a large depressed wave 1 h 45 min to 2 h after the initial tremors and caused a withdrawal of the sea at the coast. A resurgent bore followed, reaching up to 8 m in height. Data from the tide gauge at Tapaonoi Island, southwest of Phuket, confirmed that the tsunami reached the coast as a negative wave, with the sea level dropping to a level corresponding to normal low tide for 20 min. This was followed by 2 successive wave crests. Subsequently, the sea surface continued to oscillate for the rest of the day (Dalrymple and Kriebel, 2005).

Tsunami wave heights along the mostly flat plain of the Andaman coasts of Thailand reached 5–8 m above mean sea level, with the maximum height at ~12-14 m recorded at Khao Lak (Hori et al., 2007; Kelletat et al., 2007; Tsuji et al., 2006). The wave run-up height at Namkhem Fishing Village was 7-8 m, at Pakarang Cape 5-7 m, and at Bang Niang Beach, it was 10-12 m (Thanawood et al., 2006). Kelletat et al. (2007) reported that the fourth wave to strike rose on top of the third wave and caused the maximum run-up height (in excess of 10m) at Khao Lak. Chaimanee and Tathong (2005) also reported a tsunami wave height at Khao Lak ranging from 6 to 10 m. The maximum run-up height was generally found closer to the shoreline and dropped as the waves moved further inland due to the friction caused by the vegetation and man-made structures.

Across the Thai coastal area tsunami run-up varied by a factor of almost three, from 4 m high at Nai Yang beach to approximately 11 m in the Khao Lak tourist region of

Phang-nga province. At Khao Lak the wave reached the roof of three-storey buildings, which is approximately 8 m in height (Ghobarah et al., 2006). Madsen and Fuhrman (2007) reported that the tsunami waves in 12 m water depth off Phuket Island (recorded by echo sounder onboard the Yacht Mercator off Naihan Bay, southwest Phuket) were composed of 3 main waves, the first of 6.6 m height, the second at 2.2 m and the third at 5.5 m, with wave periods of approximately 13-14 min.

Dalrymple and Kriebel (2005) reported that the tsunami wave broke far offshore in the Khao Lak area, and reached the coast as a vertical wall of water at a high speed of around 11 to 17 m/s (40-60 km/h) while the tsunami speed in the nearshore zone of Phuket and Khao Lak areas of Thailand slowed to 5.5-11 m/s (20-40 km/h) when it reached the land (Ghobarah et al., 2006). Warnitchai (2005) reported that the tsunami flow depth at Khao Lak was approximately 7-8 m, with a wave velocity of around 6-8 m/s, producing a dynamic pressure of 20-30 kN/m².

3-3 Tsunami Effects and Devastation

3-3.1 Natural Geomorphologic Changes

Tsunami action results in great changes to coastal areas, especially in terms of physical change to the coastal landscape and sedimentation. The extent of the damage from the 2004 tsunami varied with distance (Rajendran et al., 2007). Geomorphologic changes, for example beach erosion and the enlargement of stream openings, were observed along the Andaman coast of Thailand.

Tsunami deposits ranging from 10 to 70 cm thick are to be found from the coast of India to the Andaman and Nicobar Islands. The characteristics of the 2004 tsunami sedimentary deposits provide useful recognition criteria for comparative historical events. Furthermore, scouring of the beaches and river banks, as well as deposits of sand and debris found inland provide evidence of the inundation pattern resulting from the tsunami pattern on land (Rajendran et al., 2007). Kelletat et al. (2007) point out that the tsunami wave washed out beach sediment and deposited it inland. These sediments are composed of quartz, feldspar and mica and covered the soil and grass. Heavy minerals are also found as stratified layers. Brown mud originating from the deep offshore zone was identified on land. Beach sand sediments along the Andaman coasts

of Thailand were removed by the tsunami waves and carried landward to be deposited in the inundation zone. In the Khao Lak area, beach sand and vegetation were eroded by the tsunami waves. Sediment in the tidal creeks and streams was flushed landwards by the incoming wave run-up, and then the receding wave later moved the sediments and floating debris back towards the sea. The seaward flow of the receding wave generally moved down the streams with high velocity. Later, sediment transported by these receding waves was deposited in the nearshore zone (Dalrymple and Kriebel, 2005).

Hori et al. (2007) concluded that some topographic features, notably scarps and slopes, controlled the distribution of the tsunami sediments in the Khao Lak area, as no tsunami sediments were deposited on the upper part of the slope below terraces and high ground. Tsunami sediment from the 2004 event covered the low-lying coastal plain of Khao Lak and extended more than 1 km inland. However, sediment thickness in this area did not clearly decrease landward as would normally occur in tsunami sediments deposition. Deposition of tsunami sediment further inland was halted by the steep slope and terrace scarp behind the coastal plain, resulting in large amounts of sediment being deposited along the front of these vertical hillsides. Thick sediments were also deposited in depression areas. Along one transect at Namkhem Fishing Village, fining-upward sediment and multiple layer deposits were found as was to be expected. However, the basal sediment shows the fining landward characteristic, as the grain size of basal deposition was influenced by the power of the up-flow waves. Multiple wave action represented by layers of coarse-grained sediment overlain by fine-grained material was found in some locations (Hori et al., 2007). Mollusc shell fragments are commonly found in coarse-grained tsunami sediments in Khao Lak, suggesting that the sediments came from the beach and shallow sea bottom (Hori et al., 2007).

Khao Lak is one of the most attractive tourist beaches in Thailand and long-term loss of the sand from the beaches is detrimental to the tourism industry. However, beaches along Khao Lak initially recovered within a month of the tsunami attack and now most beaches show no obvious damage from the tsunami. It can be inferred from this that nearshore and offshore sand is the significant source of the beach sand refilling the eroded beaches. Some re-deposited sediment may be transported from the tidal creeks and streams and carried back to be deposited on the beach after the tsunami event.

However, some parts of the beach along this area, for example the Pakarang Cape, located north of Khao Lak, were severely destroyed, and have taken a long time to recover (Dalrymple and Kriebel, 2005).

The 2004 tsunami diminished soil and water quality and destroyed coral reefs, sea grass beds and beach forests along the Andaman coast of Thailand (Thanawood et al., 2006). Beach erosion and damage to coral reefs were reported in several areas. Agricultural land as well as groundwater and subsurface ponds were intruded by saltwater.

3-3.2 Loss of Life and Physical Damage to Property

The 2004 earthquake caused severe destruction to the countries located around the Indian Ocean. The earthquake itself caused severe damage to the areas adjacent to the epicentre, e.g. Sumatra and the neighbouring islands and also on distant islands and coastal zones around the Indian Ocean. The earthquake damaged many structures in western and Northern Sumatra, the Andaman and Nicobar Islands of India. The shift of the ocean floor created a tsunami that affected 19 countries, causing more than 300,000 deaths and destruction in 12 countries including Indonesia, Sri Lanka, India, Thailand, Somalia, the Maldives, Malaysia, Myanmar, Tanzania, the Seychelles, Bangladesh, and Kenya (Ghobarah et al., 2006; Liu, 2005). Compared to other tsunamis during the period 1992-1998, which resulted in 3,000 deaths (including the disastrous tsunami in Papua New Guinea in 1998 that caused 2,100 fatalities), the destructive power of the 26 December 2004 tsunami was that of a mega-tsunami. The number of victims of the 2004 tsunami is more than that of all other tsunami fatalities in the past 300 years combined (Synolakis et al., 2005).

More than 230,000 were reported dead or missing in Indonesia, and there were more than 50,000 fatalities in Sri Lanka and India (Liu, 2005). In Thailand, there were 5,395 deaths, with 2,822 missing and unaccounted for. The worst-affected part of the Andaman coast of Thailand was Phang-nga province (which includes Khao Lak) (Thanawood et al., 2006). At Khao Lak, there were 4224 fatalities with 5597 injured and 1733 missing people. The fatality to Thai nationals was almost equal to that foreign dead. In addition, there were approximately 5000-7000 of dead and missing Myanmar workers in Thailand (Jonathan et al., 2008).

In Khao Lak, the extensive damage and loss of life resulted from its low-lying coastal plane, which permitted the development of a high turbulent bore that travelled almost 1.5 km land inwards (Dalrymple and Kriebel, 2005). Loss of life and the property damage in Khao Lak was exacerbated by the restriction caused by the surrounding elevated ground and hills that served to strengthen the receding tsunami wave (Thanawood et al., 2006). At Bang Niang Beach in Khao Lak, a 10-12 m tsunami wave inundated and destroyed beachfront hotels, resorts and infrastructures. More than 200 guests, especially those tourists staying in ground-floor rooms of the seaside hotels and resorts adjacent to the beach, lost their lives.

Both luxury hotels and local fishing villages close to the seashore were destroyed. Tsunami waves washed away and destroyed many fishing boats. They demolished culture ponds along with aquaculture infrastructures and facilities (Thanawood et al., 2006). In contrast Dalrymple and Kriebel (2005) reported only minor building damage at Patong Beach, Thailand, where tsunami run-up was 2-3 m; only the beachfront structures were damaged and most places recovered within a week. The tsunami wave that hit Patong Beach broke very close to the shore as a plunging breaker due to the steep offshore bathymetry. Most of the major seaside buildings and infrastructures, for example Phuket airport, bridges and roads, survived the tsunami.

The extent of building damage and the degree of devastation as a result of the tsunami was also dependent on construction type and strength of the buildings located in its path. Ghobarah et al. (2006) described the demolition of engineer-designed and non-engineer-designed structures in the tsunami-affected areas of Thailand. The structures suffering the most damage on the coast of Thailand were wooden, residential houses with tile or corrugated steel sheet roofs. Non-engineer-designed buildings, such as wood-framed structures and straw houses, were totally destroyed by the 2004 tsunami in most areas. On the other hand, well-designed and reinforced concrete buildings with good foundations survived the tsunami waves; reinforced concrete hotel buildings, situated on the isthmus of Phi Phi Island, were not structurally damaged by the tsunami waves, as the building foundations were well-designed and strong enough to withstand the scour of the receding waves. However, most wooden structures in that area were absolutely devastated. Loss of support for the structural foundations was generally

observed in the areas where wave run-up exceeded 8 m, such as there at a three-story resort in Khao Lak.

Chapter 4 Numerical Modelling of Tsunami Propagation and Inundation Forecasting.

Tsunami waves are characteristically long waves, for which the wavelength is much longer, and the wave amplitude significantly less, than the water depth; they act as linear waves, except during the run-up process in the vicinity of the coast (Karlsruhe et al., 2005; Segur, 2007). Therefore, a depth-averaged linear numerical model is used to study tsunami generation and propagation in deepwater. Non-linear wave interactions, wave breaking actions and energy dissipation are needed to predict the dynamics of tsunami waves in the nearshore area, and are necessary to obtain a deep understanding of the specific tsunami pattern (Geist et al., 2007).

Tsunami propagation and inundation patterns and the degree of damage are the result of complex interactions between the moment release, the slip distribution, local and regional bathymetry (McCloskey et al. (2008). Tsunami modelling deals with the correlation of submarine earthquake ruptures, seafloor deformation, tsunami wave amplitude in the open ocean, tsunami wave propagation and inundation based on seafloor topography. Numerical modelling is one of the most significant tools to determine a trustworthy tsunami risk zone map, tsunami evacuation route maps, a tsunami safety shelter plot and tsunami mitigation plans for the future. There are 3 major numerical tsunami models used for the simulation of tsunami propagation and inundation: Cornell Multi-grid Coupled Tsunami Model (COMCOT) developed at Cornell University, the Method Of Splitting Tsunami (MOST) the computational model developed originally by the University of Southern California, and TSUNAMI N2, the model developed at Tohoku University (Liu, 2005).

The TSUNAMI N2 model, which is now widely employed for simulation of tsunami patterns, was modified from the TUNAMI N2, developed by Shuto and Imamura. TUNAMI N2 is a model based on long wave theory by means of very small ratio of water depth to wavelength in shallow water (Singh et al., 2008). The model has the potential to simulate reflecting boundaries for fixed coastlines. In the open ocean boundaries, free outward passage of the wave can be calculated; the boundary between the wet and dry points is judged by the total depth (Imamura, 1996). Usha et al. (2006), citing Imamura (1996) and Koshimura and Mofjeld (2009), state that a finite difference

code of TUNAMI N2 was utilized to forecast tsunami propagation and inundation on dry land. The model provides includes the numerical code, with a manual, for developing hazard maps of each area incorporating with tsunami mitigation plan.

The COMCOT model adopts the finite difference method to solve linear and non-linear shallow-water equations. It was used to generate tsunami propagation in the entire Indian Ocean; it is necessary to include the nearshore bathymetry and inland topography, since these factors are determinate for the direction of wave propagation and the flow pattern inland (Liu, 2005) as does the MOST model.

The MOST model, the model used in this dissertation, is described below.

4-1 Wave Propagation Modelling

The tsunami wave is initiated by the disturbance of the ocean floor but, after the initial disturbance, the tsunami motion is governed by a linear wave equation. A practical model for this stage of the wave would be a linear wave equation with varying seawater depths. Geist et al. (2007) indicated that tsunami modelling begins with a limited data set for earthquake ruptures, primarily moment magnitudes and hypocentre locations. Fault geometry, average slip and rupture are additional source parameters needed for tsunami modelling and sub-fault parameterisations are needed to forecast tsunami heights and inundation patterns. Primary source parameterisation is then, when available, refined based on data from Deep ocean Assessment and Reporting of Tsunamis (DART) buoys. Following on from this stage, the refined source is used to recalculate the propagation.

Geist et al. (2007) states that a tsunami forecasting system is composed of a pre-computed propagation database supplemented by water level data assimilated in real time. Data, acquired from the DART stations, can be used as primary inputs. Sea level observations from DART are applied to estimate the slip distribution of the tsunami earthquake. Geist et al. (2007) also pointed out that the linear term is the most important component of the equation for computing vertical displacements and offshore tsunami amplitudes. Variable degrees of slip can be allocated to each unit source and several unit sources are combined to determine the tsunami wave field for an earthquake of any given magnitude and sub-fault slip distribution. Consequently, the

propagation database is calculated as a function of location and propagation time from a specific unit source. To calculate tsunami wave propagation in the open ocean, the linear wave equation splits into 2 sets of waves propagating in different directions. For the 2004 Indian Ocean tsunami, the negative leading wave propagated eastward towards Indonesia, Thailand, Myanmar and Malaysia. The first wave to reach India and Sri Lanka was a positive wave that flooded the coastal areas, and this was followed by a large negative wave. However, the positive volume and the negative volume were far enough apart in both time and position to be treated as two separate waves (Segur, 2007).

4-2 Wave Inundation Modelling

A linear wave propagation model adequately describes the progress of the 2004 tsunami wave propagation until it reaches the shallow coastal zone. There the tsunami wavelength becomes shortened and its amplitude increased as the tsunami wave changes shape. The linear model then fails, becoming infinite as the wave amplitude develops. In the near-shore non-linear terms becomes dominant, so a non-linear long-wave model is used (Segur, 2007).

The forecasting of the run-up height of a tsunami wave is strongly related to nearshore wave propagation effects. Reliable inundation modelling depends on the accuracy, availability and horizontal resolution of the nearshore bathymetry and coastal topography which, unfortunately, are not available for most coastal areas, especially in the tsunami-prone regions around the Indian Ocean. Small-scale variations in nearshore topography may yield great differences in the run-up pattern and turbulent dissipation in the shallow continental shelf zone during the tsunami wave propagation may affect tsunami run-up heights to different degrees. For example, the broad continental shelf and the complicated bathymetry of the Thailand and Myanmar coastlines have huge effects on the run-up and the propagation of tsunami waves in this region.

Run-up prediction from numerical models is the most underdeveloped part of tsunami forecasting due to a) the lack of fine-resolution bathymetry and topography (10-50 m horizontal resolution), and b) accurate field measurements for validation. However, when such high quality data bathymetry and topography are available, MOST model

simulations are believed to be accurate enough to develop inundation maps and to assist in developing tsunami mitigation measures (Titov and Gonzalez, 1997).

4-3 MOST (Method Of Splitting Tsunami) Numerical Model

Titov and Gonzalez (1997) stated that real-time tsunami forecasting can work through a combination of data from tsunami detection buoys (DART) and the use of the Method Of Splitting Tsunami (MOST) numerical model. However for validation, the results of numerical modelling should be tested using (large-scale) laboratory modelling and field data (Liu, 2005; Synolakis et al., 2005). Tsunami inundation distance and run-up heights need to be compared with field measurements from the past tsunami events. The 2004 event provides an excellent opportunity to do this for the MOST model and waves along the Khao Lak coast.

The MOST model is a hydrodynamic model used for simulating tsunamis generated by submarine earthquakes, replicating tsunami propagation across the open ocean and estimating tsunami inundation on land. The model is based on a finite difference numerical approximation to the non-linear shallow water wave equation. The MOST model uses the dislocation field from the seismic deformation model to initialize the hydrodynamic computations. It allows for the crustal deformation from the earthquake, and computes wave generation and inundation on dry land over the newly deformed bathymetry and topography (Borrero et al., 2006). MOST modelling is carried out in three phases: deformation, propagation and inundation. First, the initial deformation state is generated by simulating the seafloor uplift and subsidence ascribed to the seismic event. Uniform slip on one or several sub-faults is assumed to be the initial condition for tsunami propagation (Geist et al., 2007).

The MOST model allows the rupture zone to be divided into sub-faults, each with its own distribution of vertical displacement (both positive and negative) across the fault (each sub-fault is 50km wide*100km long). However the model is limited in that it does not include any time dependence in displacement of the sub-faults; the model assumes all are displaced at the same moment. For the 2004 earthquake the total time for the rupture to propagate its northern end extremity was ~500 s. Slow slip in the hour

following the earthquake is also believed by several authors to have contributed to the severity of the tsunami.

To simulate a tsunami scenario with the MOST model, all three phases need input data that includes 1) the size and distribution of seafloor displacement triggered by the seismic event (deformation phase), 2) gridded bathymetry data for the propagation phase and 3) gridded Digital Terrain Models (DTM) including bathymetry and topography of the coastal zone for the inundation phase (Borrero et al., 2006). To develop reliable outcomes from the MOST model, accurate detailed bathymetry and topography and precise earthquake event sources are essential inputs.

4-4 ComMIT (Community Model Interface for Tsunami)

ComMIT is a community interface for the MOST model, developed by PMEL/NOAA and funded by USAID. MOST and ComMIT are non-commercial models, available with source code and documentation free of charge, for use by the scientific community. It can be used to develop tsunami inundation maps for coastal communities. Scientists can access the modelling tools with an internet-enabled interface. This interface allows for sharing of databases and of model results. Tsunami models can be run for tsunami forecasting and hazard assessment, using data from local and remote databases. ComMIT provides an interface that permits users to select flexible input to the model and acts as a platform to show the output as a graphical user-interface. ComMIT has been written in the Java programming language, using the Network Common Data Format (NetCDF) for model input, and can be run on MS WINDOWS, MAC OS and UNIX. Input parameters of the model are read from simple ASCII text (<http://nctr.pmel.noaa.gov/model.html>).

4-5 Numerical Tsunami Forecasts for the Indian Ocean and the Thai Coast

The MOST model has been used to simulate the tsunami pattern and to calculate tsunami heights and arrival times (e.g. Liu, 2005; Titov et al., 2005; Geist et al., 2007) for the 2004 Indian Ocean tsunami. The results show that there are some discrepancies between the numerical results and the tide-gauge data in both the arrival times and the

wave heights. The model predicts the correct phase of leading waves toward Sri Lanka when compared with data from Jason and Topex/Poseidon satellites' images, and the tide-gauge data of Sri Lanka and the Male (Maldives); wave heights at Colombo and Gan correspond very well to the measured data but are over-predicted at the Male. The arrival time of the leading waves was 10-20 min before those calculated using the model. The numerical results match very well with the tide gauge data when applying the low grid resolution (2 min) with the complexity at the Maldives (Liu, 2005; Titov et al., 2005).

Geist et al. (2007) compared the wave heights from different tsunami prediction scenarios with the observed heights of the 2004 tsunami around the Indian Ocean. An earthquake of magnitude M_w 9.4 was used as the source for the wave propagation calculation. In most areas the modelled tsunami wave heights are equivalent to the observed mean regional and local tsunami run-up amplitudes, except for those in line with the main lines of propagation of the tsunami, for example Sri Lanka and Thailand, which were underestimated. It also underestimated the tremendous run-up at Banda Aceh, due to the unforeseen high slip along the southern part of the rupture zone; the Geist et al. (2007) study used ~ 9 m. When they used a higher slip (16 m) this resulted in the over-predicted of results everywhere, except for Banda Aceh.

Geist et al. (2007) recommend that a small scale finite-difference grid is needed to compute numerical tsunami inundation models for specific sites. Also, Vallee (2007) suggests that the merging of different datasets is useful for the numerical modelling of tsunami inundation. Highly detailed bathymetry is also of significant value for the distant propagation since tsunami refraction, trapping and refocusing in the distant area also depend on the bathymetry of the source location. For instance, tsunami propagation towards the Seychelles and the Oman Islands was controlled by refraction, trapping and refocusing of the tsunami waves at the Maldives (Kowalik et al., 2007).

Another reason for the discrepancies between modelled and observations can be the uncertainty in the fault-plane mechanism. The initial impact of the 2004 tsunami, using free-surface profiles based on a NOAA fault-plane mechanism, was overestimated especially on the Sri Lankan and eastern coasts of India. This was due to the excess energy computed by the NOAA fault-plane mechanism as well as the effect of the

spread of the rupture further north. Numerical modelling of the tsunami based on this mechanism would have predicted severe damage to the Sri Lankan and Indian coasts. By contrast, the simulations based on the USGS fault-plane mechanism considerably underestimated the tsunami amplitudes for both countries (Liu, 2005).

Borrero et al. (2006) used the MOST model to study inundation areas and flow depths for the western Sumatra tsunamis in 1797 (Padang) and 1833 (Bengkulu), using a system of 3 nested, geophysical coordinated, rectangular grids. Regional scaled areas were modelled using 1200 m and 600 m coarser outer grids while the area of interest was modelled at 200 m resolution. Their results matched with the report that stated that a large vessel was carried roughly 1 km inland into the town, and a small boat that was carried further upstream. Both sources of the earthquakes and the presence of offshore Islands controlled the degree of severity, inundation distances and flow depths. Nonetheless, Borrero et al. (2006) suggests that finer grid spacing for better detail is needed to obtain estimates of inundation and operational inundation maps, as the 200 m grid resolution is too coarse. For example, 75 to 250 m resolution was used to produce inundation maps in California (Borrero et al., 2006).

Karlsrude et al. (2005) proposed that numerical modelling for forecasting tsunamis for the Thai coast should start with the 2004 Indian Ocean tsunami ($M_w = 9.3$) as this can provide a seismological scaling reference. Their studies made use of a 3D depth-averaged linear model for tsunami generation and propagation in deep water; a 2D Boussinesq model, including non-linear effects, was applied in the nearshore area. There was no inundation included; their shore-line was represented by a vertical, impermeable wall (no-flux boundary conditions), that provided a doubling of the surface elevation due to reflection see (Harbitz and Pedersen 1992). An important strength of the MOST model over that used by Karlsrude et al. (2005) is its inclusion of inundation and run-up.

Karlsrude et al. (2005) simulated seven tsunami scenarios and predicted their impacts on the Thai Andaman coast. The seven scenarios sought a balance between the seismological data and the surveyed tsunami wave heights data, the first scenario being the 2004 event. The average rigidity on the rupture was assumed to be 40 GPa, which yielded a seismic moment of 1.10×10^{23} Nm; the slip seismic potential then decreases

gradually northward along the Nicobar-Andaman Subduction Zone. The other 6 scenarios were used to consider what might happen in the future. They divided the 1360 km rupture zone into 6 segments with various lengths ranging from 100 to 360 km, 140-210 km widths and thrust heights from 4 to 18 m. Varying earthquake magnitudes were applied for the different segments, including $M_w = 7.0$, 7.5 and 8.5 between Sumatra and the Nicobar Islands, $M_w = 8.5$ and 7.5 between the Nicobar-Andaman Islands and $M_w = 7.5$ north of the Andaman Islands. These composite motions were used to generate seabed displacements and seabed displacements were converted to produce a smooth sea surface disturbance.

For the inundation along the Andaman coast of Thailand, Karlsrude et al. (2005) reported that the 3D simulation results are comparable to the observed tsunami run-up heights and time series for Patong Beach and Bang Niang Beach (4-6 m wave height at Patong Beach and 8-9 m wave height at Bang Niang Beach).

For their $M_w = 8.5$ scenarios, a maximum surface elevation of 1-2 m is forecast along the Andaman coast of Thailand, considerably smaller than that of the $M_w = 9.3$ scenario, and the waves at Bang Niang Beach for $M_w = 8.5$ did not break. Karlsrude et al. (2005) recommend that the $M_w = 8.5$ scenario, with maximum surface elevation of 1.5-2.0 m above sea level should be implemented as a design basis for the short to medium term for Patong Beach, Bang Niang Beach and Namkhem Fishing Village.

Chapter 5 Regional Setting & Methodology

5-1 Regional Setting

5-1.1 General Location of Khao Lak, Phang-nga Province.

Thailand is situated in the Southeast Asian region, and judged to be a tectonically stable zone compared to the other countries in this area. The west coast of the Thai peninsular is composed of many islands, drowned valleys, steep cliffs, short and narrow beaches, and truncated headlands with small embayments. Steep-gradients and short rivers form floodplains of thin deposits of Quaternary sediment and narrow bays backed by crescent-shaped sand ridges are also found in the high energy coastal erosion regime of the west coast of Thailand (Dheeradilok, 1995; Sinsakul, 1992). Khao Lak is part of the west coast of the Thai peninsular and is one of the most famous tourist spots of the Andaman Sea coast of Thailand. It is located between 8° 38' N to 8° 50' N and 98° 13' E to 98° 17' E, and situated in Khukkhak sub-district, of Takua Pa district, in Phang-nga province (Figure 5-1). Khukkhak sub-district has an area of 147 km² and encompasses 7 villages - Bang Khaya, Thung Kamin, Pak Weep, Khukkhak, Bang Niang, Bang Niang Tai and Bang La-On (Sajjakul, 2005).

The Khao Lak area is part of the Khao Lak- Lam Ru National Park which has its headquarters situated on the headland of Hin Chang headland, the southern-most part of the study area. The National Park has an area of 125 km² and consists of tropical evergreen-forested hills, sea cliffs and beaches. The mountains of Khao Lak, Khao Bang Niang and Khao Buang San are located on the east side of Khao Lak. Freshwater lagoons are also found behind the sandy beaches in this area, especially in the low land behind Pakarang Cape and Khukkhak Beach. Headlands between bays, e.g Hin Chang headland, normally have steep cliffs and truncated rock spurs due to the effect of high-energy wave action.



Figure 5-1 Study area of Khao Lak (red box on inset map) showing the main beaches and coastal features.

5-1.2 Geological Setting

The Ranong and Klong Marui faults, with north & northeast-southwest strike-slip motions, are positioned on the Thai peninsular and are some of the main geological characteristics of the west coast of Thailand (Dheeradilok, 1995). In addition, the associated initial extrusion has resulted in a clockwise rotation of continental blocks in Southeast Asia. Both Ranong and Klong Marui faults are related to crustal movements. Igneous deposits dominate the geology of Khao Lak. Mountain ranges in Khao Lak consist of dome-shaped granite rocks. The granite rocks found in this region are rich in mica and were laid down between 60 and 140 million years ago during the Cretaceous period. These granite rocks yield tin deposits, which were mined in this region about 20 years ago.

The western coast of Thailand has been influenced by the Quaternary crustal movements. Quaternary sediment on the west coast of Thailand is formed by the short, steep-gradient, swift rivers which flow to the Andaman Sea and are usually deposited as thin layers at the head of the bays. The average thickness of Quaternary sediment on the Andaman coast is approximately 20 m. It is also composed of Pleistocene sediments which are mostly residual fluvial deposits of stiff clay, silt and coarse sands and gravels. The Pleistocene deposits overlay the Tertiary deposits or older rocks and are capped by intertidal Holocene silt sediments with intermittently interbedded beach sand (Sinsakul, 1992).

Evidence of Holocene eustatic sea level fluctuations, such as shell remains found 5-10 m above mean sea level (dated to 3530-5740 BP), is related to the tectonic uplift along the west coast of Thailand in the past 6000 years; it is also a source of heavy mineral deposits that are mined in this area (Dheeradilok, 1995; Sinsakul, 1992). The top soil is classified as loamy sandy acid soils. More acidic sandy mud is set in the lower layer.

5-1.3 Coastal Geomorphology of Khao Lak

The Andaman coast of Thailand consists of steep cliffs interspersed with narrow beach ridges mostly formed in embayments (Sinsakul, 1992). Khao Lak has a coastal plain, about 12 km long with sandy beaches situated on the west and mountainous ranges located on the east. There are four main streams running from the mountainous areas to coast: the Bang Niang, Pak Weeb, Pong and Kukkak canals. Natural changes to the

creeks and main canals, and the effects of reclamation and landlord alteration of land plots, have affected the water drainage of the whole area (Sajjakul, 2005).

Khao Lak extends from the rocky beach of Khao Lak Lam Ru National Park (near Bang La-On village) in the south to Pakarang Cape and Pak Weep Beach on the northern end. The study area (Figure 5-1) comprises Nang Thong Beach, which includes two main beaches at Bang Niang village and Bang La-On village: local people and tourists sometimes refer to these as Bang Niang Beach and Bang La-On or Nang Thong Beach. Khukkhak Beach is located north of the Bang Niang Beach, and is part of the study area. North of the Khukkhak Beach is the Pakarang Cape and the small beach between two hills named Pak Weep Beach, which are also incorporated in the study area.

Pak Weep Beach is a small beach between two hills. Backshore of Pak Weep Beach is not particularly wide and consists of small hills and natural water ponds which are found sparsely in the whole area. Pak Weep canal is the main stream with its opening located at this beach. Pakarang Cape is a flat plain, the tip of which points to the North-West. Coral reef patches are located around the cape. Casuarinas pines occur naturally, with coconut plantations at the backshore of Pakarang Cape.

Khukkhak Beach is located between Pakarang cape and Bang Niang Beach. The coastal plain of Khukkhak beach is approximately 1.5-2.5 km wide, from the coastline to the low inclined hill, with distinct steep slopes in some part of the backshore. Sand dunes are normally found along the beach. Khukkhak Canal is the main stream that runs through this beach.

Bang Niang Beach is a low gradient beach with a backshore area of a flat coastal plain. Casuarina pines and coconuts are the local flora of the area. Sand dunes are also found along the beach. Small creeks and natural swamps also originate in the backshore area. Pong canal and branches of Khukkhak canal run through and open at the beach. Nang Thong Beach (or Bang La-On Beach and Sunset Beach) is a low gradient beach with some rocky outcrops appearing at the intertidal zone. The backshore of this beach is a narrow lowland strip extending to the main road and the mountain behind (Sajjakul, 2005).

5-1.4 Climate

The tropical monsoon pattern dominates Thailand's climate. Dry season dominates in the western coast of Thailand during November to May with high temperatures (27-36°C) and low humidity; this is the most popular period for the tourists. In this season, there is a cool breeze and a calm sea state. The rainy season, the Southwest monsoon, starts in June and continues until October. August and September are the wettest months of the year with heavy showers although sunny intervals sometimes occur. Waves are highest during the Southwest monsoon season. Beaches are windswept and less scenic in this period. Beaches generally suffer from coastal erosion due to the monsoon waves.

5-1.5 Economic Development and Land Use.

The tin mining industry had an economic impact on the area from 100 until 20 years ago. The only traces of the tin mining industry are old mining pits that remain as irregular shaped ponds and mounds in this area. Tourism is now the main industry. According to the Provincial Office of Tourism, Recreation and Sports statistics, 548,515 foreign tourists visited Phang-nga in 2007 (<http://secretary.mots.go.th>) and generated more than £45m income. In addition, more than 17000 visitors visit the Khao Lak_Lam Ru National Park annually. It is a favourite resort area, particularly for northern Europeans. Many hotels and resorts have been established in the area, especially along the four main beaches: Khukkhak Beach, Bang Niang Beach, Nang Thong Beach and Bang La-On beach.

Beach forest dominates in Khao Lak coastal areas. Along the beach casuarinas, coconuts and pandans are present. Mangrove forests are frequently found around tidal flats, and occur as fringes to tidal creeks and accumulation flats. The west coast of Khao Lak is utilized for commerce and tourism while the residential areas are typically in the northern zone. Commercial and residential areas are also situated along the main road that lies between the beaches and the mountainous zones.

5-2 Acquisition& Preparation of Detailed Data.

5-2.1 Data Acquisition

The bathymetry of the nearshore area off the Khao Lak coast was surveyed using an Innomar SES-2000 Light parametric digital echo-sounder (Figure 5-2 and Figure 5-3), an instrument designed for shallow water (5-200 m) and small area sediment surveys (up to 50 m penetration) with small beam-widths at low frequencies (3.5 -15 kHz) and accurate ($0.02 \text{ m} + 0.02 \%$ of water depth) depth measurements with the high (100 kHz) frequency. The vessel speed was 5-7 km/h. Depths were calculated from time duration that wave travels using the speed of sound in water adjusted for temperature and salinity. Tide tables were used for correcting tide effects; this limited the accuracy of the final survey data – no local tide gauge was available. Depths were adjusted to mean sea level value. The survey accuracy was estimated to be $\pm 0.5\text{m}$.



Figure 5-2 Conducting the bathymetric survey along the Andaman coast.



Figure 5-3 The Innovar SES-2000 Light digital parametric echo-sounder used for measuring the water depth of the study area.

Detailed topography of the area around Bang Niang and Nang Thong Beaches was conducted using a two-frequency Real Time Kinematic (RTK) Differential Global Positioning System (RTK-DGPS) Model Leica GS 1200 (Figure 5-4). The coordinate system used for this survey is WGS 84 on a UTM grid and using mean sea level of the Andaman Sea of Thailand as the base of vertical height (vertical datum).

The RTK-GPS system is composed of two parts: a base unit and a rover unit. The base unit, which serves as the reference, is mounted on a tribrach on a tripod leg and is set exactly over a known reference station. For this survey, reference stations constructed by the Royal Thai Survey Department, and the Department of Public Works and Town & Country Planning were used. Typically the locations of these reference station (WGS 84) are known to a horizontal accuracy of better than ± 0.05 m and a vertical accuracy of ± 0.01 m. The base unit sends signals which allow the rover units(s) to correct its position caused by small drifts in the orbit parameters of the GPS satellites. Normally the base unit used in this survey was placed not farther than 5 km from the rover to ensure the continuity of data gathering.

The rover unit calculates its position using signals from the GPS satellites. Uninterrupted satellite signal reception, at both base and rover, are required from at least 4 satellites to ensure data accuracy. There were some problems in the Khao Lak area between 1.00-3.00 pm when < 4 satellites were visible. A Compact Flash card was

used to store and transfer data for analysis. Leica Geo Office software was used for post-processing the data. Data were viewed, edited and export and used to create the topography of the study areas for the modelling.

An area of approximately 160 km² (8 km wide and 20 km long) including the area of the nearshore of Bang Niang and Nang Thong Beaches and their vicinity was surveyed. Spacing of the marine survey's lines is approximately 500 m (Figure 5-5) with the survey tracked by GPS (± 4 m horizontal accuracy). Spacing of the topographical surveys ranges from 5-10 m perpendicular to the coastline and approximately 40 m parallel to the coastline. (Figure 5-6).

Surveyed bathymetric and topographic data acquired by both Innomar digital echosounder and RTK-DGPS for this research is accurate, and its resolution is fine enough for the MOST/ComMIT model simulation. Mean sea level data measured by the Hydrographic Department of the Royal Thai Navy for each survey date were used for correcting tidal effects and adjusting both surveyed bathymetric data and topographic data to a common datum.



Figure 5-4 Leica System 1200, Real Time Kinematic GPS surveys for topographic data. Rover receiver, Base unit and Base station.

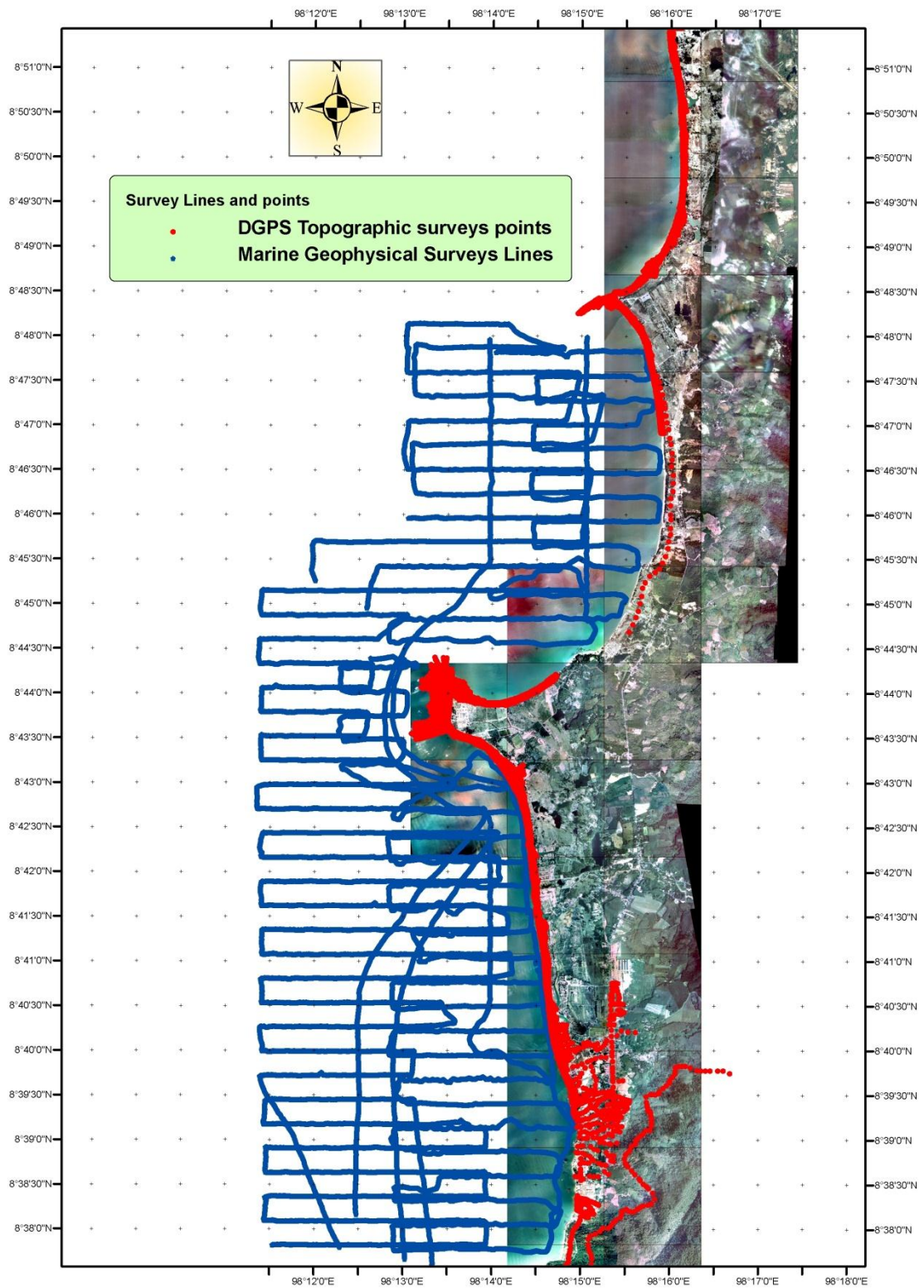


Figure 5-5 Bathymetric survey lines and topographic survey points of Khao Lak area.

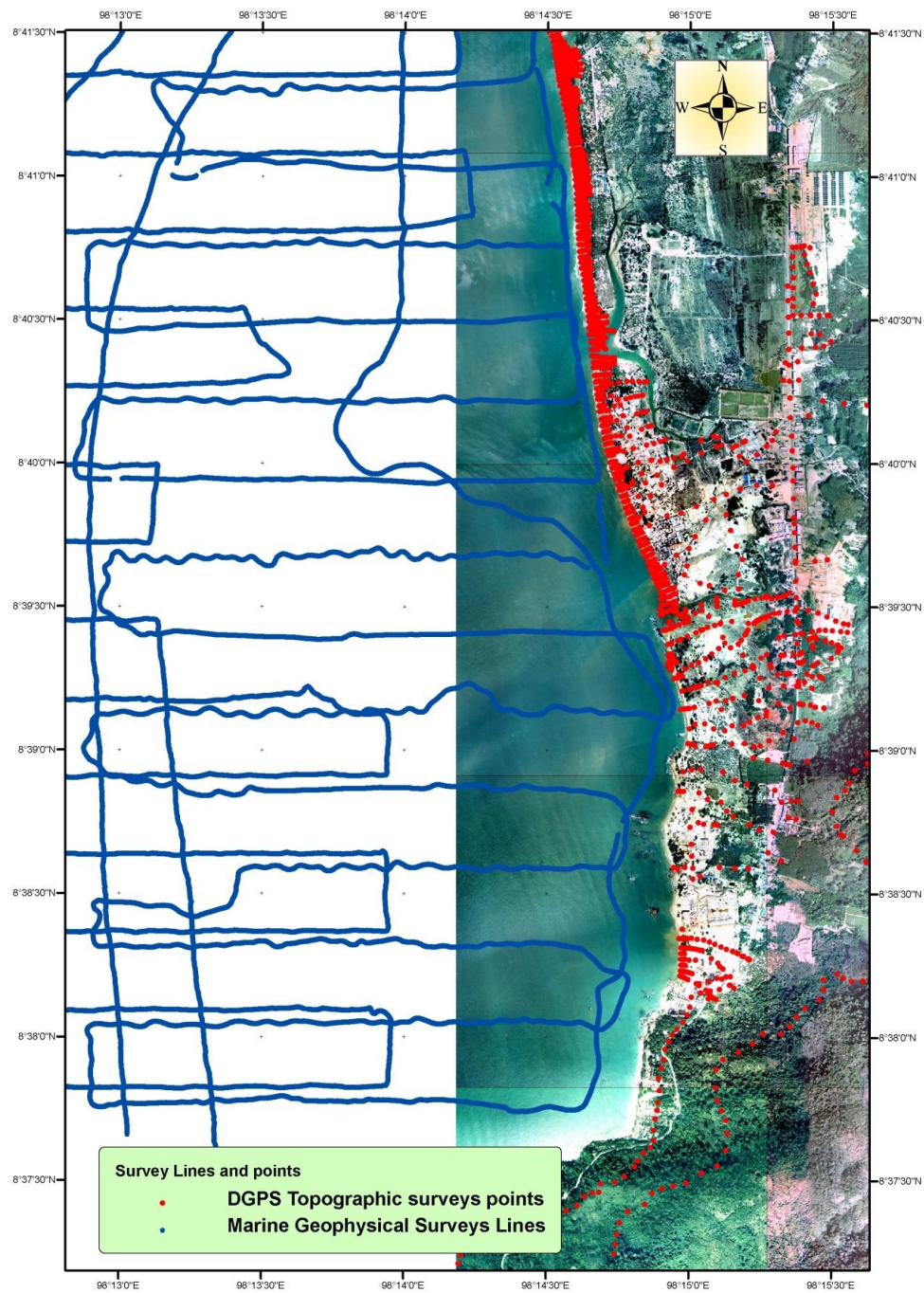


Figure 5-6 Bathymetric survey lines and topographic survey points of Bang Niang and Nang Thong Beaches.

5-1.1.1 *Preparation of data*

To study the behaviour of the tsunami wave that inundates the beaches and the backshore areas, it is necessary to supply detailed topographic and bathymetric data of

the area concerned. It was necessary to integrate both topographic and bathymetric data, which were conducted by different instruments and recorded in different formats, into the same file and the vertical datum of both datasets had to be adjusted to correspond with the mean sea level of the Andaman Sea of Thailand. Data were transformed into NetCDF format to fit with MOST/ComMIT model (as Grid C) by using MathLab software. Detail of data preparation to suit the MOST/ComMIT model included:

- Bathymetric data were adjusted using the Tide Tables of Hydrographic Department, Royal Thai Navy to mean sea level at the date, while topographic data, surveyed by using RTK-DGPS, was already set to mean sea level due to the reference base unit that set to the Andaman coast mean sea level. Then, both data set were merged together. Surfer software was used to produce the contour maps of both study area and detailed study area. Krigging method was used to interpolated data set to 40*40 m for study area and 20*20 m for detailed study area.
- The two sets of high resolution topographic and bathymetric data of the study area of Khao Lak (Figure 5-7; 40 by 40 m interpolated resolution) and detailed study area of Bang Niang and Nang Thong Beaches (Figure 5-8; 20 by 20 m interpolated resolution) were prepared separately to be the inputs for the MOST/ComMit model for detailed grid C. Moreover, 1.0 m of tide was also added to the combined bathymetric and topographic data to replicate the high tide as it occurred on 26 December 2004 at the time of the tsunami.
- Finally, topography and bathymetry were merged into one computational grid. Water depth is set to positive values while height above mean sea level is set into negative value to match with the requirement of the model. Data in UTM grid was transformed into Latitude and Longitude format (WGS 84) to match up with the MOST/ComMIT model requirement, and was interpolated to a regular grid.

- Points were checked and errors removed. Consistency between grid C dataset of bathymetry and topography and those of grid B was validated to match each other by overlaying their contours.
- Two sets of nested computational grids of grid C for study area and detailed study area were verified by using Bathymetry Correction command of ComMIT model. The smoothing algorithm was applied to the computational grids to maintain model stability by reducing potential discontinuity due to single-node cells, for example the Islands (Venturato et al., 2007a).
- Grid A and Grid B data was downloaded from ETOPO data to use in the simulation of tsunami waves by the MOST/ComMIT model in this research.

5-2.2 The Study Area

The wider study area (Figure 5-5 and Figure 5-7) is comprised of Khao Lak Lum Ru National Park, Nang Thong, Bang Niang and Kukkak Beaches, Pakarang Cape, and Pak Weep Beach, approximately 14 km in length. The detailed study area consists of the Nang Thong and Bang Niang Beaches, where many resorts and hotels are located (Figure 5-6 and Figure 5-8). Nang Thong and Bang Niang Beaches are sandy beaches, ~5 km in length, with rock outcrops extruding in some spots of the intertidal zones.

Water depth off the west coast of Phang-nga province, in front of the study area, decreases at the continental slope from 400 m depth ~250 km offshore to approximately 100-200 m depth 160 km offshore, and then gradually decreases over the continental shelf to ~30 m depth 12 km offshore. In front of the Bang Niang and Nang Thong Beaches water depth is 18 m at 5-6 km offshore (Figure 5-7). Coral reef patches can be found just off the coast. Sinsakul (1992) cited the Royal Thai Hydrographic Department report that tidal category of the west coast of Thailand is described as a semi-diurnal type. The tidal range of the west coast is approximately 2.5 m during the spring tide.

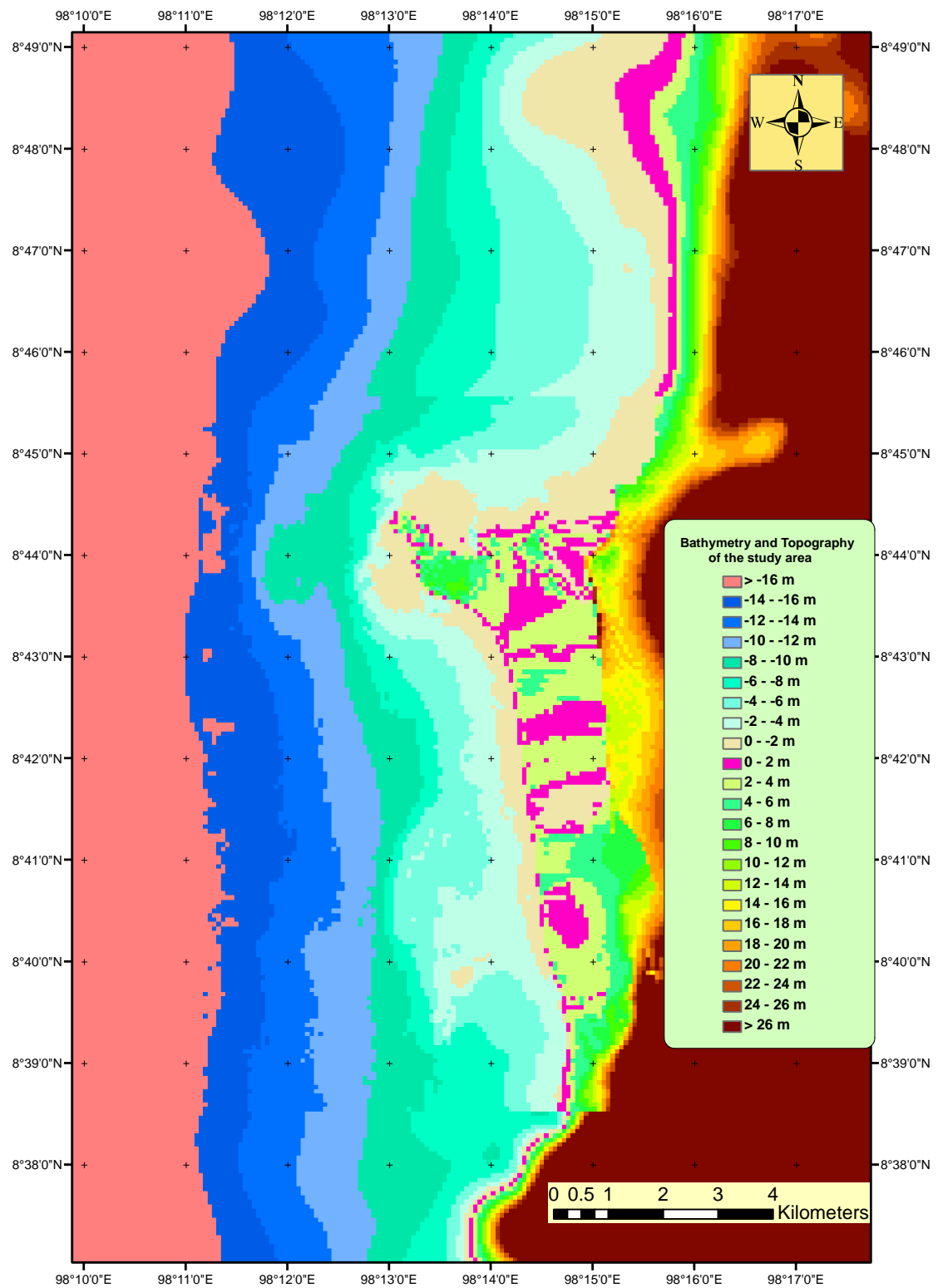


Figure 5-7 Depth and height of Khao Lak area.

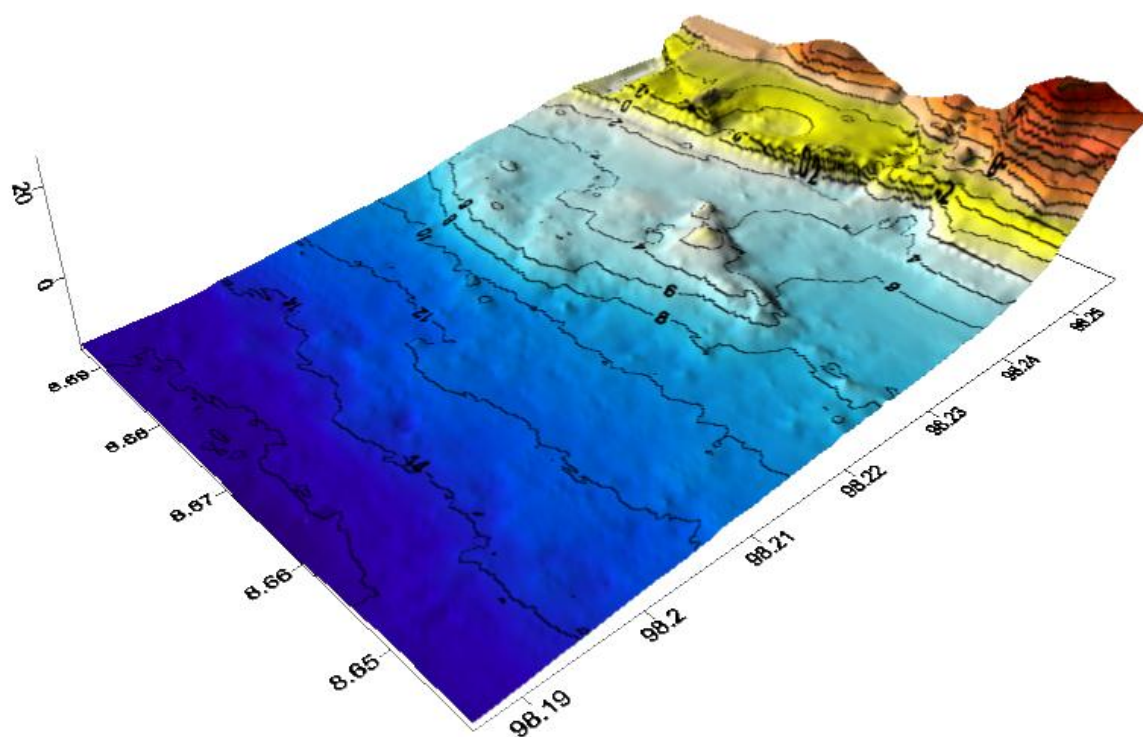


Figure 5-8 Detailed bathymetry and topography of Bang Niang and Nang Thong Beaches.

5-3 Methodology

5-3.1 The MOST/ComMIT Model.

The numerical model used in this research is the MOST (Method of Splitting Tsunami) model with the ComMIT (Community Model Interface for Tsunami) for tsunami generation, open sea propagation and for the study of the inundation in nearshore and coastal zones. The [MOST](#) model was developed by Vasily Titov of NOAA/PMEL and Costas Synolakis of University of Southern California. This model is able to simulate three steps of tsunami progression: earthquake deformation, transoceanic propagation, and inundation on dry land. The model was developed under the supervision of the NOAA Centre for Tsunami Research (NCTR) to assist coastal communities in their efforts to evaluate the tsunami risk, and mitigate tsunami vulnerability, since the model can provide information about wave arrival time, wave height and inundation areas. Maximum tsunami wave height, water velocity and maximum inundation distance are the important factors about which vulnerable coastal communities requires information. In addition, tsunami wave characteristics, including wave series and wave arrival time, are also necessary for the community to mitigate the tsunami devastation (e.g. set up evacuation routes and position critical infrastructure) by emergency management and urban planning.

The ComMIT model is a finite-difference, long-wave approximation model. It solves a long-wave approximation to the Navier-Stokes equation using the finite difference method for propagation modelling (> 50 m depth). Bottom friction is not included in the propagation model for the deep open sea but plays an important role for the inundation model in coastal areas. The equation switches to the shallow-water theory with bottom friction for computing wave inundation in shallow water and on-land flooding. The MOST model uses spherical coordinates with the Coriolis force and a numerical dispersion scheme (Dominey-Howes et al., 2007; Geist et al., 2007; Hamouda, 2006; Venturato et al., 2007a; Venturato et al., 2007b).

5-1.1.2 ***Model Setup***

The MOST/ComMIT model allows for the use of three nested computational grids, with information flowing from the coarsest, smallest-scale grid (grid A) through a grid

of intermediate resolution (grid B) to the finest large-scale grid C. Grid A is the spatially biggest digital elevation model (DEM) with coarsest resolution and has the greatest coverage. Fewer node points are needed to resolve tsunami wave patterns in the open ocean. Grid B is the intermediate DEM, and grid C is the finest resolution DEM grid with least coverage. As a tsunami wave travels across the shallow coastal areas, more node points are needed because of the shorter wavelengths (Venturato et al., 2004). The grid interaction among grid A, grid B and grid C interrelates by passing wave height and velocity interaction between nodes along their intersecting boundaries (Venturato et al., 2007a).

The three computational grids used in this research to generate the tsunami generation at the subduction zone, the tsunami wave propagation across the Indian Ocean (the Andaman Sea) and the inundation on Khao Lak and Bang Niang and Nang Thong Beaches are shown in Figure 5-9. Grid A data was downloaded from <http://sift.pmel.noaa.gov> and has a lat-long resolution of 2 minutes while grid B was downloaded from the same source at 30 seconds resolution, both in NetCDF format. Grid C, the finest one, was developed from local topographic and bathymetric surveys by the author and the Department of Mineral Resources' staff to gain a high resolution grid which matches with the model requirement (more detail about grid C can be found in Data Acquisition and Preparation Section).

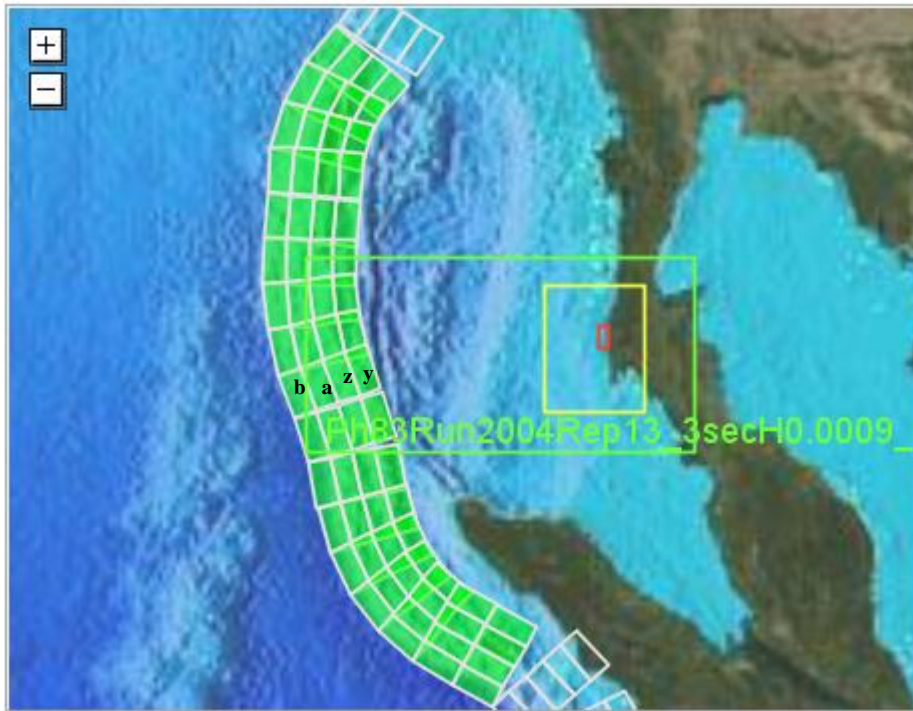


Figure 5-9 Three nested grids used for studying tsunami generation, propagation and inundation of Khao Lak: Grid A; Green rectangular, Grid B; Yellow rectangular and Grid C; Red rectangular. (Also shown in green is the rupture zone)

5-1.1.2.1 Rupture sources (vertical seafloor displacement heights)

To cover the entire width of Sunda Subduction in the case of the Indian Ocean rupture zone, 4 parallel sub-units were utilized; sub-unit 'b' was located at the outer western side of the subduction zone, followed by sub-unit 'a', sub-unit 'z' and finally sub-unit 'y' on the eastern side of the subduction (Figure 5-9). Each sub-unit can be selected or not-selected depending on earthquake characteristics. Several sets of horizontal units can be placed together to represent the ruptures of each earthquake (Figure 5-9). Sub-units of the Sumatra section are represent by b1, a1, z1 and y1, sub-units of the lower Nicobar section represent by b2, a2, z2 and y2, the upper Nicobar section by b3, a3, z3 and y3, and the Andaman section by b4, a4, z4 and y4 (Figure 5-10).

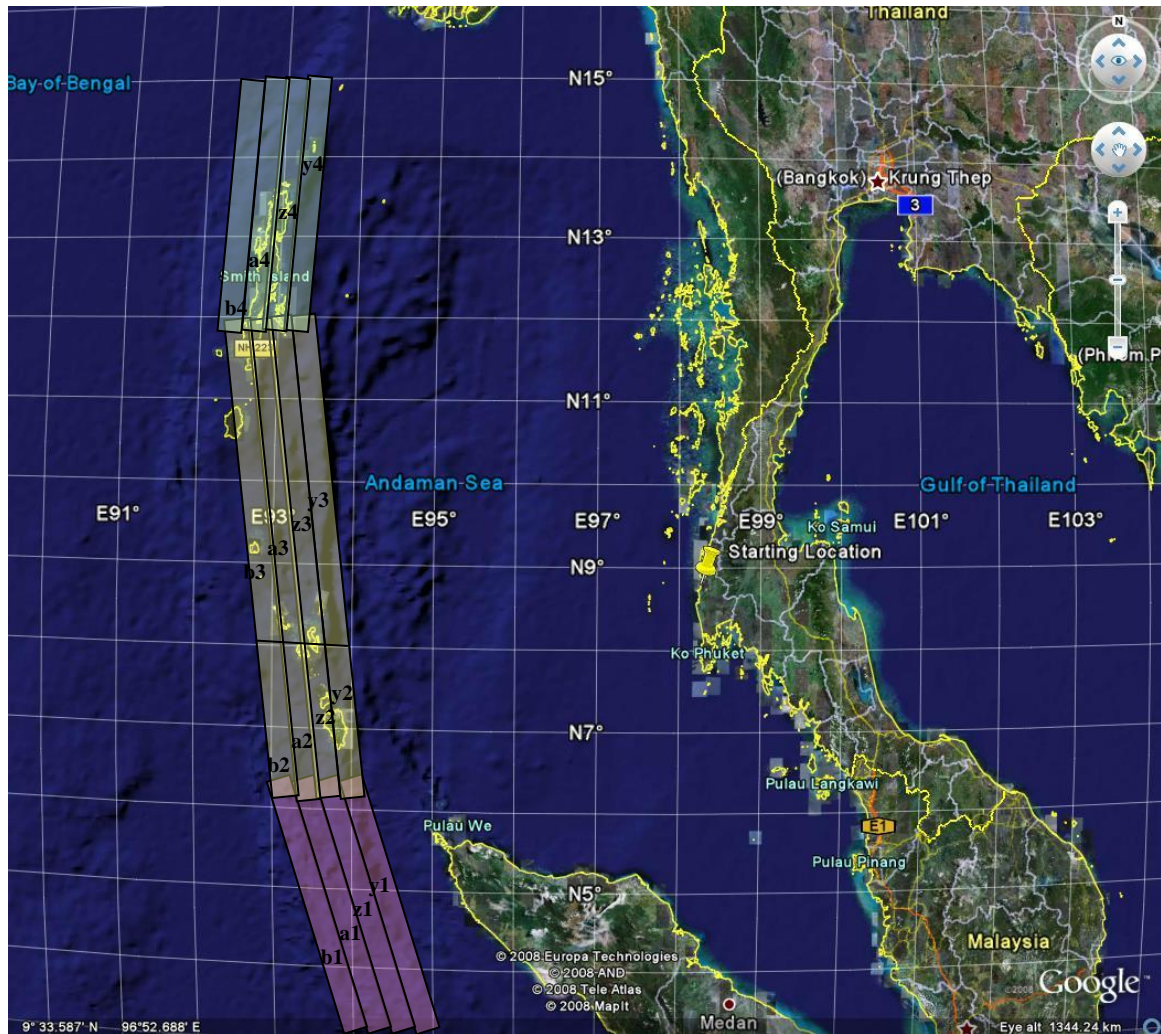


Figure 5-10 Subduction zone showing sub-units used for simulating the 2004 Indian Ocean Earthquake-generated tsunami by MOST/ComMIT model.

5-3.2 Simulation of the 2004 Tsunami

The 2004 tsunamigenic earthquake deformation was simulated in the MOST/ComMIT model by varying the slip of the earthquake sources referenced by various concerned documents (Table 5-2). The MOST/ComMIT model was set up to represent different rupture scenarios suggested by various authors. The slip of the Sunda subduction related to the 2004 Indian Ocean earthquake is divided into 3 sections: Sumatra section, Nicobar section and Andaman Section with the Nicobar section itself divided into 2 subsections (Figure 5-10). 16 scenarios relating to different estimated earthquake characteristics of the 2004 earthquake from Table

1-1 were considered by varying the rupture heights of the sub-units. Details of 16 scenarios simulated were as follows:

5-1.1.3 *Scenario 1 and 2*

According to Plafker (1997) and Synolakis et al. (2005) tsunami run-up, by the Plafker rule, is never higher than twice the slip so rupture heights were selected depending upon the run-up on the areas perpendicular to those specific coastlines. Moreover, Lay et al. (2005) and Vallee (2007) stated that the vertical displacement height of the 2004 earthquake at Sumatra Section was approximately 20 m. Scenario 1 assumed that the run up height of Sumatra coasts varied from 16-32 m so 8-16 m slip was used. Gahalaut et al. (2006) suggested that the slip height of the Nicobar Section was 11-15 m. For the Nicobar section the tsunami run up height was ~20 m so 8-10 m of rupture were used for this section. For Scenario 2 ruptures of 9-17 m were selected for Sumatra section and 8.5-9 m for the Nicobar section. Both scenarios have an M_w of 9.4 (Figure 5-11).

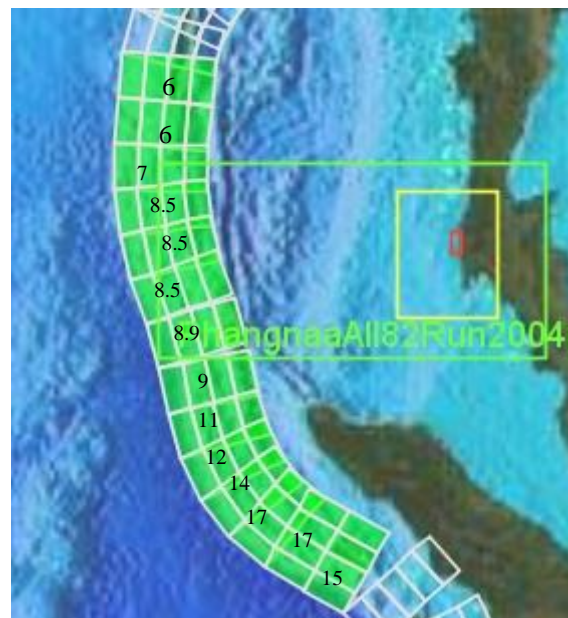


Figure 5-11 Vertical seafloor displacement heights of scenario2

5-1.1.4 *Scenario 3, 4, 5 and 6*

According to Gahalaut et al. (2006) and Lay et al. (Lay et al., 2005) high slip of 20 m occurred along the Sumatra section and decreased to 2m height at the Andaman section. In

addition the Nicobar section slip height was approximately 10 m (Gahalaut and Catherine, 2006; Vallee, 2007). Scenario 3 set the rupture height of the Sumatra section to 16 m (since the highest tsunami wave height at Sumatra coast was approximately 32 m), 8 m for the Nicobar section (16 m wave height occurred at Pakarang Cape of Thailand), and 3 m for the Andaman section (6 m tsunami wave height occurred along Myanmar's coast). To match up with the average of the slip height of 15 m for the whole rupture, slip height of Sumatra Section of 14 m was applied for scenario 4 (Ammon, 2006; Sinadinovski, 2006; Stein and Okal, 2005b; Stein and Okal, 2007). In Scenario 4 rupture height was increased to 11 m for the Nicobar Section according to (Gahalaut and Catherine, 2006; Piatanesi and Lorito, 2007; Tanioka et al., 2006). Scenario 5 has rupture heights of 17, 14 and 4 m for the Sumatra, Nicobar and Andaman sections. Scenario 5 is similar to scenarios 3 and 4 but with slightly increased slip height of 14m along the Nicobar Section to 14 m (Gahalaut et al. (2006). The M_w of all these three scenarios are 9.3. Scenario 6 considers the most extreme case with 18 m of rupture along the Sumatra section, and 12 m and 8 m for the Nicobar and Andaman sections; with these very high rupture values, the M_w of Scenario 6 was 9.5. The scenario 6 applied high slip along the Sumatra Section (Lay et al., 2005; Piatanesi and Lorito, 2007; Tanioka et al., 2006; Vallee, 2007) to represent vertical displacement of 18 m. Then, 12 m of slip height of the Nicobar Section, and 8 m of slip height of the Andaman Section were derived from Gahalaut et al. (2006) and Tanioka et al (2006).Scenario 7, 8, 9 and 10

Song et al. (2008) concluded that vertical deformation was not enough to generate the enormous 2004 Indian Ocean tsunami; it was not just the vertical dislocation of the seafloor, but the horizontal impulse of the slip of the 2004 earthquake that made up two thirds of the satellite-observed tsunami height. The horizontal impulse of the faulting continental slope generated kinetic energy 5 times higher than that associated with the vertical dislocation. The asymmetrical tsunami pattern of leading-elevation waves toward Sri Lanka against that of leading-depression waves toward the Andaman Sea coast of Thailand is evidence of a horizontally-forced mechanism.

Song et al. (2008) state that the 2004 earthquake displacement shows the seafloor uplift occurred on the west side with high horizontal displacement to the north-west direction at the Sumatra section, with lower horizontal displacement for the Nicobar section and the smallest at the Andaman section. Sea bottom subsidence took place along the east side of the eruption area (Song et al., 2008). Two-dimension shallow water theory might not be adequate to

represent the tsunami generation mechanism and 3-D motions of faulting continental slopes, which generate near-bottom water movement, might be necessary. Titov et al. (2005) divided the 2004 ruptures into 4 segments and set slip values for 21, 13, 17 and 2 m over each segment to recreate the seafloor deformation but Song et al. (2008) disputed the tuned displacements of Titov et al. (2005) model stating they over-estimated the GPS measurement and seismic inversion data. Inclusion of the horizontal impulse momentum may be necessary for tsunami mechanism clarification (Gahalaut and Catherine, 2006).

The following scenarios represent different characteristics of the 2004 event by varying the rupture heights to mimic horizontal rupture effects because the model could not directly input horizontal displacement of the sea-bed.

5-1.1.5 Scenario 7, 8, 9 and 10

In these four scenarios low slip height was used in the 2 central rectangular sub-units, and higher slip height in the 2 outer rectangular sub-units. Slip height of the Sumatra section (which had the highest the vertical displacement) varies from 10 m (Piatanesi and Lorito, 2007) to 20-23 m (Lay et al., 2005; Vallee, 2007). Therefore, slip height of this section of approximately 16-18 m were applied to simulate the tsunami with horizontal displacement effect for scenarios 7, 8 and 9. Scenario 7 used 18 m at the outer and 16 m at central sub-units of the Sumatra section, 14 m and 12m were applied to the outer and central sub-units of the Nicobar section and 8m and 6m to the Andaman section. Gahalaut et al.(2006) and Tanioka et al. (2006) reported that the Nicobar Section's slip heights are 11-15m and 10-15m respectively so slip heights of 12-14 m were applied to simulate the effect of horizontal displacement for the Nicobar Section for scenarios 7 and 9. Moreover, For, Slip heights of 6-8 m were used for the Andaman Section (Gahalaut et al.(2006). The M_w of Scenario 7 is 9.5.

A slip height of 10 m of the Nicobar Section is reported in Vallee (2007) so scenario 8 uses 12 m and 10 m for the Nicobar section rupture heights. Scenario 9 is similar to scenario 7, except 5 m and 3 m were applied to the Andaman section (Gahalaut et al.(2006) and a slightly decreased slip height of the Sumatra Section from 16-18 m to 15-17 m according to varied slip height range presented in Lay et al. (2005), Piatanesi and Lorito (2007) and Vallee (2007). Scenario 10 has 17 m and 15 m for the Sumatra section, from Lay et al. (2005) and 12 m and 10 m for the Nicobar section (Vallee, 2007) and 8m and 6 m for the Andaman section (Gahalaut and Catherine, 2006). The M_w of scenarios 8, 9 and 10 were 9.4.

5-1.1.6 *Scenario 11, 12 and 13*

Slip heights varied as in the previous scenario but is higher in the two western sub-units than in the eastern sub-units. For the Sumatra Section, slip heights vary between 10 and 23 m (Lay et al., 2005; Piatanesi and Lorito, 2007; Vallee, 2007). Slip heights of 14-18 m were selected for tsunami wave simulation of scenario 11 and 12, and those of 16-18 m were chosen for Scenario 14. For The Nicobar Section, slip heights of 8-12 m were selected for scenario 11 and 12 according to Gahalaut et al.(2006), Tanioka et al (2006) and Vallee, 2007. In Scenario 11, rupture heights of the Sumatra section were set to 18 m for the two western sub-units and 14 m for the eastern sub-units, 12m and 8 m, and 5 m and 3 m for the Nicobar and Andaman sections respectively. To compare the effect of friction coefficient, scenario 12 was set to the similar rupture heights as Scenario 11 but the friction coefficient was set to 0.0009 instead of 0.0003. The M_w of both Scenarios 11 and 12 are equal to 9.4. In scenario 13 the slip height of the Nicobar and Andaman Sections was set to low values to test the effect of a smaller earthquake; the slip heights were reduced to 14m and 12 m along the Sumatra section, to 8m and 5m for the Nicobar section and 5 m and 2 m for the Andaman section, yielding an M_w of 9.3.

5-1.1.7 *Scenario 14*

According to Pietrzak et al. (2007), the largest region of slip was situated between 3° to 5° N (along the Sumatra section; inverted from co-seismic GPS data) but may have extended northwards to about 6° N. Another patch in the north between 8° N to 10° N (along the Andaman section) shows a high degree of rupture. This corresponds to the Jason-1 images that the tsunami propagated outwards from the northern patch of slip between 8° to 10° N. A zone of lower slip was between 7° to 8° N. Slip heights of this section were derived from Vallee (2007) and Tanioka et al., (2006), who reported that slip heights of the Sumatra Section was 20 m and the Nicobar Section was approximately 10-15 m. These slip heights were integrated with Pietrzak et al. (2007) who reported the different slip height of different sections. Therefore, Scenario 14 was set up to represent estimated rupture heights from Pietrzak et al. (2007); slip heights were highest in the Sumatra section, lowest in Nicobar section; slip heights were again higher in the western sub-units and lower in the east (Sumatra 18m and 16m, the upper part of the Nicobar section and the Andaman section 12 m and 10 m,

the lower part of the Nicobar section 6 m and 4 m, and 10 m for the 2 eastern ones). M_w was 9.4.

5-1.1.8 ***Scenario 15 and 16***

Finally, according to Ioualalen et al.(2007), the average rupture of the 2004 earthquake was about 10 m of uplift and up to ~6 m of subsidence over the 1200-1300 km of the Andaman-Sunda trench. Bilham (2005) stated that the 2004 earthquake generated up to 10 m of uplift and subsidence from the earthquake elastic rebound. Furthermore, Kowalik et al. (2007) indicated that the fault plane is broken into 2 segments and that the maximum uplift is 5.1 m with the maximum subsidence roughly 4.7 m. The following two scenarios were conducted to simulate the deformation relating to both uplift and subsidence effects by setting rupture heights for uplift motion as positive values, and subsidence as negative values.

In scenarios 15 and 16, slip height has the highest uplift in the Nicobar segment, lowest in Andaman segment, positive (uplift) in the west and negative (subsidence) in the east. For the Sumatra section, the rupture height (Scenario 15) was set to 12 m in the west and -6m in the east, and rupture heights of 6 m and -2 m for the lower Nicobar section. The Andaman section and the upper Nicobar sections were set to 8 m and -4 m. Scenario 16 is similar but has a higher M_w than Scenario 15, 9.3 compared to 9.2

| Sources | Scenarios | | | | | | | | | | | | | | | |
|--|---|---|---|---|---|---|--|--|--|--|--|--|----|---|----|---|
| | 1 | 2 | 3 | 4 | 5 | 6 | 7 | 8 | 9 | 10 | 11 | 12 | 13 | 14 | 15 | 16 |
| (Ammon et al., 2005) slip=15-20 m width 200 km | | | | Apply 14 m for Sumatra Section | | | | | | | | | | | | |
| (Bilham, 2005) Uplift =10m, subsidence=10m | | | | | | | | | | | | | | | | Apply + 16m slip height and - 7m of Nicobar |
| (Lay et al., 2005) Slip =20m (Sumatra) <2m (Nicobar& Andaman) Width =160-170km | Apply max slip height of 16 m for Sumatra section | Apply max slip height of 17 m for Sumatra section | Apply slip height of 16 m for Sumatra Section and 3 m for Andaman Section | Apply slip of 3 m for Andaman Section | Apply slip height of 17 m for Sumatra section and 4 m for Andaman Section | Apply slip height of 18 m for Sumatra section | Apply slip height of 16-18 m for Sumatra section | Apply slip height of 16-18 m for Sumatra section | Apply slip height of 16-18 m for Sumatra section | Apply slip height of 15-17 m for Sumatra section | Apply max slip height of 18 m for Sumatra section | Apply slip height of 14-18m for Sumatra section | | Apply slip height of 16-18m for Sumatra section | | |
| (Stein and Okal, 2005b), (Stein and Okal, 2007) Slip=12-15m width=200km | - | - | - | Apply 14 m for Sumatra Section | | | | | | | | | | | | |
| (Gahalaut and Catherine, 2006) Slip=3.8-7.9m (Andaman) 11-15m (Nicobar) Width=120-160km | | | | Apply slip height of 11 m for Nicobar Section | Apply slip height of 14 m for Nicobar Section | Apply slip height of 12 m for Nicobar Section | Apply slip height of 12-14m for Nicobar Section, and 6-8 m for Andaman Section | Apply 6-8 m for Andaman Section | Apply slip height of 12-14m for Nicobar Section, and 3-5 m for Andaman Section | Apply 6-8 m for Andaman Section | Apply slip height of 12-14m for Nicobar Section, and 3-5 m for Andaman Section | Apply slip height of 12-14m for Nicobar Section, and 3-5 m for Andaman Section | | | | |

| | | | | | | | | | | | | | | | |
|--|---|--|---|--|--|--|--|--|--|--|--|--|--|---|---|
| (Sinadinovski, 2006) Slip=15m Width=50km | - | - | - | Apply 14 m for Sumatra Section | | | | | | | | | | | |
| (Tanioka et al., 2006) Slip =23 m at Aceh coast 21 m at Simeulue 10-15 m at Little Andaman and Car Nicobar | Apply slip height of 8-10 m for Nicobar Section | Apply slip height of 6-9 m for Nicobar Section | Apply slip height of 8 m for Nicobar Section | Apply slip height of 11 m for Nicobar Section | | Apply slip height of 12 m for Nicobar Section | Apply slip height of 12-14m for Nicobar Section, | | Apply slip height of 12-14m for Nicobar Section, | | | | | | |
| (Ioualalen et al., 2007) Uplift =10m, subsidence=6m | | | | | | | | | | | | | | Apply + 12m slip height and - 6m for Sumatra | Apply + 12m slip height and - 6m for Sumatra |
| (Kowalik et al., 2007) Uplift =5.1m, subsidence=4.7m | | | | | | | | | | | | | | Apply + 6m slip height and - 2m for Nicobar and + 8mand - 4m for Andama n | Apply+8 m and - 4m for Andama n |
| (Pietrzak et al., 2007) 3-5 ⁰ N=high slip, 8-10 ⁰ N=high slip 7-8 ⁰ N=low slip | | | | | | | | | | | | | Apply slip height of 16-18 m for Sumatra, 4-6 m for Lower Nicobar and 10- 12 m for Upper Nicobar and | | |

| | | | | | | | | | | | | | | | | |
|---|---|---|---|--|--|--|--|--|--|--|--|--|--|---------------------|--|--|
| | | | | | | | | | | | | | | Andaman Sextions | | |
| (Piatanesi and Lorito, 2007) slip= 10m at South 5° N Max=30 (Aceh) =10m at 6.5-11° N= =20m at Northernmost 11- 14° N | Apply min slip height of 8 m for Sumatra section | Apply min slip height of 9 m for Sumatra section | - | Apply slip height of 11 m for Nicobar Section | | | | | | | Apply min slip height of 14 m for Sumatra section | | Apply height of 12-14 m for Sumatra section | | | |
| (Vallee, 2007) Slip=20 m at Sumatra 10 m at Nicobar | Apply slip height of 8-10 m for Nicobar Section | | | | Apply slip height of 17 m for Sumatra Section | | Apply slip height of 16-18 m for Sumatra section | Apply slip height of 16-18 m for Sumatra section and 10- 12m for Nicobar Section | Apply slip height of 16-18 m for Sumatra section | Apply 10-12m for Nicobar Section | | | | | | |

Table 5-1 slip height Detail according to various documents used for simulation of tsunami wave by using MOST/ComMIT model in 16 scenarios.

| Scene | Slip along sub-faults(m) | | | | | | | | | | | | | | | | M _w |
|-------|--------------------------|------|------|------|-----------------|-------|-------|-------|-------|-------|-------|-------|-----------------|----|----|----|----------------|
| | Sumatra Section | | | | Nicobar Section | | | | | | | | Andaman Section | | | | |
| | b1 | a1 | z1 | y1 | b2 | a2 | z2 | y2 | b3 | a3 | z3 | y3 | b4 | a4 | z4 | y4 | |
| 1 | 8-16 | 8-16 | 8-16 | 8-16 | 10 | 10 | 10 | 10 | 8-9 | 8-9 | 8-9 | 8-9 | - | - | - | - | 9.4 |
| 2 | 9-17 | 9-17 | 9-17 | 9-17 | 8.5-9 | 8.5-9 | 8.5-9 | 8.5-9 | 6-8.5 | 6-8.5 | 6-8.5 | 6-8.5 | - | - | - | - | 9.4 |
| 3 | 16 | 16 | 16 | 16 | 8 | 8 | 8 | 8 | 3 | 3 | 3 | 3 | 3 | 3 | 3 | 3 | 9.3 |
| 4 | 14 | 14 | 14 | 14 | 11 | 11 | 11 | 11 | 3 | 3 | 3 | 3 | 3 | 3 | 3 | 3 | 9.3 |
| 5 | 17 | 17 | 17 | 17 | 14 | 14 | 14 | 14 | 14 | 14 | 14 | 14 | 4 | 4 | 4 | 4 | 9.3 |
| 6 | 18 | 18 | 18 | 18 | 12 | 12 | 12 | 12 | 12 | 12 | 12 | 12 | 8 | 8 | 8 | 8 | 9.5 |
| 7 | 18 | 16 | 16 | 18 | 14 | 12 | 12 | 14 | 14 | 12 | 12 | 14 | 8 | 6 | 6 | 8 | 9.5 |
| 8 | 18 | 16 | 16 | 18 | 12 | 10 | 10 | 12 | 12 | 10 | 10 | 12 | 8 | 6 | 6 | 8 | 9.4 |
| 9 | 18 | 16 | 16 | 18 | 14 | 12 | 12 | 14 | 14 | 12 | 12 | 14 | 5 | 3 | 3 | 5 | 9.4 |
| 10 | 17 | 15 | 15 | 17 | 12 | 10 | 10 | 12 | 12 | 10 | 10 | 12 | 8 | 6 | 6 | 8 | 9.4 |
| 11 | 18 | 18 | 14 | 14 | 12 | 12 | 8 | 8 | 12 | 12 | 8 | 8 | 5 | 5 | 3 | 3 | 9.4 |
| 12 | 18 | 18 | 14 | 14 | 12 | 12 | 8 | 8 | 12 | 12 | 8 | 8 | 5 | 5 | 3 | 3 | 9.4 |
| 13 | 14 | 14 | 12 | 12 | 8 | 8 | 5 | 5 | 8 | 8 | 5 | 5 | 5 | 5 | 2 | 2 | 9.3 |
| 14 | 18 | 18 | 16 | 16 | 6 | 6 | 4 | 4 | 12 | 12 | 10 | 10 | 12 | 12 | 10 | 10 | 9.4 |
| 15 | 12 | 12 | -6 | -6 | 6 | 6 | -2 | -2 | 8 | 8 | -4 | -4 | 8 | 8 | -4 | -4 | 9.2 |
| 16 | 12 | 12 | -6 | -6 | 16 | 16 | -7 | -7 | 8 | 8 | -4 | -4 | 8 | 8 | -4 | -4 | 9.3 |
| | | | | | | | | | | | | | | | | | |

Table 5-2 Eruption sources for model calculation for the 16 different scenarios.

Chapter 6 Comparison of Model Outcomes and the 2004 Tsunami Surveyed Data

6-1 Comparison of Maximum Tsunami Wave Heights from Modelling and Surveyed Data

Siripong, et al. (2005) measured tsunami run-up along the Andaman coast of Thailand, including Bang Niang Beach, using GPS and Total Station systems. Run-up heights were adjusted for tidal correction to match up with the Mean Sea Level (MSL) of the Andaman's coast. Jarusiri and Choowong (2005) conducted a survey of the tsunami disaster areas of Thailand and created a diagram showing tsunami heights (above ground level) along Bang Niang Beach which can be used to compare with the model outcomes of this research. Matsutomi et al. (2005) surveyed tsunami effects along the west coast of Thailand, especially in Phang-Nga and Phuket. Khao Lak was one of the main areas of interest. Traces on the ground and on buildings were used for estimating inundation and run-up of tsunami waves at Khao Lak and Phuket. Tide tables for Phuket were used for tidal corrections. Maximum tsunami wave heights, inundation distances, inundation area, cross section profiles of the wave, tsunami arrival time and wave interval from the model were compared to surveyed data.

Results generated by the ComMIT model for the 16 'rupture scenarios' were compared with surveyed data from the 18 locations where observations had been made by Siripong, et al. (2005), Jarusiri and Choowong (2005) and Matsutomi et al. (2005) using NCBrowse software. Tsunami maximum wave heights from the surveyed data, and those from the model are plotted along the coastline of Khao Lak. These results are shown in Figure 6-1 to Figure 6-5.

As the exact form of the 2004 earthquake rupture pattern was uncertain a number of different model scenarios were set-up and their outcomes compared to the observations. Scenarios 1 and 2, which vary their rupture heights by using half of the tsunami wave heights of the area perpendicular to the rupture, yield low tsunami wave heights when compared to the surveyed data, using either a low or a high friction coefficient (Figure 6-1). According to Scenarios 3, 4, 5 and 6, whose rupture heights vary by dividing

their ruptures into 3 sections, with each block in the same section having the same uplifts, also produce tsunami wave heights that are lower than those recorded by the surveys, especially for the northern part of the study area. However, the model outcomes are generally consistent with the surveyed data at Bang Niang and Nang Thong Beaches, except for Scenario 5.

In Scenarios 7, 8, 9 and 10 (Figure 6-3), the earthquake rupture is simulated using higher uplift of the two middle blocks and lower uplift of the two outer blocks. Scenario 7, which represents $M_w = 9.5$ earthquake rupture, yields tsunami waves which are too high, especially along the Bang Niang and Nang Thong Beaches compared to the surveyed data (Figure 6-3). Scenario 9 ($M_w = 9.4$) has higher uplift for the Nicobar Section also predicts higher wave than those observed from the surveys. Scenario 8 (also $M_w = 9.4$) has moderate rupture height at the Nicobar Section and predicts tsunami wave heights in general agreement with the surveyed results.

Scenarios 11, 12 and 13 (Figure 6-4) were generated by varying the rupture heights by placing higher uplift for the two western blocks and lower uplift for the two eastern blocks. Scenario 13 ($M_w = 9.3$), using the lowest rupture heights with the greatest friction coefficient, resulted in a tsunami which is too low. Scenario 12 with a moderate rupture ($M_w = 9.4$) but with high friction coefficient also yields a tsunami wave which is too low. Scenario 11, with moderate slip and low friction coefficient, yields the optimal tsunami wave height, in general agreement with the surveyed data. Scenarios 15 and 16 (Figure 6-5) predicts a tsunami wave crest that reaches the Thailand coast before the trough, which is the opposite of the real situation of the 2004 tsunami so Scenarios 15 and 16 were discarded from our further consideration.

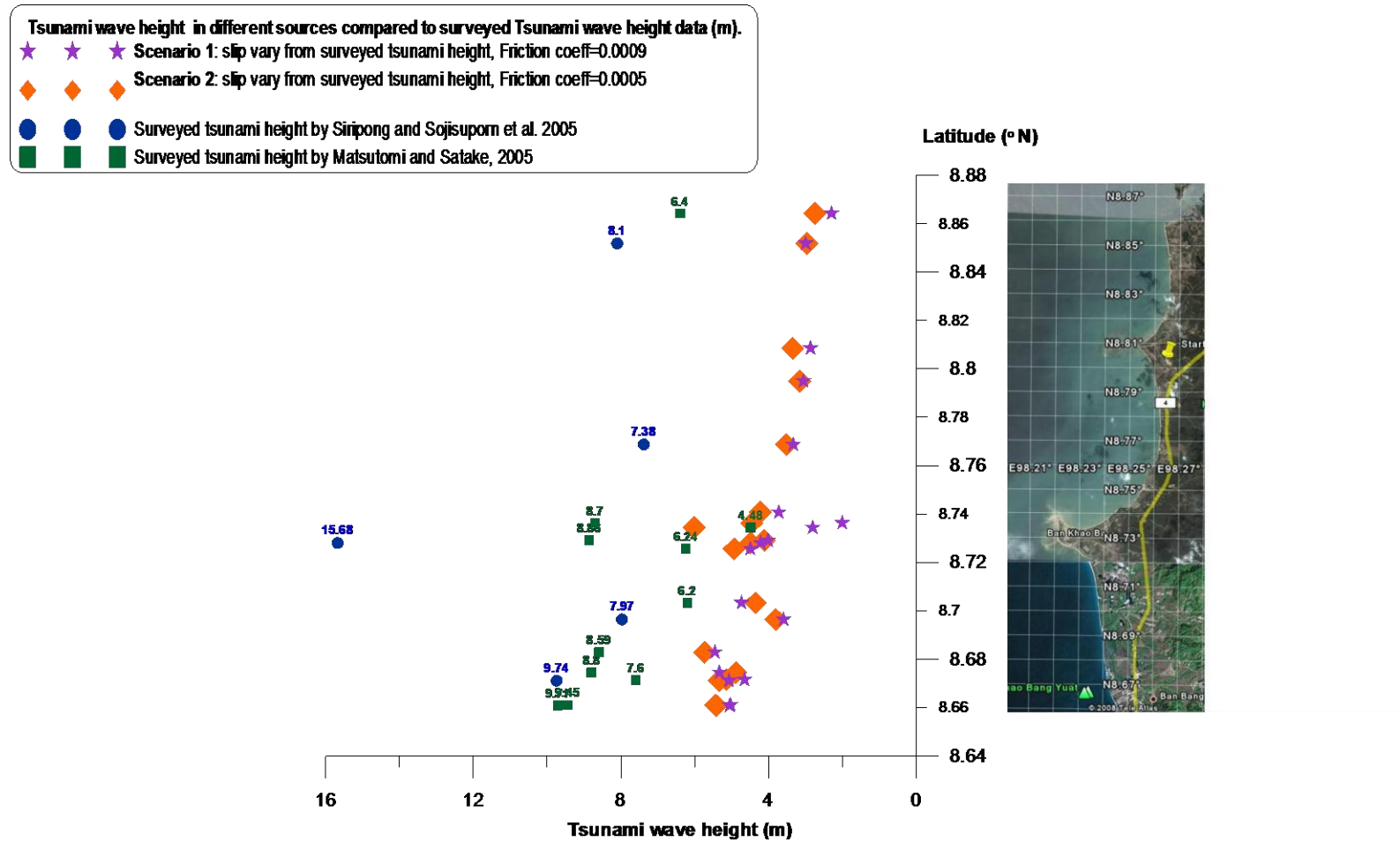


Figure 6-1 Comparison of tsunami wave maximum height of scenarios 1 and 2 with surveyed data.

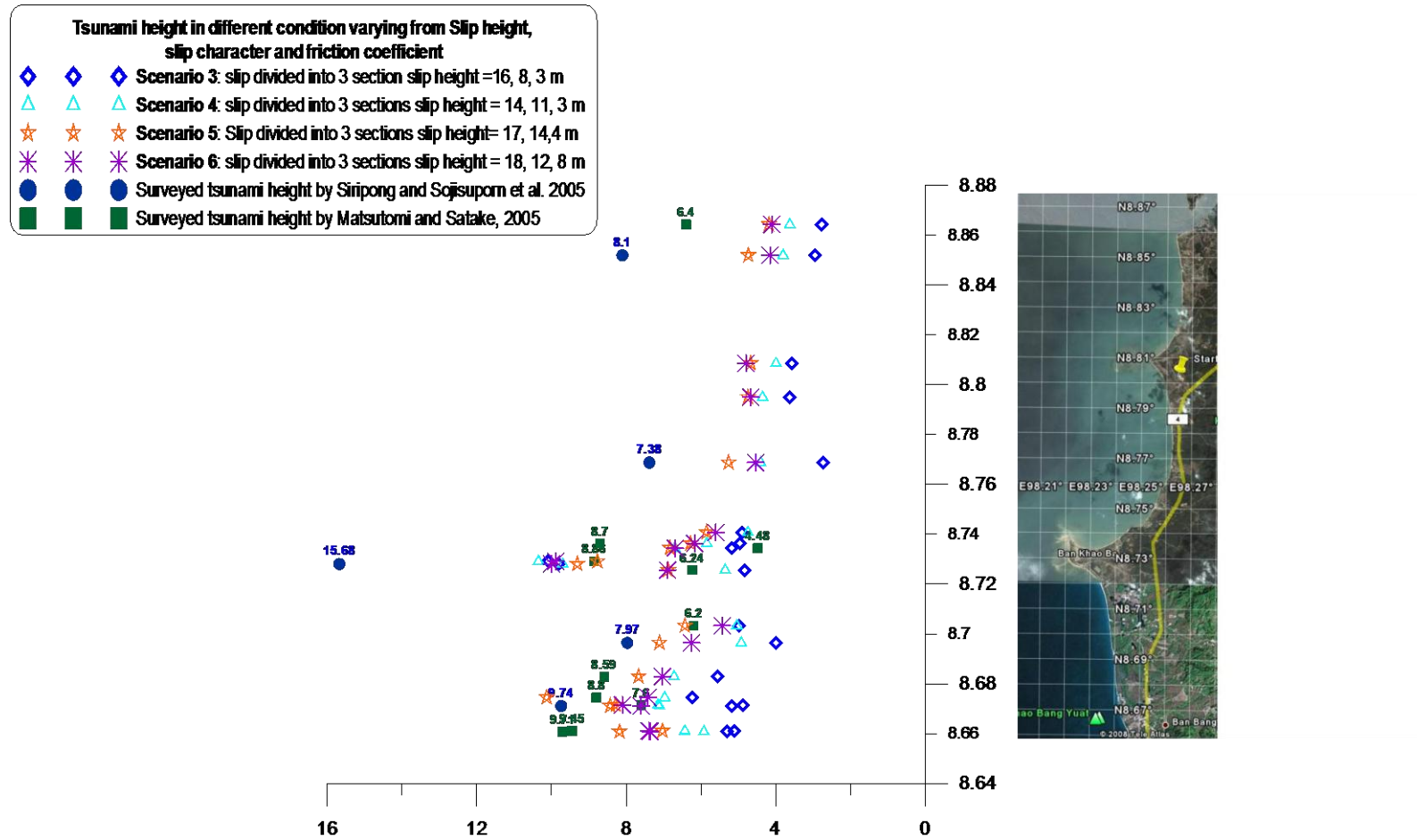


Figure 6-2 Comparison of tsunami maximum wave height from scenarios 3, 4, 5 and 6 with surveyed data.

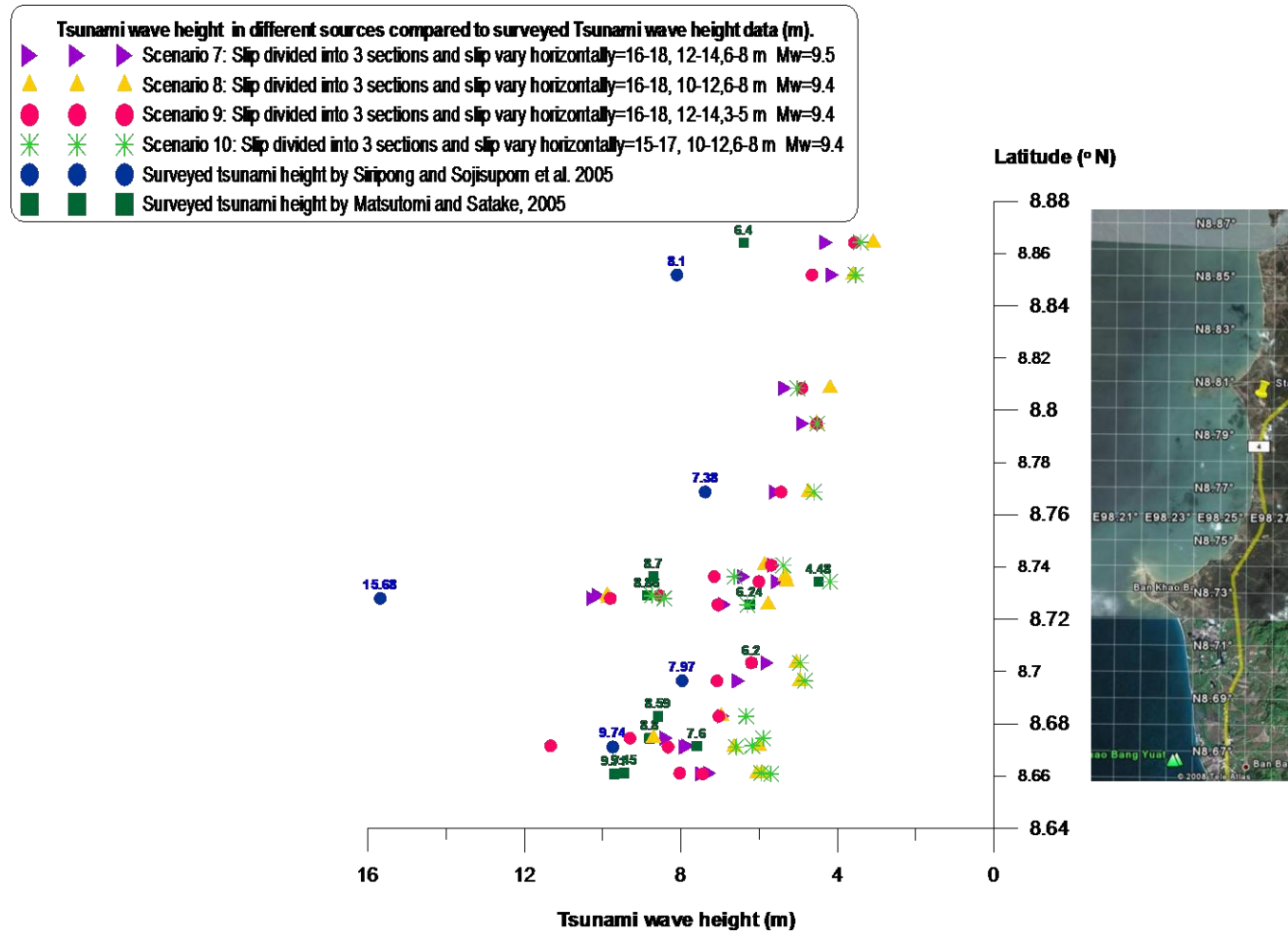


Figure 6-3 Comparison of tsunami maximum wave height from scenarios 7, 8, 9 and 10 with surveyed data.

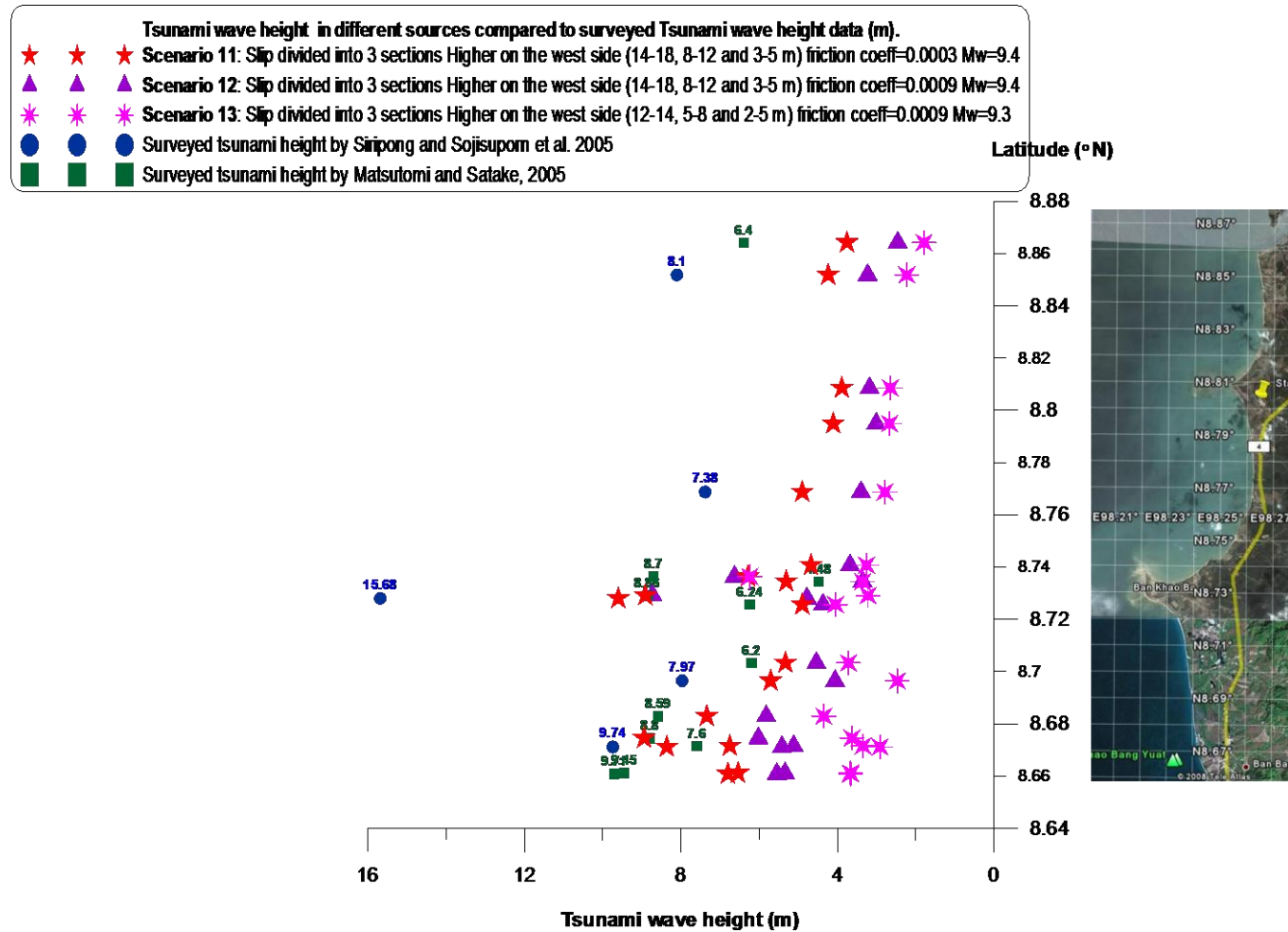


Figure 6-4 Comparison of tsunami maximum wave height from scenarios 11, 12, and 13 with surveyed data.

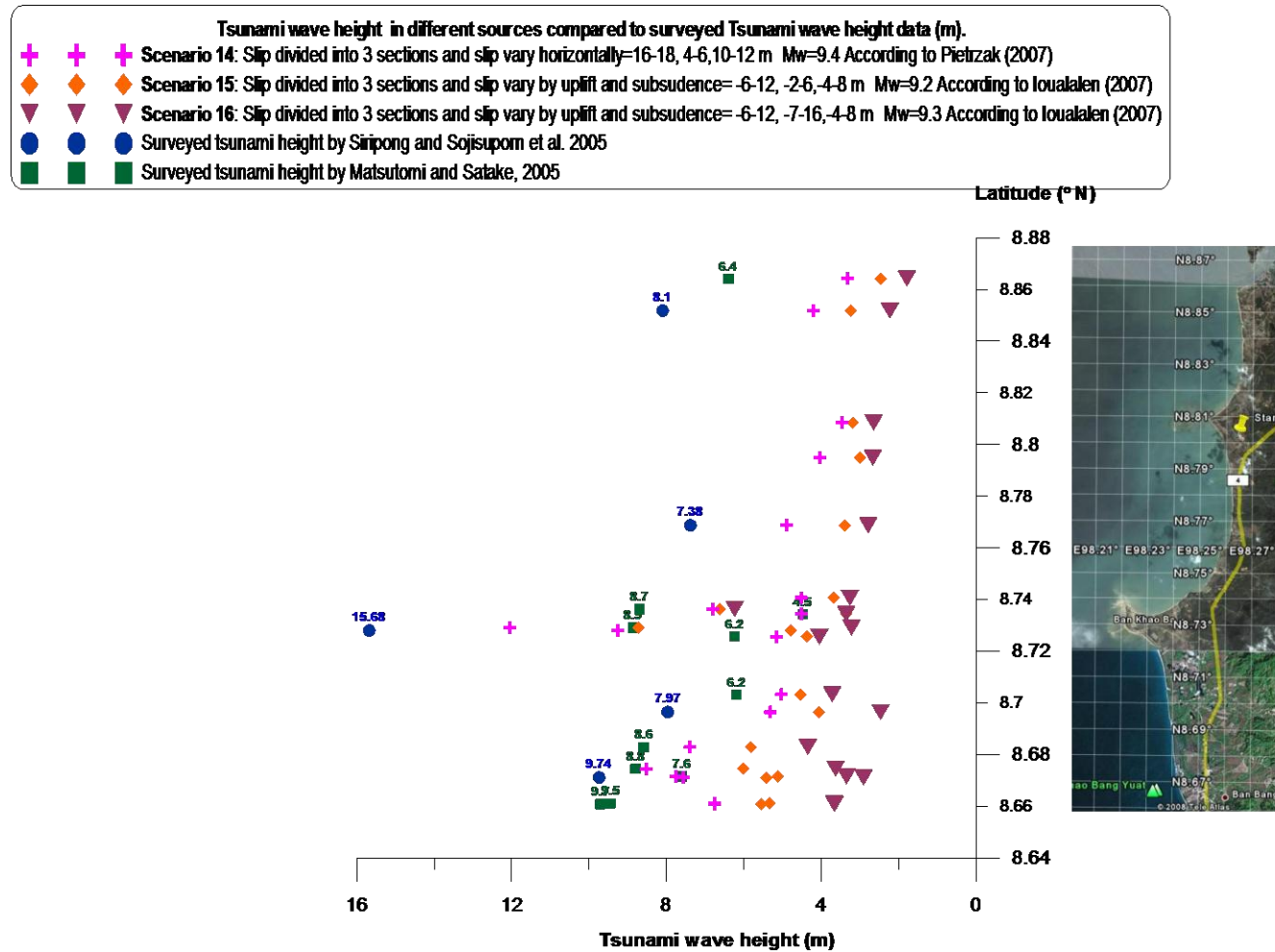


Figure 6-5 Comparison of tsunami maximum wave height from scenarios 14, 15, and 16 with surveyed data.

Apart from the direct tsunami wave height comparison, linear regression between the model results and the surveyed data of maximum wave heights for the same locations were can be used to objectively assess the degree to which the model explains the patterns of observations. The R^2 value (where R is the correlation coefficient) measures the proportion of the variance explained by the model. Comparison between the linear regression lines of the maximum modelled and observed tsunami wave height of 14 (excluding 15 and 16) scenarios for the observations of Siripong et al. (2005) and Matsutomi et al. (2005), and the combined data, are shown in Figure 6-6, Figure 6-7 and Figure 6-8. In addition, the R^2 values for the linear regressions between maximum wave heights predicted by the model and by the surveys of Matsutomi et al. (2005) and Siripong, et al. (2005) individually, and the R^2 of the combined data, are shown in Table 6-1.

The model Scenario 11 shows the best overall agreement ($R^2 = 0.514$) with the surveys; Scenario 3 has the highest R^2 (0.976) in comparison to Siripong, et al. (2005) but is poor in comparison to Matsutomi et al. (2005) ($R^2 = 0.140$). In terms of the *absolute* height predictions none of the Scenarios predict the higher (>12m) waves observed by Siripong, et al. (2005) although Scenario 11 is one of the best predictors. Scenario 11 was therefore selected for use as the prototype model for the 2004 Indian Ocean tsunami and future tsunami simulations in the region can be implied that scenario 11 from the model, which represents the idea of horizontal movement and high uplift on the west side of the rupture, yields wave heights that correspond to the surveyed maximum wave height, and should be selected to use as a prototype for the 2004 Indian Ocean tsunami and future tsunami simulations. It corresponds to Lay et al. (2005), who divided the 2004 rupture into 3 segments: a 420 km Sumatra segment, a 325 km Nicobar segment and a 570 km Andaman segment. In addition, the Sumatra segment had large rapid slip, and the Nicobar and Andaman Segments had a slow slip of around 5 m. Also, two to three times of slip is required for the northern part of the 2004 eruption (the Andaman Segment). Moreover, the uplift occurred on the west side and the submerged happened on the east side of Nicobar and Andaman Islands.

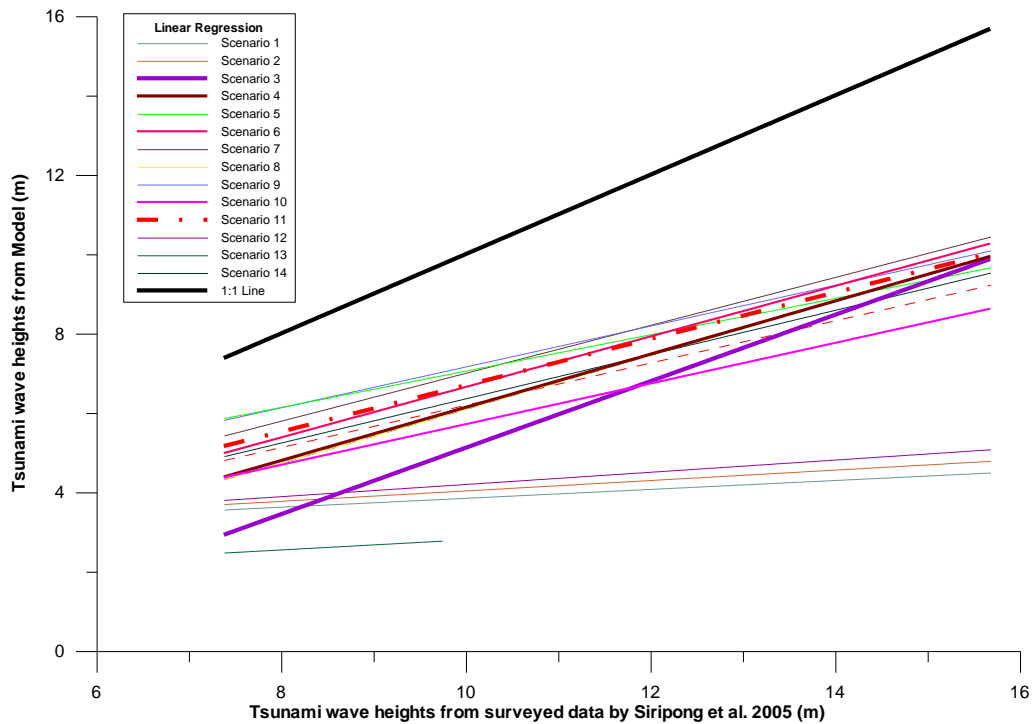


Figure 6-6 Linear regression lines of modelled maximum tsunami wave heights of 14 scenarios against the surveyed data by Siripong, et al. (2005). Also shown is the one-to-one line (black).

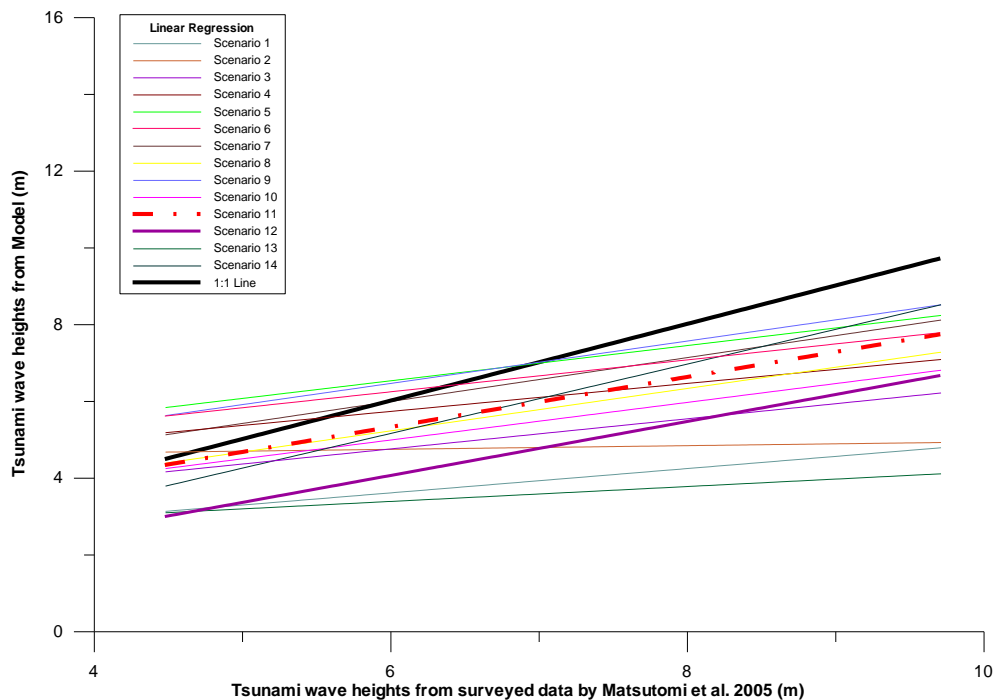


Figure 6-7 Linear regression lines of modelled maximum tsunami wave heights of 14 scenarios against the surveyed data by Matsutomi (2005). Also shown is the one-to-one line (black).

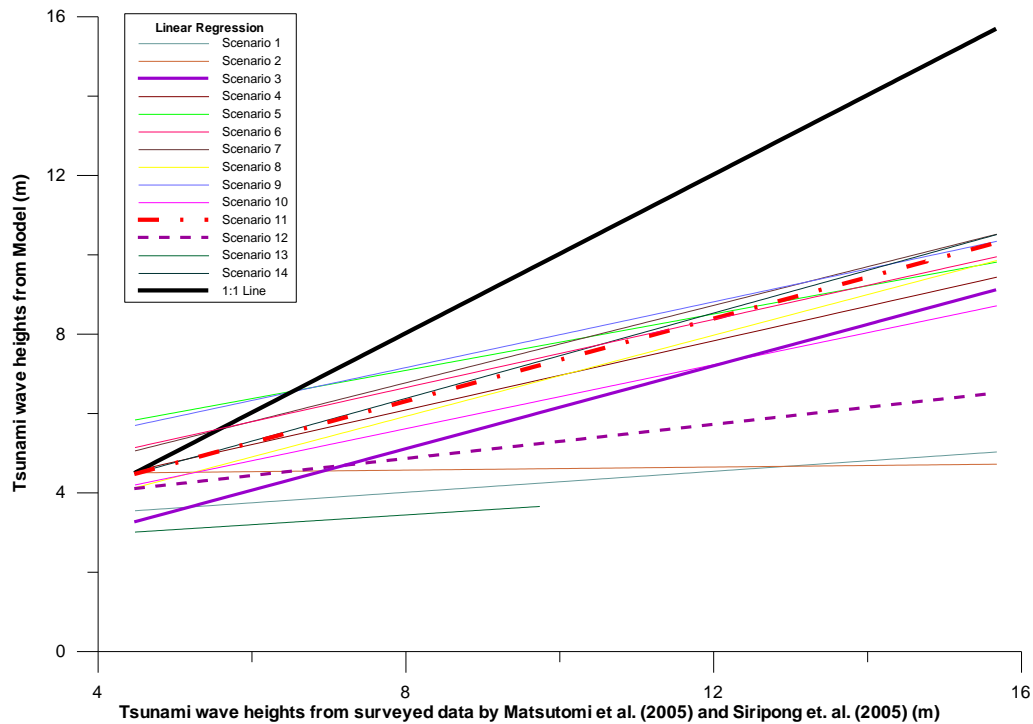


Figure 6-8 Linear regression lines of modelled maximum tsunami wave heights of 14 scenarios against the combined surveyed data by Matsutomi (2005) and Siripong, et al. (2005). Also shown is the one-to-one line (black).

| Scenario | Model compared to Siripong, 2005 R^2 | Model compared to Matsutomi, 2005 R^2 | Model R^2 compared to combined surveyed data |
|----------|--|---|--|
| 1 | 0.218 | 0.183 | 0.085 |
| 2 | 0.236 | 0.007 | 0.002 |
| 3 | 0.976 | 0.14 | 0.372 |
| 4 | 0.892 | 0.133 | 0.325 |
| 5 | 0.628 | 0.244 | 0.28 |
| 6 | 0.826 | 0.223 | 0.363 |
| 7 | 0.783 | 0.382 | 0.463 |
| 8 | 0.739 | 0.256 | 0.406 |
| 9 | 0.704 | 0.217 | 0.267 |
| 10 | 0.826 | 0.351 | 0.424 |
| 11 | 0.747 | 0.464 | 0.514 |
| 12 | 0.32 | 0.497 | 0.117 |
| 13 | 0.172 | 0.094 | 0.032 |
| 14 | 0.822 | 0.414 | 0.35 |

Table 6-1 R^2 values for the linear regression of predicted against observed (Matsutomi et al. (2005) and Siripong et al. (2005) tsunami wave heights for 14 rupture scenarios

6-2 Comparison of Modelled Tsunami Profiles of Scenario 11 with Surveyed Data

Model outcomes from Scenario 11 were compared to the cross section profiles surveyed by Siripong, et al. (2005), Jarusiri and Choowong (2005) and Hori et al. (2007). From the modelling, the maximum height of the tsunami wave that inundated Bang La-on Beach (part of Nang Thong Beach) is shown in Figure 6-9. The whole area was inundated by the tsunami wave run up reaching +8-10 m (above MSL). The inundation wave height at Bang La-on Beach from Siripong, et al. (2005) were extracted and plotted to compare with the model results along the same profile (Figure 6-9). The tsunami wave heights along the Bang La-on Beach profile peaks at +10 m above MSL at 120 m from the shoreline (water depth 7.5 m) in good agreement with the +9.6 m surveyed by Siripong, et al. (2005) (Figure 6-9). However, the model yields a lower wave height than that surveyed by Siripong et al. (2005), close to the beach. Both sets of data show a drop in tsunami wave height to +8 m above MSL at ~160 m from the shoreline.

In Figure 6-10, model outcomes are compared to Siripong, et al. (2005) and Jarusiri and Choowong (2005) data of the same profile of Nang Thong Beach. Tsunami wave height from the model shows an approximately uniform wave along the profile (+7-8 m MSL) from the coastline to 1200 m inland. In contrast, data from Siripong, et al. (2005) show a maximum of +12 m at the coastline and 200 m, dropping to approximately 8.2 m at 300 m and 1100 m from the shore. Data from the Jarusiri and Choowong (2005) survey shows a pattern of lower waves than Siripong, et al. (2005). The Jarusiri and Choowong (2005) survey, estimated waves of ~10-11 m high at the beach, and dropped to almost reach approximately 4 m above sea level before it rose up again at 350 m inland, and the overall wave height was only 3-6 m for 400-800 m from the coastline. Mean sea level adjustment and poorly defined location of the Jarusiri and Choowong (2005) survey location may have resulted in the discrepancy between the two surveys.

Figure 6-11 shows a comparison of the wave heights from model outcomes along a cross section with wave heights at specific points surveyed by Hori et al. (2007). Both sets of data yield comparable wave pattern, particularly in the nearshore area. Both

yield a wave of ~7-8 m above MSL high 200 m inland but the wave height 700 m inland from the survey is 1-2 m lower than that indicated by the model.

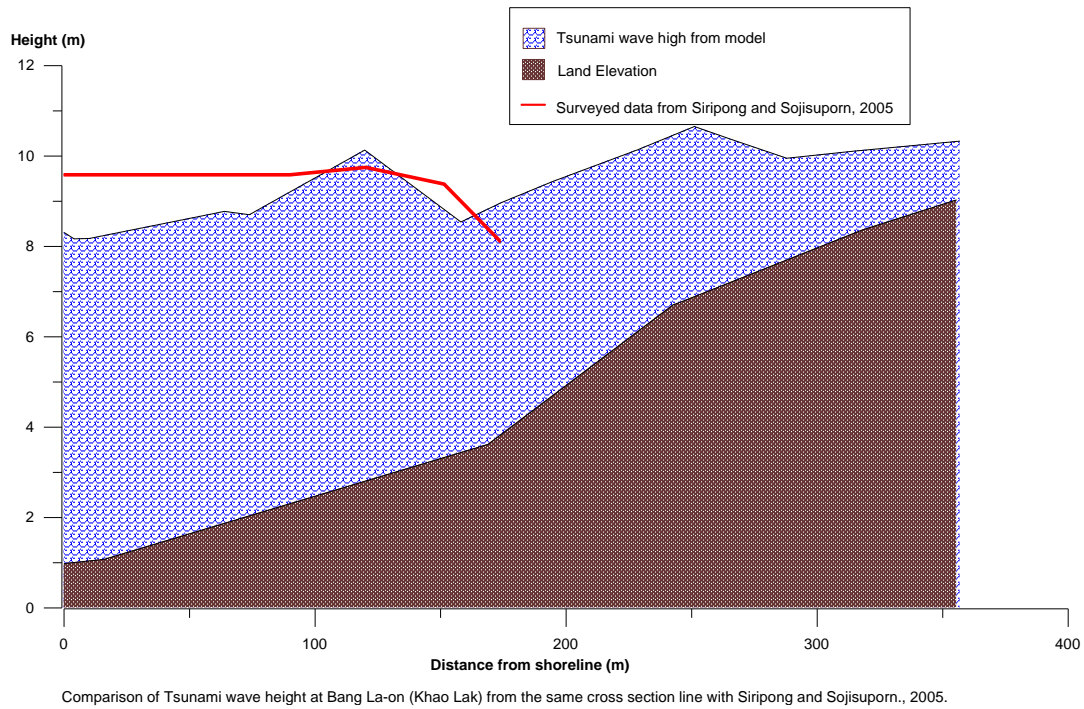


Figure 6-9 Comparison of tsunami wave height at Bang La-on beach along the same cross section line with Siripong, et al. (2005)

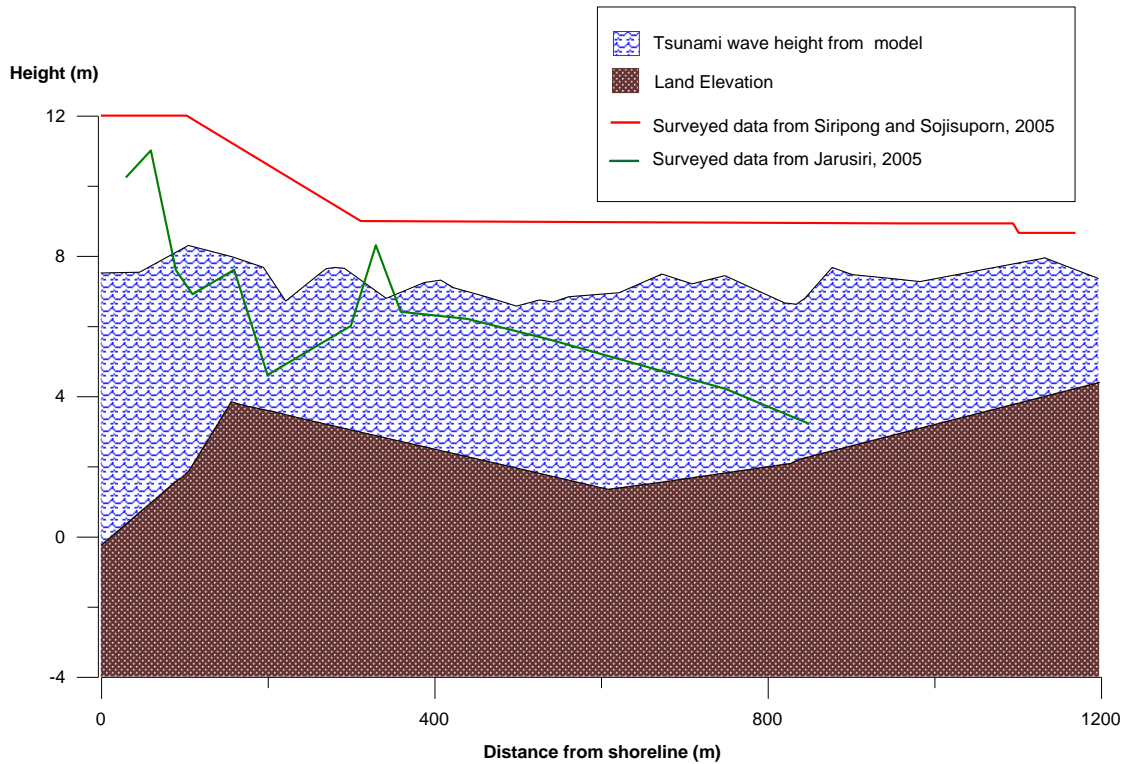
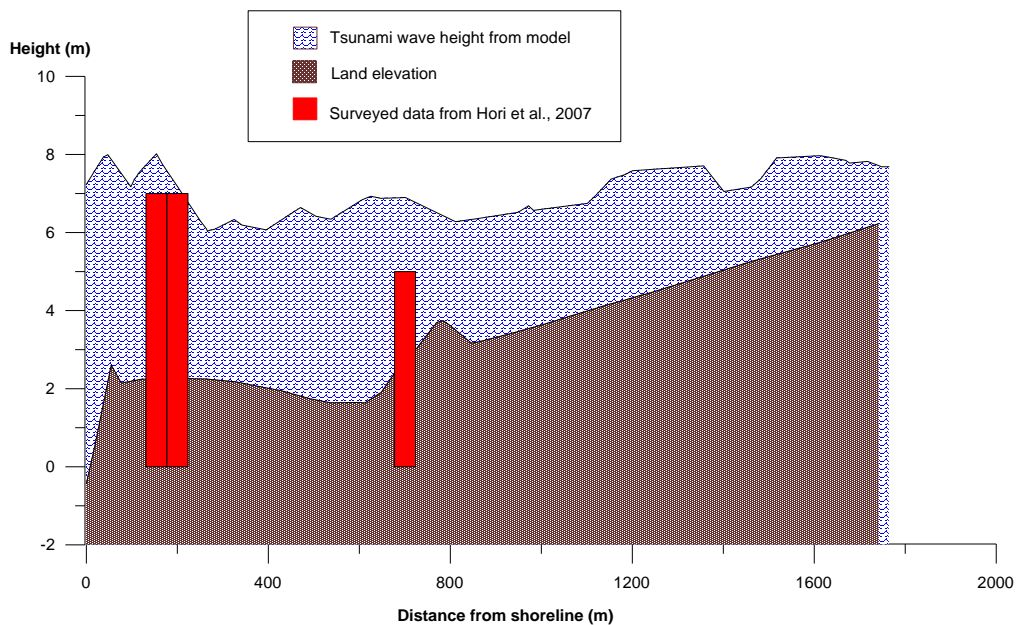


Figure 6-10 Comparison of tsunami wave heights at Nang Thong Beach along the same cross section line as Siripong, et al. (2005) and Jarusiri and Choowong (2005).



Comparison of Tsunami wave height at Khao Lak from the same cross section line with Hori et al., 2007

Figure 6-11 Comparison of tsunami wave heights across Bang Niang Beach through the specific points surveyed by Hori et al. (2007)

6-3 Comparison of Tsunami Inundation Area from the Model with Surveyed Inundation Area of the 2004 Indian Ocean Tsunami.

Inundation distance and area are the other significant parameters used for validating the model results with the surveyed data to evaluate the accuracy of the model. Inundation area of Khao Lak (from Khao Lak National Park to Namkhem Fishing Village) inundated by the 2004 tsunami was derived from aerial photos of the area taken shortly after the event incorporating with the 2004 tsunami inundation data conducted by the Department of Mineral Resources of Thailand staff (Figure 6-12). At Namkhem Fishing Village, the aerial photos show that the inundation area covered the low-lying plain along the banks of the Pak Ko Canal but the model misses the inundation along the canal banks (Figure 6-12: A) probably because of the absence of reliable bathymetry of the canal and topography along both sides of the canal. So, for simulating flooding and inundation along the canal due to a future tsunami it will be necessary to produce a more accuracy bathymetry and topography of this area. The lack of the detailed topography along the Pak Ko embankment also resulted in a smaller inundation area for the backshore and less inundation along the west side of the canal than the actual occurred. Inundation areas at Tabtawan Beach and Bang Sak Beach compare well with the aerial photos.

The area which shows distinctly differences between the model and surveyed is Pak Weeb Beach, located north of Pakarang Cape. Pak Weeb Beach is situated between two hills and the model does not predict well in this region of complex topography (Figure 6-12: B); the model predicted that the inundation area covered the Pak Weeb Beach although this area was not flooded during the 2004 tsunami. For the future research, more detailed topographic data of the slightly high altitude should be included to ensure more reliable inundation map for mitigation.

In general, the inundation area from the model compares well with the aerial photo data of Khukkhak Beach, Bang Niang Beach and Nang Thong Beach; however, the inundation area from the model slightly floods beyond that of the survey, except for the southern part of the detailed study area (backshore of Nang Thong Beach and Sunset Beach) (Figure 6-13). This might be the effect of wave reflection and refraction from

nearby coastal areas and adjacent islands and capes that cause complex wave pattern for the southern part of Nang Thong Beach, which the model cannot completely simulate. Also, the headland of the Khao Lak National Park (Hinchang Cape) partly blocks the wave that travels from the southwest in the model simulation, resulting in less effect of the wave on the southern part of Nang Thong Beach.

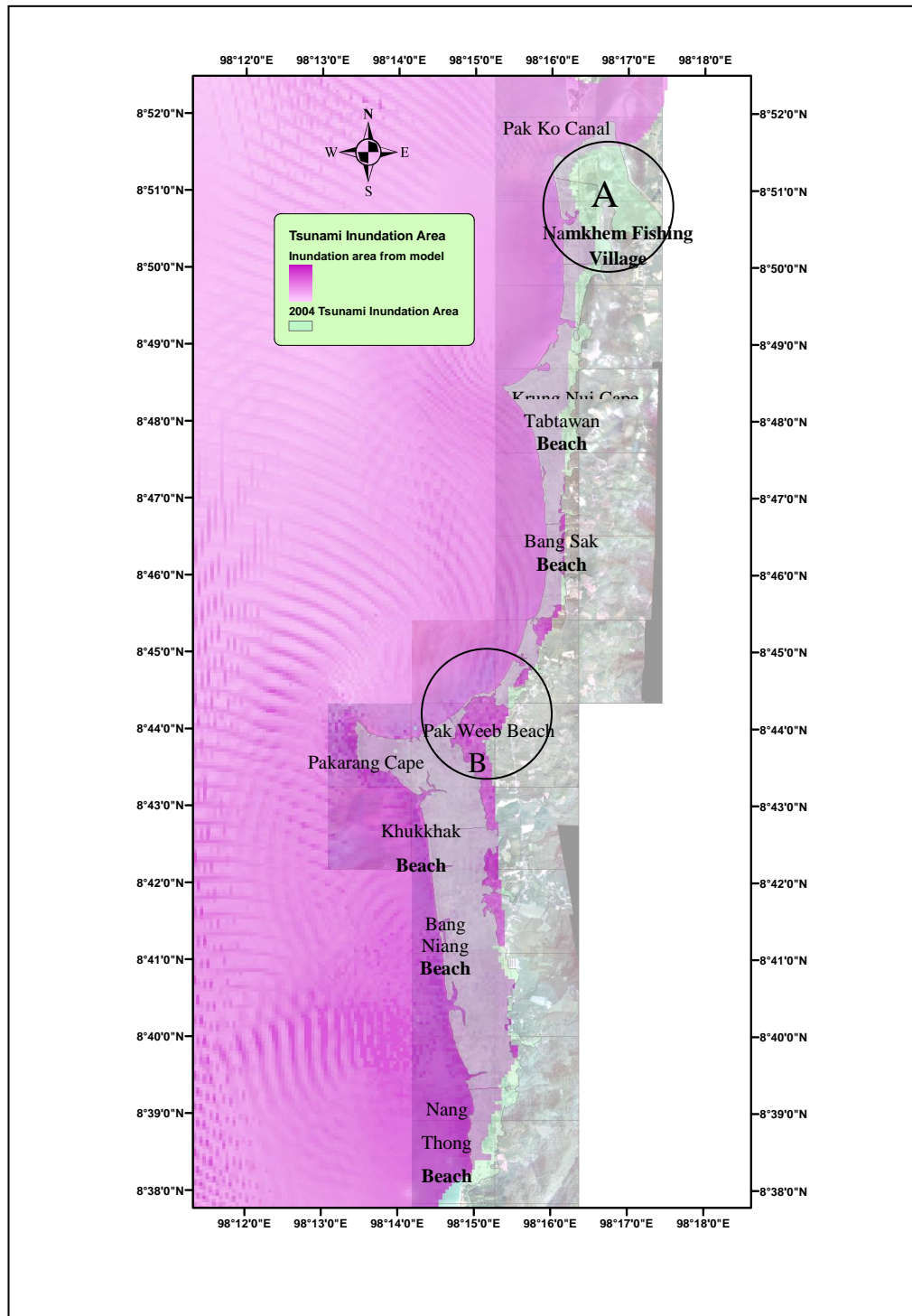


Figure 6-12 Comparison of tsunami inundation area of Khao Lak from model with real inundation from the surveyed data of the 2004 tsunami.

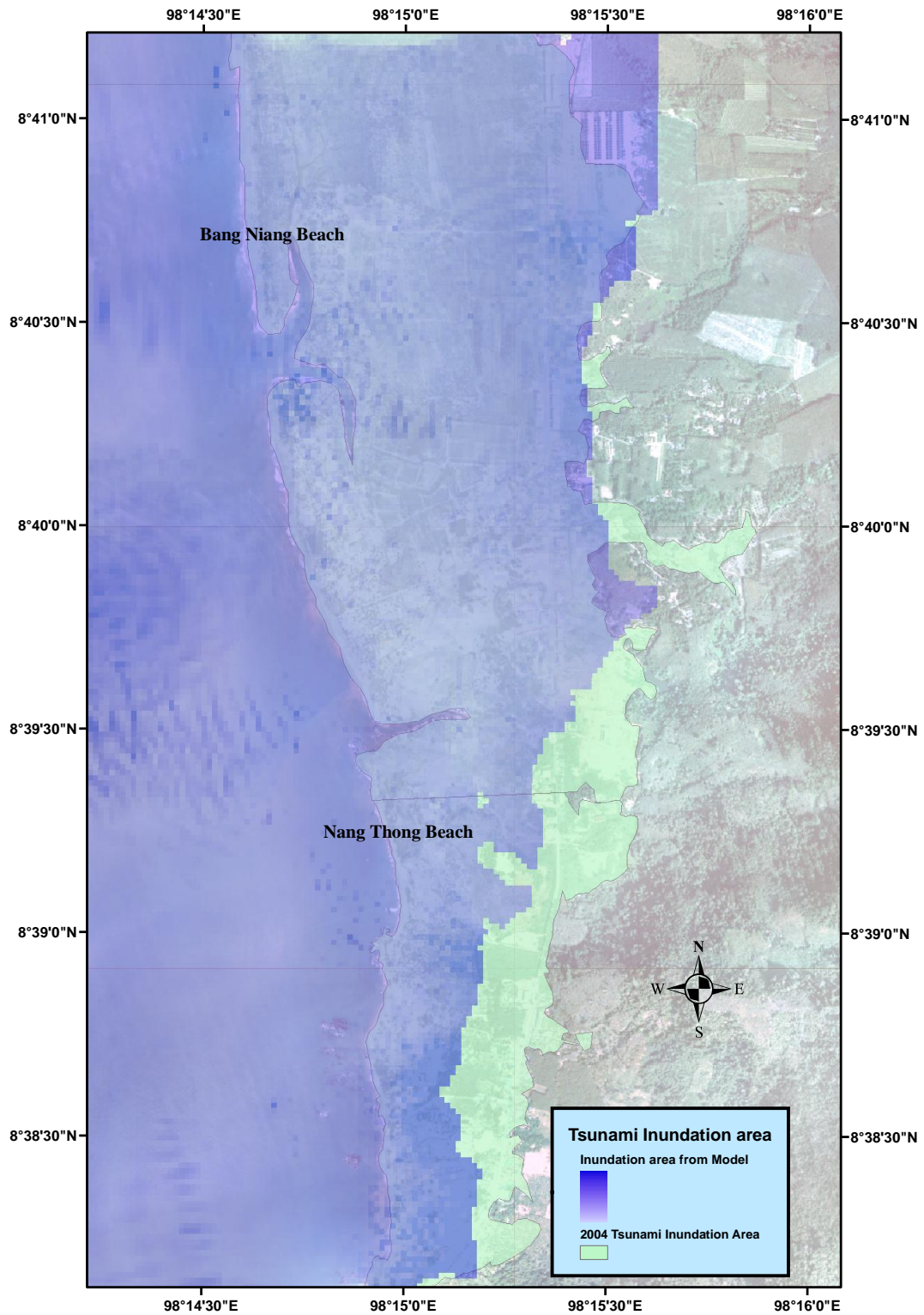


Figure 6-13 Comparison of tsunami inundation area simulated by model vs. real inundation area from surveyed data of Bang Niang and Nang Thong Beaches.

6-4 Effects of Tide on Tsunami Wave Height and Inundation Distance

Tide plays an important role in controlling both tsunami height and inundation distance and is a significant factor which influences the tsunami intensity. The inundation distance of the model, which includes +1 m tide effect (Figure 6-14), is 200-600 m further inland than those where the tidal effects have been excluded (Figure 6-15). The maximum tsunami wave height in specific areas also changes; maximum heights of the tsunami wave with +1 m tide are approximately 1.0-1.5 m higher than those without tidal effect. Inclusion of the high tide in the model, resulted in more reliable results when compared to the surveyed data (Figure 6-13), bathymetric and topographic data of Bang Niang and Nang Thong Beaches were adjusted by adding 1 m tide to represent the effects of high tide and were used as inputs for the MOST model to study the differences of effects of high tide influences.

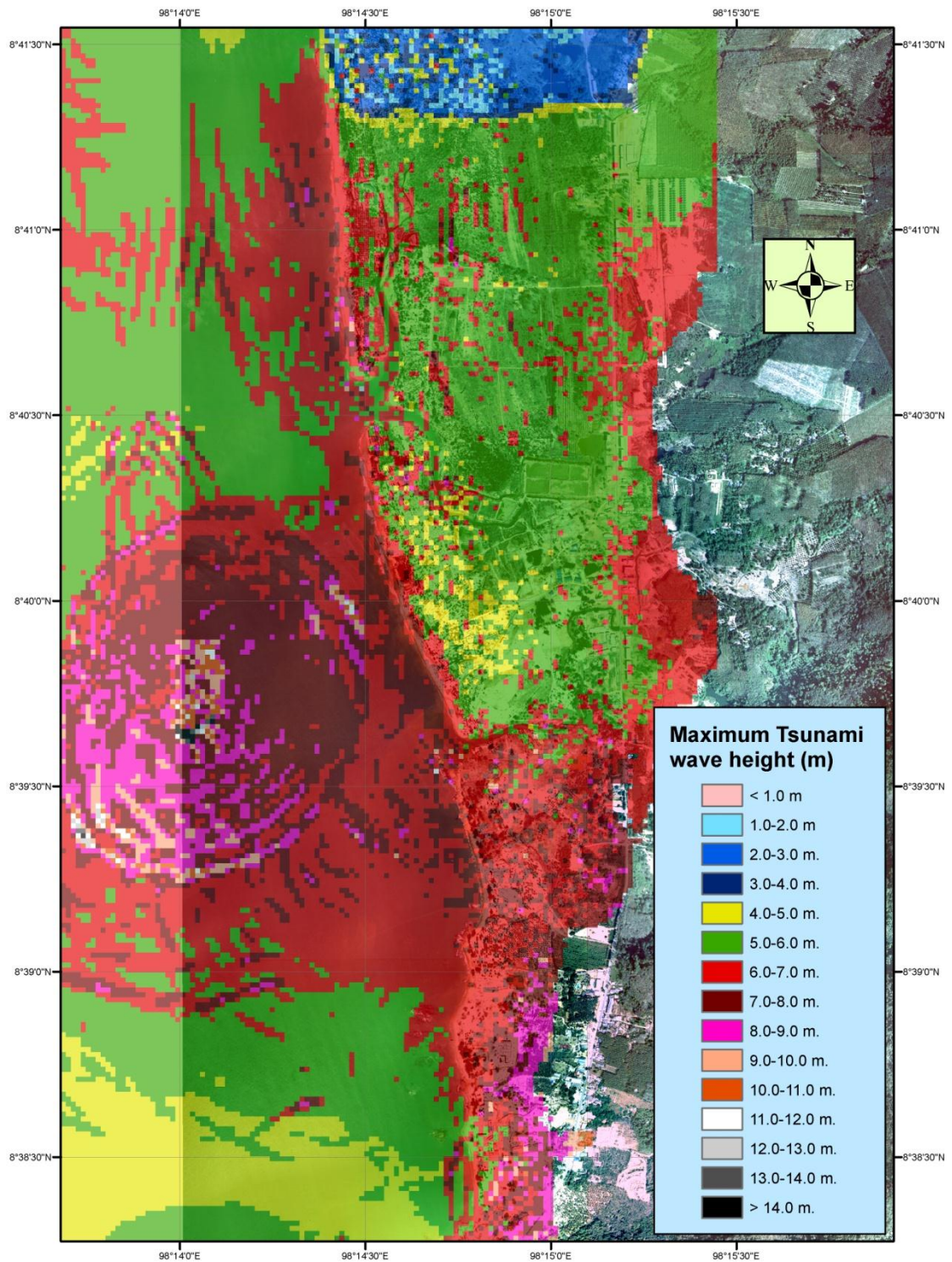


Figure 6-14 Inundation area and maximum wave height of tsunami wave along the Bang Niang Beach and Nang Thong Beach with 1.0 m tide.

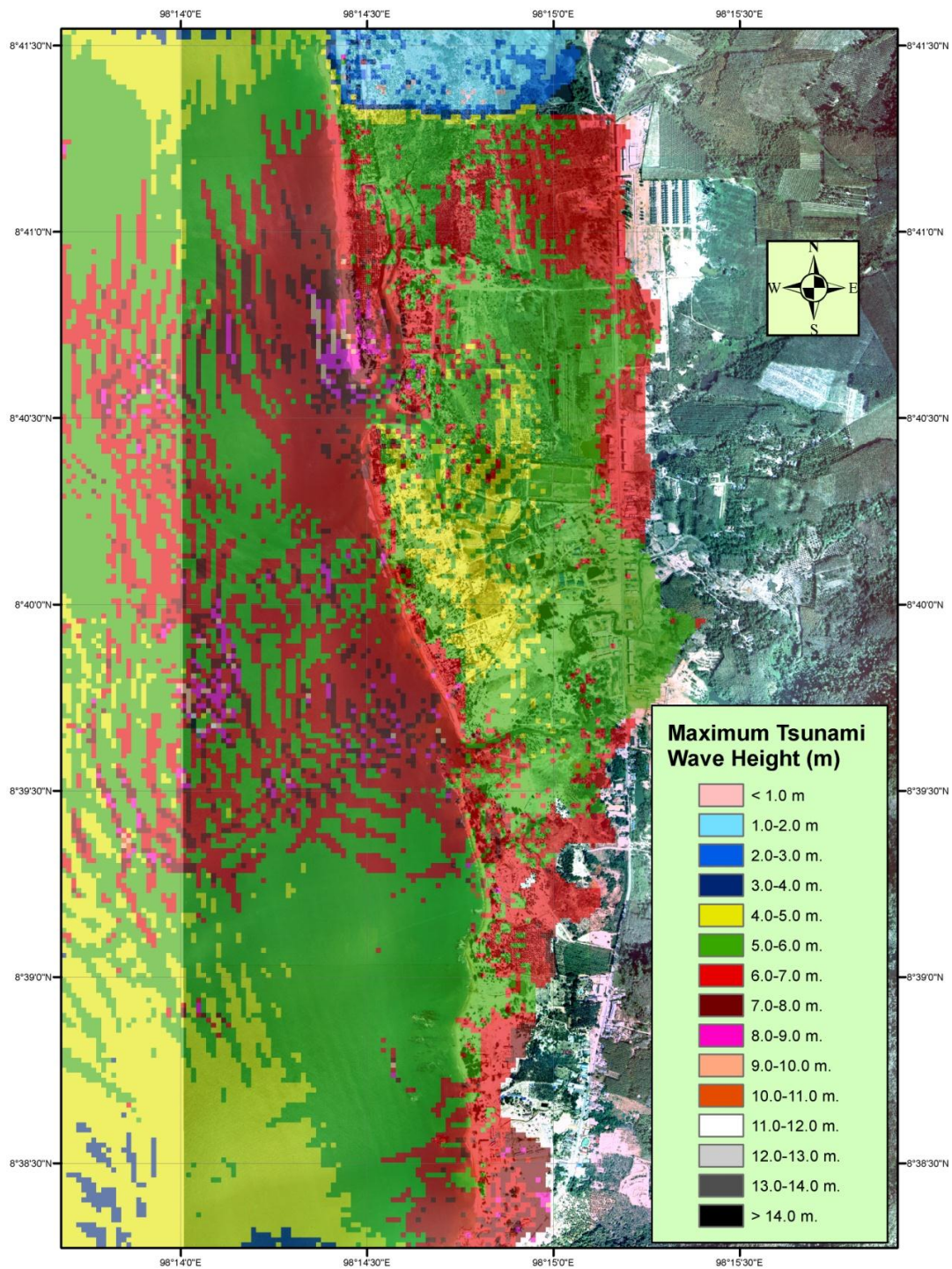


Figure 6-15 Inundation area and maximum wave height of tsunami wave along the Bang Niang Beach and Nang Thong Beach without tidal effects.

6-5 Comparison of Tsunami Arrival Time from the Model and Tide Gauge Records of Kuraburi.

The Tsunami waves reached different regions of the Andaman coast of Thailand at different times and with different patterns. Tsunami wave characteristics at Kuraburi tide gauge station (Figure 6-16) shows a similar pattern of wave characteristics as those computed by the model for Bang Niang Beach but with different arrival times. The wave trough arrived at the Kuraburi tide gauge station before the wave crest (Tsuji et al., 2006) which corresponds to the model. The tide gauge recorded at least 5 significant wave crests reaching the station which is again comparable to the model result (Figure 6-16). At Kuraburi, the third wave is the maximum one; also, the third wave is the highest from the model, especially at Bang Niang Beach. Rabinovich and Thomson (2007) reported that the first 3 tsunami waves, recorded by tide gauge station at Kuraburi, had a similar height of 1.35-1.4; the model also shows that the characteristics of the first 3 wave crests were similar, ranging from 5 to 6 m high at the shoreline.

Tsuji et al. (2006) reported that the first trough arrived at the Kuraburi tide gauge station at 10.32 am (+2h 34 min after the earthquake) indicated by 0 in Figure 6-16. The water level continued to drop and reached the maximum regression at 10.58 am (+3h 00 min). First wave crest arrived at the station at 11.12 am (+3h 14 min) indicated by 1 in Figure 6-16. The maximum tsunami height (expressed as deviation from the expected astronomical tide at Kuraburi) was recorded at 14.28 (+6h 30 min) for 1.40 m (indicated by 5 in Figure 6-16). The period between the wave crests was approximately 40 min. However, the arrival time recorded at this tide gauge appeared not to be consistent due to an instrumental error. Rabinovich and Thomson (2007) state that tide gauge at Kuraburi is an analogue device which is designed for measuring tides, not for the shorter wave-length tsunami wave. The arrival time recorded by the tide gauge at Kuraburi station seems to be not reliable due to timing errors. Tsuji et al. (2006) state that the tide gauge arrival time was shifted 12 min in advance of the exact time. After correcting the time by 12 min the arrival time of the first trough, the first crest and the fifth wave reached the station at +2 h 22 min, +3 h 2 min and +6 h 18 min. However, the model shows the first wave crest arrives at Khao Lak at 2 h 27 min, which is supported by many independent observations and time-stamped photographs taken

around Khoa Lak. The patterns of the wave arrival from the model and the tide gauge data are broadly consistent and helpful for the study of wave pattern.

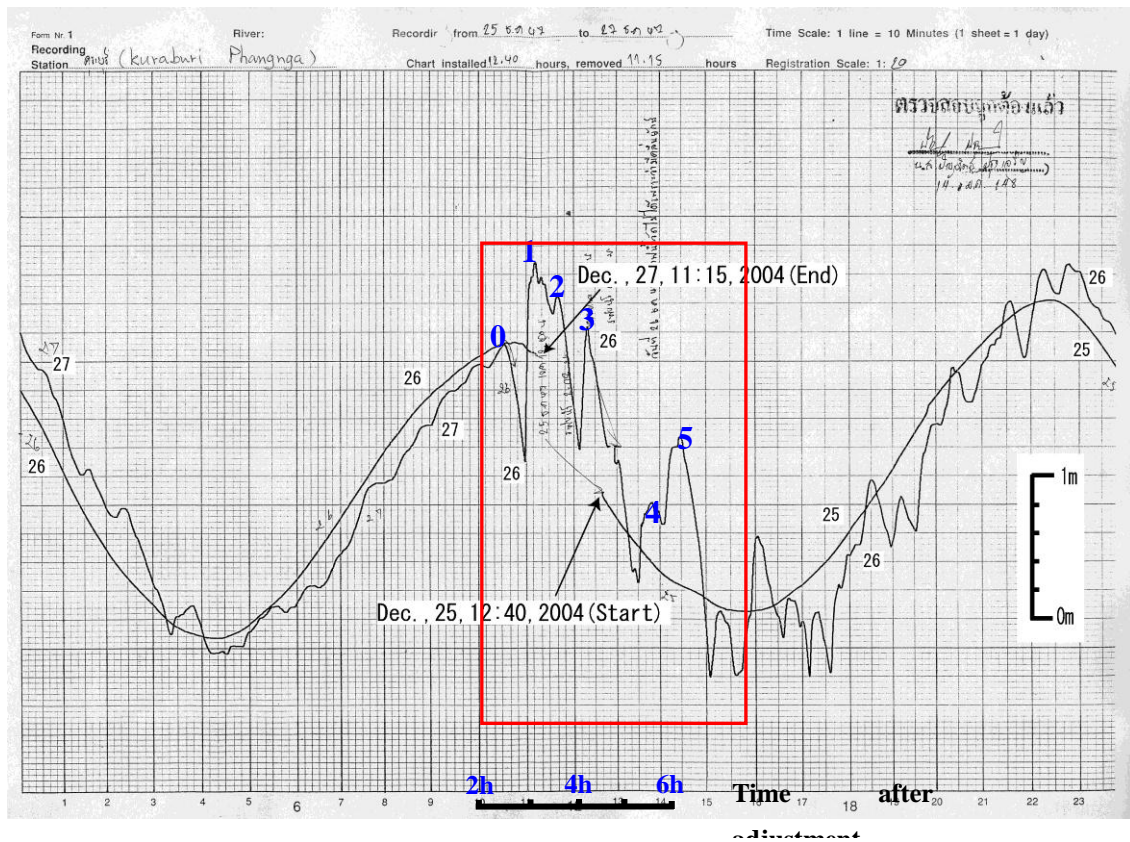


Figure 6-16 Tide gauge data from Kuraburi Naval station, Phang-nga province, north of the study area.

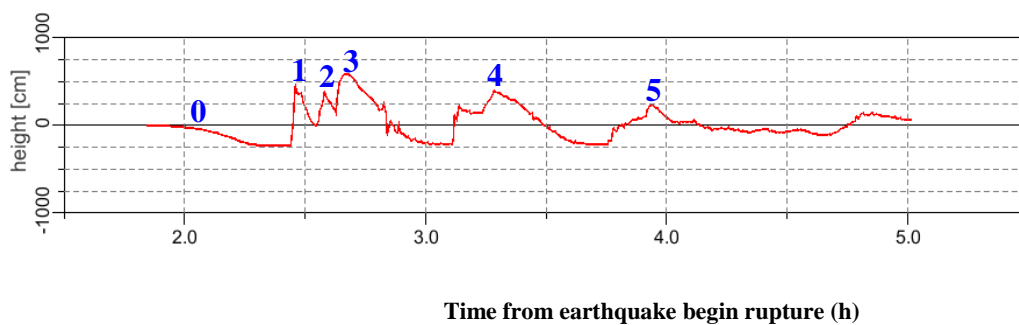


Figure 6-17 Tsunami wave height vs. arrival time at Bang Niang Beach computed from the MOST model and the ComMIT interface of the 2004 Indian Ocean tsunami.

Chapter 7 The 2004 Indian Ocean Tsunami Wave Pattern at Khao Lak: Model Simulation

Numerical modelling is a fundamental tool for understanding past tsunami events and simulating future tsunamis. This research uses the MOST model with the ComMIT interface to simulate the tsunami wave propagation from the 2004 Indian Ocean earthquake. Also, the tsunami from a possible future earthquake in the Indian Ocean which might cause significant effects to the coastal areas of Thailand is used as a source to consider the mitigation needed to protect the coastal population.

Scenario 11 is consistent with the post-tsunami field surveys of maximum run-up made by Siripong et al. (2005) and Matsutomi et al. (2005) and was selected to represent the 2004 Indian Ocean tsunami event which reached the Andaman coast of Thailand from the beginning of the earthquake and tsunami generation to 5 h after the earthquake.

7-1 The 2004 Indian Ocean tsunami wave propagation from the model

The 2004 tsunami wave was mainly generated at the subduction zone near the Nicobar and Andaman Islands as a depressed wave but also propagated from the adjacent sources areas, which contributed to the overall pattern of wave propagation along the Thai coast.

The tsunami wave propagates as a long wave. The height of the tsunami waves in the open ocean is around 0.5-1.5 m. The first trough of the wave reaches the Similan and Miang Islands (~70 km west of Phang-Nga) 1 h 12 min after the earthquake (henceforth +1 h 12 min); the water recedes for 16 min before the first run-up wave arrives at the beach. The sea level drops as much as 7 m on the west coast of the Similan Islands during the first trough. The first tsunami wave crest inundates the Similan Island for 10 min with a maximum height of 6-9 m. A second recession occurs before the second wave floods the Islands for 16 min with the maximum run-up height of 2.5 m. Intermittent flooding of the Islands then occurs for another hour before a high wave crest, reflected back from the Phang-Nga coast, attacks the east coast of the island, 3 h after the earthquake. This 2-3.25 m high wave overwhelms the Islands for 32 min. The

irregular occurrences of recession and flooding continues to occur over the Islands for more than 7 h after the earthquake with decreasing height and severity.

The tsunami wave reaches the Surin Islands at +1 h 40 min. The maximum sea level drop was between 5-7 m for about 20 min before the first crest reaches the beach on the west side of the Islands at +2 h 8 min. The first wave crest moves around the Islands from the west to the east; with a wave run up of 2-5 m inundating the Island for approximately 20 min. Recession and inundation then occurs irregularly for a further 5 h due to incoming waves and reflected waves from the mainland and the adjacent Islands. A reflected wave from the small Tasai Island, located to the south, generated a 3 - 4 m high wave crest that attacks the southwest and southern part of the Surin Islands 4 h after the earthquake.

7-2 Nearshore Tsunami Propagation and Inundation along Khao Lak's Coast.

7-2.1 The first wave trough and crest

According to the model, the first tsunami wave arrives at the nearshore zone of Khao Lak from the southwest as a depression wave (a trough) at +1 h 36 min resulting in a sea level drop. The tsunami draw-down begins between +1 h 45 min and +1 h 50 min. and results in the exposure of the seafloor in the subtidal area (Figure 7-1). At +2 h 8 min, sea level drops to ~1 m below MSL at the tip of Pakarang Cape; maximum draw-down (5-6 m) for the area occurs around +2 h 22 min, resulting in the maximum exposure of the subtidal area (Figure 7-2); rock outcrops along the Nang Thong Beach (Figure 7-2) and coral patches along the Pakarang Cape are exposed. Also, the distinct Pah Island, situated at the mouth of Pak Koh Canal, is completely exposed and visibly emerges in the model scene (Figure 7-1). The seabed in the nearshore stays exposed for more than 20 min before the first crest arrives).

In the model the seafloor emerges up to 10 km from the shoreline (+2 h 22 min), the coral patches around the Pakarang Cape and the rock outcrops along the Nang Thong Beach become totally exposed. This is consistent with the real situation of the 2004 Indian Ocean tsunami which reached the Khao Lak area at 10.11 am local time, (+2 h 13 min); rock outcrops which are entirely submerged even during low tides were exposed (Figure 7-2 and Figure 7-3) and can be compare to the model results from +2 h 3 min to +2 h 22 min.

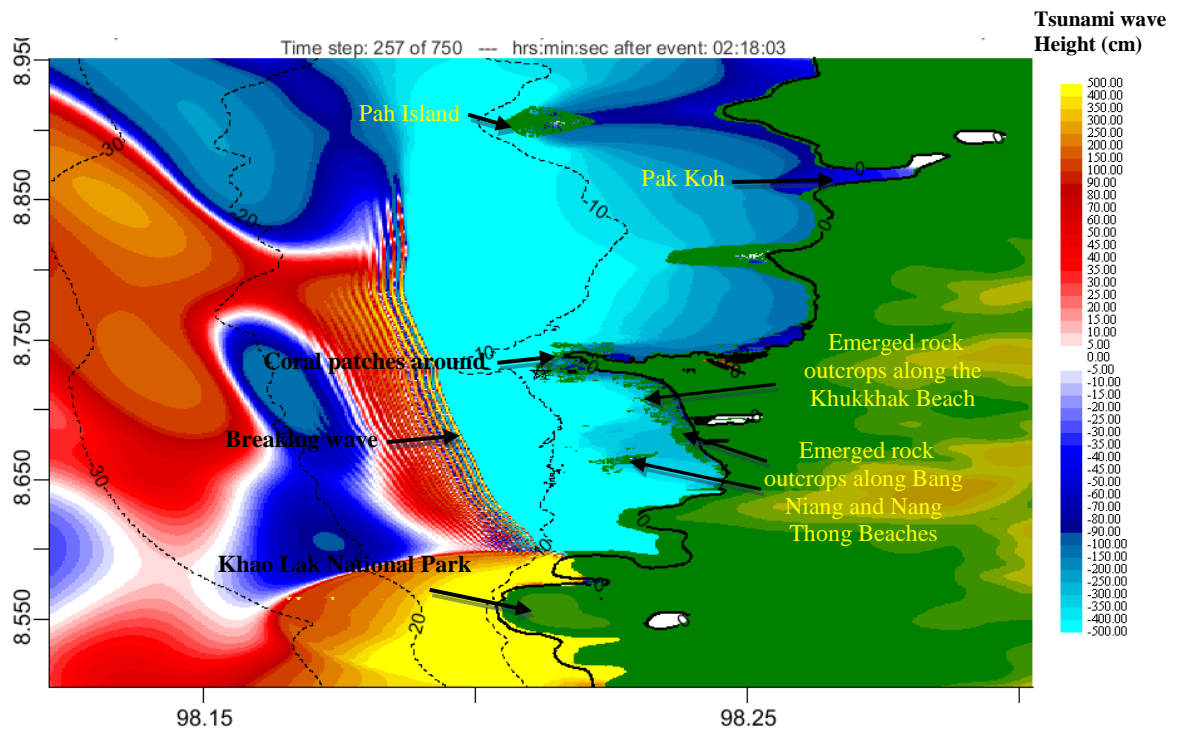


Figure 7-1 (+2 h 18 min) First tsunami trough causes the sea level to recede along the Khao Lak coast. Rock outcrops and coral patches, also island bases emerge. The first tsunami wave crest arrives from the west as a series of breaking waves and from the south-west as a single steep-faced crest



Figure 7-2 (top) View of Khao Lak area. This picture was taken from the Khao Lak National Park, in the south of the study area; it shows the drawdown of seawater due to the first tsunami wave trough that reached the area at 10.11 am (+ 2 h 13 min). Submerged rock outcrops which are never normally exposed come into view (Captured from video: <http://www.radarheinrich.de/tsunamiarchiv/videos14/thailand/sunset-beach-tsunami-original.wmv>).



Figure 7-3 Khao Lak area in ‘normal conditions, November 2008 during a low tide.

From the model, the first tsunami wave crest to reach the Khao Lak coast, approaches the shore from an orientation of 245-260° (Figure 7-1). Firstly, small consecutive breaking tsunami waves occur at 15 m water depth (confirmed by the photograph of the exposed nearshore and a series of white breaking waves in the background (Figure 7-4). The white breaking waves occurs between +2 h 18 min and +2 h 22 min, reaching the coral patches around Pakarang Cape, the emergent Pah Island and the exposed rock outcrops along the Nang Thong Beach. To the south, the crest of the first tsunami wave hits the rocky beach and headland of the Khao Lak National Park Headquarters, arriving from the southwest without the occurrence of the small consecutive breaking tsunami waves.



Figure 7-4 The first wave trough reached the Khao Lak at around 10.11 am of 26 December 2004. On the horizon the first of the series of breaking waves (Figure 7-1) can be seen approaching the coast.

(This picture is part of a sequence of six pictures was taken by Mr and Mrs John and Jackie Knill of North Vancouver, Canada, who were on a beach at Khao Lak resort just before 10:11 a.m. on 26th December 2004. They saw the tsunami coming and took a series of pictures that are among the most impressive photographs to come out of the disaster. Their camera was found later, washed up on a beach among other debris. Its chip still contained the couple's last pictures. Mr and Mrs Knill died seconds after their last picture. Their bodies were found and identified: <http://www.tsunamis.com/john-knill-jackie-knill-tsunami.html>)

The tsunami wave first arrives from the west-southwest, peaking at about 14 m in height. The tsunami wave first inundates Pakarang Cape at +2 h 27 min and reaches Khukkhak Beach 2 min later; it reaches Nang Thong and Bang Niang Beaches 3-4 min later (+2 h 31 min after the earthquake).

As a result of offshore bathymetry and local geomorphology of Khao Lak coastal region, the headlands, capes and small pocket beaches act as a barrier to the propagation of the tsunami wave and result in the reflection and refraction of the incoming waves in various directions; the incoming waves interact and flood the Khao Lak area for approximately 25 min. (Figure 7-1, Figure 7-5 and Figure 7-6). Most of Pakarang Cape is totally flooded as waves inundate the Cape initially from the west but also from the southwest (Figure 7-5). Another set of waves from the west refracts southward to attack the Cape from the north-northwest. Namkhem Fishing Village, Khukkhak Beach and Nang Thong Beach also are entirely submerged by the first wave (Figure 7-6); the model suggests that the crest of the incoming wave is > 9 m above MSL, especially in the area between Nang Thong Beach and the Khukkhak Beach where two sets of waves collide (~ 10 -14 m) (see Chapter 3 Section 3-2 where the wave heights have been compared to those predicted by the model).

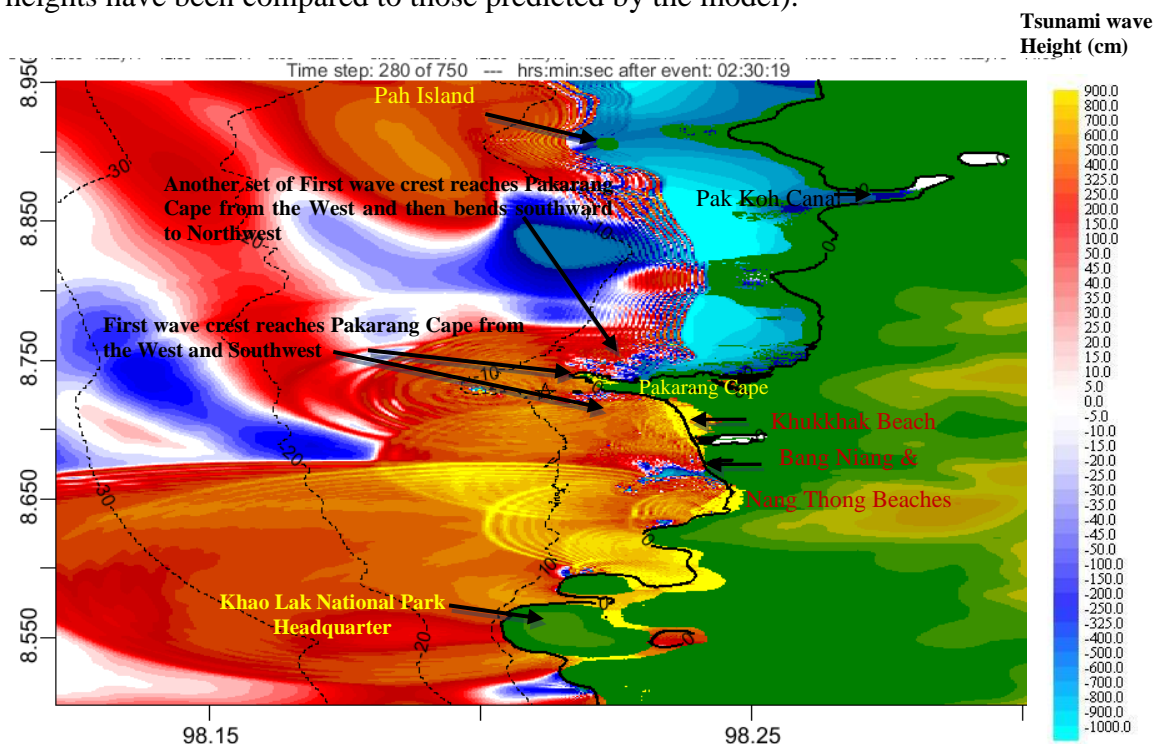


Figure 7-5 (+ 2 h 30 min) First tsunami crest has started to inundate the southern part of Khao Lak , from the National Park Headquarters to Pakarang Cape while the northern part of the Khao Lak coast is still exposed in the initial trough.

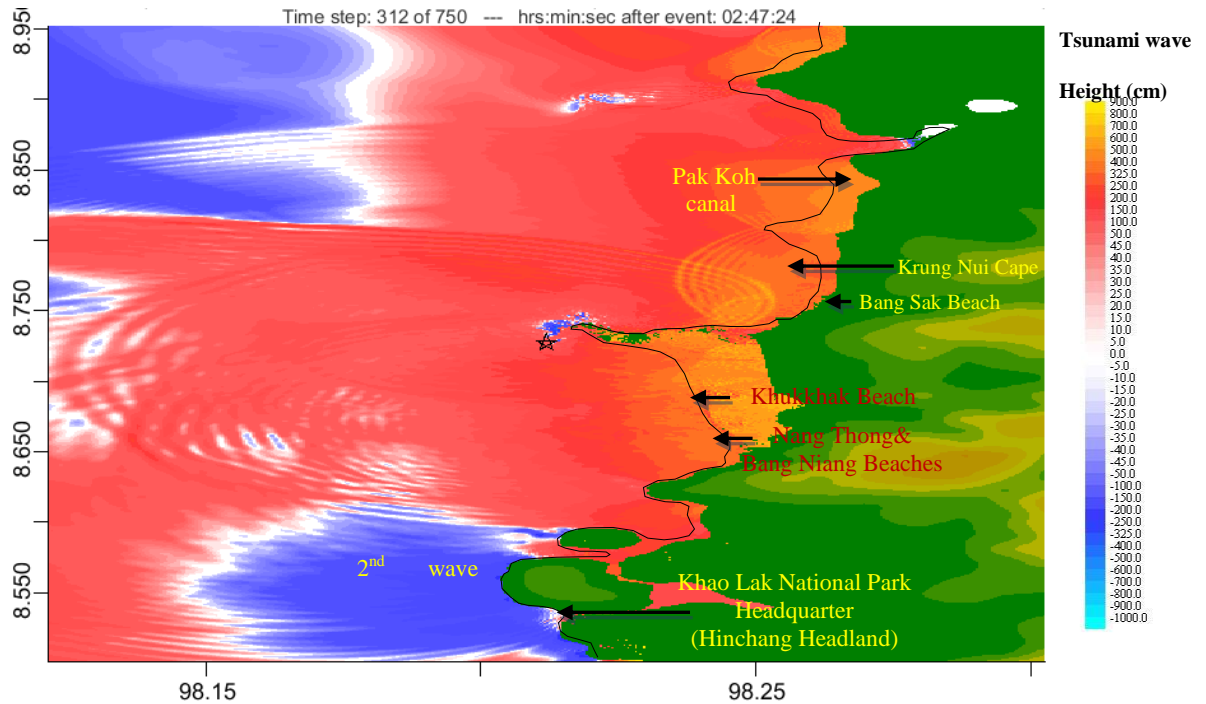


Figure 7-6 (+ 2 h 47 min) The whole of the Khao Lak coast is totally flooded by first tsunami wave including Pakarang Cape where waves inundate from both the north-west and south-west.

7-2.2 The Second and Subsequent Waves

The behaviour of the second wave is different in the southern area, (Khao Lak National Park Headquarters to Pakarang Cape) from the northern area (Pakarang Cape to Namkhem Fishing Village). The second trough arrives at the southern area from the south-west while the beaches in the northern area, including the Pak Koh Canal, are still flooding from the first wave set (Figure 7-7: +2 h 55 min).

The second recession occurs at the rocky beach of Khao Lak National Park Headquarters for a short period of time (Figure 7-7). Between the Nang Thong Beach and the Pakarang Cape the water recedes for ~20 min (+ 2 h 53 min to + 3 h 13 min): it occurs around 20 minutes later in the northern area (+3 h 10 min to +3 h 40 min - Figure 7-9).

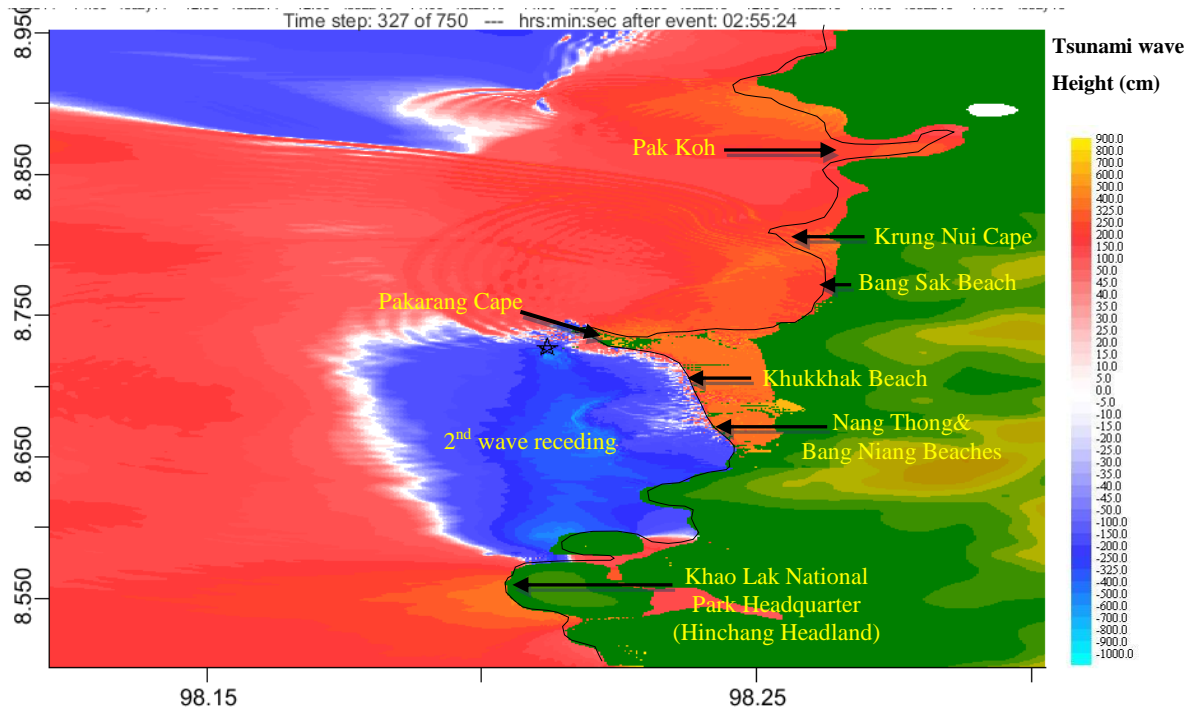


Figure 7-7 (+ 2h 55 min) Second tsunami crest attacking Khao Lak

The second wave crest reaches the rocky beach in front of Khao Lak National Park Headquarters at +2 h 55 min (Figure 7-7) and propagates northwards reaching the south side of Pakarang Cape at +3 h 9 min and Nang Thong and Bang Niang Beaches 4 minutes later (Figure 7-8). The largest waves occur when a wave crest from Khukkhak Beach collides with a crest from the Bang Niang Beach. The wave propagates northwards reaching Krung Nui Cape at +3 h 13 min (Figure 7-9). Another wave crest from west reaches Krung Nui Cape at +3 h 38 min; the inundation of the coast north of Pakarang Cape continues for 24 min until + 4 h 2 min.

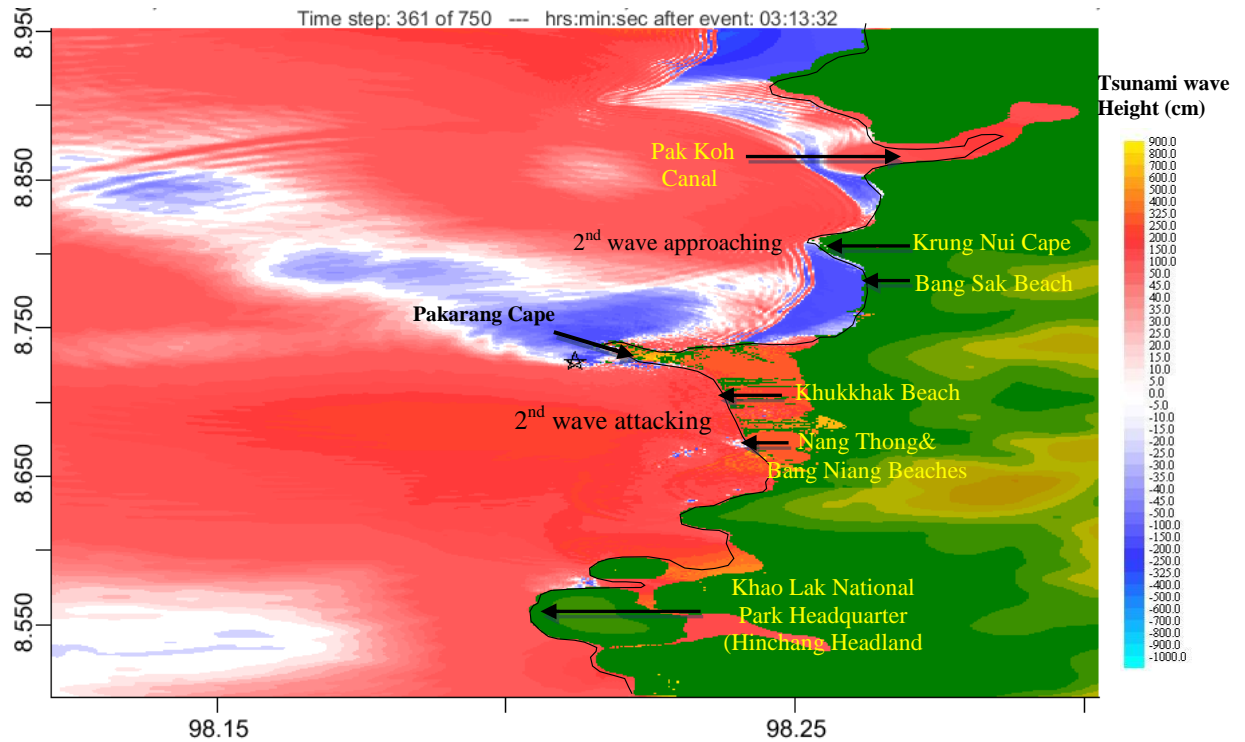


Figure 7-8 (+ 3 h 13 min) Second tsunami wave crest attacks Khao Lak at 3 h 13 min.

A third tsunami wave hits the area located south of Pakarang Cape at + 4 h 7 min inundating the area for 40 min, although the wave height is less than 1 m. Tsunami waves continue to attack the Khao Lak area for several more hours, with the similar behaviour but with decreasing wave height and wave destruction. Waves continue to reflect and refract from the nearby coast and the adjacent islands generating recession and run-up over the region. The model shows that 5 sets of tsunami waves flood Khao Lak region in the 6 h after the earthquake, decreasing in height with time (the third wave crest is the highest one from the model). Wave inundation periods of each wave set are approximately 15-30 min; however, the fourth inundation period is the longest one that lasts for about 40 min.

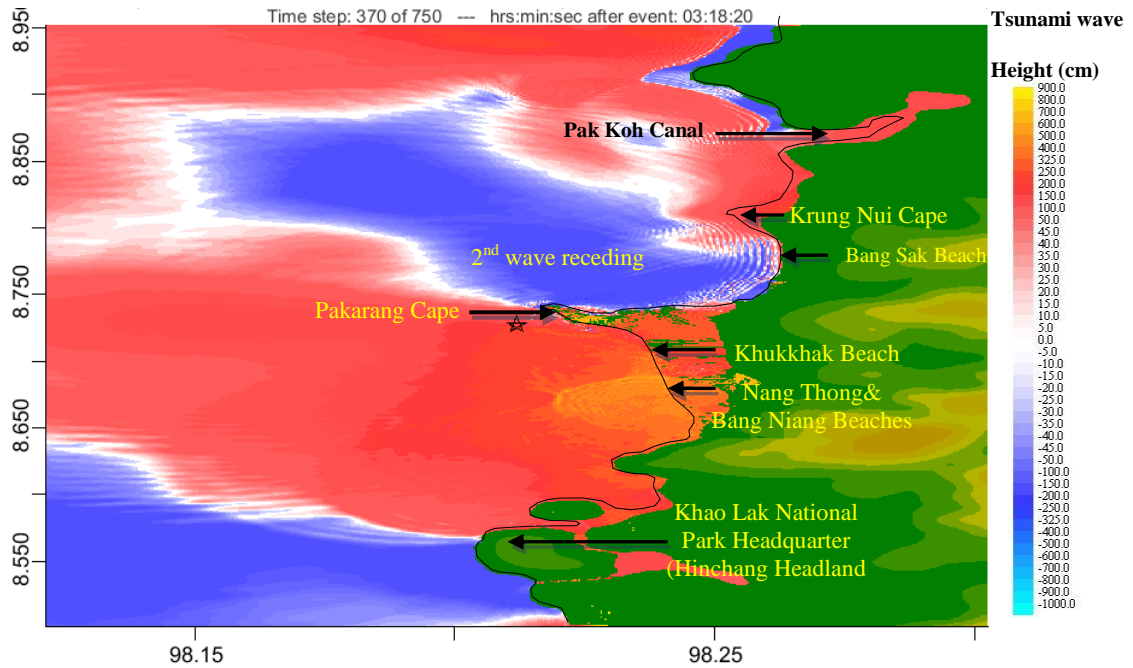


Figure 7-9 (+ 3 h 18 min) Two second tsunami wave crest, approaching from different directions collide at Nang Thong Beach and cause the high magnitude of run up level.

7-3 Detail of Tsunami Wave Behaviour of the Model at Nang Thong and Bang Niang Beaches and Comparison with the Tsunami Observations.

7-3.1 First wave recession along Nang Thong and Bang Niang Beaches

The tsunami wave had very severe effects on the Nang Thong and Bang Niang Beaches and the other tourist beaches between the Khao Lak National Park Headquarters and Pakarang Cape. Water recession initially occurred at these beaches at + 1 h 50 min. Sea level 5 km offshore drops more than 5 m below MSL; 3 km offshore it drops between 2.5 - 3 m at +2 h 12 min. Rock outcrops located along the shoreline emerge from the sea (Figure 7-10 and Figure 7-11 as white patches) and were easily seen by tourists as shown in Figure 7-12. The model shows water drained from nearshore zone with flow rates of between 2 - 6 m/s (Figure 7-11 +2 h 12 min). Water is also drawn from canals and lagoons alongside the beach with outflow rates of up to 2 m/s. The direction of the water recession due to the wave trough initially occurs obliquely to the beach then changes to be perpendicular to the beach. Flow speeds increase to 2 - 4 m/s at 1.5 km offshore.

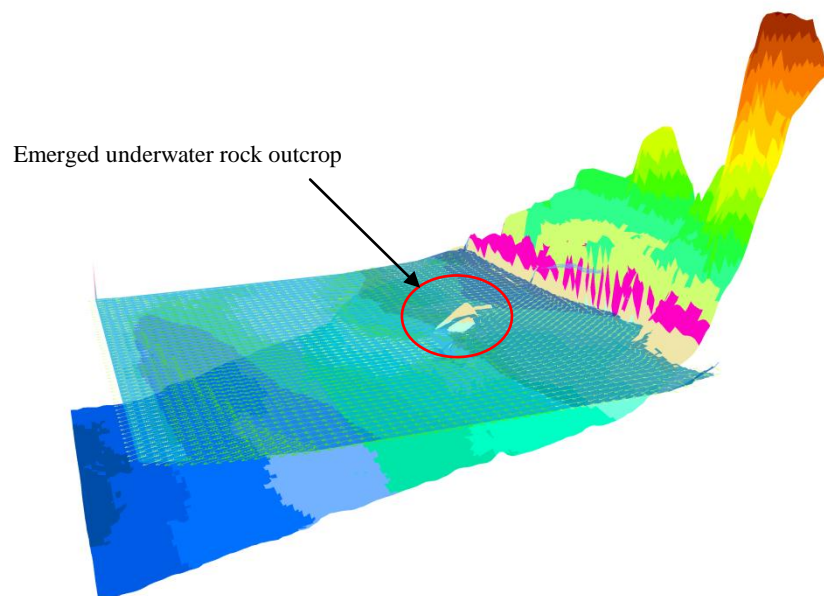


Figure 7-10 3-D diagram of the simulated 2004 Indian Ocean first tsunami wave trough which approaches the coastal area of Bang Niang and Nang Thong Beaches viewed from the southwest, covering the same area as Figure 7-11. The lower (blue shades) surface is the offshore bathymetry (colour contours every 2 m) and the upper (partially transparent) surface is the instantaneous water level with current vectors superimposed. Brighter colours are the onshore topography.

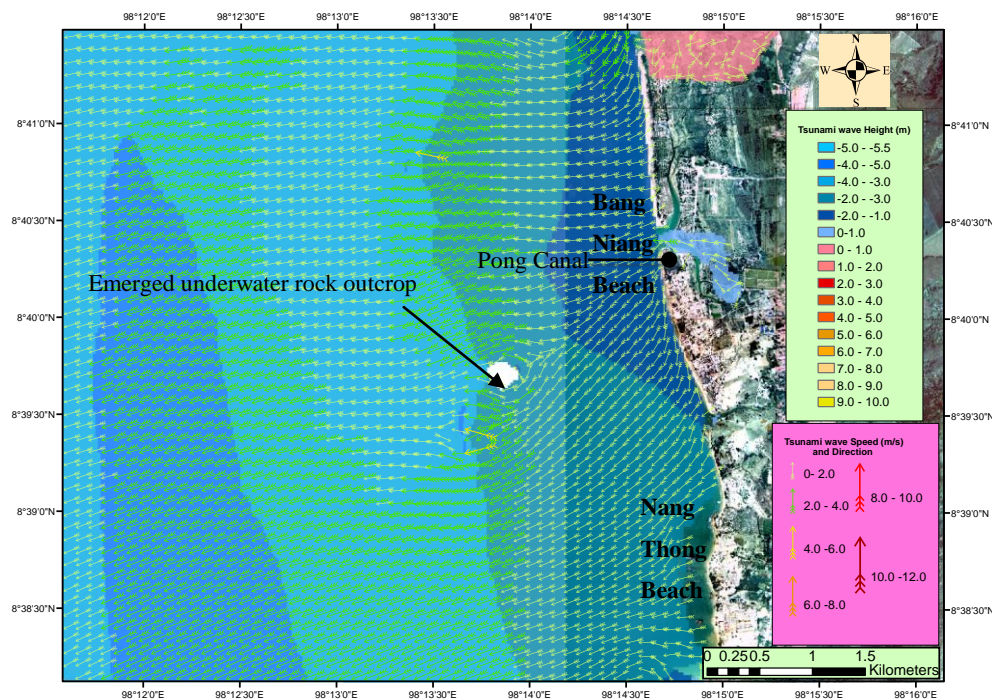


Figure 7-11 (+ 2 h 12 min) Sea level recession and the depth-averaged water current speeds caused by the arrival of the first tsunami wave trough at Bang Niang and Nang Thong Beaches. The alongshore distance is ~ 6 km, on-offshore ~ 6 km

The wave recession predicted by the MOST model was compared with those that actually occurred using pictures taken by a Thai photographer from the Khao Lak National Park scenic view point, to provide a qualitative evaluation of the modelled tsunami pattern. From the view point (Lat. 8.63° N and Long. 98.24° E) it could be seen that rock outcrops emerged from the intertidal and subtidal zone of Nang Thong and Bang Niang Beaches (Figure 7-12). Underwater rock outcrops were clearly seen during this period before the first tsunami crest reached the shoreline; the typical state of the same area is shown in Figure 7-13. There is also clear qualitative correspondence between the model results (Figure 7-14 and Figure 7-15) and those shown in a video record of underwater rock outcrops (between 300-1000 m offshore) at the same site which had never before been seen, and were exposed during the first tsunami wave recession.

At +2 h 20 min (Figure 7-14 and Figure 7-15), the water recession reaches its greatest extent (between 4 and 7 m below MSL - Figure 7-16 and Figure 7-17). This corresponds to the wave recession images in Figure 7-15 and Figure 7-18.



Figure 7-12 Water level recession resulting from the first tsunami wave trough that impacted the Khao Lak area. This image was taken from the scenic view point near the National Park Headquarters showing the exposed rocks and seabed resulting from the seawater drawn down on 26 December 2004 (time unknown) (<http://www.radarheinrich.de>).



Figure 7-13 Khao Lak area in November 2008 during a normal low tide. This image is of the same area as Figure 7-12.

7-3.2 The behaviour of the first wave crest.

When the first tsunami wave crest reaches the offshore area of Bang Niang Beach and Nang Thong Beach the wave speed is very high at the front of the incoming wave crest (Figure 7-14), travelling at a speed of 6 - 12 m/s. The tsunami wave approaches the shoreline with an angle of almost 90° , flooding the exposed sea-bed and the underwater rock outcrops. In Figure 7-15, Figure 7-16 and Figure 7-17, multiple wave crests are found from the modelling, especially in the area in front of Nang Thong Beach. About 2 km offshore, the maximum height of the wave crest reaches 7 m at Bang Niang Beach and 8.5 m at Nang Thong Beach as the waves move into shallower water and shoaling effects intensify (Figure 7-16 and Figure 7-17, +2 h 20 min) which correspond to Figure 7-19. Later multiple waves represented by consecutive wave crests reach Nang Thong Beach (Figure 7-19 and Figure 7-20 +2 h 25 min). These correspond to the multiple wave crests seen in Figure 7-1 and Figure 7-5. However, most of these wave crests merge before reaching the land producing the very high wave which attacked Nang Thong Beach.

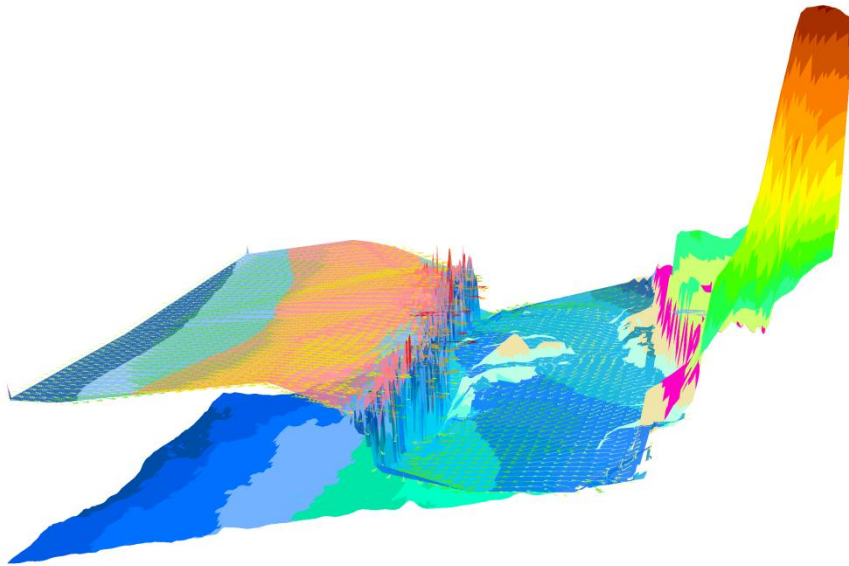


Figure 7-14 (+ 2 h 20 min) 3-D diagram of the simulated 2004 Indian Ocean first tsunami wave crest approaching the coastal area of Bang Niang and Nang Thong Beaches and viewed from the south. Alongshore distance is ~6 km, cross-shore ~6 km. The lower surface (blue shades) is the offshore bathymetry (colour contours every 2 m). The upper surface (partially transparent) is the instantaneous water level with current vectors superimposed; pinks and reds are the highest water levels. Brighter colours are the onshore topography.

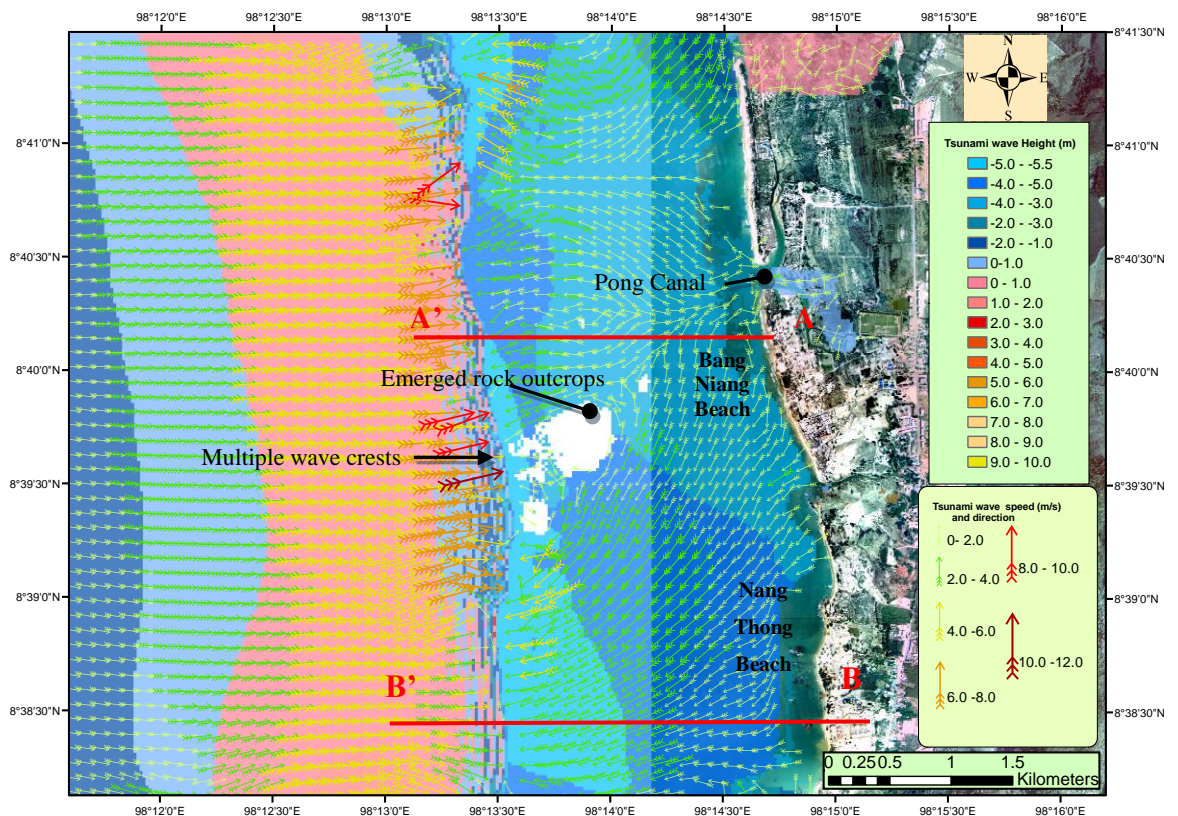


Figure 7-15 (+2 h 20 min) The wave trough continues to cause water regression close to the shore. At the same time the wave crest is approaching the coastline as a wall of water with multiple breaking crests. The white patch in the centre of the image is an exposed rock outcrop.

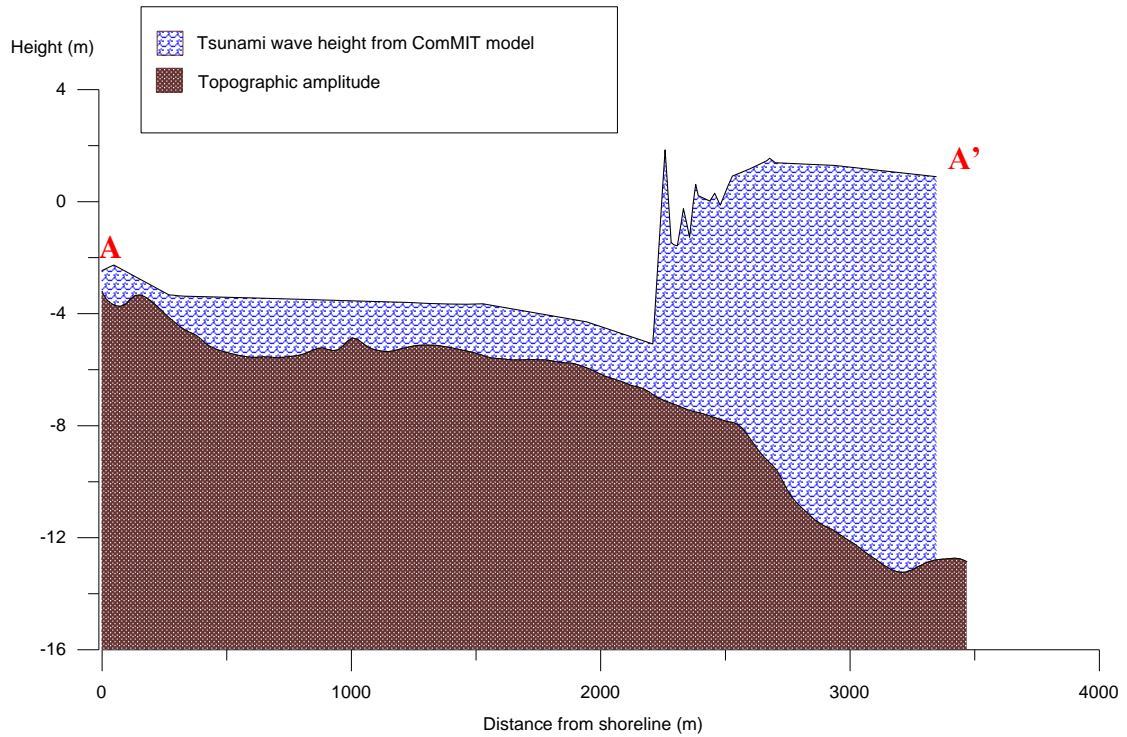


Figure 7-16 Cross section diagram of the first wave trough and wave crest at Bang Niang Beach +2h 20 min. The wave is moving from right to left.

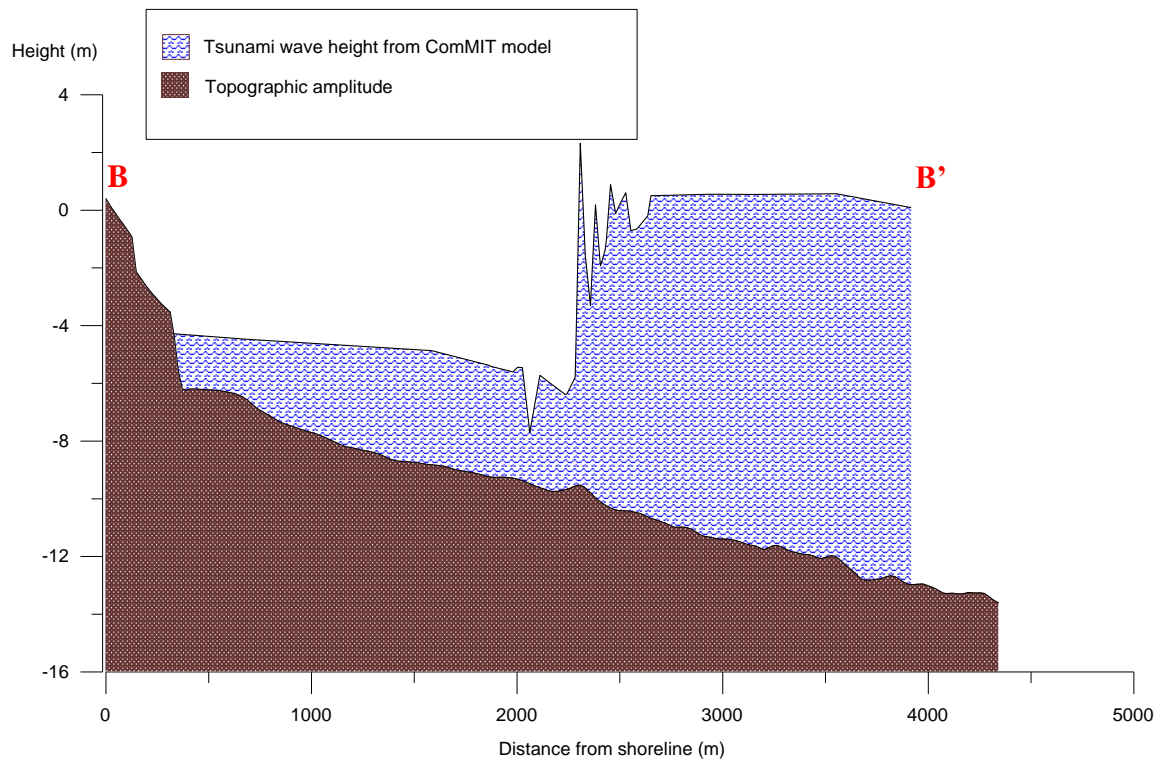


Figure 7-17 Cross section diagram of the first wave trough and wave crest at Nang Thong Beach +2h 20 min. The wave is moving from right to left.



Figure 7-18 Tsunami Recession at Nang Thong Beach 10.20 am (+2h 22 min)
<http://www.radarheinrich.de/wbblite/thread.php?threadid=2844>

At + 2 h 25 min (Figure 7-19 and Figure 7-20), the crest of the first tsunami wave, approaching from the west and the southwest, has almost reached the coastline. The two waves merge, resulting in enhanced effects to Nang Thong and Bang Niang Beaches. Wave speeds along Nang Thong Beach range between 6-12 m/s but are greatest for the southern part of Nang Thong Beach (8-12 m/s). These high waves speed at Nang Thong Beach might be the most important factor that caused the severe damage of the area. Wave speeds at Bang Niang Beach are smaller than those at Nang Thong Beach (4-8 m/s) possibly as a result of the rock outcrops situated in front of Bang Niang Beach, blocking and dissipating energy from the tsunami wave travelling from the southwest, resulting in diminished wave power. However, the speed of the wave which attacks part of Bang Niang Beach located north of the Pong canal is as high (8 m/s) as that at Nang Thong Beach.

Rock outcrops, both underwater and emerged ones, may play an important role in controlling wave behaviour and severity of the tsunami wave. Fewer underwater rock outcrops located in front of Nang Thong Beach might result in the more severe destruction by tsunami waves at Nang Thong Beach which had no rock outcrops in front of it to provide protection to the beach and backshore of the southern section. Mukdara Beach Resort, which was destroyed by the tsunami waves, has no natural

barriers, such as underwater rock outcrops, to provide protection from waves approaching from the southwest.

Headlands and nearshore bathymetry also play an important role in altering wave direction and wave power. The Hinchang Headland, located south of Nang Thong Beach, has significant effects on wave propagation and inundation of Nang Thong Beach. It partly blocked the tsunami approaching from the southwest, and the wave refracted and diffracted around the headland before combining with the wave from the west.

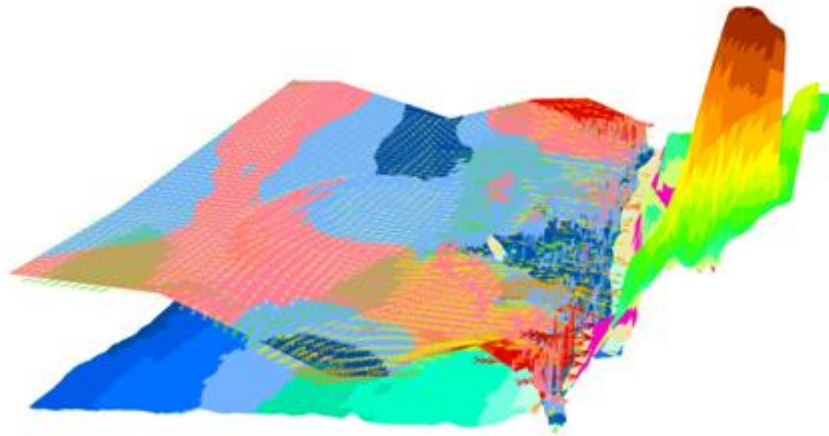


Figure 7-19 (+2 h 25 min) 3-D diagram of simulated first tsunami wave crest to attack the coastal area of Bang Niang and Nang Thong Beaches looking north. Area, scale and colour contours are the same as Figure 7-10 and Figure 7-14. The tsunami wave approaches from two directions (west and southwest) producing very high water levels where they interact – see the red areas to the south along Nang Thong Beach.

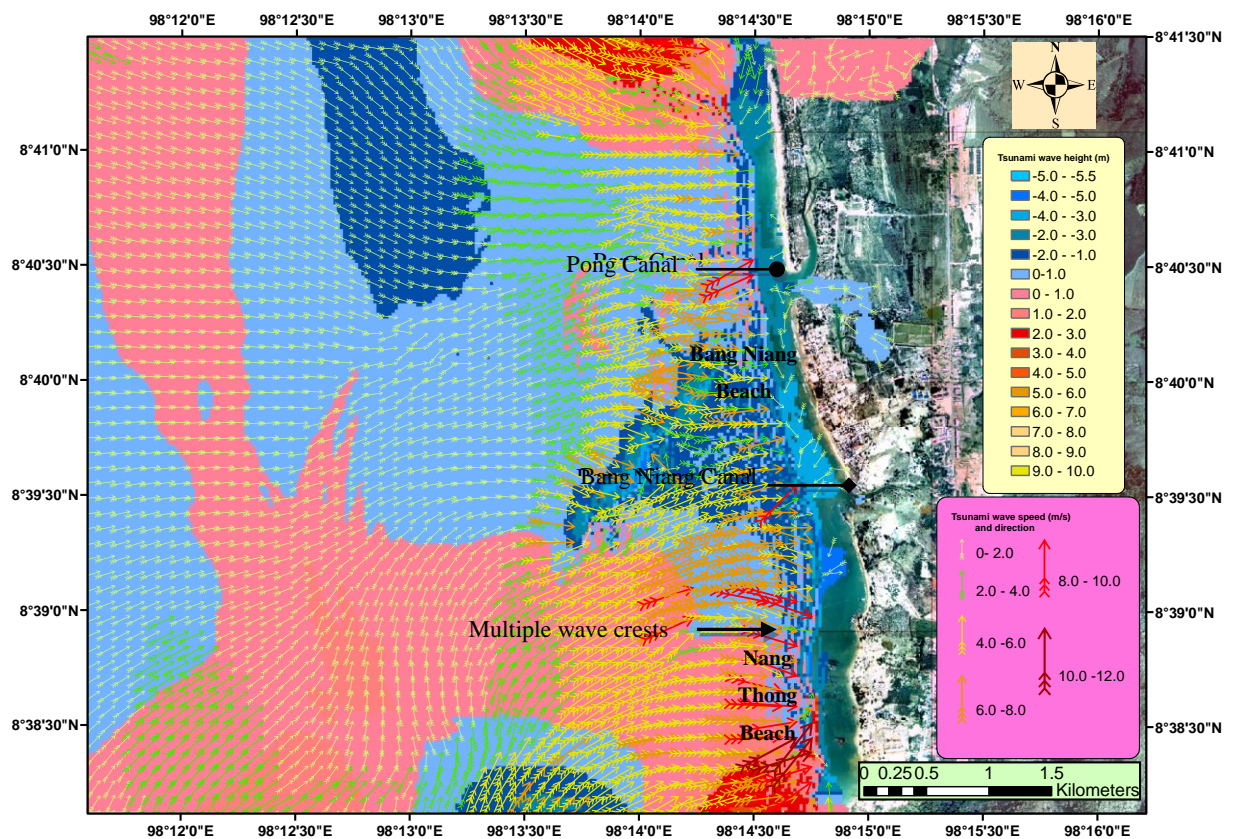


Figure 7-20 (+2 h 25 min) Simulated tsunami first wave crests reaching Bang Niang and Nang Thong Beaches from the west and from the southwest around the Pakarang Cape Headland, combining to produced the highest and fastest wave crests along the southern part of Nang Thong Beach.

7-3.3 Comparing tsunami wave pattern at Sunset Beach and south of Nang Thong Beach

To verify the model predictions of wave heights, directions, speed and timings for the 2004 tsunami, the major sources of evidence are photographic images, video clips and interview reports, which have been collected and analyzed for comparison of the observed wave patterns and characteristics with those from the model. Photographs and video clip taken from Sunset Resort and Palm Beach Resort on Sunset Beach (a small pocket beach located south of Nang Thong Beach; sometimes recognized as part of Nang Thong Beach) and Nang Thong Beach, located in the south of the study area, show clearly the wave pattern of the first tsunami wave on 26 December 2004. From the model results shown in Figure 7-1, the first wave crest attacks Sunset Beach before reaching Nang Thong and Bang Niang Beaches, with a high degree of wave power. The tsunami waves approached the Sunset and southern Nang Thong Beaches with 6-12 m/s wave speed before inundating the coastline with a 5.5 m high wave (their speeds has dropped to 2-6 m/s at this point –see Figure 7-21, Figure 7-22 and Figure 7-23). This corresponds to evidence from an image in Figure 7-24 and a video clip in Figure 7-25 taken from a restaurant overlooking the Sunset and Nang Thong Beaches, which shows the tsunami wave crest reaching Sunset Beach. Time-stamped photographs taken from both Nang Thong Beach and Sunset Beach Figure 7-24 and Figure 7-26 to Figure 7-31 show similar arrival times (between 10.25-10.29 am, +2 h 27 min to +2 h 31 min; Figure 7-24, Figure 7-26 and Figure 7-29). The first wave from the model (Figure 7-1 and Figure 7-22) which initially hits south of Nang Thong Beach is very similar to the wave pattern reached at the front of Sunset Resort in Figure 7-24 and another view of the same wave crest in Figure 7-25. The first wave in the model reaches the coastline at +2 h 27 min (Figure 7-22 and cross section profile in Figure 7-23) a few minutes earlier than the times of the photographs. The reason for this delay might be the time of propagation of rupture activity along the subduction because the rupture was not synchronous along the fault. The rupture of the northern part of the subduction occurred between 3-8 min (200-480s) from the beginning of the earthquake. However, the present version of the MOST model cannot represent the time delay of along the subduction; it can simulate a single synchronous event only.

A video recorded by a Thai hotel owner shows that the wave crest started to shoal while approached the rocky cliffs and moved like a straight wall before hitting the beach; the model also shows the wave approaching perpendicular to the beach as a wall and later moving to southeast and northeast (Figure 7-22). The rock outcrops, located in front of the Khao Lak and Khao Lak Seaview Resorts on Sunset Beach, are the examples of the large barriers that enhanced wave breaking (Figure 7-27) and reduced wave inundation inland.

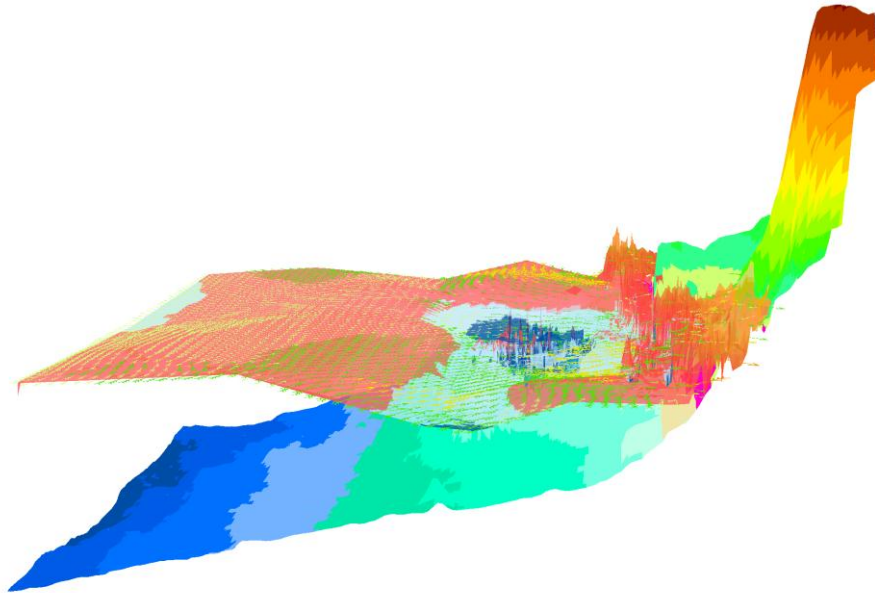


Figure 7-21 3-D diagram of the first tsunami crest attacks Bang Niang Beach and Nang Thong Beach at +2 h 27 min after the quake.

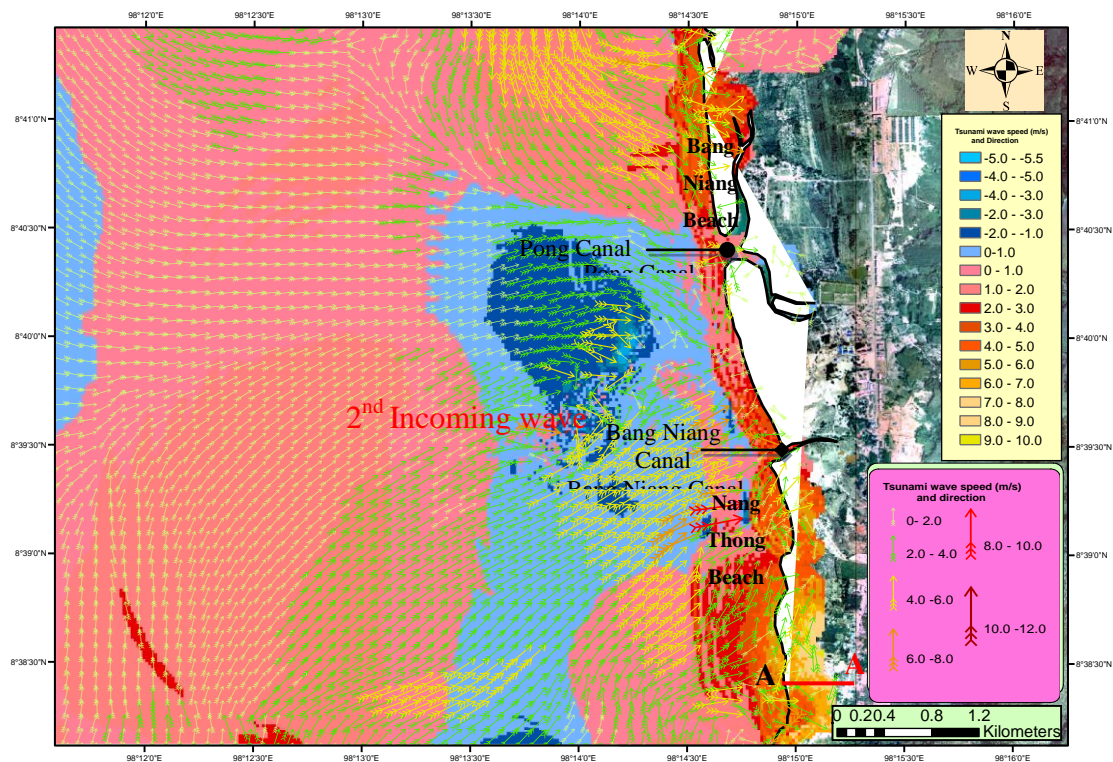


Figure 7-22 Simulated first 2004 Indian Ocean tsunami wave crests attacks Bang Niang Beach and Nang Thong Beach at +2 h 27 min, while the second tsunami wave closely follows the first one.

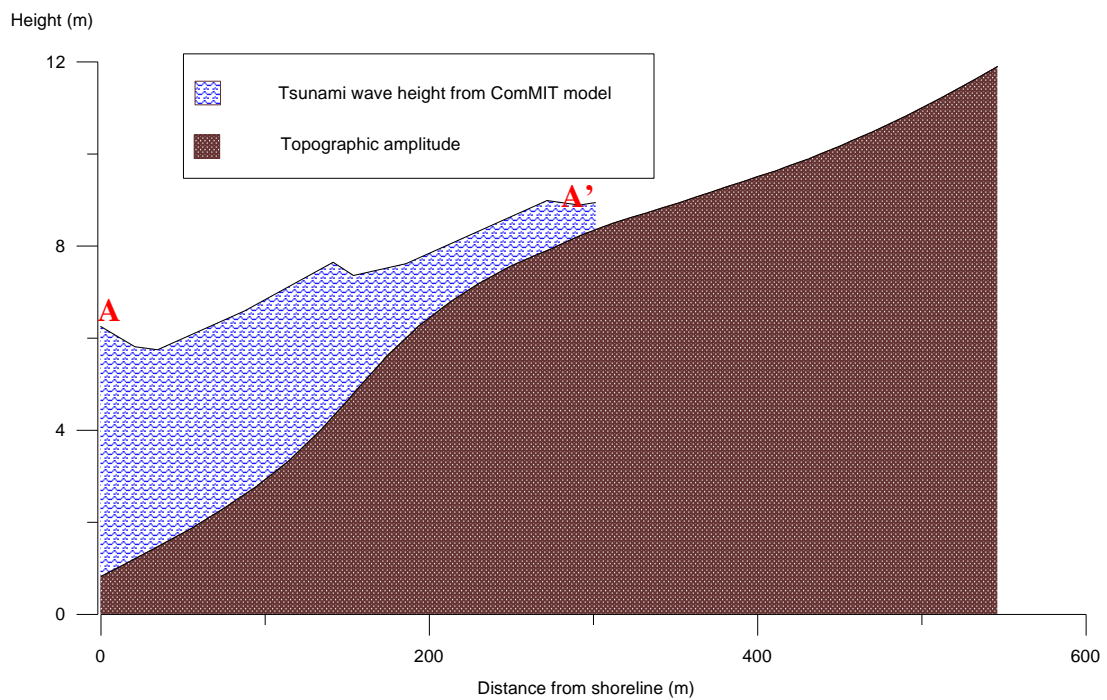


Figure 7-23 Cross section diagram of first wave trough and wave crest at Nang Thong Beach +2h 27 min



Figure 7-24 The first wave crest arriving at Sunset Beach (a small pocket beach, and considered to be part of Nang Thong Beach)

(Sunset Resort, Sunset Beach, Thailand, December 26, 2004, 10:29: AM (+2 h 31 min) Some of these people died 15 seconds later, all other people on this picture were injured; <http://www.radarheinrich.de/tsunamiarchives/tsunami2004.html>).



Figure 7-25 Top view of first wave crest that reached Sunset Beach, a small beach close to the Khao Lak National Park taken from a headland (seen to the left in Figure 7-24; <http://www.radarheinrich.de/wbblite/thread.php?threadid=322>).



Figure 7-26 First tsunami wave crest reached Nang Thong Beach after 10.25 am (+2h 27 min) (<http://www.radarheinrich.de/wbblite/thread.php?threadid=2844>).



Figure 7-27 Breaking of the tsunami wave around rocks outcrops at Sunset Beach (Right), and wave receding following by the first tsunami wave crest was going to reach Bang Niang Beach (on Top Left) (<http://www.radarheinrich.de/tsunamiarchiv/videos14/pc-dvd-ui/videos/thailand-tsunami.html>).



Figure 7-28 Typical Sunset Beach, Nang Thong Beach and Bang Niang Beach in November 2008 during low tide (compare to the tsunami event which attacked the same area on 26 December 2004 in previous figure).



Figure 7-29 High tsunami crest reached Sunset Beach, Khao Lak on 26 December 2004 at 10.29 am (+2 h 31 min) (http://news.bbc.co.uk/2/hi/in_pictures/4293123.stm).



Figure 7-30 Sunset Beach in November 2008 during low tide (Left), showing flat beach with few rock outcrop compared to the day tsunami attacked this beach in December 2004 (Right: (<http://www.radarheinrich.de/wbblite/thread.php?threadid=1689>)).



Figure 7-31 Breaking of tsunami wave on the shore of Sunset Beach (http://news.bbc.co.uk/2/hi/in_pictures/4293123.stm).

The other area showing some correlation between model results and photographic records of the tsunami is at Palm Beach Resort on Sunset Beach. Three consecutive pictures (Figure 7-32, Figure 7-33 and Figure 7-34) taken by a tourist, show the actual pattern of the tsunami wave that struck Sunset Beach and compare well with the model predictions at +2 h 20 min (Figure 7-15), at +2 h 25 min (Figure 7-20) and at +2 h 27 min (Figure 7-22). Following the drop in water levels at Palm Beach Resort, the wave crest approached the beach, increasing in height due to shoaling, as the wave moved into shallower water and over the rock outcrops towards land (Figure 7-32). Multiple crests surged together resulting in high wall of water that flooded the beach and inundated farther inland (Figure 7-33 and Figure 7-34).

Underwater rock outcrops are easily seen from both Figure 7-15 (+2 h 20 min) and the first picture (Figure 7-32) due to water recession due to arrival of the wave trough. According to the model water level drops 3-5 m below MSL. A small wave crest estimated to be not more than 3 m high can be seen in Figure 7-32, followed by a high wall of second wave crest (Figure 7-33). From the model, wave speed is very high in this zone. It could be as fast as 12 m/s. The model also shows that the wave crest height

at the shoreline (Figure 7-23 + 2 h 27 min) exceeded 5 m; the wave photographed in Figure 7-34 is consistent with the height predicted by the model.



Figure 7-32 First tsunami wave recession in front of Palm Beach Resort, Sunset Beach, Khao Lak. First small wave crest followed by the second huge wave can be seen from this view (<http://ourworld.worldlearning.org>)



Figure 7-33 Surging of tsunami waves caused high wave crest reached the area in front of Palm Beach Resort (<http://ourworld.worldlearning.org>).



Figure 7-34 Inundation due to the tsunami wave which attacked Palm Beach Resort on 26 December 2004 (<http://ourworld.worldlearning.org>).

7-3.4 Comparing Tsunami Wave Pattern at Nang Thong Beach.

Video and photos show a multiple breaking tsunami wave, rather than a single crest (Figure 7-32, Figure 7-35 and Figure 7-36) approaching the coastline of Nang Thong and Bang Niang, and confirms the multiple crest predicted by the model (Figure 7-1, Figure 7-15, Figure 7-16 and Figure 7-17). The video record shows considerable wave breaking due to rock outcrops. The wave crest elevation increases from 2-3 m (red colour in Figure 7-37) to 5-6 m (yellow colour) as it approaches the beach. Wave propagation, surging and recession are shown in a video clip of the nearshore area while appearing in the model as a gyre (Figure 7-38, Figure 7-40 and Figure 7-42); the gyre was caused due to the combination of receding water from the first tsunami and the incoming second wave. The model shows the first wave approaching Nang Thong Beach from two directions (Figure 7-37) but no evidence of such wave behaviour has been found from video and photographic images to support this.

The first wave crest approaching the area was detected from a photograph (Figure 7-35) time-stamped 10.17 am (+2h 19 min). The model shows the first tsunami wave crest

reaches the coastline of Nang Thong and Bang Niang Beaches at +2 h 27 min (Figure 7-22) while the images in Figure 7-24, Figure 7-25 and Figure 7-26 show the first crest reached the coastline at Nang Thong Beach at 10.25-10:29 am local time (+2h 27 min to +2h 31 min). The arrival time from the model is approximately 4 minutes ahead of that of camera recorded of arrival time. The model predicts that the first tsunami wave has a speed of 6-12 m/s as it reaches the shore. The wave comes from two directions, the southwest and the northwest and attacks the centre part of Nang Thong Beach with that high degree of wave velocity as seen in Figure 7-21 and Figure 7-22. The incoming wave from the southwest has a height of 2 m with its velocity of 4-12 m/s. Later, as the northwest wave arrives, its height increases to 6-10 m above MSL (Figure 7-23) its speed decreases to 2-6 m/s as it moves inland (which correspond to Figure 7-36). It took about 4 minutes for the water to reach its peak height at the shoreline. The peak wave height of approximately 10 m occurred south of Nang Thong Beach (at Country Side Resort; Figure 7-37). The tsunami heights surveyed along the Khao Lak coast by Matsutomi et al. (2005) and Siripong et al. (2005) were between 8.3-9.9 m. which is in close agreeable with the model. Along the northern section of Bang Niang Beach, wave crest speed was around 8 m/s; it reached the nearshore zone from the northwest with a height of 4-6 m.



Figure 7-35 The first wave crest approaching the coastal of Khao Lak.



Figure 7-36 The first wave crest shoaling as it approaches land after the first recession (<http://www.radarheinrich.de/wbblite/thread.php?threadid=364>).

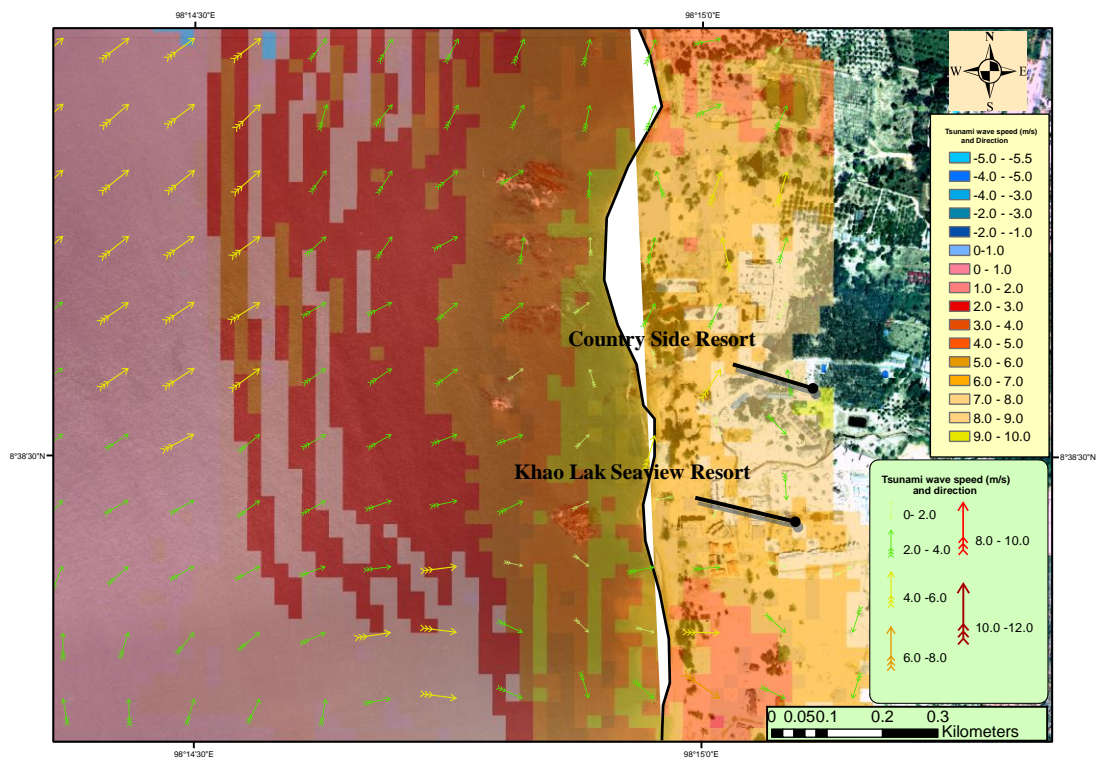


Figure 7-37 Detailed diagram of wave speed and direction that attacks Nang Thong Beach at +2 h 27 min.

At +2 h 30 min, the first wave crest reaches the nearshore of Nang Thong and Bang Niang Beaches. Sea level rises up and increases its height to approximately 4-6 m while

reaches the area within 1.5 km from the beaches. After the first wave inundated, the first wave rundown flows parallel to the coast in 2 opposite directions; then, merges together and acts as a current at the centre of the area with its run down velocity of as high as 8-12 m/s (Figure 7-38). Then, the tsunami wave crests creat the high wave run up of around 3-5 m in height at the coastline (Figure 7-39). The model suggests that the second wave crest height was 1-4 m at ~2 km offshore but increased to 7.0-8.5 m (Figure 7-16 and Figure 7-17) at the shoreline due to shoaling and combining with the first wave run down. The second wave crest reached the shoreline at +2 h 35 min (Figure 7-40 and Figure 7-41). Wave velocity of the second tsunami wave is of the order of 2-6 m/s and its run up direction was from both northwest and southwest (Figure 7-22). It is corresponding to the interviews and video clips which state that the second wave to reach the area was the highest one to hit the Nang Thong and Bang Niang Beaches (approximately 4.5-9.8 m (with an unusual maximum wave height = 15.7 m).

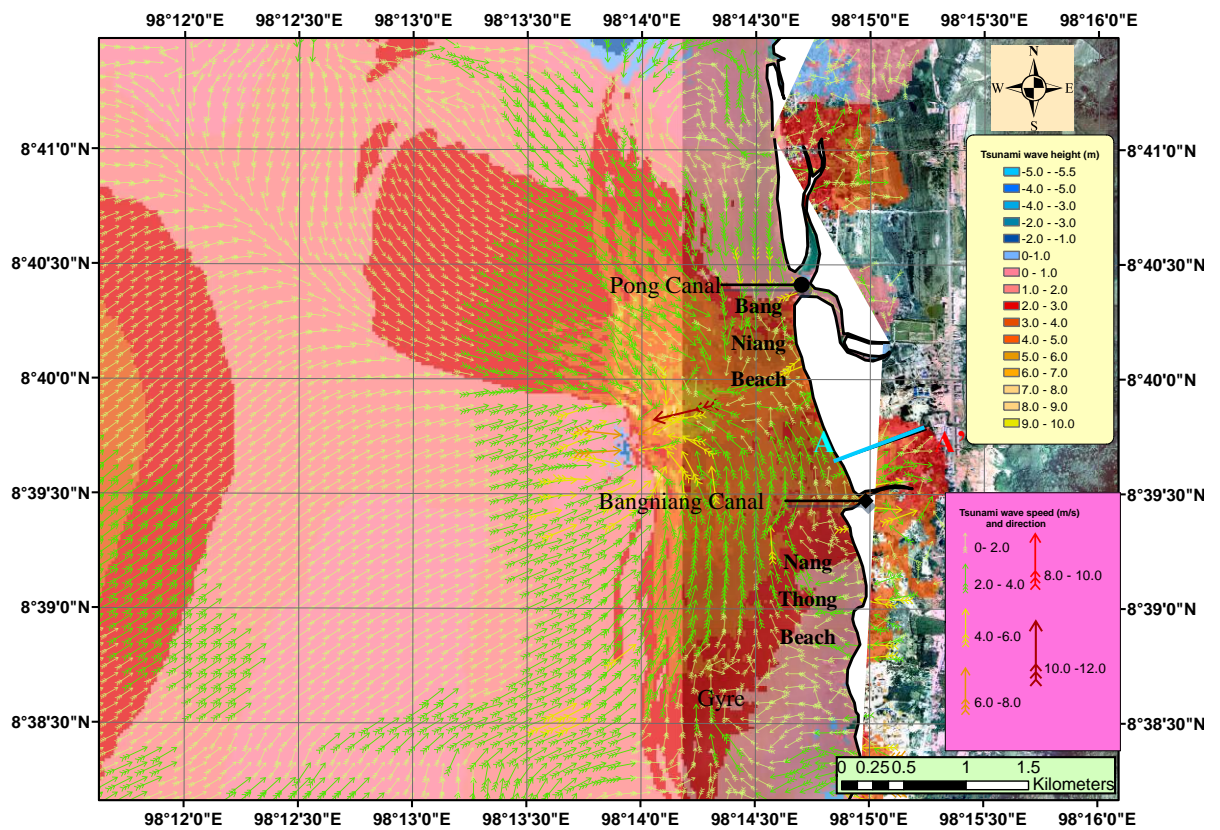


Figure 7-38 Tsunami wave from the model attacks Bang Niang and Nang Thong Beaches at +2h 30 min (10.32 am).

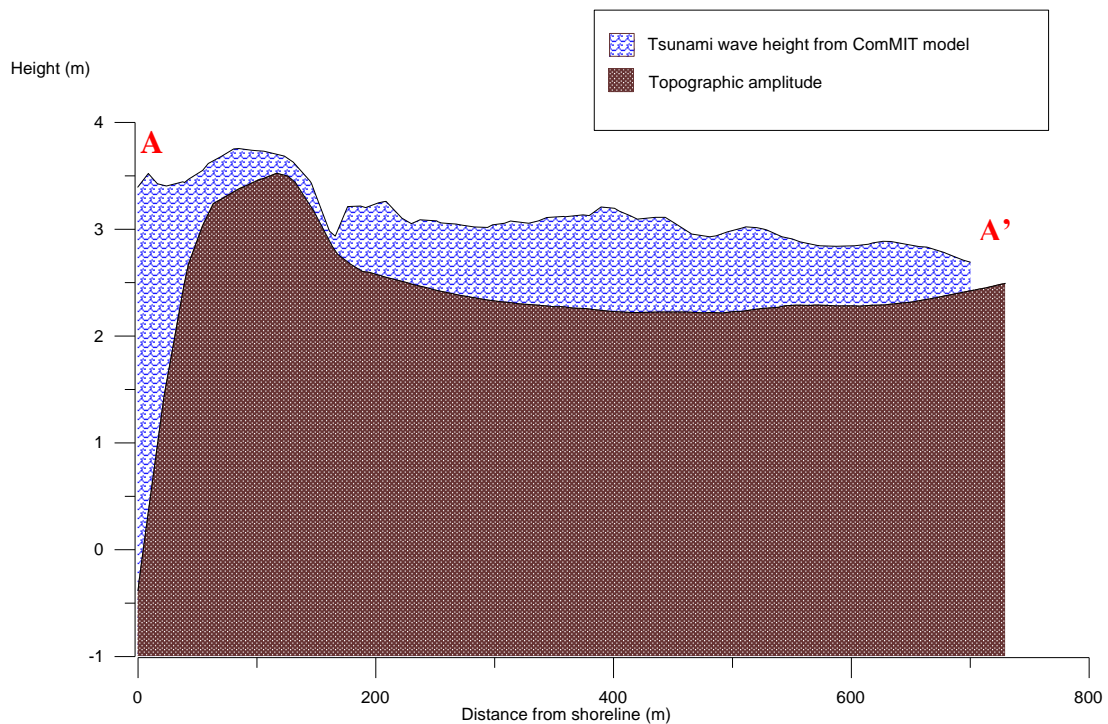


Figure 7-39 Cross section diagram of tsunami wave at Nang Thong Beach +2h 30 min

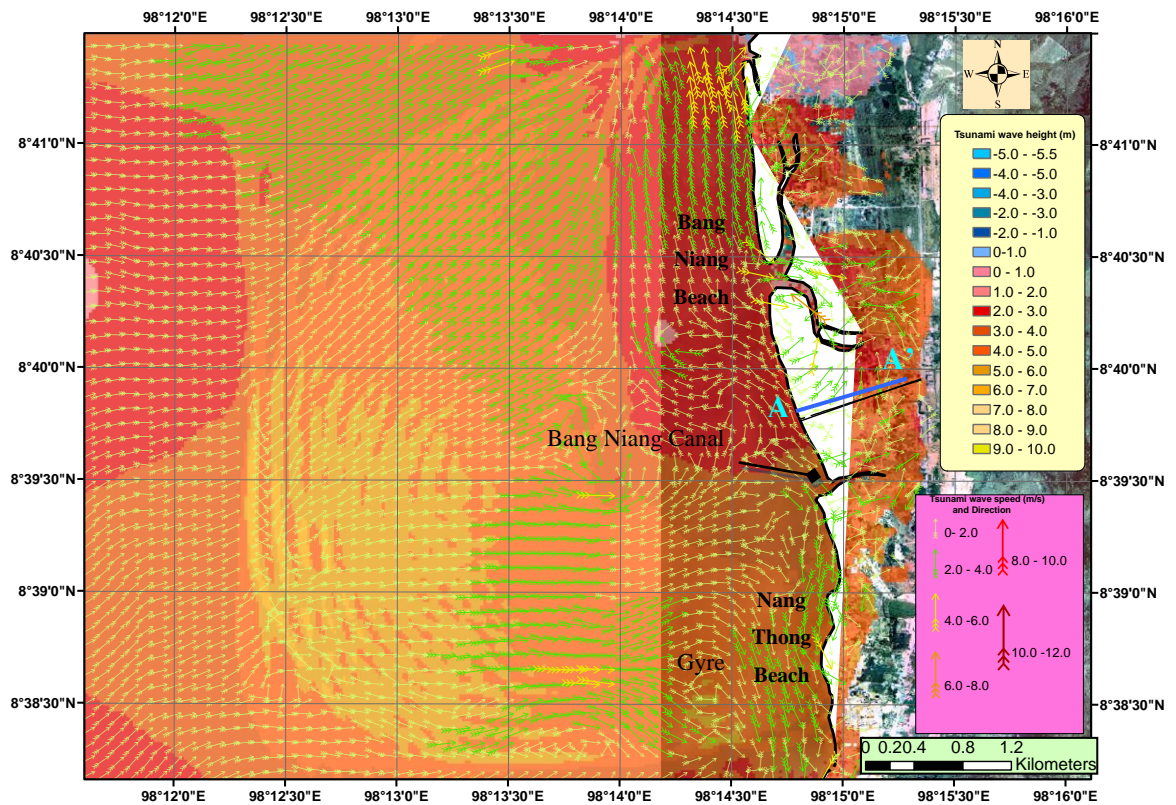


Figure 7-40 Tsunami waves from the model attacks Bang Niang and Nang Thong Beaches at +2h 35 min (10.33 am).

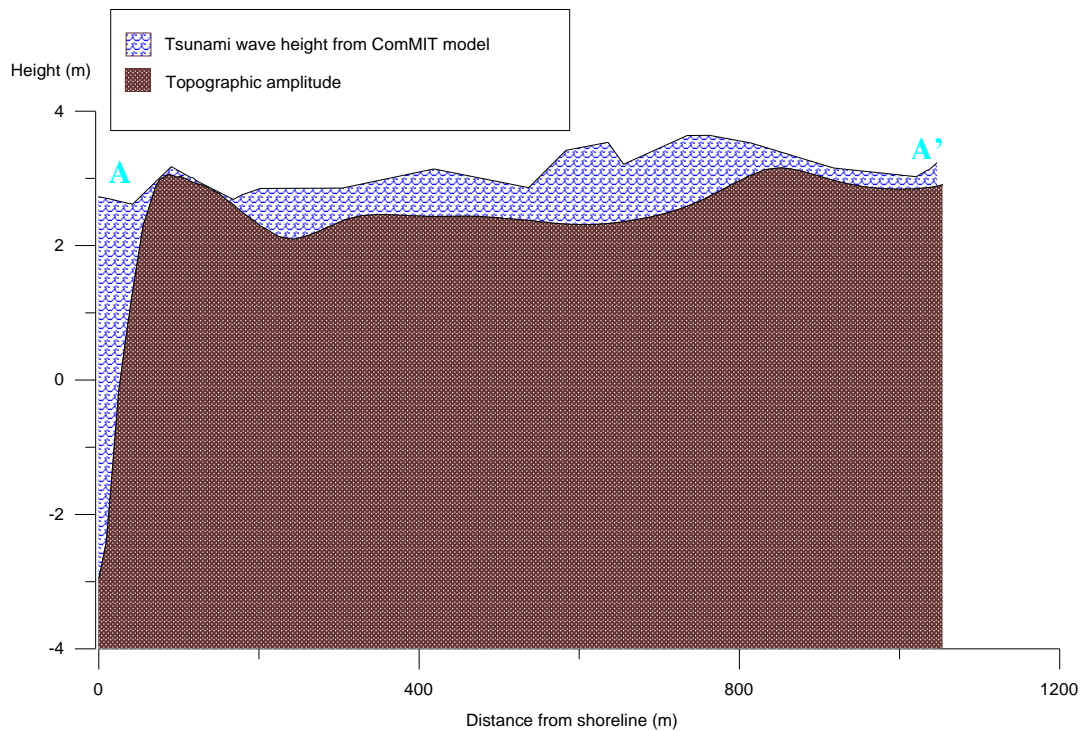


Figure 7-41 Cross section diagram of tsunami wave at Bang Niang Beach +2h 35 min

According to the model, the third wave reaches the centre part of the Bang Niang and Nang Thong Beaches at +2 h 46 min (Figure 7-42); the wave height is between 2 -5 m at the coastline, and inundates the whole area back to 1 km with 2-3 m of water (Figure 7-43). Unfortunately it is difficult to find evidence to validate the model predictions for the second and the subsequent waves. Most evidence is found for comparison to the first wave's actions than of the second and the later waves, except some video footage.

The maximum inundation distance and area occur as the third wave surges into the recession of the second wave (Figure 7-42). The inundation distance of the third wave reaches beyond the main road ~1.5 km from the shore (Figure 7-42, + 2h 46 min). This is consistent with the surveyed data of inundation distance of the 2004 tsunami, except at Sunset Beach where the inundation distance from the model is slightly shorter than that of the surveys. While the third wave was still flooding the area the fourth wave (+3h 16 m), inundates the whole of Khao Lak including Bang Niang and Nang Thong Beaches. The wave speed is quite slow, < 2 m/s. Recession due to the trough ahead of the fifth wave trough occurs around + 3 h 29 min causing sea level drop by 2-7 m. Around 4 h after the rupture, while the seawater still floods the area, the fifth wave crest arrives and inundates the backshore.

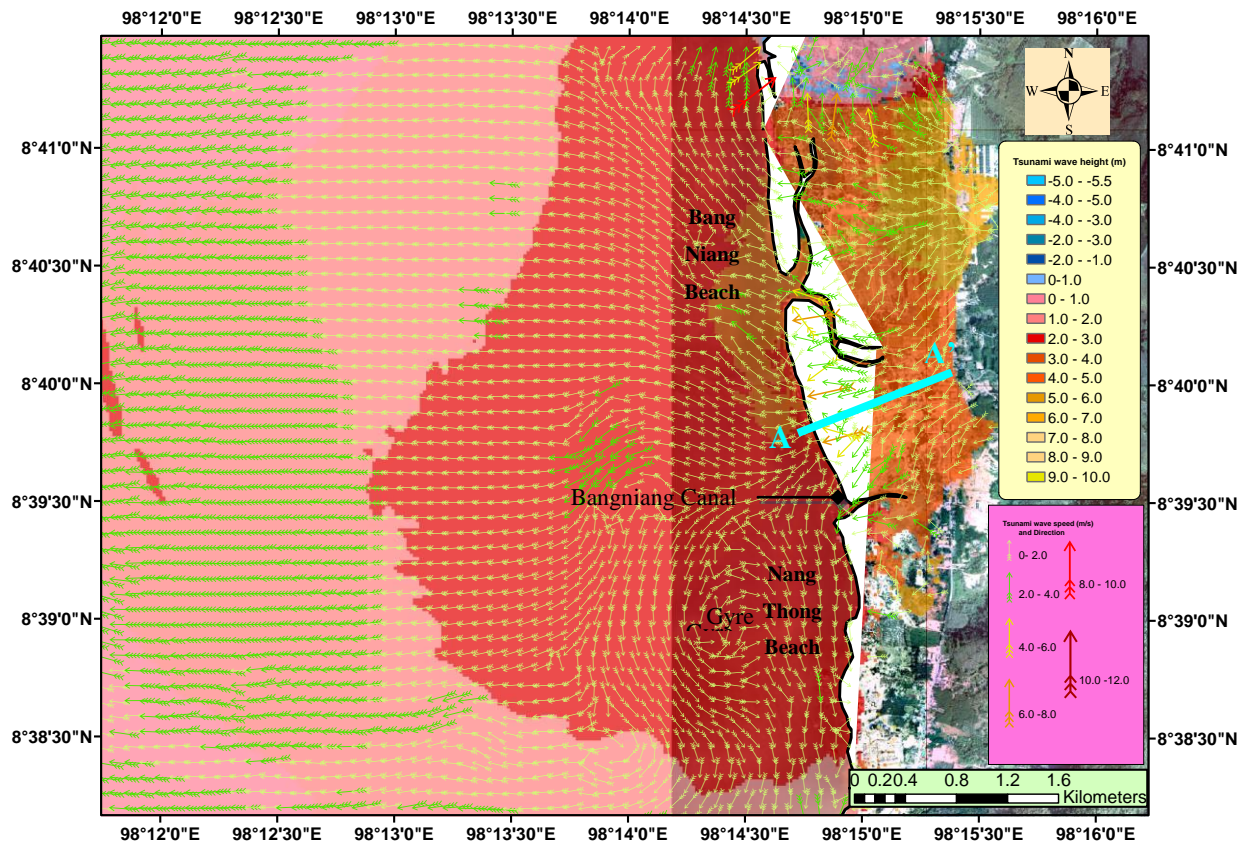


Figure 7-42 +2h 46 min, The maximum inundation distance and area were due the combined effects of the second wave run down and the third wave run up.

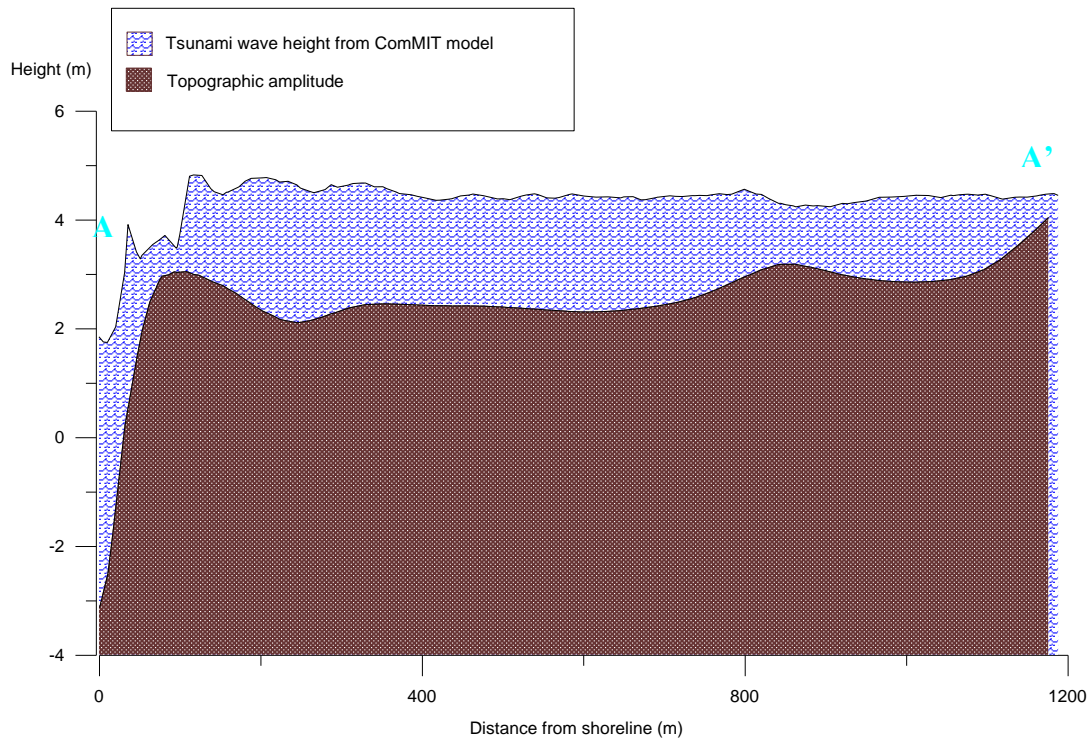


Figure 7-43 Cross section diagram of tsunami wave at Bang Niang Beach +2h 46 min

According to the model, the tsunami wave came from southwest and moved to the northeast at Nang Thong Beach (Figure 7-44). The police patrol boat was moved ~2.6 km away from its original site to a location 1.25 km from the coastline, in a northeast direction (Figure 7-44 and Figure 7-45) in a direction corresponding to the wave direction from the model. A set of images of police patrol boats, taken from Nang Thong Beach, can also be compared to the tsunami wave direction and offshore wave height predicted by the model (Figure 7-46 to Figure 7-50). Two police patrol boats were moored offshore of Nang Thong Beach on 26 December 2004. One patrol boat was sunk but the other was transported 2.6 km landward by the tsunami wave. Draw-down effects resulting from the wave trough arrival can be seen from the first scene (Figure 7-46 and Figure 7-47).

The offshore tsunami wave high can also be estimated. The first wave crest that reached the offshore Nang Thong Beach is higher than the police patrol boats which are ~5-6 m high (Figure 7-47 and Figure 7-50). The breaking wave is about 1/3 higher than the police patrol boats and estimated at roughly 8-9 m (Figure 7-48 and Figure 7-50). This agrees with the offshore tsunami wave heights displayed in Figure 7-16 and Figure 7-17. From these pictures, the first tsunami wave crest reached the offshore Nang Thong Beach as a broad wall of water (Figure 7-48). Figure 7-49 and Figure 7-50 show the wave simultaneously impacting the police patrol boats.

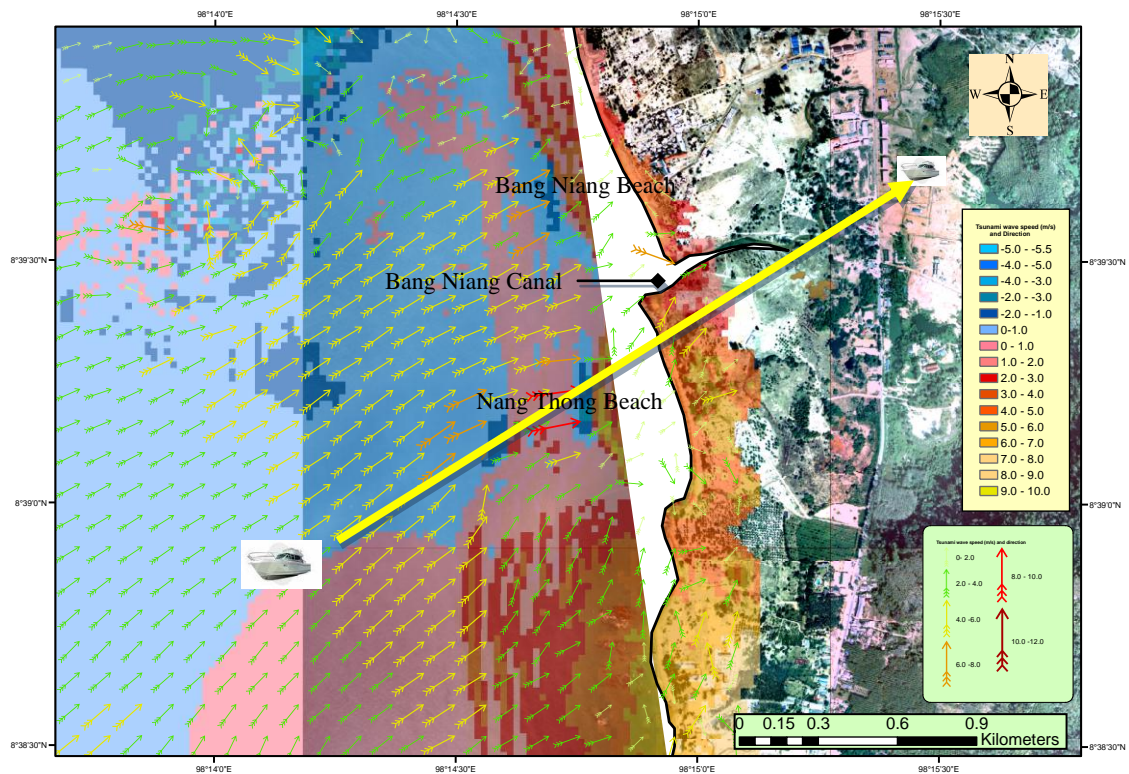


Figure 7-44 Path of Police patrol boat transported by the tsunami on 26 December 2004 at offshore Nang Thong Beach.

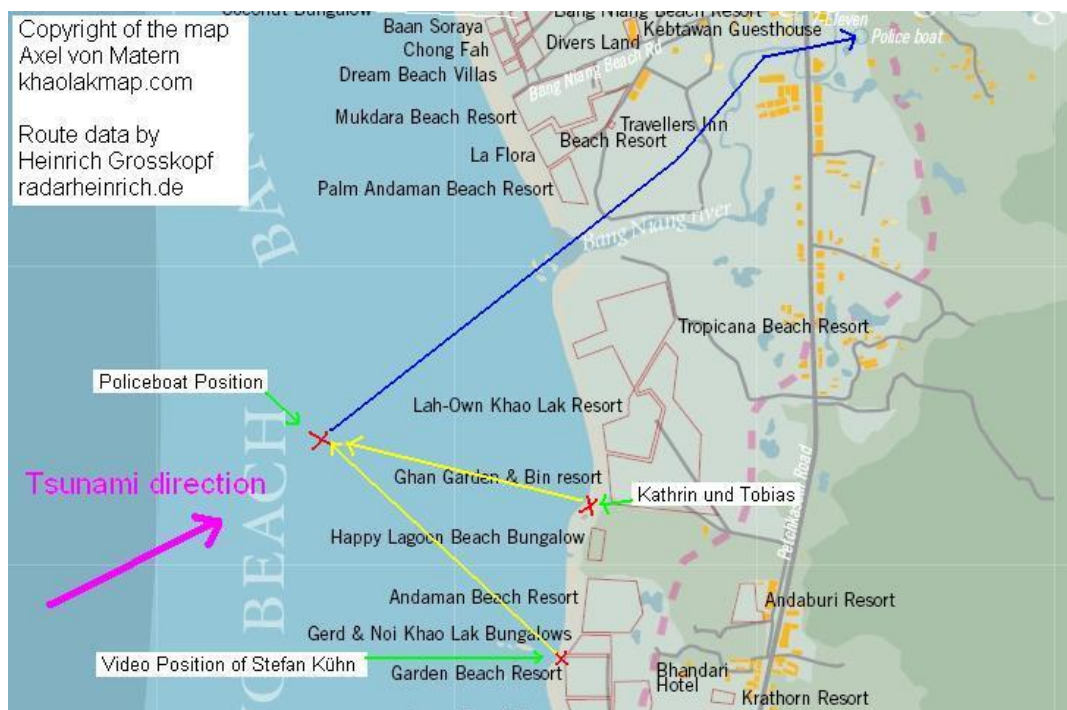


Figure 7-45 Comparison of wave direction in front of Nang Thong Beach and map showing the direction moved of the police patrol boat by the tsunami wave (www.khaolakmap.com).



Figure 7-46 First wave crest approaching nearshore Nang Thong Beach before reaching the two police patrol boats.

(<http://www.radarheinrich.de/wbblite/thread.php?threadid=2844>).



Figure 7-47 First tsunami wave at nearshore Nang Thong Beach was as high as police patrol boats heights (<http://www.radarheinrich.de/wbblite/thread.php?threadid=321>).



Figure 7-48 First tsunami wave trough reached offshore Nang Thong Beach causing water drawn down, while the first wave crest broke at the underwater rock outcrops resulting in high breaking waves (<http://www.radarheinrich.de/wbblite/thread.php?threadid=321>).



Figure 7-49 First tsunami wave crest reaching Nang Thong Beach and attacking the two Police patrol boats, causing one to sink; the other was transported 2.6 km away (<http://www.radarheinrich.de/wbblite/thread.php?threadid=321>).

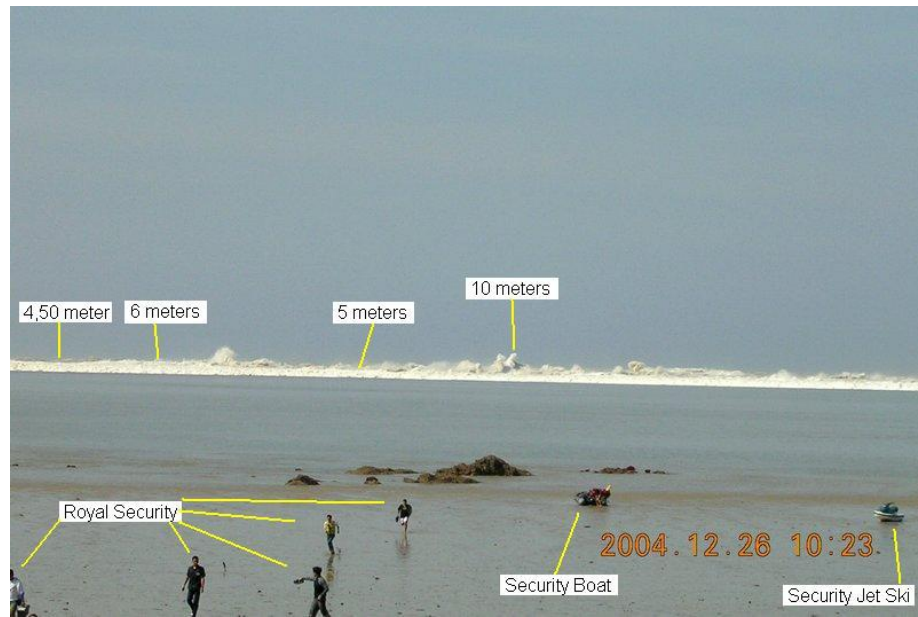


Figure 7-50 Estimated height of first tsunami wave crest which reached and broke at nearshore Nang Thong Beach (<http://www.radarheinrich.de/wbblite/thread.php?threadid=2844>).



Figure 7-51 Police patrol boat Number 813 was transported by tsunami wave. This image was taken 1 week after the 2004 tsunami event.



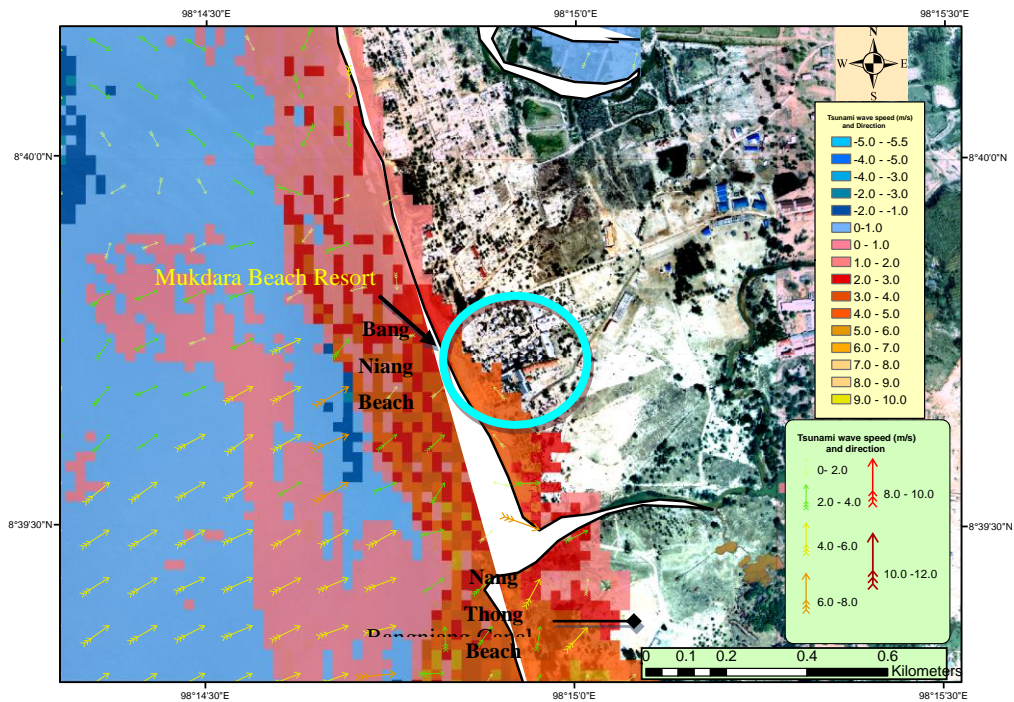
Figure 7-52 Police patrol boat was moved 2.6 km from its mooring and stranded 1.25 km from the coastline due to the high energy tsunami wave that attacked Khao Lak on 26 December 2004. The height of police patrol boat is about 5 m.

7-3.5 Comparing Tsunami Wave Pattern at Bang Niang Beach.

At Bang Niang Beach, the wave pattern from the modelling can be compared to photographs taken from Mukdara Beach Resort. Mukdara Beach Resort is located at the southern end of Bang Niang Beach, north of the Bang Niang Canal. The resort was totally flooded during the tsunami period. At +2 h 27 min (Figure 7-53), the model shows a tsunami wave approaching Bang Niang Beach; at the Mukdara Beach Resort itself, the tsunami wave was 4-6 m above MSL, its velocity was 4-6 m/s and it approached from the southwest (Figure 7-54). Time-stamped photographs show the first wave overwhelmed the ground floor of the hotel at 10.29 am, +2h 31 min (Figure 7-55). Water 1-2 m deep flooded the ground floor of the resort (compare to model outcomes in Figure 7-39). The resort is situated about 3-4 m above mean sea level, so first wave which initially overwhelmed the ground floor of the resort is ~4-6 above MSL which corresponds well with predictions from the model. Water depth increased more than 2 m in the next 3 minutes reaching ~4 m at 10.32 am (Figure 7-58), ~7 m above MSL with many kinds of floating debris drifting everywhere. Five minutes later

water had inundated the main building of Mukdara Beach Resort to a depth > 5 m. This photographic evidence is also consistent with the survey data from Siripong et al. (2005) and Matsutomi et al. (2005).

Later, the wave from southwest merges with the wave arriving from the west inundating the whole of Bang Niang Beach to depths of 2-5 m high (Figure 7-62 and Figure 7-63; +2 h 46 min) before starting to draw back to the sea. The tsunami wave inundation distance is 1.6 km inland. Inland the speed of the run-down is < 2 m/s but this increases to 4-8 m/s at the coastline. Wave run-down direction is generally to the west, perpendicular to the shoreline. The model shows a gyre (Figure 7-62) caused by the combination of the first wave's draw-down and the second wave's run-up wave.



Nang Thong Beach

Figure 7-53 Diagram of wave speed and direction of the first tsunami wave to attach Bang Niang Beach at +2 h 27 min. The blue oval shows the location of Mukdara Beach Resort

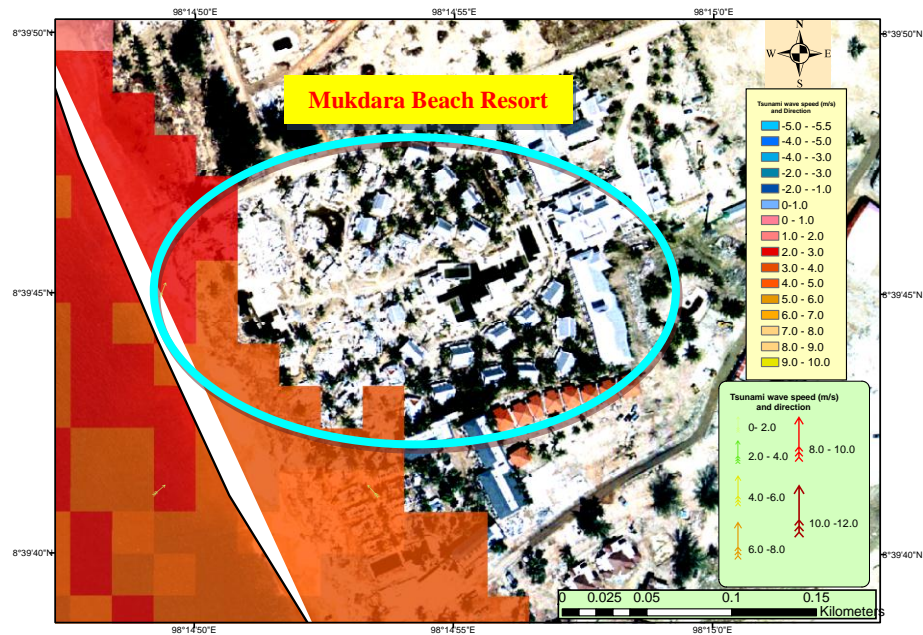


Figure 7-54 Detailed diagram of wave pattern around Mukdara Beach Resort at +2 h 27 min. Wave speeds are ~4-6 m/s, heights are 4-6 m above MSL and the wave approaches Mukdara Beach Resort from the southwest.



Figure 7-55 First wave reached Mukdara Beach Resort at +2h 31 min (10:29 am) (<http://www.radarheinrich.de/wbblite/thread.php?threadid=3178>).



Figure 7-56 The flooded buildings and small road has now been replaced by the corridor to the conference hall but the green water tower still remains and appears in the both pictures.

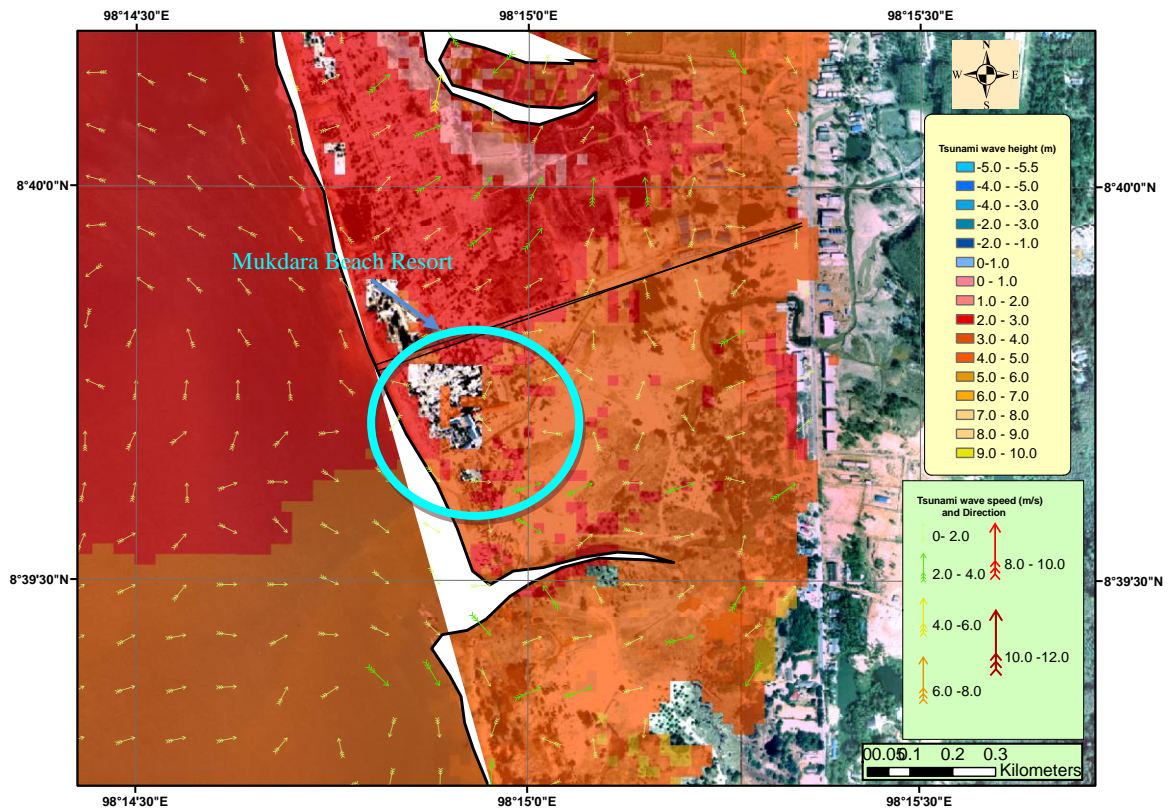


Figure 7-57 Detailed diagram of tsunami wave which inundates the Mukdara Beach Resort area, Bang Niang Beach at +2 h 35 min.



Figure 7-58 Photograph taken at 10.32 am on 24 December 2004 (+2h 34 min) of the first wave overwhelming Mukdara Beach Resort. Water depth from the known height of buildings is estimated to be 3.7 m (<http://www.radarheinrich.de/wbblite/thread.php?threadid=3178>).



Figure 7-59 This building is approximately 5 m high and was almost submerged by the first tsunami wave that attacked Nang Thong Beach.



Figure 7-60 Water depth due to the tsunami wave was approximately 3 m above the ground floor at 10.37 am on 26 December 2004 and rising rapidly (<http://www.radarheinrich.de/wbblite/thread.php?threadid=3178>).



Figure 7-61 This wall was underwater during the first tsunami wave attacked on 10.37 am of 26 December 2004.

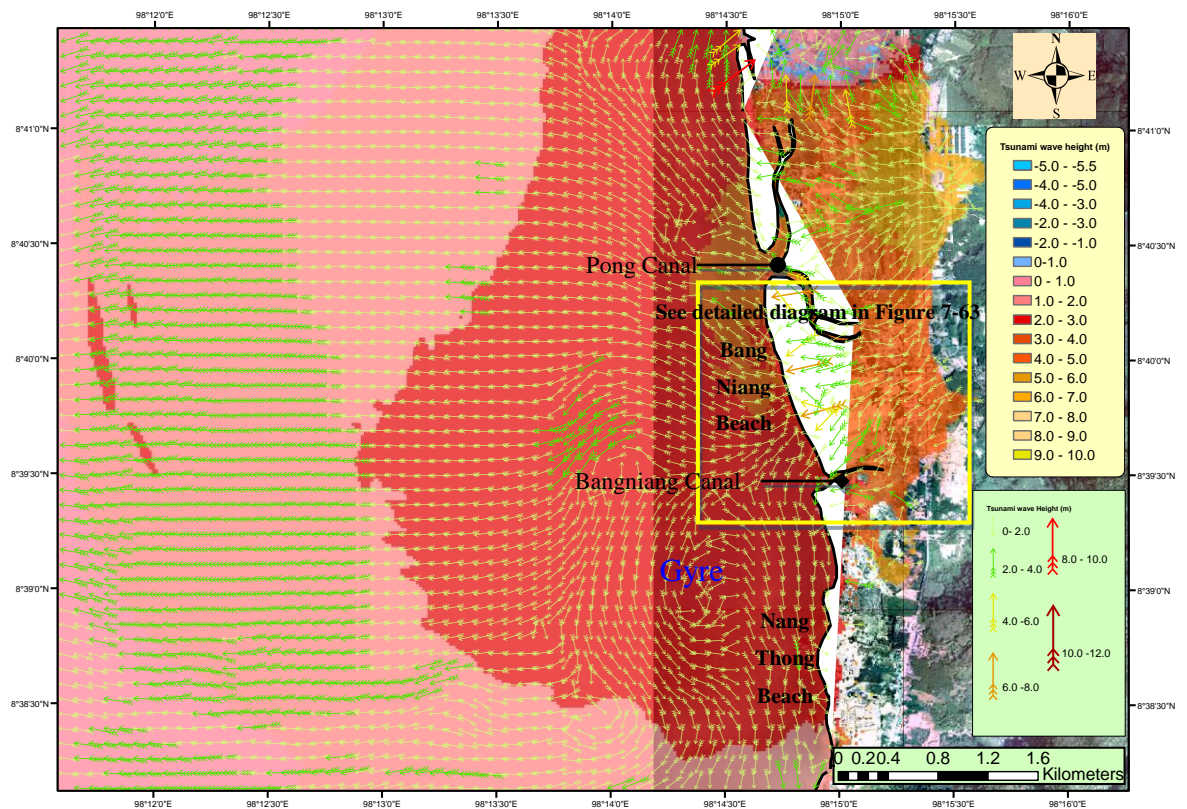


Figure 7-62 Inundation due to the wave from the southwest merging with the wave from the west at Bang Niang Beach and Nang Thong Beach at +2 h 46 min.



Figure 7-63 The wave that totally flooded Mukdara Beach Resort (Bang Niang Beach) starts to draw back (+2 h 46 min).

At 10.59 am exactly 3 hours after the earthquake, the model shows that the water levels offshore have receded prior to the arrival of the next wave (Figure 7-64 and Figure 7-65). The waters which inundated the shoreline are running back to the sea ($\sim 2\text{--}4\text{ m/s}$) although there is still considerable water around the Mukdara Beach Resort. The model shows much of the water in this area returning to the sea by flowing north or south towards the Pong and Bang Niang canals where flow speeds were very high ($\sim 6\text{--}8\text{ m/s}$) (Figure 7-64). Scars remaining on the canal banks provide evidence of this rapid retreat of water. New channel openings formed in the Pong Canal due to the high speed and power of the run-down flows, breaking through its existing shore-parallel banks.

The model results of flow back through the canals are supported by a photograph taken at the Mukdara Beach Resort at 10:59 am (Figure 7-66) looking towards the sea, which shows relatively calm, debris-laden water over the Resort, with depths of 1-2 m, but no indication of flow back to the sea across the Resort. The next incoming wave can also be seen from Figure 7-66.

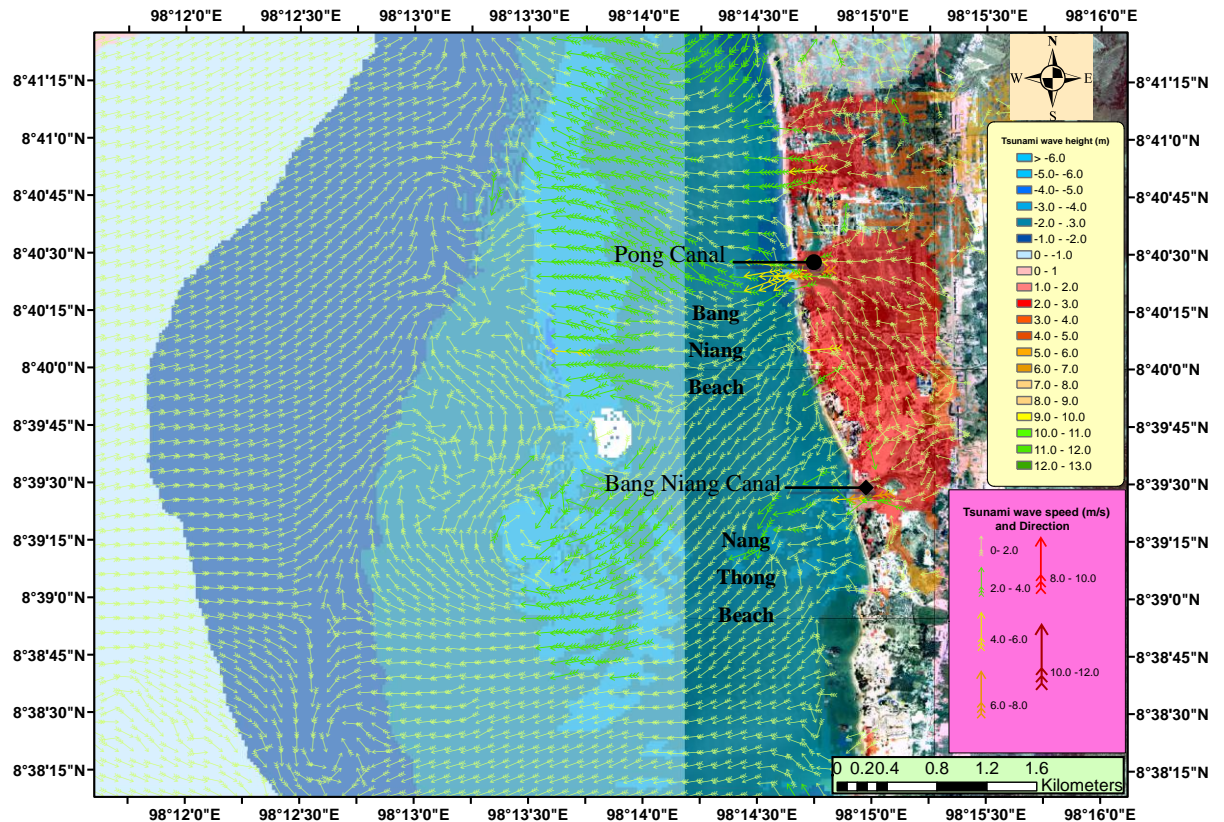


Figure 7-64 Wave retreating at +3 h 00 min (10:58 am).

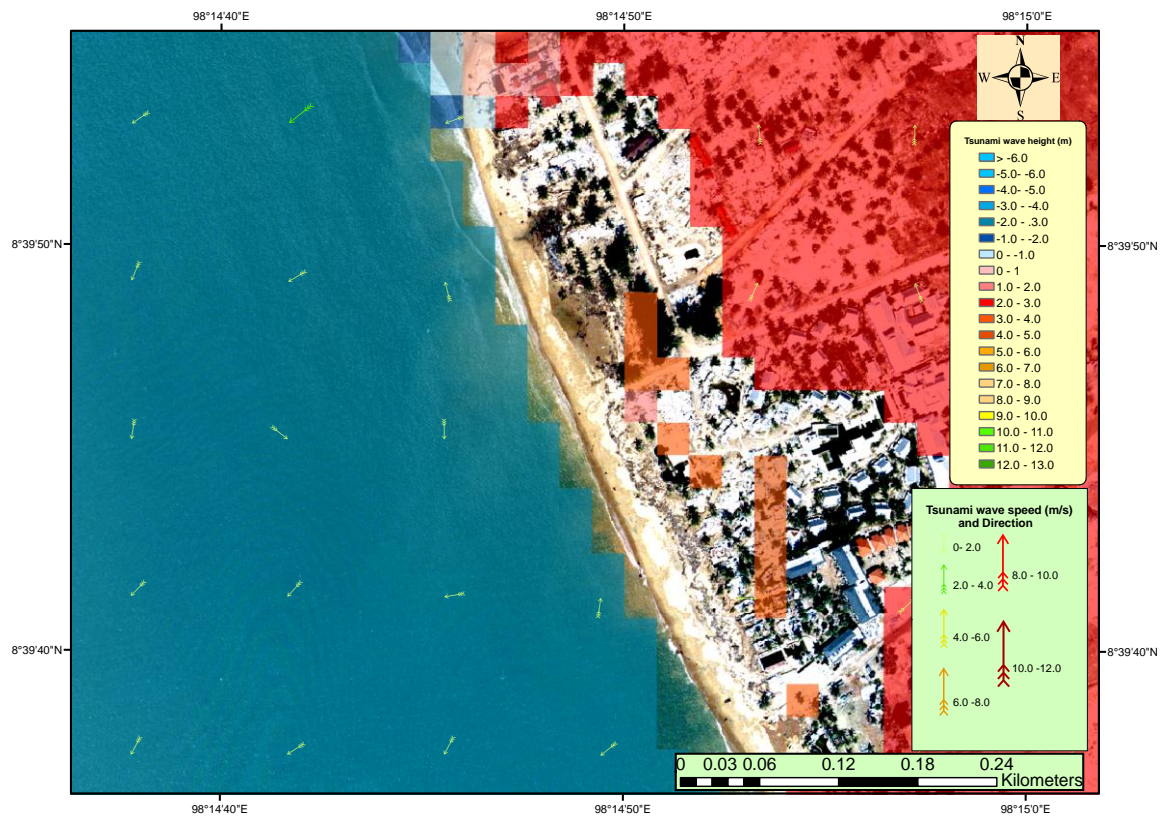


Figure 7-65 Detailed diagram of water height, speed and direction around Mukdara Beach Resort at 3 h 00 min.



Figure 7-66 Mukdara Beach Resort looking seaward at 10.59 am (3 h 01 min)
(<http://www.radarheinrich.de/wbblite/thread.php?threadid=3178>).



Figure 7-67 Mukdara Beach Resort in November 2008 taken from the same location as figure above.

A set of images taken from the Khao Lak Orchid Hotel can also be used to compare the modelled wave patterns with the tsunami that actually occurred. Khao Lak Orchid Hotel is located on Bang Niang Beach, north of the Pong Canal entrance, 200 m from the beach. The northern branch of the Pong Canal runs parallel to the beach behind the hotel. The hotel buildings are about 3-4 m above mean sea level. There are patches of Casuarina trees along the beach in front of the hotel. According to the hotel owner, the first crest only reached the swimming pool which located ~200 m from the shoreline and was about 3-4 m high; it slowly overwhelmed the front garden and the small road in front of the hotel. On the other hand, shortly after this a second crest (part of the first tsunami wave) came from the canal opening, located south of the hotel, inundating the hotel from the rear and flooding the hotel to a depth of 7 m. From the model, the tsunami wave behaves in a similar way, except for the inundation distance. In Figure 7-68, a wave crest first approaches from the west-northwest and is ~3-5 m high (above MSL, ~1 m above ground level) reaching the front of the Khao Lak Orchid Hotel and the canal behind the hotel (Figure 7-69); the inundation in the model is further than the actual inundation. The model shows a second crest, with the water reaching 5-6 m above MSL (~2-3 m above ground), inundating the hotel with flow speeds of 2-4 m/s (Figure 7-70). This agrees with the hotel owner who stated that the “second wave” inundated the hotel to about 3-4 m above the basement (~6-7 m above mean sea level; Figure 7-71). However, in the model it is difficult to distinguish between the effects of the first and the second crests because the waves arrive within a few minutes of each other and surge together creating the high wave flooding.

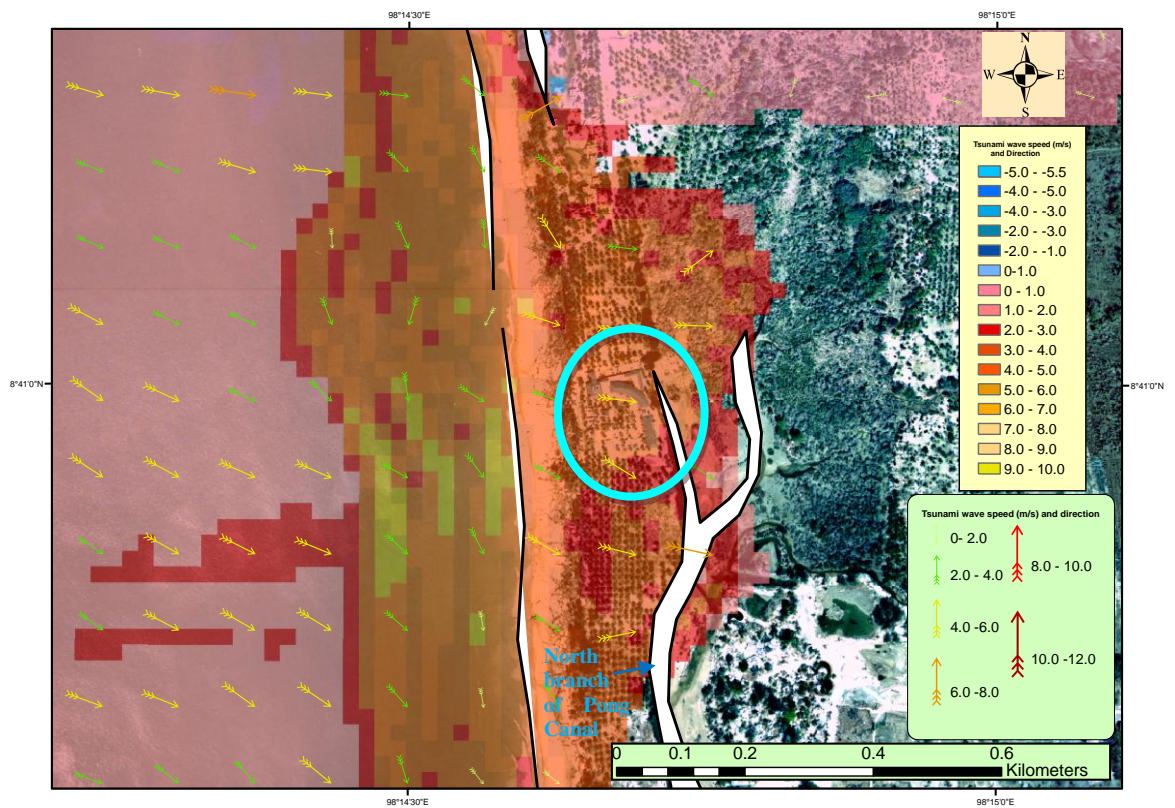


Figure 7-68 First wave crest reaches beyond the swimming pool and the buildings of Khao Lak Orchid Hotel to the canal behind the hotel.



Figure 7-69 Swimming pool in front of the Khao Lak Orchid Hotel



Figure 7-70 A second wave crest came from the canal entrance, flooding from south to north, passing the rear of the hotel without reaching a height that would flood the 2nd story of the hotel.



Figure 7-71 Khao Lak Orchid Resort was flooded by the tsunami to the floor of the 2nd story buildings which is approximately 6-7 m high.

The model results and the various lines of evidence collected at the time of 2004 tsunami show an encouraging, although not precise, degree of correspondence. It shows that the model captures most of the features of the observed waves and allows an understanding of how the wave inundated the nearshore region, including wave period, wave height, wave speed, wave direction and wave inundation distance, and gave sufficient confidence in the MOST model to allow it to be used to model future tsunami scenarios from which tsunami mitigation plans can be created to minimize tsunami impacts.

7-4 Vulnerability of the Khao Lak Area to Tsunami Generated by Earthquakes in the Future.

Khao Lak is one of the most important resort areas along the Andaman coast of Thailand. Many luxurious resorts and hotels have been re-established in this area (rebuilt along the beach-front after the 2004 tsunami) and generate important income for the local people so the safety and well-being of both tourists and local population are important to ensure the security of the tourism industry, especially for Bang Niang Beach and Nang Thong Beach. The wave characteristics from the model will be used to develop the mitigation plans and measures for providing a safer environment for the community.

To prepare for a potential tsunami that might affect Khao Lak in the future, the tsunami history of the area and earthquake sources of possible tsunami that might occur in the future along the Sumatra and Nicobar sections of the Sumatra Subduction zone must be considered. According to Section 2-5, a great earthquake of M_w between 8.5 and 9.0 is likely to occur along the Nicobar section of Sunda subduction in the next 100-500 years. However, it is impossible to forecast earthquakes with present technology. The 1960 Chilean earthquake, $M_w = 9.5$ which is the highest magnitude earthquake on record, caused a mega-tsunami resulting in severe destruction after which it was believed the fault would be inactive for several hundred years but another great earthquake ($M_w = 8.8$) and tsunami occurred again in February 2010.

Earthquake magnitude is known to correlate, or 'scale', with rupture parameters such as length and displacement (Henry and Das, 2001; Wells and Coppersmith, 1994). Wells and Coppersmith (1994) compiled source parameters (seismic moment, subsurface

rupture length, down-dip rupture width & average surface displacement) from 421 historical earthquakes between 1857 and 1993 including 50 thrust and 20 normal earthquakes in range $2 \times 10^{16} \text{ N m} < M_0 < 3 \times 10^{20} \text{ N m}$, and developed empirical relationships with the objective of being able to predict the expected value of a dependant parameter from an observed parameter. They found no significant difference (at 95%) between their regression constants depending on tectonic setting.

Henry and Das (2001) used data from Wells and Coppersmith (1994) but extended the range to include many of the large dip-slip earthquakes that have occurred since 1977. They showed that the ratio of rupture length to rupture width increases systematically with length for lengths $> 40 \text{ km}$ and slip to be proportional to rupture length over range $10^{17} \text{ N m} < M_0 < 3 \times 10^{21} \text{ N m}$, and that seismic moment scaled approximately as L^3 supporting Romanowitz (1994) who stated that the $M_0 \propto L^3$ relationship extended to the largest scale events.

Figure 7-72 shows a plot of rupture length L (km) against Seismic Moment M_0 (10^{20} N m) of all the dip-slip thrust earthquakes with $M_w > 7.5$, taken from Table 1 in Henry and Das (2001) which includes those from Wells and Coppersmith (1994), with the addition of our 2004 and the 2005 Nias earthquake. The line solid is the best fit line

$$\log(L / \text{km}) = -5.58 + 0.37 \log(M_w / \text{Nm})$$

from Henry and Das (2001), valid for $M_0 < 3 \times 10^{21} \text{ N m}$, but which fits the five largest events very well. The Wells and Coppersmith (1994) correlation (dashed line) is also shown. For the selection of a tsunamigenic earthquake to use for the design of mitigation measured to protect the Khao Lak coast the relationships for dip-slip earthquakes suggested by Henry and Das (2001) are used. The solid dot on Figure 7-72 shows the event finally selected.

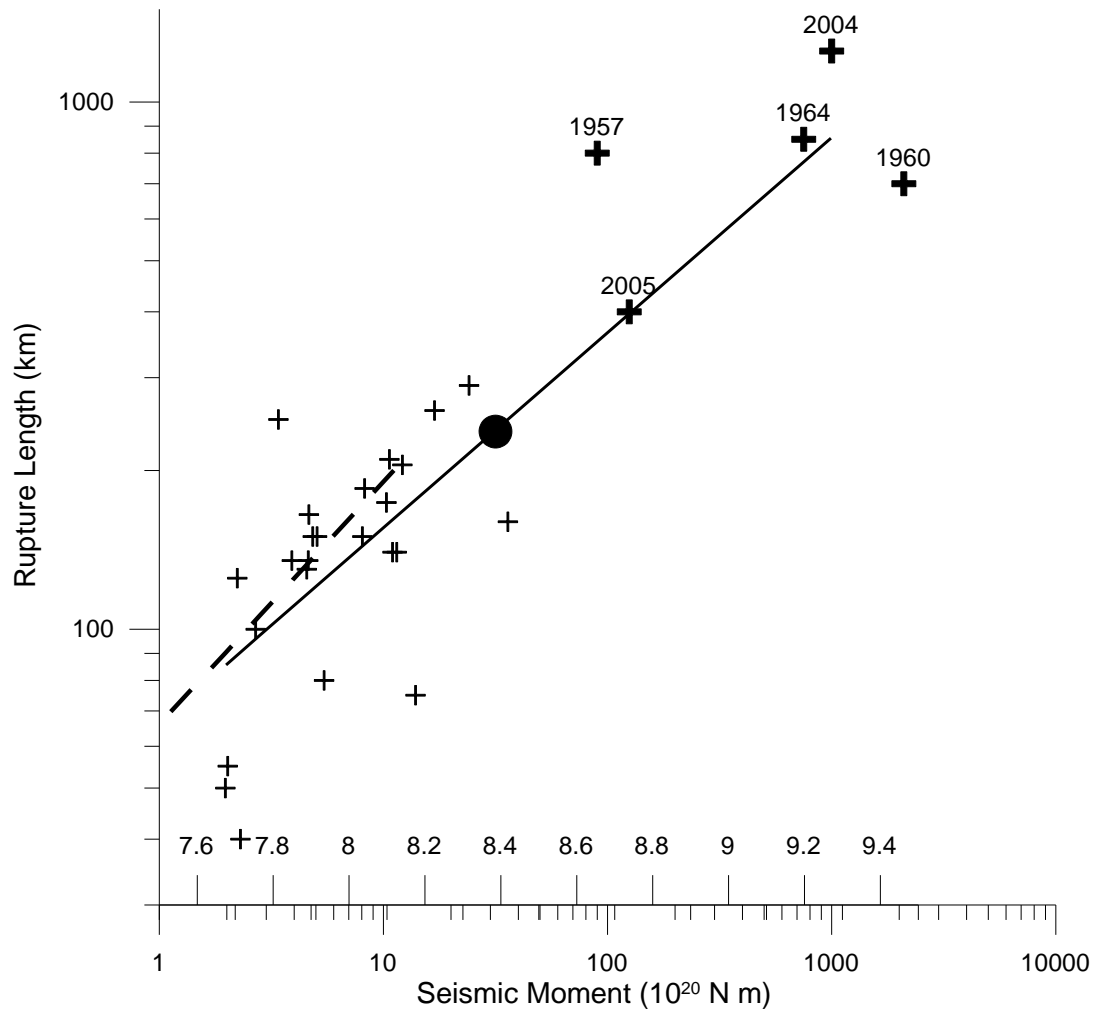


Figure 7-72 The relationship between rupture length and seismic moment M_0 for dip-slip earthquakes with $M_w > 7.5$ taken from Henry and Das (2001) with the addition of the 2004 Indian Ocean and the 2005 Nias events. The solid line is the best-fit correlation from Henry and Das (2001); the dashed line is from Wells and Coppersmith (1994). The solid dot is the $M_w = 8.4$ event selected for the mitigation scenario.

The vulnerability of the Khao Lak area to tsunamis generated by earthquakes of different magnitudes is summarized in Table 7-1. The rupture parameters in Table 7-1 were generated using the regression equations for dip-slip earthquakes in Henry and Das (2001). The tsunami wave parameters were generated using the MOST model using the closest values for rupture lengths and rupture widths permitted by the model for a rupture along the Nicobar section of the fault (Figure 7-73); the tsunami wave heights were for position close to the shoreline near Bang Niang and Nang Thong beaches.

| Magnitude M_w | Seismic Moment (10^{20} N m) | Rupture Length (km) | Rupture Width (km) | Average Displace- ment (m) | Max Wave height (m) | Inundation Area (km^2) | Inundation distance (km) |
|--------------------|---------------------------------------|---------------------------|-----------------------|----------------------------------|---------------------------|---|--------------------------------|
| 8.0 | 11.2 | 162 | 54 | 4.3 | 0.7 | 1.33 | 0.10 |
| 8.2 | 22.4 | 209 | 69 | 5.1 | 1.4 | 1.54 | 0.11 |
| 8.4 | 44.7 | 269 | 90 | 6.2 | 10.3 | 5.89 | 1.60 |
| 8.6 | 89.1 | 348 | 116 | 7.4 | 20.3 | 7.19 | 1.93 |
| 8.8 | 177 | 449 | 150 | 8.8 | 12.2 | 6.05 | 1.52 |
| 9.0 | 355 | 580 | 193 | 10.5 | 10.7 | 6.21 | 1.62 |

Table 7-1 Maximum tsunami wave height, inundation area and distance at Khao Lak from the MOST model, for earthquakes of magnitudes between 8.0 and 9.0 centred on the Nicobar section of the fault. Rupture length, width and displacement (slip) are from the regression equations in Henry and Das (2001)

The earthquake selected for the mitigation was magnitude 8.4 although there was very little difference between the heights (10.3-12.2 m) and inundation areas (5.9-6.2 km^2) of the tsunami resulting from 8.4, 8.8 and 9.0 earthquakes. This was chosen as the forecast scenario for tsunami mitigation, and for the development of tsunami resilience for the communities of Bang Niang and Nang Thong Beaches, because it produced significant tsunami effect on the Khao Lak coast and would not have too long a return period.

The very large wave (>20 m) near Khao Lak by an $M_w = 8.6$ earthquake predicted by the MOST model appears to be due to the interaction between the third wave crest and the water drawing back to the sea after the second wave, but this does indicate the considerable uncertainty likely to be associated with the details of a future tsunami. The sensitivity of the model to the location the earthquake hypocentre was tested by moving the hypocentre of hypothetical $M_w = 8.4$ earthquake north or south by 100km. The waves differed in detail but the wave height and inundation distances were similar.

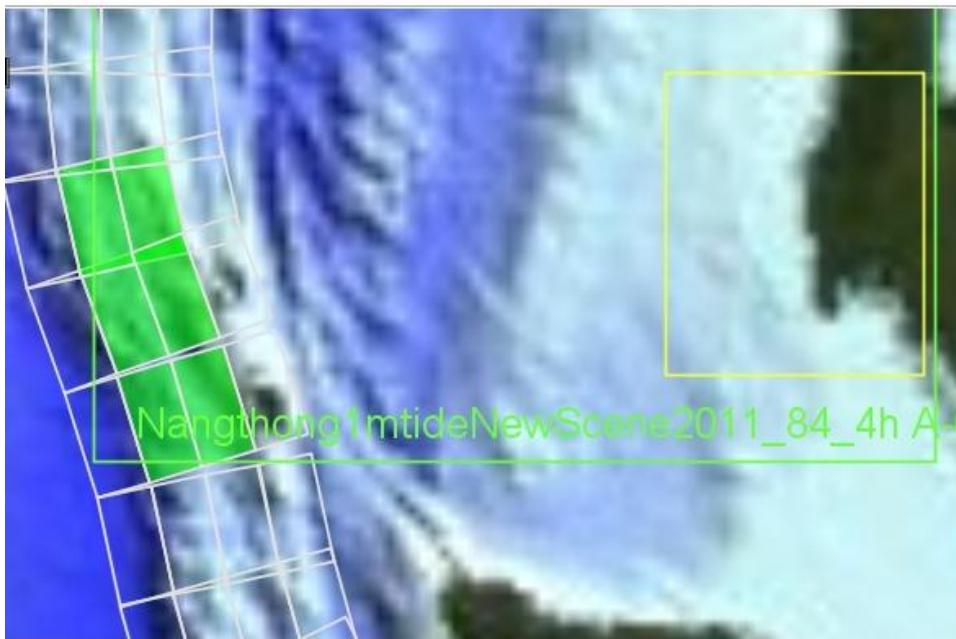


Figure 7-73 Sections along the Nicobar section of the fault used to generate the $M_w = 8.4$ tsunami, shaded green, using the MOST model; each box is 100 km x 50 km. The green box is Grid B, and the blue box, centred on Khao Lak is Grid C.

Chapter 8 Tsunami Mitigation

The loss of life and property due to natural disasters, including tsunamis, is increasing, not because the disasters occur more often but due to the pressures of human population. New settlement in the coastal risk areas increases the vulnerability of coastal communities. A recent UN report stated that three-quarters of the world's population will reside in coastal cities (Intergovernmental Oceanographic Commission, 2005).

Harinarayana and Hirata (2005) state that the key issue in natural hazard mitigation is preparation. Many communities do not realise the necessity of adopting preparatory measures and having mitigation plans until the hazard occurs. The probability of a tsunami is high in some areas of the world, such as countries along the Pacific Rim, especially Japan, where significant tsunamis occur on a decadal scale. As a result, research documents and the technology needed for tsunami alleviation are in an advanced state of development in this region. On the other hand, the risk of a powerful tsunami in the Indian Ocean region was thought to be very low before 2004, much lower than that in the Pacific Ocean, where many tsunamis have occurred there in the recent past. Of the 63 tsunamis events in the Indian Ocean since 1750, listed by the National Geographic Data Centre, only 8 were classified as major events. Thailand had never been hit by a tsunami in its recorded history and the 2004 tsunami in southern Thailand was the first such tragedy to have happened there (Dalrymple and Kriebel, 2005; Thanawood et al., 2006). Consequently, prior to the 26 December 2004 event, the tsunami was an unknown and unforeseen hazard for the Thai people. Thailand was unprepared for such a catastrophe and no mitigation plans existed to reduce the effects of a major tsunami on the people who lived along the Thai coast. Conversely, as mentioned in Bernard et al. (2006), tsunamis happen at least once a year somewhere in the world and living near the coast means living with the risk of this geo-hazard.

Synolakis et al. (2005) state that tsunami hazard mitigation involves three components, detection, forecasting and emergency preparedness. Direct tsunami detection data can be obtained from tsunameters; buoys to detect tsunami in real time are currently deployed across the Pacific, and now in the Indian Ocean. For tsunami forecasting, not

only numerical models, but also a trustworthy database of inundation is needed for verification and planning the mitigation programmes. Furthermore, as reported in Rajendran et al. (2007), the 2004 Sumatra-Andaman earthquake and tsunami were the first events to have occurred in the era of broadband seismometry and space-based geodesy. Geist et al. (2007) suggested that the availability of a global network of broadband seismic stations, regional GPS, post-tsunami surveys and tide gauge data, led to a better understanding of subduction mechanisms. These data can also be used to reconstruct the evolution of the Sumatra-Andaman tsunami from the earthquake that led to it, and this, in turn has brought about an improved understanding of tsunami patterns.

8-1 Tsunami Mitigation at Policy Level

To assist in the achievement of a full capacity tsunami mitigation scheme, the United States Agency International Development (2007) reviewed the disaster management in Thailand and concluded that a collection of policies, laws, institutional frameworks and clear guidelines needed to be put in place, including the integration of the technical, socio-economic and ecosystem background required for decision-making. However, without public participation the formulation of an appropriate policy might cause subsequent problems. For example in Sri Lanka, the short-term policy issued by the Sri Lankan government prohibiting reconstruction in the coastal buffer zone (100-200 m from the sea), resulted in a slow recovery after the 2004 tsunami. Another example involved fishermen, who were relocated 2 km from the sea and could not continue fishing. The main reason for these problems was a lack of a public consultation in the formulation of processes to be implemented. From these examples it can be seen that it is essential to understand the local people and the work they do in the different areas and pay more attention to community involvement (Ingram et al., 2006). Comparable problems also occurred in Thailand. The slow recovery of Phi Phi Island and Namkhem Fishing Village can be ascribed to similar reasons. Effective policy should balance the sustainable usage of natural resources and human needs. Public and political support can be built up by emphasising the comparative losses to communities that have no risk-reduction plans and policies compared to those communities with effective measures in place to strengthen the community preparedness (Eisner, 2001). Rittichainuwat (2006) recommended that government should have clear strategies backed up by sufficient funding. The lack of practical policies and adequate funding

tends to block the recovery process in the tsunami-affected area and prevent reconstruction in the tsunami safe zone.

After a disaster, governments immediately take charge of the tasks of rescuing victims, building temporary shelters and rebuilding damaged infrastructure. In such a situation it is difficult to institute policies to cope with the long-term vulnerability. Ingram et al. (2006) state that policies such as the relocation of local communities and the institution of buffer zones result in reducing exposure for the short term but are not easy to implement and sustain in the longer-term.. In Thailand, even though the government and the military provided financial and logistical support for the local community to build new houses in a tsunami safe zones, the local people insisted on rebuilding their houses on their own land located in the tsunami risk area (United States Agency International Development., 2007). Eisner (2001) points out that a disaster such as a tsunami yields the opportunity to minimise future losses by offering the opportunity to reshape existing, unsuitable patterns of development. The introduction of a coastal buffer zone and setback policies, will then guarantee safety for the people who reside along the coast. The main strategy for reducing tsunami impact for the long-term is therefore a policy of adaptation but such reactive policies need to be in agreement with the prevailing socio-economic, environmental and political conditions.

Government agencies are responsible for developing emergency policies and strategies to meet the needs of communities, including raising the awareness of the people, developing a warning system, reducing false alarms, and providing evacuation maps (Jonientz-Trisler et al., 2005). Eisner (2001) recommended that local governments or communities select a group of specialists to assist them, including researchers, architects, and geotechnical, coastal and structural engineers from local academic institutions, government agencies, and professional associations. Bernard et al. (2006) recommended that policy makers address three strategies to reduce tsunami impacts:

1. awakening the realisation that tsunamis constitute a potential hazard that faces the communities,
2. setting up scientific standards for tsunami forecasting and
3. maintaining public awareness of the tsunami phenomenon by developing regular community activities such as training, exercises, research and development.

In Thailand, it is the lack of a comprehensive policy framework that gives rise to a deficiency of cooperation among the stakeholders. National and local agencies need to develop well-integrated strategies instead of working in isolation, and the skills of national and local officers in charge of these services must be applied to develop an effective early warning system (United States Agency International Development., 2007). Sonak et al. state that the level of implementation is as significant as the policies themselves in achieving the optimal results, and policies should be reviewed periodically to allow for the effects of changes in the local demography and economic developments in the community.

8-2 The Concept of Tsunami Community Resilience

Resilience is defined as the ability to absorb (withstand), adapt and recover from losses (Berkes, 2007). Tsunami-ready communities are those that have tsunami response plans and conduct occasional tsunami drills. Jonientz-Trisler et al. (2005) suggested three components relating to building a tsunami-resilient community, viz. hazard assessment, warning guidance and mitigation.

Scientists conducting active research and modelling are responsible for hazard assessment and proposing warning guidance to suit the community. Tsunami prone areas must be identified and warning information should be given to the local population. For mitigation, an emergency manager applies the available science and technology to create plans and education products; it should be noted that social scientists are helpful in providing input for delivering right message to motivate the populace. Pomeroy et al. (2006) recommended rehabilitation livelihood principles to avoid the mistakes of the 2004 tsunami. Firstly, it is necessary to understand the diversity of the coastal population. Secondly, to build up the involvement of the community, and thirdly to create long-term plans to build up sustainable, resilient communities based on the recognised vulnerabilities.

Community resilience begins with tsunami hazard assessment by determining the sources and impacts of potential tsunamis. Numerical modelling can be used to estimate the effects of potential future tsunamis. The risk of a future tsunami disaster is a function of the forecasted hazards and the scale of the vulnerability of the local

population residing in the danger zone. Risk assessment is carried out by making an integrated assessment of the vulnerability of the community to the potential hazards, the infrastructure and economic activity in the area, and the level of local preparedness ($\text{risk} = \text{hazard} \times \text{vulnerability}$). Annaka et al. (2007) use the Probabilistic Tsunami Hazard Analysis (PTHA) method for estimating tsunami risk for the Japanese coasts. PTHA represents the relationship between the predictable tsunami height and the probability of this being exceeded. This method comprises a tsunami source model to generate an estimation of tsunami height, which is used for quantitative tsunami risk assessment. Logic-trees are created for tsunami sources induced by earthquakes and the resulting tsunami height estimations. The estimated preparedness of the community, based on the risk assessment outcome, is then applied to reduce susceptibility.

From Jonientz-Trisler et al. (2005) point of view, a tsunami-resilient community is a community that has action plans, products and policies to reduce the impacts of tsunami hazards. In a resilient community, such tsunami preparedness plans will have been publicised and practiced by the population. For the safety of life and property during and after a devastating tsunami, part of the preparedness must be the education of the public about tsunami waves. The plans should be regularly updated to improve the resilience level for the future, by adapting them to incorporate the lessons learnt from recent tsunamis both in and outside the area. Wood and US Geological Survey (2007) stated that the greater resilience the community achieves, the lower the community vulnerability to disaster. The tsunami-ready community that has an educational program, a frequent evacuation drill and a practical post-disaster recovery plan, is more capable of efficient response and has a shorter recovery period than the community without such practical measures in place.

Historical records of tsunamis, both local tsunami and distant, are the first information that should be collated for evaluating tsunami risk in an area. It is then necessary to understand the tsunami wave patterns, including the number of waves, wave heights, arrival times and inundation distances anticipated. Knowledge of aspects of plate tectonics and seismology are necessary to forecast the future occurrence of mega-earthquakes and tsunamis; Potential future seismic events and tsunami-triggering scenarios should be identified together with an estimation of tsunami run-up heights under different seismic conditions. Tsunami reduction measures, such as physical

barriers, vertical land reclamation, new building codes and land use planning, should be implemented. Knowledge of tsunami prediction is necessary for decision makers at all levels from the regional to the global scale since it is essential to bring together the knowledge of geology, oceanography, engineering and architecture to create the tsunami-safe area with proper mitigation measures (Dalrymple and Kriebel, 2005).

Mitigation involves sustained measures to reduce long-term tsunami risk. The mitigation issue is mainly concerned with coastal land use planning, the maintenance of the environment and ecological stability such as mangrove and beach forest enrichment, the protection of sand dunes and the setting up of buffer zones. Building regulations for protecting critical facilities and infrastructures are also part of mitigation. Tsunami-resistance should be considered when drawing up legislation for building codes, building design and construction practices (National Science and Technology Council, 2005; Thanawood et al., 2006; Wood and Geological Survey (U.S.), 2007). The design and layout of buildings have to be considered as they will affect evacuation and recovery plans as well as controlling resistance to destruction. Systematic coastal zone management, including land-use planning and coastal zoning is a practical means of reducing loss from potential tsunamis (Siripong et al., 2005).

Coastal zone management and the restoration of ecosystems need to be balanced with coastal development projects (Srinivas and Nakagawa, 2008). The environmental implications for any disaster preparedness concept to reduce tsunami vulnerability are significant, as the deterioration of environmental conditions, such as deforestation or dune removal, may serve to increase the impacts of the disaster. Sand dunes, mangrove forests and coral reefs act as barriers to reduce the power of the tsunami waves. After the tsunami, these natural forms of protection can recover relatively quickly and provide continued protection for the coast, whereas the reduction of ecosystems as a consequence of coastal development may reduce such resilience. Coastal reforestation will result in an increase in the forests' ability to protect the coastal areas from erosion due to storm surges and enhance its capability to absorb wave energy. Buffer zones and no-build (set back) areas will ensure the security of the tsunami affected zones.

8-2.1 Tsunami Warning Systems and Emergency Planning

Rittichainuwat (2006) reported from her surveys of tourists in Phuket, Khao Lak, Krabi and Phi Phi Islands that western tourists were concerned about the lack of an adequate tsunami warning system and that the Thai government must install such a system to meet international standards. Injury and loss of life from the tsunami wave can be reduced if people are warned that a tsunami is approaching. For that reason, complete area coverage and built-in redundancy in the warning system are important for improving the standards of safety. However, due to the differences between coastal communities, no complete warning and evacuation systems has been devised that can suit all coastal communities (Oregon Emergency Management and Oregon Department of Geology and Mineral Industries, 2001).

For Khao Lak the probability of a 'distant' tsunami is greater than that of a 'local' tsunami as the likely earthquake source is the Sunda Subduction zone. Effective forecasting is therefore essential for the design of a warning system, with the added requirement for recognising and discarding false alarms. Oregon Emergency Management and Oregon Department of Geology and Mineral Industries (2001) reported that due to the slow rate of subduction, earthquakes generating devastating tsunamis tend to occur along short segments and for these it is difficult to issue a warning, due to the subdued response of the coastal landmass. It is therefore essential that the warning system should include the recording of seismic signals and have the critical ability to assess the likelihood of tsunami generation.

However, with a view to increasing public confidence and reducing the number of false alarms, tsunami warnings cannot depend upon seismic data alone. Stein and Okal (2007) reported that the Pacific Tsunami Warning Centre first estimated the magnitude of the 26 Dec 2004 earthquake using long-period body waves and concluded that the magnitude of the earthquake was $M_w = 8.0$, with little possibility of tsunami generation. 45 minutes later, the magnitude estimate was increased to $M_w = 8.5$ and an ocean-wide tsunami became possible. Four hours later, the earthquake magnitude was re-calculated, using longer-period surface waves, and yielded $M_w = 9.0$ with the very high risk of a tsunami. By that time, Indonesian, Thai and Sri Lankan coasts had already been devastated. As a result of this, Stein and Okal (2007) suggested that the traditional measures of earthquake size, determined shortly after major seismic activity, are

inadequate for issuing tsunami warnings. Although, an earthquake with $M_w < 8.0$ may be too small to generate a far-field tsunami the hazard to nearby coasts can still be large. It is a serious difficulty in the process of tsunami warning to decide whether a warning should be issued or not, or whether to cancel it if the tsunami forecasting system is unreliable.

Seismic sensors, seismographic networks, sea level observing networks and deep sea pressure sensors are real-time instruments that can assist in the early identification of tsunami (Intergovernmental Oceanographic Commission, 2005). Real time sea-bottom pressure recorders (tsunameters) incorporated with the DART system can be used to detect a tsunami in the deep ocean before it reaches the coastal and to bring about more reliable tsunami prediction. Networks of these instruments serve have improved both the 'tsunami approaching' prediction and provided additional information to reduce false alarms (Bernard et al., 2006; Jonientz-Trisler et al., 2005). Synolakis et al. (2005) stated that the best means of alleviating the next Indian Ocean tsunami disaster is the combination of a trustworthy prediction of the tsunami using the network of real-time deep ocean buoys and public education.

Synolakis et al. (2005) state that seismic observations and tide gauge data may not sufficient for tsunami prediction as some tide gauges will not show high frequency content as they are designed to measure tides at periods much longer than those of tsunami waves (Piatanesi and Lorito, 2007). An effective but costly way is to deploy an ocean bottom crustal deformation monitoring system together with a offshore direct tsunami observation system. For the Thai coast, digital tide gauges (with a frequency response high enough to record tsunami effects) deployed on Miang Island or the Similan Islands is one of the most cost-effective methods for tsunami detection and will give up to one hours warning of a tsunami event impacting the mainland coast of Thailand. Mexico are installing a system to detect and monitor tsunami waves using high-frequency sea-level tsunami gauges operating continuously with 1 min interval recording. These tsunami gauges are to be installed every 200 km along the Mexican Pacific coast (Farreras et al., 2007).

Rittichainuwat (2006) recommended that any official tsunami warning system should be enhanced e.g. by supplementary systems installed by the hotels and communicating

directly with the individual guestrooms. These would serve to build the confidence of the guests that all is being done to ensure their safety. These measures could even be supported by periodic drills and rehearsals of tsunami evacuation. However, the warning system is not only dependent on technology, but also relates to organisation and management. A successful warning system needs to reach all groups of people and to inform them what they need to do. After this, it becomes a question of how the population responds to the warnings.

The other crucially important measure to be incorporated within the tsunami warning system is an integrated emergency preparedness plan. The availability of emergency responses could have saved a large number of people along the Indian Ocean coasts from the fatal outcome of the 2004 tsunami. Many of the Indian and Sri Lankan people who live along the coasts could have been saved if the warning had been issued on 26 December, after the tsunami hit the Andaman and Nicobar Islands i.e. approximately 2 hours before hitting the Indian mainland and Sri Lanka. Fortunately, some hotels in Phuket, Thailand, evacuated their guests to the upper floors immediately after feeling the earthquake and some sailors at the Langkawi Island yacht harbour in Malaysia sailed their yachts offshore after a short-wave radio report that a big wave had hit Aceh, Indonesia. Many hotels in southern Sri Lanka were warned by a sister hotel of the approach of a freak wave from the east. These fortunate hotels and some of their neighbours evacuated their guests to a higher floor after the first wave hit (Synolakis et al., 2005).

Most deadly tsunamigenic events reach the coastal communities within 30 minutes to 1 hour of the triggering earthquake. Synolakis et al. (2005) suggest that 15 minutes warning is enough time for evacuation in places such as the Maldives. After Malle Island had been struck, the Ministry of Atolls of the Maldives warned the outer islands 15 minutes before the tsunami arrived, and saved many villagers who had enough time to evacuate to the centres of the islands. In the event that the local people feel the earthquake strongly enough to disrupt normal or everyday activities, it can be presumed that sea level might change, and that evacuation should take place immediately from the low-lying areas and the beaches. For this to happen it is necessary for both the local residents and visitors to know something of the geophysical history of the area. Importantly, they should know how to evacuate without delay to high ground inland or

to a higher floor in an engineered building which has survived the earthquake. For sensitive places such as schools, it is crucial that evacuation drills be repeated regularly.

The National Disaster Warning Centre of Thailand, established in May 2005, receives and analyses hazard observation data and issues warnings through warning towers, radio and television channels and approximately 20 million mobile phones in Thailand. Approximately 80 warning towers have been installed along the coastline of Thailand. These towers receive warning signals from satellites and broadcast warning message in five languages. Sirens and loudspeakers operated by the local administration officials are incorporated into the warning system; the next step is for local radio broadcasting stations to receive the warning signal directly via the Asia Star Satellite (United States Agency International Development., 2007).

8-2.2 Coastal Zoning and Land Use Planning.

Tsunami risks can be mitigated by minimising the exposure of people and property through land use planning (Eisner, 2001). Hence, development must be controlled in tsunami-affected zones. Sonak et al. stated that coastal zone management and development should be integrated with environmental and social services to fill the gap between the sciences and other disciplines.

To assure the safety of communities from tsunami risk, it is necessary to identify tsunami risk areas, to generate evacuation maps and evacuation routes, and to identify tsunami-safe zones (Bernard et al., 2006). Human vulnerability is the highest priority in mitigating the effects of a tsunami, with the reduction on the economic impact a secondary priority. A trustworthy scientific organisation should be responsible for setting the scientific standards for tsunami prediction and it should be the task of national or local government agencies to produce inundation and evacuation maps to suit each specific community.

To achieve a trustworthy level of tsunami forecasting, Harinarayana and Hirata (2005) propose that detailed seafloor bathymetry and shallow subsurface structure surveys be carried out using high resolution mapping devices, especially near the possible sources of potential tsunamigenic earthquakes. Detailed bathymetric and topographic data are needed for numerical modelling computations designed to study tsunami wave propagation in the open sea and inundation in the nearshore zones. As tidal effects can

change the inundation patterns tsunami risk maps should ideally indicate the risk as a function of tidal conditions for the areas concerned. If a tsunami occurs during high tide, the effect of the wave is likely to be worse than that at low tide. The average high tide along the Thai Andaman coast is normally +1.0 m MSL, and +1.5 m MSL at spring tides. Karlsrude et al. (2005) recommended that the risk management measures to be implemented for the next 50-100 years should be designed using a maximum level of +3.0 to +3.5 m MSL (1.5 - 2.0 m for the tsunami wave plus 1.5 m due to possible high tide). To protect vulnerable communities from mega-tsunami over the next 100-200 years need further investigation but, meanwhile, the design maximum level for such an occurrence should be considered to be 5-10 m above mean sea level. Sensitive buildings, such as schools and hospitals, should be located outside these tsunami risk zones.

Geographical Information Systems (GIS) and indicator-based computer decision support tools play an important role in the assessment of hazard vulnerability and are utilised in the preparation of risk maps (Dominey-Howes and Papathoma, 2007). GIS-based evacuation maps were developed by integrating tsunami modelling output with geographical data (Jonientz-Trisler et al., 2005). Wood and US Geological Survey (2007) reported that GIS is being used to identify tsunami-prone areas of the Oregon coastal zones. GIS can also be used to combine data on socio-economic conditions (distribution of developed land, human populations, economic assets and locations of critical facilities) with data on tsunami inundation zones.

At present, there is no complete set of tsunami risk maps and related information for the tsunami-affected areas of Thailand. As a consequence, land use planning and coastal zone management frameworks are incomplete. For example, roads and highways construction groups do not take disaster risk reduction into account. Significantly, setback policy has not been implemented for the reconstruction in the tsunami-affected areas after the 2004 tsunami event due to a lack of law enforcement. The setback policy initially proposed for reconstruction in the coastal zones was 100 m; this was then reduced to 50 m and again to 30 m but finally no setback has been enforced. Neither were the guidelines for land use and reconstruction in the tsunami-affected area put forward by United States Agency International Development (2007) put into effect. For Bang Niang Sub-district Administrative Office, there are some local regulations issued

by the office to enforce for zoning and building codes. The regulations are referenced by the Department of Public Works and Town & Country Planning.

Escape routes should be well marked and easily accessible (Karlsruhe et al., 2005). Evacuation routes should lead to a safe place or area where evacuation shelters are available. These safe areas can be natural (elevated land) or man-made shelters. These safe places should be accessible and lie within 500 m of the shoreline. Evacuation routes should also indicate the locations of vertical evacuation shelters in the event that the horizontal safe zones are too distant. Vertical evacuation to the higher floors of strong buildings also becomes crucial for shelter if the warning time is short (Dalrymple and Kriebel, 2005). Eisner (2001) suggested that vertical evacuation is also essential in densely populated zones where horizontal evacuation is limited by road capacity. Buildings of 2-3 stories and more are most appropriate for vertical evacuation. Building size, access and the available facilities, are factors determining the capacity of vertical shelters. A list of buildings to be used as vertical shelters in case of emergency should be made public, to both the local population and tourists.

It was not only the power of the tsunami itself which created the casualties and damage, but also the floating debris carried by the swirling waters. Debris carried by the incoming and receding waves was a major cause of destruction (Dalrymple and Kriebel, 2005). The first wave demolished buildings and produced debris which was supplemented by cars and other unfixed objects for the subsequent waves to use for further demolition. To minimise such consequences it is necessary to locate potential debris-producing objects and structures such as parking lots, wooden buildings etc., as far landward as possible (Dalrymple and Kriebel, 2005).

In the long-term, new construction must be able to withstand tsunami forces. Critical facilities such as hospitals and schools, and basic infrastructure such as main roads and bridges should be relocated to safe areas (National Science and Technology Council, 2005). Wood and US Geological Survey (2007) reported that fatalities in Indonesia were high for children under 5 years of age and for senior citizens over 65 years of age; they suggest that facilities for the dependent population, such as care homes, child care centres and emergency-services facilities (police station and fire station) and medical facilities (hospitals and physician offices), should be also be located well clear of the

anticipated tsunami inundation zones. Hospitals and physicians' offices make up an essential part of the emergency services, as they are vital to the handling of casualties during and after a disaster. As a result, it is an important requirement that medical facilities are located in safe zones that are still easy to access in the event that roads are blocked by evacuating crowds or debris from the disaster. Further infrastructure that needs to be relocated outside the hazard zones include the basic services such as electricity and water supply facilities (Wood and Geological Survey (U.S.), 2007). Eisner (2001) noted that critical infrastructures will need to be up and operating as soon as possible after the disaster, and in case of damage must be repaired at once.. Moreover, Eisner (2001) recommended that critical facility buildings should be designed to withstand an increased force level, suggesting 15-50 % above the calculated standard. Public venues such as national parks, and museums, that are widely used during the daytime, need special measures to protect employees and visitors. Tourists and visitors may dominate the population in coastal tsunami risk areas during the daytime. Generally speaking, tourists, visitors and seasonal or temporary employees will be among the people who know least about tsunami waves and evacuation procedures. Farreras et al. (2007) also recommended that the relocation of railway tracks and roads further inland will help to minimise fatalities and loss of property.

Standard tsunami evacuation signage, for example hazard zone signs, evacuation routes and education signs, are significant tools that need to be incorporated into a practical evacuation plan. For example, the State of Washington has placed warning and evacuation signs in popular locations and tsunami inundation maps of the area have been put on display in prominent positions (Johnston et al., 2005). Signs should be clear enough and make sense to both residents and visitors. They should not mislead the people by directing them to safe places far away from their current position.

8-2.3 Standards for Building Regulations

Building regulations constitute one of the main aspects affecting the degree of destruction resulting from tsunami waves. A building engineered to high standards is able to withstand a strong tsunami wave. It is remarkable that places of worship are constructed to a higher standard than many residential buildings, and remain standing after the tsunami, for example churches and Buddhist temples in Sri Lanka and

mosques in Banda Aceh, Indonesia (Synolakis et al., 2005). Harinarayana and Hirata (2005) also noted that if a high magnitude earthquake occurs in a country with poorly-prepared building codes of construction, the casualties are likely to be considerably greater than by a similar event happening in a well-prepared country. Lack of attention to the building regulations generally results in poor construction. The degree of destruction by tsunami waves can be limited by issuing and enforcing suitable standards and construction codes, designed for the particular area. All available knowledge concerning potential tsunami waves, for example, wave speed direction and height, as well as land use planning decisions need to be pooled in developing appropriate building standards. New developments should be encouraged in the tsunami-safe zone, and infrastructures in the high-risk tsunami areas should be actively discouraged. All buildings in the inundation zone must be designed to withstand the force of the tsunami waves; tsunami-resistant building design standards should be implemented in the tsunami affected communities.

If building is permitted in the zones most prone to the potential of high tsunami waves open-plan buildings, especially for the first (ground) floor, and buildings on elevated land should be encouraged. For example, the Safe Islands concept was planned by the Government of the Maldives to set up communal high buildings and buffer stocks of provisions in specially constructed zones located on higher ground (National Science and Technology Council, 2005). Eisner (2001) recommended 4 ways to reduce risk when developing a construction project in a tsunami affected area: avoiding risk by raising the land and structures above the flood level or placing infrastructure on higher land; slowing the wave by using the friction provided by forests, slopes and berms; steering the wave by diverting the wave away from densely populated zone; and blocking the wave by building hard structures to obstruct and reflect the wave forces.

Most houses and small buildings in southern Thailand are built on shallow spread footings embedded less than 1 m below ground level. As a result, scouring is one of the main factors causing most non-engineered buildings to collapse in the flood zone. Collapse of such buildings can be avoided by putting in well-designed and deeper foundations in the tsunami-prone areas. Large buildings, piers and harbour structures should have scour-resistant foundations and all structures should incorporate proper anchoring to the foundations (Dalrymple and Kriebel, 2005).

Siripong, et al. (2005) divided the areas flooded by the 2004 tsunami in Thailand into 3 zones; the flood zone, the wave-attacked zone and the zone most-strongly attacked by the wave. Buildings in the wave-attacked zone need to be specially designed to withstand the high-speed water velocities and flooding; buildings in the zone most-strongly attacked by the wave need even more advanced design construction to tolerate the impacts of high-speed breaking waves. More consideration should be given to the population density in each building, the height of the building, and the evacuation shelter it provides. Phuket and the Phang-nga provinces of Thai coast are major tourist destinations and it is impractical to prohibit local people from living and working in these tourist spots so it is important to build a safe environment for them. Experience gained from the severe destruction caused by the 2004 tsunami underlines the need for better-engineered building design. Dalrymple and Kriebel (2005) suggest that buildings with flow-through lower floors are suitable for the tourist beaches of southwest Thailand; they use less valuable land and can reduce the loss of life since well-designed, flow-through buildings experience lower hydrodynamic forces. Debris is dangerous for people and buildings, so car parks and heavy items should be placed on the inland sides of buildings (Dalrymple and Kriebel, 2005). Karlsrude et al. (2005) advised that construction in the tsunami risk zones of Khao Lak should be located on elevated ground or on land raised for new construction. Eisner (2001) suggested that no infill houses should be built in the tsunami risk zone, and that buildings should have ample spacing between them. Warnitchai (2005) recommended that infill masonry is used on the ground floor of buildings these should be constructed of weak panels which are easily ripped off by the waves, although it must be noted that debris generated by these panels may cause subsequent damage elsewhere.

Further studies are needed on the design of resilient structures that can withstand tsunami waves. Findings should be verified by laboratory experiments and field surveys. The dynamic factors of tsunami flooding, such as flow velocities, friction, drawdown velocity and strain acceleration are also in need of further study. The output from this research can then be used to create procedures and guidelines for design, planning and construction in tsunami-affected areas (Bernard et al., 2006). A guidance document entitled “Designing for tsunamis”, developed by the State of California is one

of the guidelines illustrating planning, site development and construction configuration approaches which mitigate the effects of tsunamis.

The Department of Public Works and Town & Country Planning of Thailand had formed a committee to investigate the damaged buildings in tsunami affected zones, and to provide engineering and architectural advice for renovation and reconstruction. In 2005 the Department issued Coastal Planning Regulations for Phang-nga province. No residential building higher than 7 m and larger than 90 m² or non-residential flat-roofed buildings higher than 7 m and larger than 150 m² are permitted closer than 75 m to the coastline. No building must be situated within 30 m of the coastline. No building construction higher than 12m, factory, entertainment building, transportation station, market, gas and petrol station, religious building, school, hospital, warehouse and hazardous warehouse in the area located 225 m from the coastline (Department of Public Works and Town & Country Planning, 2005). Standard manuscripts for designing buildings and evacuation shelters in intermediate tsunami-affected areas were issued in 2008 (Department of Public Works and Town & Country Planning, 2008).

8-2.4 Tsunami Protection

8-2.4.1 *Natural Protection*

Environmental degradation can result in natural disasters being more catastrophic. Managing natural resources cleverly will help to secure the land against the worst hazards for the next generation. The degree of devastation from a tsunami will vary from area to area due to the presence of natural barriers such as sand dunes, mangroves, coral reefs, sea grass and coastal vegetation.

8-2.4.1.1 Beach Forests and Mangrove Forests.

Coastal areas that have trees experience less damage than the areas without this natural protection as the trees can reduce both wave amplitude and wave energy (Danielsen et al., 2005). Sonak et al. quoted a UNEP report that undisturbed coastal forests in the Maldives, composed of a high diversity of plant species, were the most resilient to the tsunami forces. Mangroves provide a bioshielding effect, and are able to dissipate the wave energy and decrease the rate of water flow. However, Alongi (2008) argued that it is difficult to assess the ability of mangroves to protect against tsunamis as mangrove

forests are normally located in naturally shelter zones such as enclosed bays, lagoons and estuaries and are not located on the open coast. The protection against tsunamis provided by mangroves may therefore be overstated and distract from the main effort put into mitigation. To date there is no statistical evidence or scientific data to prove or disprove the ability of mangroves to reduce the loss of life from tsunami waves. However, it can be shown that mangroves reduce the damage to buildings located behind them. Cochard et al. (2008) supported the notion that it is difficult to compare the capabilities of different ecosystems to withstand tsunami waves across different areas due to the high level of inconsistency in wave speed and energy along the various zones.

At present, climate change might cause a loss of 10-15 % of mangrove forests. Rising sea level together with the same rate of sediment deposition will decrease the mangrove area by 1-2% each year (Alongi, 2008). These factors are aggravated by coastal development projects which destroy the natural ecosystems and result in an overall loss of their resilience (Srinivas and Nakagawa, 2008). Williams (2005) stated that tourist and industrial developments, including aquaculture farms, enhanced the tsunami impact and hasten environmental degradation. With reduced natural protection, severe damage resulted along the Indian, Sri Lankan and Indonesian coasts during the 2004 tsunami.

Located in the proper areas, mangrove and beach forests, can act as the first line of defence in the reduction of the tsunami wave intensity (Dalrymple and Kriebel, 2005; Thanawood et al., 2006). Tanaka et al. (2007) recognised that trees are also important for increasing the drag coefficient, trapping floating debris and providing vertical shelter. The effectiveness of coastal vegetation depends on its density, size and species composition (Cochard et al., 2008; Danielsen et al., 2005; Tanaka et al., 2007). Cochard et al. (2008) recommended that detailed spatial and hydro-dynamic analyses of the effects of a tsunami wave on vegetation are required before hazard vegetation interaction measures are included on the risk maps, with factors such as stand size, density, species composition, structure and homogeneity being verified against tsunami patterns. Sonak et al. reported that casuarinas trees along the coast of Nagapattinam Town in India reduced the loss of life, injuries and damage due to the 2004 tsunami (areas of the Thai coast have dense casuarinas forests). Danielsen, et al. (2005) reported that casuarinas plantations protected the villages of Cuddalore located behind them.

The degree of removal of the vegetation by the tsunami waves depends on the species and sizes of the trees, substrate characteristics and the wave character. Sparse forest is not useful as a buffer zone.

At least 100 m of mangrove forests is required to reduce the wave energy (Danielsen et al., 2005). Siripong et al. (2005) recommended that, to achieve the best protection, the variety and the density of flora in both beach forests and mangrove swamps is obtained by copying nature; introducing multiple species to reduce and dissipate the wave energy. Tanaka et al. (2007) reported that casuarinas trees provided the best protection against tsunami waves < 10 m high, with small sized trees grown in dense patches being most resilient as these trees are not broken by the waves. However, a mixture of small and large trees could provide added protection since small casuarinas serve to reduce the wave speed whilst the large trees trap floating debris. Alongi (2008) reported that the combination of rhizophora and pandanus species also provides effective protection. Rhizophora trees, which are found in mangrove forests, play an important role for protection against waves < 5 m high due to their characteristic branch structures that do not get broken, and their complex aerial root systems. Moreover, the wave energy can be reduced by up to 50% within a 150 m belt of rhizophora-dominated forest.

It can therefore be concluded that the conservation and replanting of mangrove forests and trees in the mudflats and lagoon areas will provide some protection for communities from future tsunami (Danielsen et al., 2005) and it is therefore proposed that beach forest and mangrove restoration is implemented along the Andaman coasts of Thailand to protect the backshore zone.

8-2.4.1.2 Sand dunes

In many locations, sand dunes have proved to provide valuable protection for the backshore against tsunami attack. The dunes act as natural barriers against the incoming waves, e.g. limiting tsunami penetration during the 1994 East Java and the 1996 Peru tsunamis (Synolakis et al., 2005; Thanawood et al., 2006). Sonak et al. reported that the presence of sand dunes at Pulicat Lake fishing village in India reduced the effect of the 2004 tsunami waves. Umitsu et al. (2007) pointed out that some backshore areas of Banda Aceh were protected in 2004 by sand dunes and recognised that beach ridges

and natural levees prevented the tsunami from penetrating further inland. In Sri Lanka, the hotels located behind modified sand dunes suffered far greater damages than those situated behind natural sand dunes (Synolakis et al., 2005).

Unfortunately, most sand dunes along the Thai coast have been removed for the construction of hotels, beach resorts, roads and footpaths (Thanawood et al., 2006). They were cleared to improve the appearance of the seafront. This was not the case for Karon Beach, located in Phuket province, which was one of the beaches least damaged in 2004. Here there are long, wide, elevated and vegetated sand dunes along the beach front. Commercial and residential buildings established behind these sand dunes, were largely safe from the tsunami waves. The dunes reduced the wave speed, so there was less structural damage in this area; slow flooding occurred from the tsunami that overtopped the dunes (Dalrymple and Kriebel, 2005). On the other hand, sand spits, located between the beaches and lagoons, are one of the areas prone to greatest destruction, augmented by a lack of escape routes due to blockage, caused by the overflow of waves over the sand spits. Rivers, canals and tidal creeks are also susceptible to tsunami destruction as they act as channels that funnel the tsunami wave and convey it further inland. Siripong et al. (2005) recommended that evacuation routes and shelters should be located far from any river or canal.

8-2.4.1.3 Sea grass beds.

Sea grass beds, acting as a wave buffer, constitute another important ecosystem that reduces tsunami impact by helping to reduce wave height by increasing bed friction. The effectiveness of wave attenuation by the sea grass depends on the characteristics of the sea grass itself (length, density and flexibility of the sea grass blades). Sea grass blades as high as the water depth tend to dissipate more wave energy (Cochard et al., 2008).

8-2.4.1.4 Coral reefs

Dominey-Howes and Papathoma (2007) reported that fringing reefs around coral islands can help to shield them from a tsunami wave, for example at Guraidhoo Island in Maldives which sustained a wave +3.4 m above MSL. By contrast, narrow intertidal zones without a continuously protecting reef, combined with poor building construction, resulted in severe destruction. Ingram et al. (2006) supported this

conclusion and reported that communities located behind reefs degraded by coral mining, sustained more damage and casualties than the areas with healthy coral reef protection. However, Chatenoux and Peduzzi (2007) reported that tsunami-affected areas of the Indian coast located behind coral reefs were more affected experiencing a wider area of flooding due to thereefs, located in shallow water with a shallow slope, continuing inland and this helping to increase the wave height and consequently, high wave intensity. The bathymetry of the area without coral is generally deep and steep which can block the tsunami wave, resulting in a shorter inundation distance inland. Chatenoux and Peduzzi (2007) citing the United Nations Environmental Programme (2005) reported that fringing reefs also resulted in higher levels of damage for the area sheltered by them as the fringing reef can induce a channelling effect, which allows the tsunami waves to break closer to the shore. Cochard et al. (2008) state that closed and unbroken coral reefs can provide some protection but discontinuous reefs may cause channelling effects and cause greater destruction. This may have occurred at Pakarang Cape (or Coral Cape), located north of Bang Niang Beach, which suffered severe destruction which is surrounded by patches of degraded coral. Areas behind coral reefs are not necessarily safe from tsunami waves and it is not recommended that critical facilities and high occupancy buildings be located in zones behind the coral reefs.

8-2.4.2 *Man-made Protection*

Artificial barriers such as sea walls and breakwaters are alternative options for protecting the backshore. In Thailand, the low sea wall along Patong Beach played a significant role in protecting the buildings behind it, deflecting some of the momentum of the wave upwards and reducing the wave forces impacting on the buildings along the backshore. The end result was that only 0.5 km of flooding occurred with little destruction. However, because the sea wall along Patong Beach has spaced openings for pedestrian access, building destruction and scour on the beach relating to these openings. The receding wave flowing seawards via these openings caused additional damage and scouring. A pedestrian crossover (over the seawall) instead of the opening in the seawall would have decreased the damage considerably. Conversely, the high wall at the northern end of Patong Beach created some devastation. This non-vertical seaward facing wall acted as a ramp for a run-up jet that launched a mass of water onto the buildings located behind it. A vertical sea wall on the beach face served to protect

the runway at Phuket International Airport, and school buildings and playgrounds at Kamala Beach, Phuket, were also protected by a vertical sea wall. These examples demonstrate that vertical or concave seaward facing walls of proper design can provide suitable protection for the backshore zones (Dalrymple and Kriebel, 2005).

Seawalls can be of benefit for some tsunami risk areas, but it is essential that the position and form of such a potential barrier be thoroughly investigated, as seawalls can be a costly. This was demonstrated on Okushiri Island, Japan, where a 4.5 m high seawall was built to protect the Aonae peninsula. Tsunami waves overtopped this wall in 1993 and the wall also acted as a channel which concentrated the tsunami waves into a densely populated part of the town, though it did protect the low population zone; the ultimate value of that wall is still being debated (Dalrymple and Kriebel, 2005; Synolakis et al., 2005). Apart from the high cost of construction, a wall can also block the view of the sea, which is an important consideration for attracting tourists. This is particularly important for the Andaman coasts of Thailand. Even so, many countries along the Indian Ocean, including Thailand are trying to decide whether the building of sea walls is an effective way of reducing losses from future tsunamis, and if so, what type of structure to build.

In areas facing a threat from high tsunami waves, seawalls and offshore breakwaters can be used to reduce wave speed and wave height and to alter wave direction. Vertical reinforced retaining walls, which are flexible structures, can be used to protect the backshore areas from a tsunami (Srivastava and Babu (2009), though it is necessary to study the hydrodynamic forces on the structure to decide on the best design. Flexible structures have the advantage of absorbing the kinetic energy of the waves, but they should be designed to prevent scouring and undercutting if the structure is to remain secure. Wave breaking, wave reflection and beach grain-size distribution of the area are all considerations affecting the geotechnical and hydraulic design. A successful example is the reinforced concrete seawall and tetrapods surrounding the Male coast, which helped to reduce the impact of the 2004 tsunami. Silva et al. (2000) suggest that underwater breakwaters may be able to control tsunami waves by absorbing, reflecting and dissipating the wave energy. Similarly, permeable breakwaters would reduce the reflected tsunami wave by virtue of their porosity.

Along the Phang-nga coast, which used to be a tin mining area, an artificial hill resulting from the dumping of mine tailings acted as a vertical shelter, providing a safe place for the local people who were familiar with the area. Long et al. (2007) state that ground elevation is the main factor in reducing the effects of the tsunami, and protecting the backshore; this may be as a result of man-made barriers such as high road embankments, artificial sand dunes or other earth works, or natural features.

Geosynthetics can also play a role in the protection and mitigation scenario. To improve the safety of the Andaman coast of Thailand, Long et al. (2007) recommended the use of geotextiles for building artificial sand dunes and hills to reduce the impact of the tsunami and to offer vertical shelter. Geotubes or geobags, filled with sand, silty sand and clay, can be used to build artificial sand dunes; piles of geosynthetics can be integrated into the building of artificial hills or escape mountains for vertical evacuation. Long et al. (2007) recommend these be built in pyramidal shapes of 30 m by 50 m dimension and 3-5 m high. The escape mountain has the advantage of being more easily accessible than the vertical tower as it can be reached from any direction. Geotextiles could be used to re-enforce embankments to give added resistance against failure and erosion.

Man-made structures for tsunami protection can be costly and have disadvantages as well as advantages; they can block the view from tourist hotels, alter the environmental conditions along the coastline and make it difficult for fishermen to moor their boats. Softer choices such as the replanting of mangrove and beach forests, discussed above, may have advantages for many areas and, although these cannot guarantee 100% protection from future tsunamis, they would serve to reduce some impacts and provide more beautiful scenic views to benefit the tourist business.

8-2.5 Public Knowledge

Bernard et al. (2006) stated that communities that are aware of the tsunami hazard and the tsunami's physical indicators suffer a substantially decreased loss of life. Public knowledge and awareness are critical components that need to be built into mitigating the effects of a tsunami. Emergency preparedness requires an understanding of the tsunami characteristics and patterns in order to provide the necessary information to the public. The best way to mitigate the effects of the next tsunami is to combine real-time

tsunami forecasting with public education (Synolakis et al., 2005). The lack of a tsunami warning system around the Indian Ocean rim and the lack of knowledge about precautionary behavioural response, such as recognising the implication of a rapid and unusual sea level retreat before the approach of the tsunami crest, were examples of the poor state of public awareness that led to the massive loss of life as a result of the 2004 tsunami.

Several thousand visitors from European countries lost their lives in Thailand due to their inadequate knowledge of the dangers of tsunamis, they waited and watched the seawater receding instead of evacuating to higher ground. Visitors to the Thai coast from countries where tsunamis are unknown need to be made aware of the risks and hazards of tsunami waves. The coastal community should be informed of the dangers of tsunamis and earthquakes, of the tell-tale precursors of a tsunami, of the available evacuation routes and of the details of existing warning systems.

The National Science and Technology Council (2005) state that the impact of a severe tsunami is aggravated by lack of public awareness, effective warning arrangements and the implementation of mitigation measures. The community should receive information based on scientific knowledge and applied engineering aspects affecting the area. Jonientz-Trisler et al. (2005) proposed the use of various materials, such as bookmarks, magnets and emergency contact cards to educate the children and the public at large in the tsunami-threatened community. Booklets and brochures with information on the characteristics of a tsunami, evacuation route maps and shelter locations, should be produced and placed in hotels, in the community, across businesses and in public venues.

The local community is the key to the effective implementation of tsunami mitigation strategies and should be the first priority group to prepare for the hazards. The experience gained from a past tsunami event will only be passed on through one or two generations and the society may lose its knowledge of tsunami as memories fade away and conscious awareness vanishes (Intergovernmental Oceanographic Commission, 2005). The social memory of natural hazards, such as a tsunami is probably limited to not more than 20 years and social memory is crucial to the reduction of fatalities in the next event. Stein and Okal (2007) proposed that the long return period of tsunami

events in the Indian Ocean regions, induces loss to the cultural memory. The mitigation strategy must be put into action for the long-term to reduce the tsunami susceptibility of people. Research concerning the understanding of people about tsunami hazards in the State of Washington and reported in Johnston, et al. (2005), concluded that visitors and tourists are less aware of tsunami hazard than residents, but students in general prove to have a good awareness of tsunami impacts (Johnston et al., 2005). This confirms the necessity of raising the awareness of tourists to the Andaman coast of Thailand, and that an education program on tsunami hazards for students in school would be beneficial in transferring tsunami knowledge .

An important consideration in the design of tsunami mitigation procedures for tourist areas relates to the fear of negative impacts on the economy. However, tsunami warning systems and clearly-defined evacuation measures can boost the tourists' confidence and encourage them to come back. Similarly, the media is important for distributing positive messages to tourists, for example, information on the measures being taken for their safety. However, the most important issue is that local residents themselves have confidence in the tsunami mitigation procedures prepared for the community. Significantly, the key to the success of most tsunami mitigation measures depends on the involvement and participation of the local community (Sonak et al.

Chapter 9 Tsunami Impact Reduction Schemes for Bang Niang and Nang Thong Beaches, Khao Lak.

This chapter will focus on the integration of tsunami impact alleviation strategies, the principles needed to formulate tsunami mitigation plans and measures for the Bang Niang and Nang Thong communities, and the application of these principles to improve the safety of these communities.

1. The first component to achieving these goals is to understand the nature of physical tsunami impact on the area. These relate to the geographical characteristics of the areas including the topography of intertidal and backshore zones and the bathymetry of nearshore and offshore areas. Numerical modelling plays an important role in understanding tsunami inundation patterns. Wave height, wave direction, estimated arrival time and inundation distances/areas are the main factors needed for creating tsunami mitigation plan.
2. The second component is to understand community vulnerability and build a tsunami-safe community. Several tools need to be applied including a tsunami warning system, tsunami-related zoning, and building construction codes.
3. The third component is to conserve natural environments that help to reduce tsunami impact such as sand dunes and coastal forests.
4. The fourth component is to strengthen the Local Administrative offices, e.g. Bang Niang Sub-district Administrative Office, who are responsibility for tsunami impact reduction and coordination.

9-1 Component 1: Understanding the Pattern of Tsunami waves at Bang Niang and Nang Thong Beaches

To create reliable mitigation plans and measures to mitigate tsunami impacts, it is first necessary to understand the nature of the tsunami risk. The 2004 earthquake with $M_w = 9.3$ caused severe destruction to the Andaman coast of Thailand, especially the Khao Lak area; however, the likelihood of such a high magnitude earthquake happening

again is between 400-600 years (Section 2-5) (Pietrzak et al., 2007; Stein and Okal, 2005a; Stein and Okal, 2005b). A tsunami affecting the Andaman coast of Thailand might also occur due to a smaller tectonic event on the Andaman-Nicobar Section or the Northern Sumatra Section of the Sunda subduction zone. An earthquake of M_w between 8.5 to 9.0 may occur, with dramatic consequences for the Andaman coast of Thailand, within the next 100-500 years (see Section 2-5.2 and 2-5.3). Several kinds of tools can be applied to increase the understanding of the effects of a tsunami generated by a ‘smaller’ earthquake and the vulnerability of the coastal communities to such a tsunami.

9-1.1 Tool 1: Tsunami Modelling for Prediction of Tsunami Pattern at Bang Niang and Nang Thong Beaches.

9-1.1.1 Selected source of potential earthquake eruption that might cause tsunami impact to Khao Lak.

Numerical simulation is essential to obtain realistic information on tsunami wave characteristics such as inundation distance, wave height, wave direction and wave speed, and to provide inputs for the definition of reliable tsunami mitigation plans and protective measures for Bang Niang and Nang Thong Beaches. These characteristics are the basic input for defining building regulations, evacuation routes and emergency plans.

An earthquake event with $M_w = 8.4$ occurring along the Northern Sumatra and Andaman-Nicobar sections of the zone, with larger slip for the two western rectangular components and lower slip for the two eastern rectangular components, was simulated using the MOST model with the ComMIT interface (see Section 7-4 for choice of M_w and sensitivity to M_w). The tsunami wave generated by such an earthquake would be characterised by a depressed wave propagating from the epicentre towards the Thai coast as a receding wave from the west-southwest arriving approximately 2 h 20 min later. Water levels in the nearshore would drop to 0.4-0.5 m below MSL, causing a dried-out the sea bed to become exposed for approximately 2 km offshore before the wave crest arrives.

9-1.1.2 *Tsunami pattern at Bang Niang and Nang Thong Beaches.*

According to the modelling, the first wave crest to reach the nearshore of Khao Lak (at +2 h 26 min) would have a wave height of just 0.4 m and inundate the nearshore area of Bang Ninag and Nang Thong Beaches for 24 min. The second wave trough arrives at the beach and would cause water recession to 0.5 m below MSL for 20 minutes. The first significant wave (the second wave crest) would reach Bang Niang and Nang Thong Beaches between +3 h 20 min and +3 h 33 min (Figure 9-1) and would be approximately 2 -3 m above MSL. Both beaches are flooded for 200-600 m inland. The third wave crest is largest (+4 h 0 min; Figure 9-2) Nang Thong Beach and the southern part of Bang Niang Beach would be confronted by waves up of between 4.5-5.5 m. The northern part of Bang Niang Beach would face higher waves (5.0 m above MSL, Figure 9-3) than the southern part (4.7 m above MSL at the shore and 3.0 m inland in

Figure 9-4). The northernmost part of Bang Niang Beach would also face a higher waves due to the wave flooding through the northern branch of the Pong Canal. On the other hand, the southernmost part of Bang Niang Beach would experience smaller effects of tsunami wave due to its 'high' local topography (Figure 9-5). Inundation would reach 300-350 m inland around Nang Thong Beach with high wave of 5.5-6.0 m high above MSL at +4h 0 min ;Figure 2 6). The most endangered areas from this potential tsunami wave would be around the canal that runs parallel to the coastline and the Pong Canal itself, due to the wave flooding through the northern branch of the Pong Canal (Figure 9-2). North of the canal (close to Khao Lak Orchid Resort), where the topography is higher than 2 m above MSL, the effect would be smaller.

In addition, the community must be aware that the first wave might not be the highest and the most dangerous one that affect the area. According to the model the third wave crest, which reacehes Bang Niang and Nang Thong Beaches at +4 h 0 min, is the one that cause more severe destruction than the first wave. Evacuation plan and measures should be issued in consistent with the detailed tsunami wave pattern of each specific areas. However, tsunami wave patterns (wave heights, wave periods, and inundation distance etc.) normally rely on earthquake sources which cause tsunami wave; but, the general patterns of tsunami wave should be similar.

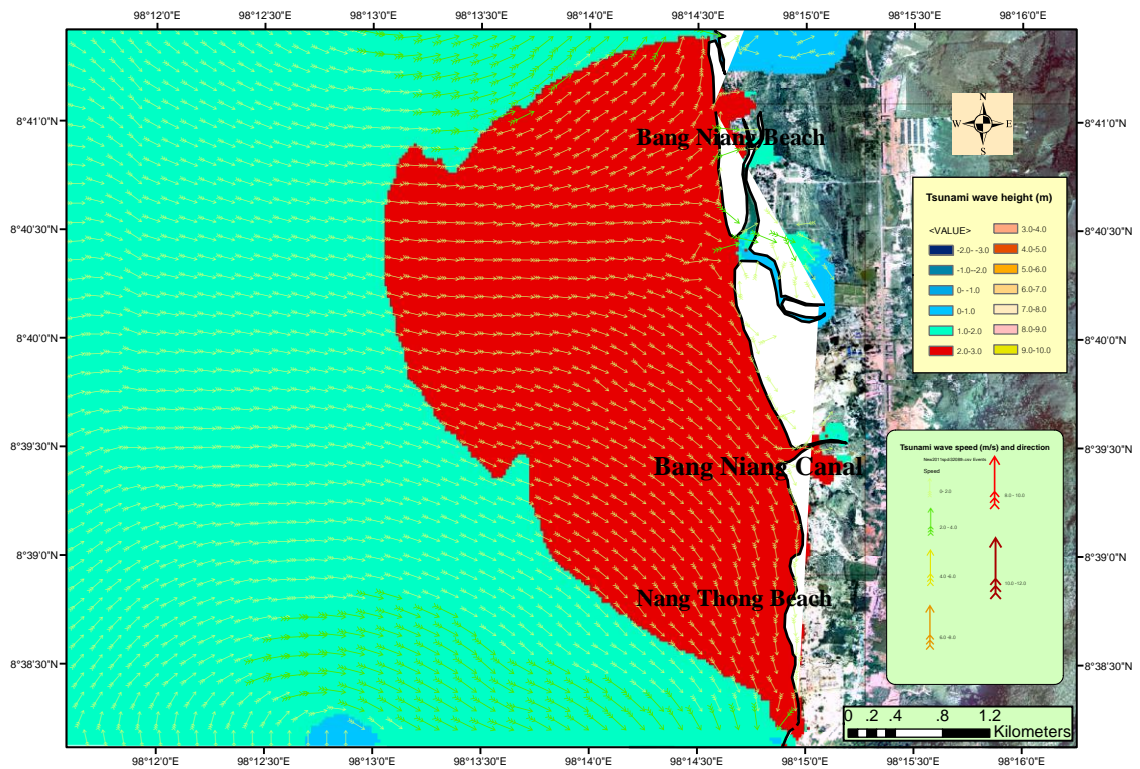


Figure 9-1 The first tsunami wave crest approaching the coastline of Khao Lak at +3h 20 min. Water at the crest of wave moves shorewards at ~2 m/s

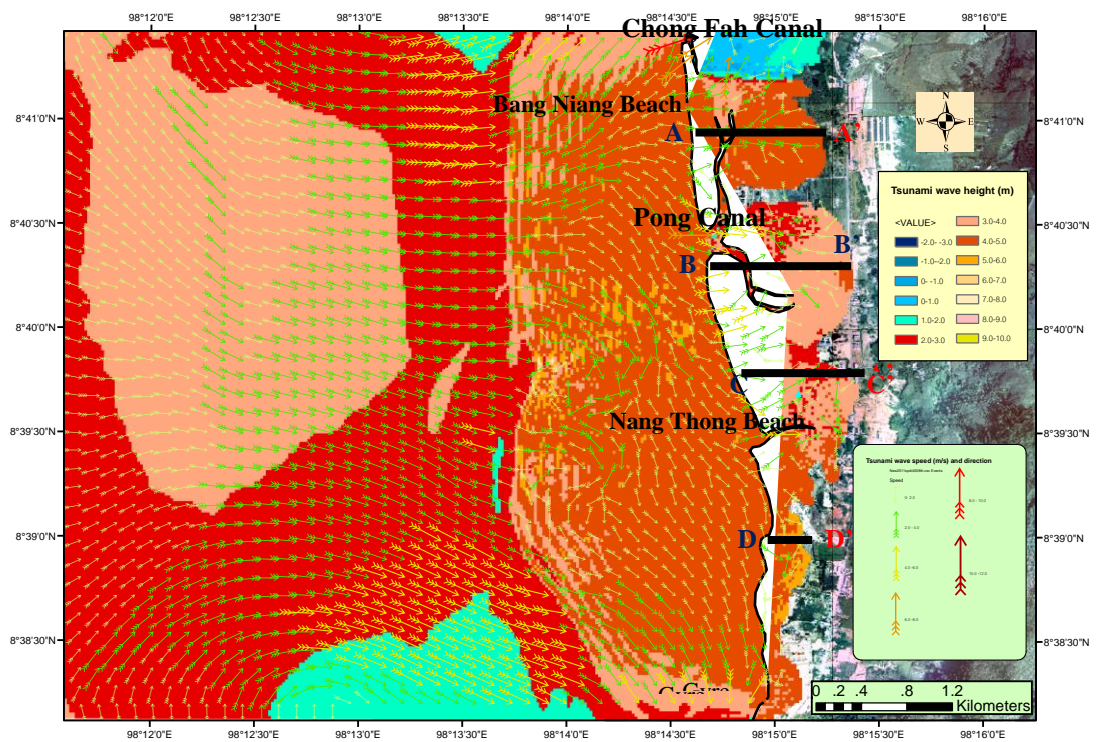


Figure 9-2 The wave crest reaches Bang Niang and Nang Thong Beaches at +4h 0 min.

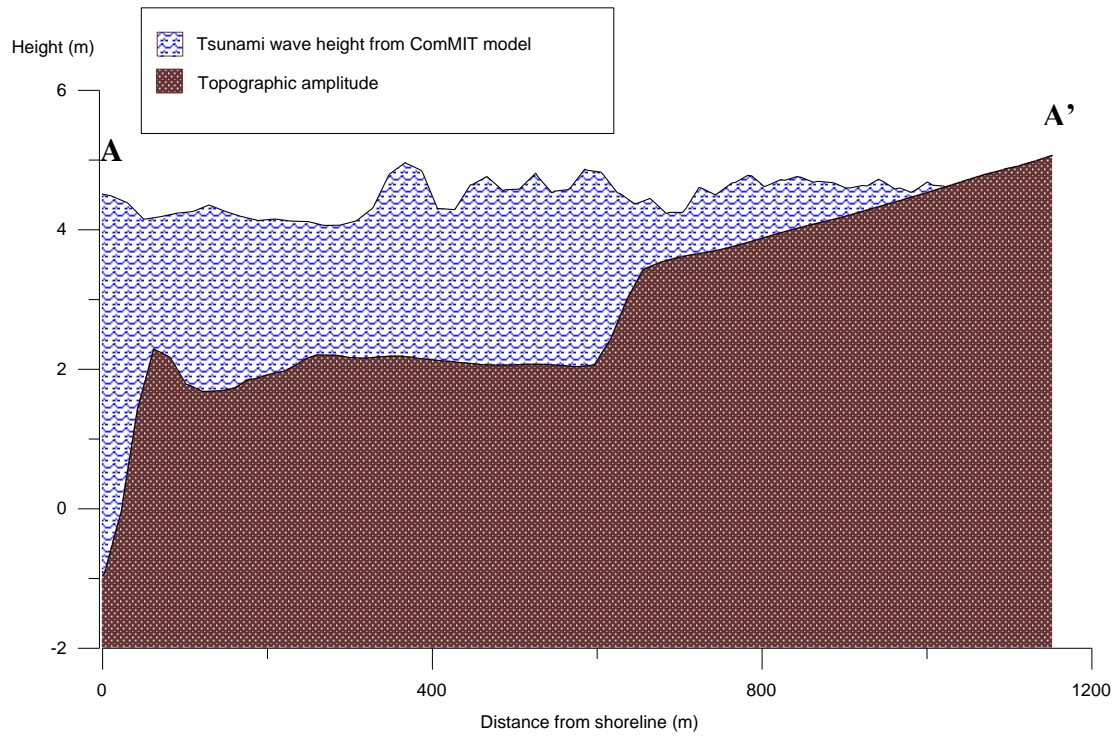


Figure 9-3 Cross-Section profile of wave inundation between A and A' (see Figure 9-2) at north of Bang Niang Beach +4h 0 min.

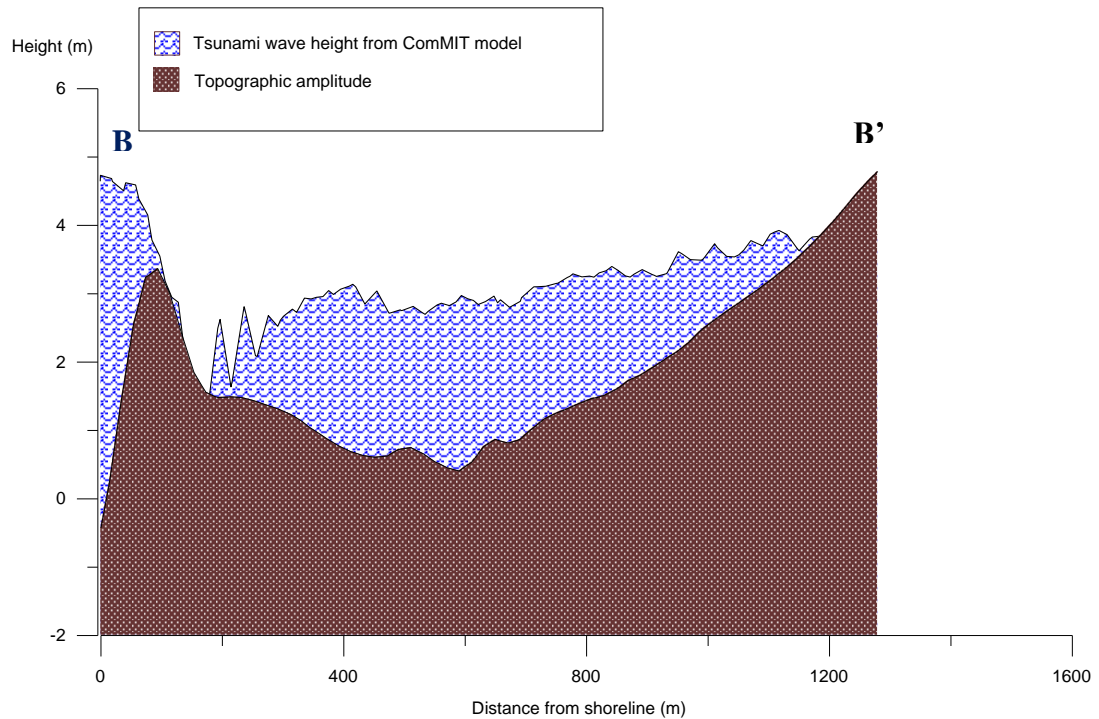


Figure 9-4 Cross-Section profile of wave inundation between B and B' at Bang Niang Beach (across Pong Canal) +4h 0 min.

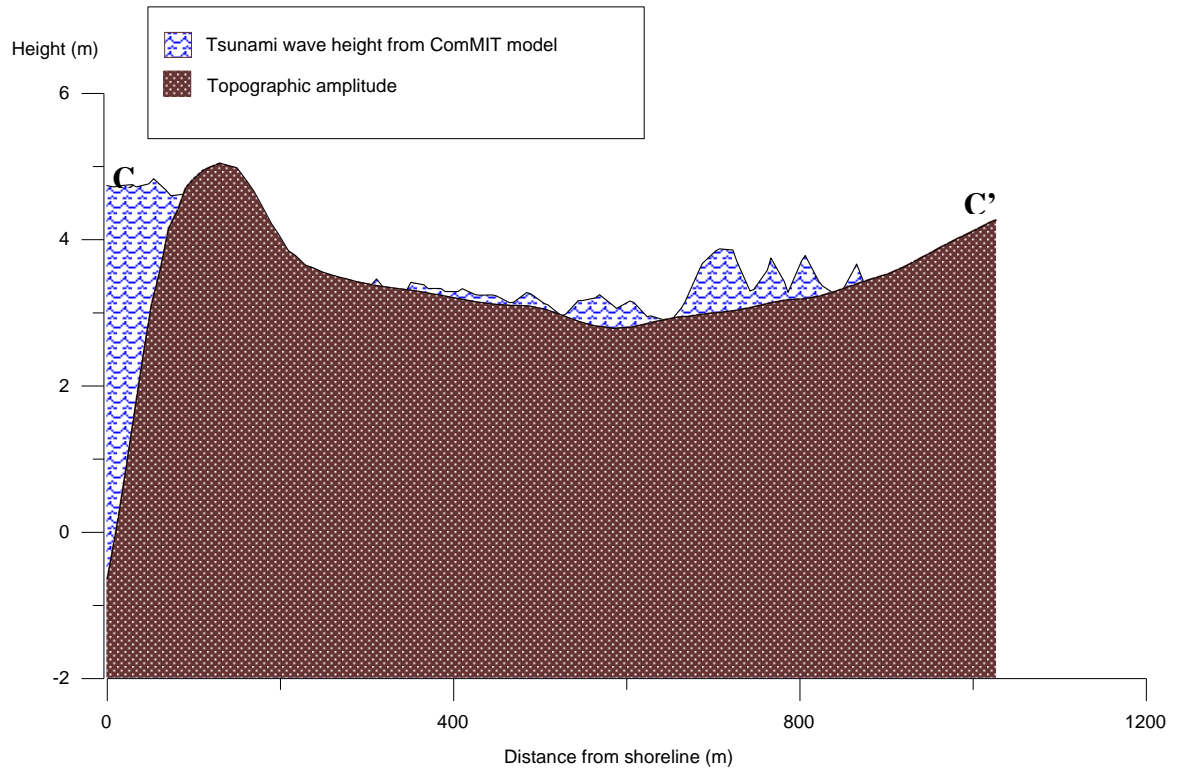


Figure 9-5 Cross-Section profile of wave inundation between C and C' at Bang Niang Beach +4h 0 min.

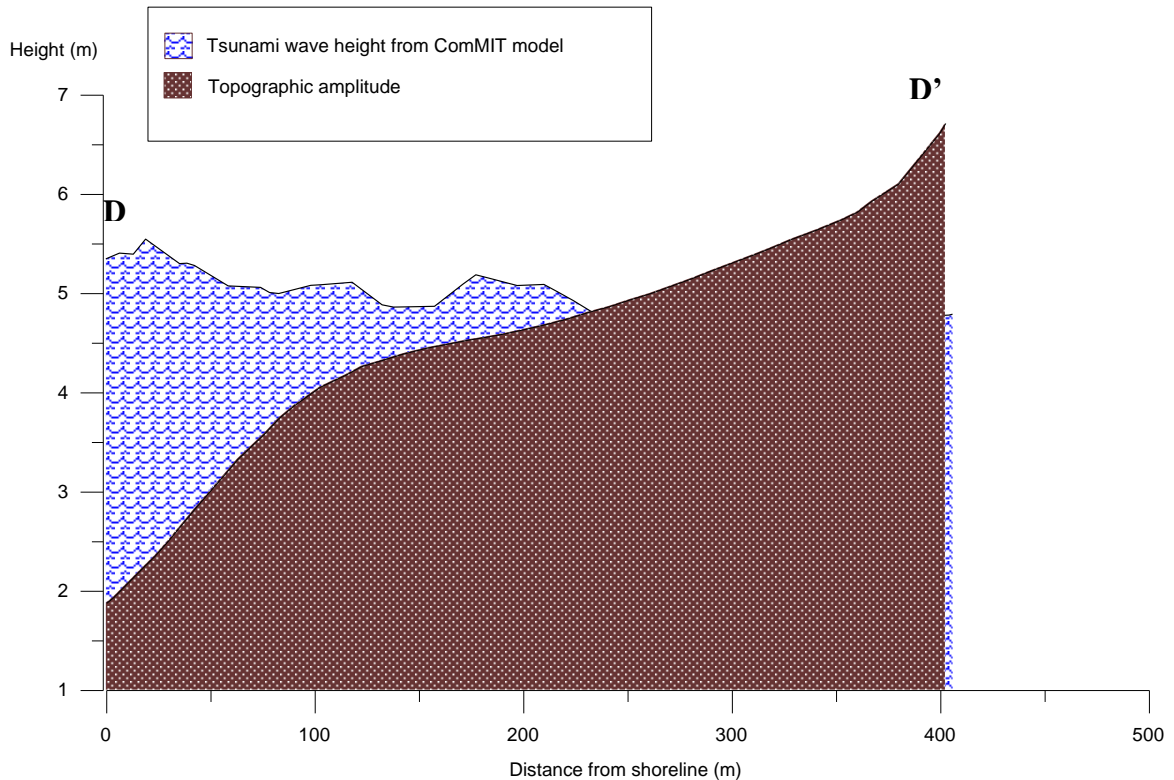


Figure 9-6 Cross-Section profile of wave inundation between D and D' at Nang Thong Beach +4h 0 min.

The inundation area of the tsunami associated with this possible $M_w = 8.4$ earthquake gives generally a similar pattern to that of the 2004 tsunami. However the maximum inundation distance is approximately half that of the 2004 event in some areas such as at the southernmost part of Nang Thong Beach (Figure 9-7). Bang Niang Beach experiences the most severe impacts; the inundation area is about 70% of that of the 2004 tsunami. Tsunami waves of 4-5 m above MSL would reach the main road, located approximately 1.2 km from the shoreline, and the areas adjacent to the Pong and the Bang Niang Canals. The maximum inundation of the coastal area at Bang Niang Beach would occur at +4 h 0 min (Figure 9-2). It is therefore necessary to design evacuation maps and prepare coastal land use plans to allow for the maximum inundation and the highest waves that would occur, especially the northern area of Pong Canal which would experience the severest wave effects. The wave speed in the Pong and Chong Fah Canals could be as fast as 6-10 m/s due to channelling effects (it would typically be 2-4m/s elsewhere). The estimated inundation area is shown in Figure 9-7. Sensitive

units such as the hospital and schools as well as tsunami shelters should be located outside the inundation area.

9-1.2 Tool 2: Classification of the Tsunami-Affected Zones.

The tsunami-affected area of Bang Niang and Nang Thong Beaches can be divided into two zones: a “severely-affected” zone and “forecast-inundation” area (Figure 9-7) which can be used for the development of land-use planning and building codes of construction for the area. The severely-affected zone is characterized by wave heights of 4.5-5.5 m above MSL (3-5 m above ground level) at the coast and wave speeds of 2-4 m/s. This is broadly in agreement with the damage classification diagram of Silpakorn University (2006) shown in Figure 9-8. The severely-affected zone (Figure 9-7) is comparable to the area severely and moderately damaged by the 2004 tsunami in Figure 9-8. Eisner (2001) and the Oregon Emergency Management and Oregon Department of Geology and Mineral Industries (2001) consider the advancing turbulent front of the tsunami wave to be the most destructive part of the wave; this turbulent front results in a high water speeds and highly energetic conditions from which it would be difficult to escape and is therefore a very dangerous region (the severely-affected zone).

The area along Bang Niang Beach, Nang Thong Beach and Bang Niang Canal banks, including the resorts and hotels, should therefore be designated as a zone that would be severely-affected by the tsunami.

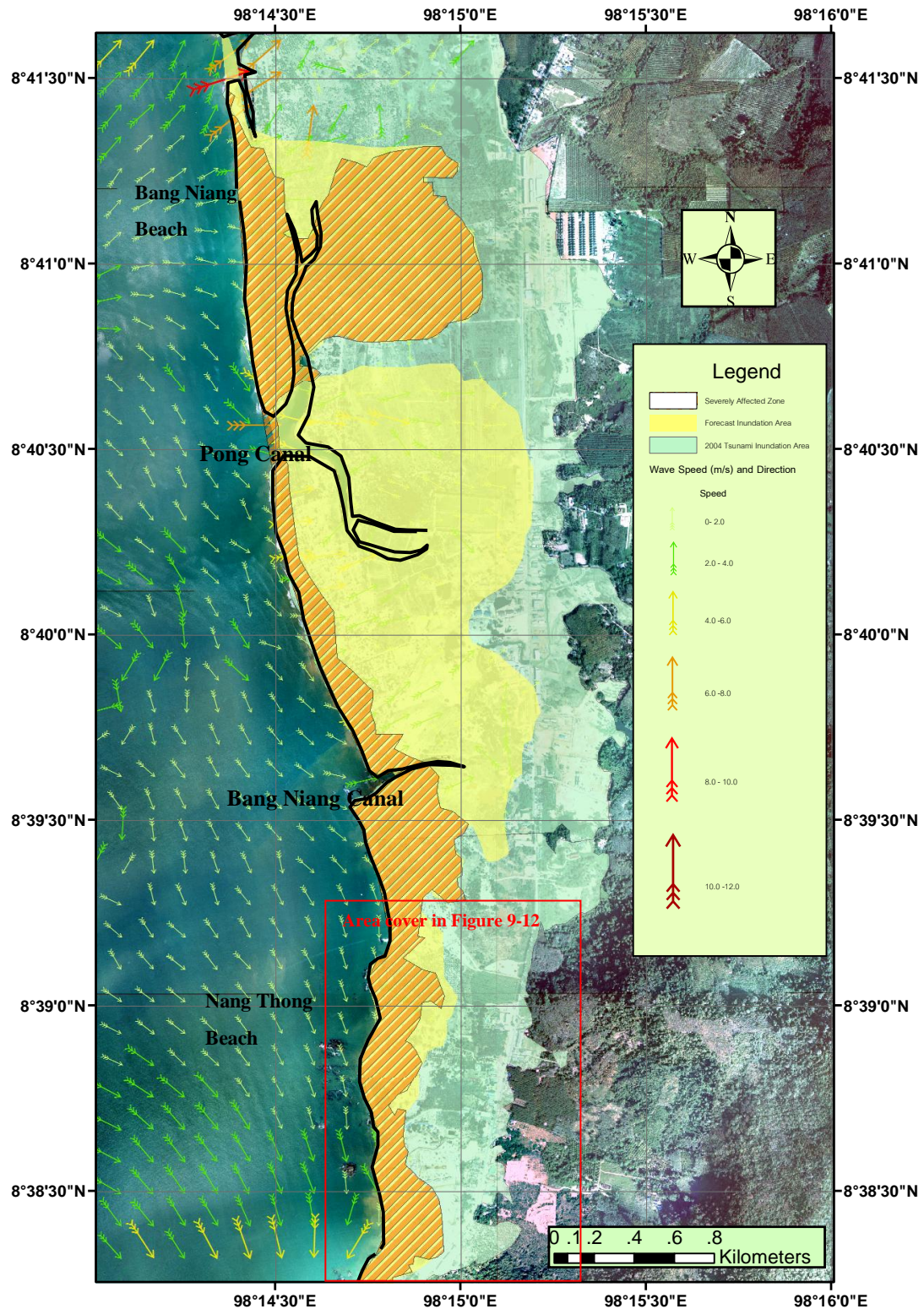
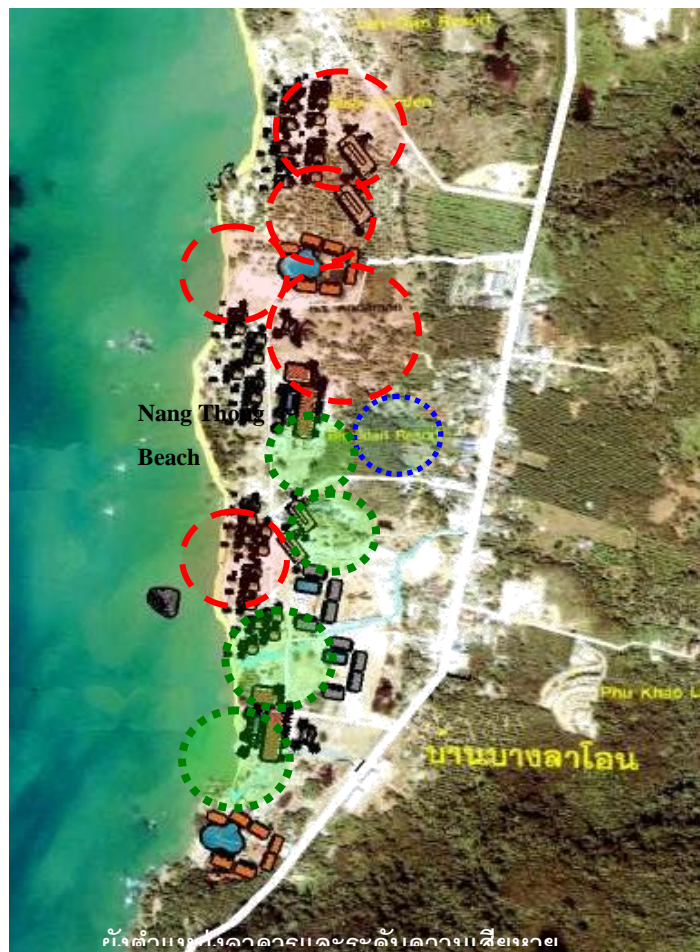


Figure 9-7 Estimated wave speeds and wave directions for the simulated tsunami that would reach Bang Niang and Nang Thong Beaches at +4h 0 min after the earthquake. The most vulnerable area would be at Bang Niang Beach, between the Bang Niang and Pong Canals, where the highest wave speeds and wave heights would be encountered.






-  Few buildings were damaged by the 2004 Tsunami
-  Buildings were moderately damaged by the 2004 Tsunami
-  Buildings were severely damaged by the 2004 Tsunami

Figure 9-8 Building damage from the 2004 tsunami waves that attacked Nang Thong Beach. (Modified from (Silpakorn University, 2006)).

9-2 Component 2: Building Resilience of the Bang Niang and Nang Thong Beach Communities.

Tsunami ‘community resilience’ is a concept developed through the integration of various strategies, plans, principles and measures, which are operative from the policy level to the implementation level, for building a long-term tsunami-safe community. Community vulnerability to both natural and technical disasters is a function of human action and customs. For a natural disaster, the level of risk is determined by the level of vulnerability combined with the degree of probability and intensity scales for each hazard. Risk reduction involves activities to reduce the vulnerability and minimise the sources of hazard. For people living in an area prone to natural hazards, the safety of buildings through the reduction of vulnerability is a key factor.

9-2.1 Tool 3: Tsunami Warning Systems and Evacuation Plans.

In the case of a submarine earthquake occurring along the Sunda subduction with the potential for the generation of tsunami waves, the first warning would come from the global seismic network of the earthquake itself. The Meteorological Department of Thailand and the Thai National Disaster Warning Centre receive the seismic signals, analyze them and issue an earthquake report, and then wait for the tsunami prediction from agencies such as the USGS and NOAA; a warning could be issued at much as 1.5 h before any tsunami wave reached the Thai coast (Table 9-1).

The first direct evidence of a tsunami wave would come from a DART[®] (Deep-ocean Assessment and Reporting of Tsunamis) buoy (Gonzalez et al, 1998) that was deployed by Thailand Meteorological Department (TMD) in conjunction with National Disaster Warning Centre at 8.905° N 88.540° E (station 23401) which is ~1020 km from Khao Lak (Figure 9-9) in deep water on the far side of the subduction zone. DART buoys were originally developed by NOAA for the US National Tsunami Hazard Mitigation Project to maintain and improve early detection and enhanced warning of tsunamis (<http://www.ndbc.noaa.gov/dart/dart.shtml>) However, this DART buoy went adrift in April 2010 and is no longer providing water column or tsunami event data. The buoy will be restored into service when it can be recovered (<http://www.ndbc.noaa.gov/>

[station_page .php?station=23401](#)). If the buoy is able to operate, it can detect a tsunami wave ~ 1.5 h before the wave reaches the Khao Lak area (Table 9-1).

Digital tide gauges, which can detect unusual changes in water level, have been installed on the Miang and Similan Islands (~67 km offshore) by the Royal Thai Navy (Figure 9-9) and are automatically transmitting their data to the National Disaster Warning Centre in Bangkok. These gauges can provide 45 minutes to 1 hour warning prior to the tsunami wave reaching Khao Lak (Table 9-1) or cancelling any false alarm previously issued. Further digital tide gauges should be installed along the Andaman Coast at 200 km intervals to provide warning of the recession of the water ahead of the first wave crest and directly connected to sirens on the Warning Towers that have been installed by the government. However, these systems must be maintained in good working order to ensure transmission of early warnings of an impending disaster to the public and tsunami drills should be conducted at regular intervals. Additional tsunami warning information should be installed in hotels' rooms in tsunami risk zone to increase tourists' confidence.

| Instruments | Activities | Warning Period |
|---|---|-----------------------|
| Seismic signal | Global system; not known if event is tsunamigenic | ~2h 30 min |
| DART buoy (8.9°N 88.5°E) 1020 km from Khao Lak | First indication that a tsunami will reach the coast of Thailand, issue warning | ~1h 15 min-1h 30 min |
| Digital tide gauge (Offshore Islands) Miang and Similan Islands | Automatic National Warning tide gauge | 45 min- 1 h |
| Water levels recede at shoreline ahead of crest | Needs local observers | < 30 mins |

Table 9-1 Estimated tsunami warning period at Khao Lak from various methods

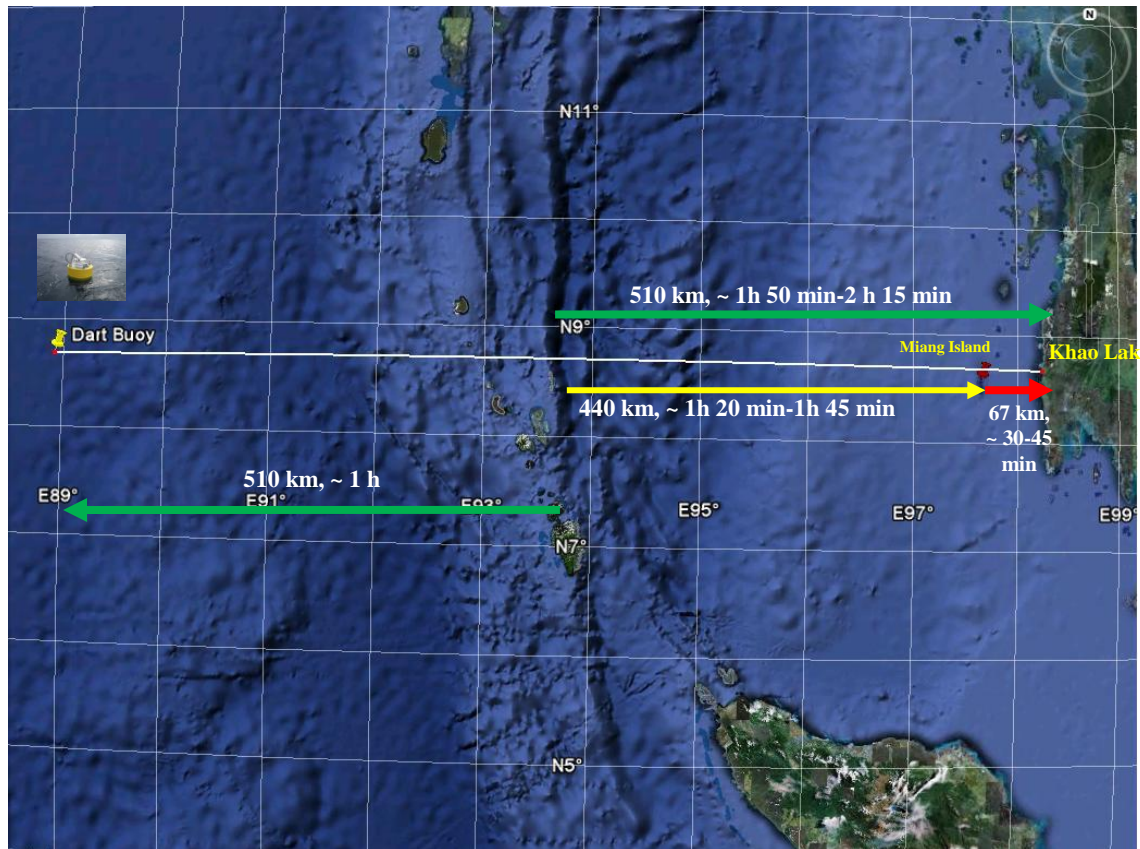


Figure 9-9 Location of DART buoy (8.905 N 88.540 E) and digital tide gauge at Miang Island relative to the Sunda subduction zone and the coast of Khao Lak, with estimated distances and tsunami travel times.

The essential requirement for reducing tsunami loss is the ‘tsunami warning period awareness’, ensuring that local people and visitors know what to do when a tsunami warning is issued. The speed of the first wave as it approaches the shoreline at Bang Niang and Nang Thong Beaches is generally faster than a human can run (1.5-5 m/s), and higher speeds still would still occur at the canal openings (Figure 9-1 and Figure 9-2). If an earthquake is felt and the seawater regression occurs, evacuation plans should provide enough time for everyone to escape to safe zones: this depends on the reliability, effectiveness and the practical planning that has been put in place ahead of the event. There is a maximum of only 30 minutes between the moment when the water levels start to fall and the first wave crest reaching the coastline so, with the safe areas approximately 1.5 km from the shoreline, tsunami mitigation plans should include the construction of vertical man-made shelters to ensure the security of all those living, working and visiting the area.

In addition, the community must be aware that the first wave might not be the highest and the most dangerous one that affect the area. According to the model the third wave crest, which reaches Bang Niang and Nang Thong Beaches at +4 h 0 min, is the one that cause more severe destruction than the first wave. Evacuation plan and measures should be issued in consistent with the detailed tsunami wave pattern of each specific areas. However, tsunami wave patterns (wave heights, wave periods, and inundation distance etc.) normally rely on earthquake sources which cause tsunami wave; but, the general patterns of tsunami wave should be similar.

9-2.2 Tool 4: Coastal Zoning and Land Use Planning for Tsunami Mitigation.

5-1.1.9 Tsunami Affected Zone and Tsunami Safe Zone

Khao Lak suffered severe damage from the 2004 tsunami due to its low-lying coastal plains, bounded by high hills on the eastern side. Again, modelling of the inundation area was used to obtain an estimated 'safe zone', beyond the severely-affected zone and the forecast-inundation areas. The extent of the flooding by the simulated tsunami generally covers the entire backshore area to a line almost to the main road.

To minimize the impact of a tsunami wave on the community, the construction of buildings of a poor standard should be prohibited in the severely-affected zone. For Bang Niang and Nang Thong Beaches, single storey building construction on low land is no longer considered suitable. Not only is there the risk of such structures themselves collapsing and generating considerable debris with the resultant loss of life, but also they lack the capacity for any escape vertically.

Recently, roads have been constructed perpendicular to the coastline in this area but these roads are narrow. More roads should be built perpendicular to the shoreline for use as evacuation routes; they should be constructed as wide as possible and reach the safe zone in the shortest distance. A high-standard, elevated road could be built parallel to the shore, close to the beach, to act as an embankment to reduce the power of the tsunami and assist evacuation but this would be unacceptable from a tourist amenity view-point; hotels are unlikely to accept their sea-view and beach access being spoilt by an elevated road however beneficial in the long-term.

Signs displaying tsunami hazard areas, tsunami evacuation routes and information about tsunamis should be placed in this zone to encourage tsunami awareness. The location of sensitive buildings such as hospitals and schools should be restricted to the 'safe zones'. The coastal zoning of Bang Niang and Nang Thong Beaches, relating to tsunami-affected zones, should be put into effect by enforcing regulation issued by Bang Niang Sub-district Administrative Office.

One successful example of tsunami mitigation is the Oregon coastal area, which utilized a GIS-based tool to create tsunami evacuation maps for each community under the supervision of Oregon Department of Emergency Management. In addition, Oregon coastal communities receive tsunami warnings from NOAA weather radio, and local officials can issue a warning by sounding 3-minute siren signals for evacuation. (<http://www.oregongeology.com/sub/earthquakes/Coastal/Tsubrochures.htm>).

A hazard related to the sea level recession is the strong currents that occurs in some areas, for example near canal openings to the sea (Figure 9-1). The water currents could be as fast as 4-6 m/s, and flow perpendicular to the shoreline, so the sea level drop and the receding water will be dangerous for anyone in the water as they would transport swimmers to the offshore area with resulting loss of life. Boats moored inshore may also be carried offshore by the receding wave and could be brought back to the shore again by the next wave crest as floating debris, which would make the wave more dangerous than it would otherwise be. To prevent more unnecessary damage it is therefore advisable to review the nearshore areas for their suitability as mooring places for small boats (fishing and tourist). Most importantly, to reduce the drawdown impact and rip-current-like effects, piers and mooring points should not be located in the areas close to canal openings.

The model predicts that a second tsunami crest would reach the area at +3h 20 min, after the second trough and associated water recession. The draw-down between the first and second waves (also the second and the third waves), would be one of the most dangerous periods of the tsunami as it would carry seawards floating debris from the previous wave, creating the possibility that this would enhance the destruction of buildings that survived the initial wave. Any boats left stranded on the seafloor after the

regression of the water may prove difficult to refloat and a later wave could swamp them.

5-1.1.10 *Set Back Policy*

For Bang Niang and Nang Thong Beaches, which are attractive tourist beaches, it is essential that land use planning is properly considered and enforced for the safety of the population. A setback policy should be implemented that secures open space of at least 50 m from the shoreline and well positioned artificial sand dunes should be constructed to reduce the wave forces and alternatively to act as vertical shelter for those unable to reach the safe zone. The planting of beach forests should be encouraged along the beaches, with Casuarinas of different size intermingled with Pandanus shrubs (Tanaka et al., 2007). However, enforcement will not be easy as this zone is important for businesses supplying tourists. Stricter codes of construction, based on the results of scientific research, should therefore be issued for the buildings in this area.

5-1.1.11 *Breakwaters and Seawalls to Reduce Tsunami Impact.*

Seawalls and breakwaters might be used as protective measures to reduce some of the tsunami devastation, but underwater structures might be better suited to the area as they do not block the view at these popular tourist beaches. A well-designed seawall located along the front of Bang Niang Beach would benefit the hotels located along the beach as well as sheltering the canal openings for the mooring of tourist and fishing boats. However, the proper design of the structure is very important as the area is densely populated and highly commercial. The pros and cons of building a seawall in the Khao Lak area are still debated among scientists, engineers, local administration officers and local people. Therefore it is will be necessary to conduct studies to determine the most appropriate designs for a seawall to reduce tsunami wave effects while minimising impacts on the tourist industry and the life-style of local fisherman.

5-1.1.12 *Evacuation Shelters*

Evacuation shelters should be located outside the inundation area, ideally in the safe zone on the landward side main road, except for an area behind Sunset Beach, where the topography is high enough to offer safety from the waves. Where these evacuation shelters are too far away from the beach or access is limited by lack of transportation,

vertical shelters are essential for the safety of the coastal population. Vertical evacuation shelters should be constructed along the beaches in locations that are too far from the high ground. Shelters should be higher than 12 m and strong enough to withstand a wave at least 6 m high with a speed of 8 m/s. Buildings of a high-standard of construction, at least 3-stories in height, can also be used for evacuation purposes (Figure 9-10). Vertical shelters should be built at intervals of 1 km along both beaches so shelters are accessible within 500m.

9-2.3 Tool 5: Recommendation for Building Code of Construction.

It is recognized that high-speed waves cause scouring of building foundations, sometimes resulting in structural collapse and destruction. Buildings located near the canal openings and facing strong wave action should be constructed to withstand such strong waves by positioning them perpendicular to the coastline, with an elevated ground floor and proper wall types as required by the appropriate building regulations, as stipulated under the land use planning directives for the area. When comparing the severely-affected area and predicted-inundation area (Figure 9-7) with the map showing the scale of damage to the buildings of Nang Thong Beach in Figure 9-8, it can be seen that the area close to the headland is protected by the headland itself and should experience less destruction than areas facing the direct force of the tsunami wave. This illustrates how the specific conditions applicable to each area need to be taken into account when setting out an appropriate mitigation plan. The important factors to be considered in defining the building regulations for Bang Niang and Nang Thong Beaches are the wave speed and direction, the wave height and the inundation depth. Bang Niang Beach, especially the area between the Bang Niang and the Pong Canals, is likely to be the area most at risk (Figure 9-7). At present, there are more than 30 luxury seaside resorts in this area. Fortunately, many are 3-4 storey high hotels and the resort buildings are built of reinforced concrete so would provide secure vertical shelters. However, the building regulations for the zone within 300 m of the shoreline should be strengthened to cope with the high waves and immense wave power that the area could be subjected to.

Although larger hotels and resort complexes located close to the beach normally comprise a number of high, reinforced concrete buildings (3-4 stories), medium-sized resorts are often composed of 1-2 story concrete buildings while the smaller resorts generally consist of small, detached bungalows and are much more vulnerable to tsunami impacts. If possible, the first floor of the building should be elevated above the maximum wave height in the area. For Bang Niang and Nang Thong Beaches, the first floor of the buildings located at the beach should be 3-5 m or more above MSL. Alternatively the elevation of the land could be raised locally, which lifts the first floor by the same amount. Buildings that let the water flow through the first floor can reduce the wave impact and help to ensure the safety of their occupants (Figure 9-10). First floor walls should be constructed of low resistance materials to permit the wave to destroy it easily, leaving the first floor as a free space to let the wave flow through; as a result, the whole building should remain as a safe shelter for vertical evacuation. The material type selected for the construction of the first floor should also be chosen to produce the least quantity of debris (a main contributor to fatalities and property damage), in an effort to reduce the impact of debris flow.

While structures with pile footings should be encouraged, (non-engineered) wooden houses and structures built on shallow spread footings should be prohibited in the zones most highly prone to damage from a future tsunami. Engineered buildings with deep scour-resistant foundations should be encouraged along the coast, especially in severely tsunami-affected areas.



Figure 9-10 Elevated and flow through first floored building designs for Khao Lak by architects at Silpakorn University. The top floor is also designed for use as a vertical shelter. (Silpakorn University, 2006).

9-3 Component 3: Conservation of the Natural Environment

9-3.1 Tool 6 Restoring Beach Forest and Sand Dunes along Bang Niang and Nang Thong Beaches.

The ecological and environmental integrity of the coastal area needs to be maintained to reduce some impacts of potential tsunami in the future. Beach forests and mangrove forests should be considered as a means of reducing the tsunami's power. Ecology needs to be balanced with coastal development projects. For example, beach forests, which naturally reside along Bang Niang and Nang Thong Beaches, are the wise way to reduce tsunami impacts (Chapter 8 Section 8-2.4.1.1). Not only are trees and bushes in beach forests able to reduce wave energy and wave height by acting as shock absorbers, they also trap floating debris and can act as vertical shelters. It will be of benefit to the

area to have a 50-m wide belt of Casuarinas of various sizes, interspersed with Pandanus shrubs, to increase the protection capacity. A 100-150 m wide of beach forest belt is even more effective, but this is unfeasible along Bang Niang and Nang Thong Beaches because most of the area is composed of hotel buildings and owned by private sector. In addition, property values in this area are very high, and the local government does not have any law or regulation to enforce a setback policy on the existing business sector.

Sand dunes have proved to protect the backshore areas in several locations from the worst effects of a devastating tsunami (Long et al., 2007). Unfortunately, sand dunes along Bang Niang and Nang Thong Beaches are not as high and stable as those of Karon Beach in Phuket. Some hotels buildings and roads are now located on sand dunes or the areas that used to be sand dunes. Some sand dunes were removed to improve the sea views from hotels and tourist resorts. In terms of reducing both tsunami impact and coastal erosion, the reconstruction of sand dunes is one of the finest ways to protect the backshore areas. (Long et al., 2007). Approximately 3-5 m high dunes built from geo-textiles not only shield the area from potential tsunami wave effects, but also protect the area from coastal erosion in the monsoon season and could act as vertical shelter.

9-4 Component 4: Strengthening Local Administrator and Community Responsibility and Cooperation among stakeholders.

A tsunami-resilient community for Bang Niang and Nang Thong Beaches can only be achieved with the cooperation of all stakeholders, including the central government, local administrative officers, researchers from the regional academic institutions and, most importantly, the local people.

9-4.1 Tool 7: Policy Formulation and Enforcement.

It is vital that the central and local government continue to recognise the economic importance of the beaches along the Khao Lak coast to tourist-related commerce. It is not only major hotel chains and resorts that are the beneficiaries; the beaches also provide income for local business and job opportunities for both local people and

seasonal employees. The government should therefore have a clear policy and provide an adequate budget to shape the area into a tsunami-safe community while maintaining its attraction as a major tourist destination.

Under the leadership of the Bang Niang Sub-district Administration Office for example, a group of experts is needed to act as an advisory committee to the local government. This should comprise researchers who study the effects of tsunamis (both in science and the social sciences) from the local university and representatives from government agencies and professional associations, to provide information and work with the community to formulate policies, strategies, plans and protective measures to reduce the effects of a future tsunami. Geologists and marine scientists can play important roles in refining simulated tsunami-forecasting models for the understanding of the tsunami pattern along the coast. This would provide data for the mapping of evacuation routes and the positioning of evacuation shelters. GIS-based risk and evacuation maps need to be prepared and made available to the public and situation should be re-appraised every few years to include the geographical changes and new developments. Coastal engineers and structural engineers should play significant roles in formulating improved building regulations and clear construction guidelines should be provided for Bang Niang and Nang Thong Beaches. It should then be the task of the social scientist to communicate the preparations to the people in the community. Most significantly, all stakeholders should exchange data and integrate them into a coastal management plan.

Integration of technical, socio-economic and ecosystem factors into the public involvement process is also required. Laws and regulations should be carefully devised and enforced by both the central government for general purpose of protecting the coastal environment, and by the local administrative office (Bang Niang Subdistrict Administrative Office) to reduce tsunami impacts along Bang Niang and Nang Thong Beaches. The policies, regulations, institution frameworks and guidelines needed for Khao Lak communities should comprised of:

- Maps showing tsunami risk areas, tsunami safe zones, evacuation routes, location of evacuation shelters; these must be issued and well publicised.

- Construction zoning maps, buildings regulation for sensitive buildings and for the protection of critical facilities, codes of construction and construction practices, including tsunami resistant design guidelines should be made available.
- New construction in severely-affected and forecast-inundation zones must comply with the policies and regulations laid down, and must be strictly enforced by the local Administrative Office

However, if the impact of the tsunami on the people and the buildings is to be reduced, the most important issue facing the community at Bang Niang and Nang Thong Beaches is the achievement of the full cooperation of the local community.

9-4.2 Tool 8: Tsunami Knowledge Distribution for the Community.

To increase the general resilience of the population it is necessary to learn to live with the hazard, to increase the range of knowledge about it, to nurture the ecological and social diversity and to create opportunities for self-help (Berkes, 2007). To live with change and the uncertainties of natural hazards, e.g. the tsunami risk along the Andaman coast of Thailand, it is necessary that reliable mitigation plans and measures be prepared and made available to the public. The more the local community understands about tsunamis the greater the benefit to the local people and tourists, and the more secure community will become.

The vibration caused by the earthquake and the sudden drop in sea level due to the receding wave should immediately be recognised by the local population as signs of an impending tsunami attack and of the imminent danger. Leaflets and booklets describing the tsunami phenomenon, giving details of the signs of a imminent tsunami attack should be distributed to the local people and tourists. Tsunami-related signage, such as evacuation routes or direction to the closest vertical shelter, should be erected on along all in tsunami-affected areas. Tsunami information documents, notice board and brochures should be placed in hotels and resort guest rooms. Bookmarks, magnets and other souvenirs should be dispersed or put up for sale to increase tsunami awareness.

Bernard et al. (2007) stated that education is the most important issue amongst tsunami mitigation activities. One of the most successful ways to raise the tsunami awareness of

the population and all stakeholders in general, and how to respond, is through tsunami-education programmes at school, especially at the primary school level. In Japan, Ohta et al. (2005) reported that tsunami mitigation education in primary schools was put into action in 1937 to bring knowledge of disaster mitigation and rehabilitation measures to children and help Japanese people to behave properly when facing tsunami waves. Furthermore, education on tsunami and other natural hazards was integrated into mainstream science curricular within both public and private schools to increase disaster awareness in the community.

An Intergovernmental Oceanographic Commission (IOC) report in 2006 stated that it is vital to integrate tsunami risk into national education programmes and develop handbooks for teachers and textbooks for primary and secondary school children (Bernard et al., 2007). In addition, the IOC recommended numerous means to strengthen tsunami awareness and preparedness in schools including, such as increased knowledge of tsunami character and risks, identifying areas in danger, and developing disaster response plans for safer schools. Well-prepared tsunami evacuation procedures for every school should be provided, and tsunami drills should be performed regularly. Furthermore, public awareness campaigns such as the development of an Early Warning Day is to be encouraged in schools. The Early Warning Day brings all stakeholder in the community together to raise awareness of all aspects of tsunami-preparedness, using educational materials such as board games, to reach out to the children.

The U.S. Tsunami Hazard Mitigation Program (NTHMP) has developed tsunami educational products, which include knowledge concerning local science, history, eye-witness accounts and Native American oral history (Bernard et al., 2007). In Mexico, Farreras et al. (2007) also recommend the use of printed material for children and adults, such as a booklet called Fasciculo on Tsunamis and other brochures to instruct the public. Schools in Japan have various activities relating to tsunami mitigation; a special course in disaster mitigation is run at Maiko High School while regular courses in disaster prevention and life saving are presented at Kitakyushu City University. Disaster imagination games conducted at schools encourage students to estimate the extent of tsunami flooding, to draw evacuation maps and find out the location of evacuation shelters (<http://www.gdrc.org/uem/disasters/japan-disaster.html#five>).

Ohta et al. (2005) recommended that people who live in the coastal zones should be given more information about tsunami, especially after the tsunami disaster in 2004. The Oregon outreach program, which conducted surveys on local residents, businesses, visitors, and children, about public tsunami awareness and preparedness actions before and after the 2004 Indian Ocean tsunami, found out that the 2004 event had an educational effect on the population of Oregon State, especially increasing the understanding of tsunami warning signs and evacuation routes. In addition, door to door visiting programs by volunteers yielded perspectives on tsunami awareness and preparedness (Bernard et al., 2007).

In case of Khao Lak today, schools are no longer located in the areas flooded in 2004 but it is still vital for the children to know more about tsunami, and to transfer their knowledge to their parents. Tsunami mitigation programmes should be conducted at schools, including for example special courses by visiting scientists, and activities which encourage students to draw up evacuation maps, identifying evacuation routes and shelters. Tsunami signage which has been placed along both beaches and roads leading to the shelters should be clearly explained to children at schools.

9-4.3 Tool 9: Encouraging More Research and Technology Development for Tsunami Impact Alleviation.

More research and technology development should be considered in several areas to reduce the impact of tsunami on the Khao Lak coast and the other areas affecting by tsunami waves. The following activities need to be undertaken:

- Research on engineering aspects of building design, to increase their ability to withstand the impacts of tsunami waves.
- Research on the advantages and disadvantages of different underwater breakwaters and seawalls, to provide reliable information for decision makers; hydrodynamic conditions of the area need to be analyzed. Seawalls and breakwaters need to be studied, using both numerical modelling and laboratory experiments; to identify the most appropriate designs and materials for this region of Thailand
- Research on the human response to tsunami waves to understand human behaviour under hazardous conditions. Research should also be conducted

on human response to warning signals, to evacuation procedures and evacuation drills, and to the post-tsunami recovery process.

Chapter 10 Discussion and Conclusions

1. Historical evidence (Chapter 2) of tectonic activity along the Sunda subduction zone suggests that the December 2004 Indian Ocean mega-tsunami cannot be considered as an isolated event and may re-occur with a return period of 500-600 years. However, it should be noted that these time-scales are based on few historical data; the difficulties in predicting such rare events are illustrated by the recent (Feb 2010) rupture along the Chilean coast - this region had previously slipped in 1960 ($M_w \sim 9.5$, the largest earthquake ever recorded). Rupture events of a lesser magnitude (M_w of 9.0 or less) could occur more frequently along the Sunda Subduction and it is necessary to have effective plans for the response to a future tsunami.
2. To assess the effects of a future tsunami on the Khao Lak coast it is necessary to have a numerical model that considers a) the generation of the tsunami wave at source from the rupture characteristics, b) the propagation of the waves across the ocean and into shallow water and c) the subsequent inundation of the shore by the waves. The MOST/ComMIT model includes these components. Its effectiveness for the Andaman coast of Thailand was tested using the 2004 tsunami. By modelling the rupture as three individual segments (Nicobar, Andaman and Sumatra), each with four blocks with different uplift or subsidence characteristics, the MOST/ComMIT model was able to produce tsunami waves of the correct height, period, inundation distances in comparison to post-tsunami surveys by Siripong, Sojisuporn et al. (2005) and Matsutomi, Satake et al. (2005), and photographic and interview evidence from those who actually experienced the tsunami first-hand.
3. The MOST/ComMIT model considers only vertical displacement of the sea bed for the generation of the tsunami but around 5 times as much energy is believed to have been associated with the horizontal displacement than the vertical (Song et al., 2008). This was accounted for by assigning a larger value of M_w in the model (9.4 as opposed to the actual seismic value of 9.2-9.3); Geist, Titov et al.

(2007) showed that a $M_w = 9.2-9.3$ produced a good correspondence to the tsunami for the Indonesian coast around Banda Aceh but less good for the Thai coast.

4. The tsunami propagated towards Sri Lanka (westward) with a *crest* leading whereas it propagated with a leading trough towards Thailand and Indonesia; this was included in the model by varying the uplift of the blocks across the sections.
5. It is assumed that any future tsunamis will have the same propagation characteristics because of similar subduction processes. However, although considerable survey work has been conducted along the Sumatra section e.g. the survey by the British Royal Navy's HMS Scott (Peplow, 2005), less is known about the Nicobar and Andaman sections because this area is in Indian territorial waters; the Indian Government have not allowed international scientific surveys of the area and no surveys conducted by the Indian Navy have been released (Giles, 2006).
6. The MOST/ComMIT model also assumes that the rupture occurs simultaneously along the whole subduction zone; it does not have the ability to model a slip that propagates slowly along the rupture. The 2004 rupture of the Sunda subduction started at 7:58 am local time on the Sumatra section and propagated northwards taking approximately 8-10 minutes to reach its most northerly extent on the Nicobar section. The timing of the arrival of the tsunami waves along the Khao Lak coastline was about 4 minutes earlier than recorded by observers on the ground probably due to the simplification in the model of 'instantaneous' slip along the whole subduction.
7. The 2004 tsunami wave speed and direction calculated from the model are in good agreement with evidence of the tsunami pictures and videos taken on 26 December, and are able to provide tsunami wave pattern information needed for future mitigation. The subduction scenario that produced results that were most highly-correlated to the surveyed data from for the 2004 tsunami wave was then used in the MOST/ComMIT model for predicting the inundation area, maximum wave heights and tsunami arrival time of a possible future event and adapted to create tsunami risk maps and for planning mitigation measures for reducing the tsunami impacts in the future.

8. The 2004 Indian Ocean tsunami, simulated by the model, shows water recession prior to the arrival of the first wave occurring along the coastline at +2h 20 min, and resulting in a sea level drop of 3-5 m at 2 km offshore, followed by multiple wave crests reached the near-shore zone. The maximum wave heights of 7-9 m with 6-12 m/s speed reached Bang Niang and Nang Thong beaches at +2h 27min, causing severe destruction. The direction of wave approach (from the southwest) and inundation distances, compared well with the movement of a police patrol boat moored offshore of Nang Thong Beach and deposited 2.6 km away inland. In addition, the modelled tsunami inundation area corresponds well with that observed from aerial surveys.
9. Photographic evidence shows that normally-submerged rock outcrops are exposed during the wave recession and cause wave breaking and locally-enhanced wave heights when the crest arrives. The rocks appear to provide some protection to the local shoreline e.g. outcrops located in front of Bang Niang Beach play a major role in dissipating tsunami wave energy, locally increasing wave heights over the outcrops but reducing wave speed and heights in areas located behind the outcrops. Therefore, inclusion of accurate nearshore bathymetry such as the location and heights of rock outcrops as essential if the tsunami wave impacts are to be correctly modelled. The surveys conducted by the author of the near-shore bathymetry were particularly important in providing accurate data for modelling. The availability of such accurate near-shore data need to be carefully considered when using models for the prediction of the impacts of future tsunami.
10. The areas close to the headland are protected from the tsunami wave and suffer less damage than the nearby unprotected beaches because headlands partly block and diminish tsunami wave energy. In addition, wave reflection from headlands, islands and nearby beaches plays an important role in tsunami wave pattern alteration.
11. Tide plays a significant role in the effect of tsunami waves on the coastline. If the tsunami occurs during high tide along the Andaman coast of Thailand, the modelled wave heights are 1-1.5 m higher and inundation distances 200-600 m greater than those occurring at MSL. For planning purposes it is therefore

advisable to run the model under high-tide conditions to ensure that impacts are not under-estimated.

12. The simulated tsunami wave patterns by MOST/ComMIT model provides confidence that this model can be used to assess the possible impact of future tsunami likely to be generated from other sections of the Sunda Subduction, and can be utilized to create risk maps and guide mitigation measures to reduce the tsunami impacts in the future.
13. Sensitivity tests were conducted of earthquakes of various magnitudes ($M_w = 8.0, 8.2, 8.4, 8.6$ and 9.0) along the Andaman-Nicobar section which might cause tsunami effects to Khao Lak. The rupture lengths and widths of these earthquakes were scaled using the results of Henry and Das (2001) and Wells and Coppersmith (1994). Earthquakes of magnitudes $M_w = 8.4, 8.8$ and 9.0 result in tsunami waves of similar maximum heights at Khao Lak ($10.3, 12.2$ and 10.7 respectively) and cause similar pattern and severity of destruction around Khao Lak, and to affect the similar areas ($5.9\text{-}6.2 \text{ km}^2$). An $M_w = 8.6$ tsunamigenic earthquake results in an unusually large maximum wave heights of 20.3 m and inundates $\sim 7.2 \text{ km}^2$. So, the $M_w = 8.4$ earthquake was selected to generate a future tsunami for mitigation purposes (allowing for the increased effect of the horizontal component of the rupture). Seismic events of between $8.5\text{-}8.9$ are estimated by Karlsrude, Bungum et al. (2005), Pietrzak, Socquet et al (2007) and Ioualalen, Asavanant et al. (2007) to have a return period of 100-430 years.
14. The physical patterns of the tsunami waves that would inundate Khao Lak is one of the most important issues that needs to be understood before developing mitigation plans and measures for tsunami resilience of Bang Niang and Nang Thong Beach communities. According to the model of the future $M_w = 8.4$ event, the first wave trough will reach Khao Lak coast $+2 \text{ h } 20 \text{ min}$ after the earthquake, and will cause water to drop $0.4\text{-}0.5 \text{ m}$ below MSL. The first wave crest to attack Nang Thong and Bang Niang Beaches occurs at $+2 \text{ h } 26 \text{ min}$, will shoal and cause a (relatively small) wave of 0.4 m above MSL, travelling with a speed of $4\text{-}6 \text{ m/s}$ at the coastline, to inundate the area for 24 min . The second wave crest is more significant and reaches both beaches at $+3 \text{ h } 20 \text{ min}$ to $+3 \text{ h } 33 \text{ min}$, inundating the area to approximately $2 - 3 \text{ m}$ above MSL. Significantly,

the third wave crest which reaches both beaches at +4 h 0 min and causes 4.5-5.5 m flooding above MSL is largest and need to be considered for mitigation.

15. The coastal areas around Nang Thong and Bang Niang Beaches were classified into either a) highly affected zones or b) inundation zones based on the wave speed and wave height (Above mean sea level).
16. Coastal zoning of Bang Niang and Nang Thong Beaches, relating to tsunami-affected zones, should be created by a group of experts and put into effect by enforcing regulation issued by Bang Niang Sub-district Administrative Office. The severely-affected zone should be carefully managed by issuing the appropriate coastal management plan, formulating building codes of construction and encouraging engineered tsunami-suitable construction. Moreover, sensitive buildings should be built outside the highly affected zone.
17. Only buildings designed to withstand the impact of the tsunami waves should be constructed in the highly-affected areas. At least 3 stories of elevated reinforced concrete building with wave flow-through on the first floor are recommended for buildings in the highly-affected areas. The first floor should be elevated or the land level should be raised to 5 m above MSL. The core structure of the building should be able to survive high wave velocities of 8 m/s; however, the first floor walls should be built with low resistant materials which would withstand 4-6 m/s velocity of tsunami wave, and produce less floating debris, to ensure the integrity of the entire building.
18. The evacuation process of this area should take no longer than 30 minutes. The tsunami waves will continue to affect this area for more than 4 hours after the earthquake, during which time it will not be safe for the rescue operations to take place. More evacuation shelters both man-made and natural, such as artificial sand dunes, should be established in the areas that are difficult to reach or far away from the elevated evacuation shelters.
19. Tsunami detection instruments such as digital tide gauges with their capability to identify any unusual patterns associated with a tsunami wave have already been installed along the Thai coast; these need to be maintained and their signals linked to use for issuing tsunami warning and to cancel the false alarms.
20. Natural protection, for example combinations of beach trees and shrubs planting in conjunction with sand dunes protection, would be an advantage for reducing

the tsunami destruction for the area. Mixture of various sizes of Casuarinas with beach shrubs such as Pandanus species could be planted on the backshore and (man-made) sand dunes. Moreover, artificial dunes might be used as vertical shelters in some areas.

21. It is important to realize that Bang Niang and Nang Thong Beaches are important tourist business spots that bring considerable economic and developmental benefits to the local and regional communities. So, a multi-disciplinary approach to tsunami mitigation, with advanced technology and research issues, is needed to provide tsunami knowledge to the coastal communities, both local and tourist e.g. ensuring knowledge of how to respond when a tsunami warning is issued, provision of tsunami evacuation maps, appropriate signs and measures. Significantly, the distribution of tsunami knowledge to the community and implementation of building regulations are crucial to alleviating the worst effects of a future tsunami and establishing a tsunami resilient community for the future.

10-1 Limitation of the Study

1. Source of submarine earthquakes and rupture characteristics of the Andaman-Nicobar sections of the Sunda Subduction are the major factors used for simulating tsunami wave modelling and for studying the patterns of tsunami waves which affect the coast of Thailand (Khao Lak); however, few data on the rupture characteristics and changes of sea bed due to the 2004 earthquake were available. Simulations of potential tsunami by modelling would undoubtedly yield more accurate outcomes if we had a better understanding of these tsunami sources along the Andaman-Nicobar sections than we achieved up until now.
2. Return periods of the tsunamis affecting the Andaman coast of Thailand, especially the rare mega-tsunamis, are quite uncertain at present (and tend to become more uncertain as the estimated return period increases). Because the return period is an important parameter for the planning of tsunami mitigation, it is necessary to integrate return periods of tsunamis of various magnitudes into decision making for tsunami mitigation. Tsunami mitigation measures along the Khao Lak should be prioritized to take account of events with the shorter

tsunami return period that might occur along the coastal areas of Thailand and the Indian Ocean rim region.

3. A tsunami model which is able to simulate tsunami waves generated by the rupture zone that includes the time taken for the rupture to propagate along the fault would yield more precise tsunami arrival times and wave crest interval than the current version of the MOST/COMmit model which has the rupture occurring at one moment.
4. A tsunami model that specifically includes the horizontal movement of submarine earthquake and deals with various 'beam' shapes of the tsunami wave from the eruption sources, especially towards the Thai and Myanmar coasts, might provide more accurate and realistic tsunami pattern that reach Khao Lak and the other area along the Andaman Thai coast.

10-2 Future Research

1. Tsunami simulation of the different areas along the Andaman coast of Thailand, and possibly in the future for the Gulf coast of Thailand, should be conducted. Initially, it should be extended to nearby areas of Khao Lak to study the correlation of the tsunami waves in adjoining locations, and to bring more understanding of tsunami pattern that will help for creating the mitigation plan of Khao Lak that relates to neighbouring zones e.g. the allocation of evacuation shelters' sites and the evacuation route to the nearby areas. Therefore, detailed topographic and bathymetric surveys of these areas need to be conducted, to ensure an accurate understanding of the inundation on land by potential tsunami waves.
2. Simulation of modelled tsunami wave by the other models e.g. TUNAMI and COMCOT for the same seismic condition and bathymetric data should be carried out for studying tsunami pattern at Khao Lak. Model outcomes from various models should be compared and analyzed to identify the advantages and disadvantages of each model outcome, and adjustments made to the mitigation plans.

3. Application of the outcomes of this research to the development of practical tsunami mitigation plans by all stakeholders should be persuaded e.g. wave speed and wave direction data, generated by this research, could be used for designing tsunami-safe buildings along the Khao Lak coast. Tsunami wave heights (above ground level) data are necessary for the arrangement of vertical shelters locations in the area. Further tsunami-related research studies in the areas of coastal engineering and coastal management should be encouraged and results of these research studies applied to the benefit of associated scientific components.
4. The scientific data generated in this thesis was for the support of local communities, and public participation in the exploitation of these research outcomes should be encouraged and integrated with other related information. The recommendations on tsunami mitigation made here, together with other documentation and preparations, must be distributed to all stakeholders to strengthen their understanding of tsunami knowledge. Tsunami education for students, seasonal workers and tourists is also essential for supporting the building of tsunami resilient community. Moreover, research topics concerning social sciences approaches e.g. the evaluation of transfer process of tsunami knowledge to local communities and students in school, should be promoted.

References

- Aitchison, J.C., 2005. The Great Indian Ocean Tsunami Disaster. *Gondwana Research*, 8(2): 107-108.
- Alexander, R. and Richard, T., 2007. The 26 December 2004 Sumatra Tsunami: Analysis of Tide Gauge Data from the World Ocean Part 1. Indian Ocean and South Africa. *Pure and Applied Geophysics*, 164(2): 261-308.
- Alongi, D.M., 2008. Mangrove forests: Resilience, protection from tsunamis, and responses to global climate change. *Estuarine, Coastal and Shelf Science*, 76(1): 1-13.
- Ammon, C.J., 2006. Earth science: Megathrust investigations. *Nature*, 440(7080): 31-32.
- Ammon, C.J. et al., 2005. Rupture Process of the 2004 Sumatra-Andaman Earthquake. *Science*, 308(5725): 1133-1139.
- Banerjee, P., Politz, P. and Burgmann, R., 2005. The size and duration of the Sumatra-Andaman earthquake from far-field static offsets. *Science*, 308: 1769-1772.
- Banerjee, P., Pollitz, F., Nagarajan, B. and Burgmann, R., 2007. Coseismic Slip Distributions of the 26 December 2004 Sumatra-Andaman and 28 March 2005 Nias Earthquakes from GPS Static Offsets. *Bulletin of the Seismological Society of America*, 97(1A): S86-102.
- Berkes, F., 2007. Understanding uncertainty and reducing vulnerability: lessons from resilience thinking. *Natural Hazards*, 41(2): 283-295.
- Berman, A.E., 2005. The Northern Sumatra earthquake of 2004: Forty years of ignoring plate tectonics. *Houston Geological Society Bulletin*, 47(6): 9-19.
- Bernard, E.N. et al., 2007. National Tsunami research plan report of a workshop sponsored by NSF/NOAA. Pacific Marine Environmental Laboratory, Seattle, Wash., pp. vii, 135 p.
- Bernard, E.N., Mofjeld, H.O., Titov, V., Synolakis, C.E. and González, F.I., 2006. Tsunami: scientific frontiers, mitigation, forecasting and policy implications. *Philosophical Transactions: Mathematical, Physical and Engineering Sciences*, 364(1845): 1989-2007.
- Bilek, S.L., 2007. Using Earthquake Source Durations along the Sumatra-Andaman Subduction System to Examine Fault-Zone Variations. *BULLETIN OF THE SEISMOLOGICAL SOCIETY OF AMERICA*, 97(1A): S62-70.
- Bilek, S.L., Satake, K. and Sieh, K., 2007. Introduction to the Special Issue on the 2004 Sumatra-Andaman Earthquake and the Indian Ocean Tsunami. *BULLETIN OF THE SEISMOLOGICAL SOCIETY OF AMERICA*, 97(1A): S1-S5.
- Bilham, R., 2005. A flying start; then the slow slip. *Science*, 308(5725): 1126-1127.
- Bird, P., 2003. An updated digital model of plate boundaries, *Geochemistry Geophysics Geosystems*, pp. 52.
- Borrero, J.C., Sieh, K., Chlieh, M. and Synolakis, C.E., 2006. Tsunami inundation modeling for western Sumatra. *PNAS*, 103(52): 19673-19677.
- Central Intelligence Agency, 2008. The CIA world factbook 2009. Skyhorse Publishing, Inc., New York, 833 pp.
- Chaimanee, N. and Tathong, T., 2005. The post-tsunami survey for coastal damage assessment along the Andaman Sea coast, Southern Thailand, Scientific Forum on the Tsunami: Its Impact and Recovery. Asian Institution of Technology, Pathumthani.
- Chatenoux, B. and Peduzzi, P., 2007. Impacts from the 2004 Indian Ocean Tsunami: analysing the potential protecting role of environmental features. *Natural Hazards*, 40(2): 289-304.

- Chlieh, M. et al., 2007. Coseismic Slip and Afterslip of the Great Mw 9.15 Sumatra-Andaman Earthquake of 2004. *BULLETIN OF THE SEISMOLOGICAL SOCIETY OF AMERICA*, 97(1A): S152-173.
- Cochard, R. et al., 2008. The 2004 tsunami in Aceh and Southern Thailand: A review on coastal ecosystems, wave hazards and vulnerability. *Perspectives in Plant Ecology, Evolution and Systematics*, 10(1): 3-40.
- Cummins, P.R., 2007. The potential for giant tsunamigenic earthquakes in the northern Bay of Bengal. *Nature*, 449(7158): 75-78.
- Dalrymple, R.A. and Kriebel, D.L., 2005. Lessons in Engineering from the Tsunami in Thailand. *The BRIDGE*, Volume 35, Number 2: 4-13.
- Danielsen, F. et al., 2005. The Asian Tsunami: A Protective Role for Coastal Vegetation. *Science*, 310(5748): 643-.
- Department of Public Works and Town & Country Planning, 2005. Criteria for defining properties utilization: application for Land use and town planning in Phang-nga province. In: P.W.a.T.C. Planning (Editor). Royal gazette, pp. 15-18.
- Department of Public Works and Town & Country Planning, 2008. Standard manuscripts for designing of buildings and evacuation shelters in intermediate tsunami-affected areas of Thailand., Bangkok, pp. 80.
- Dewey, J.W. et al., 2007. Seismicity Associated with the Sumatra-Andaman Islands Earthquake of 26 December 2004. *BULLETIN OF THE SEISMOLOGICAL SOCIETY OF AMERICA*, 97(1A): S25-42.
- Dheeradilok, P., 1995. Quaternary coastal morphology and deposition in Thailand. *Quaternary International*, 26: 49-54.
- Dominey-Howes, D., Cummins, P. and Burbidge, D., 2007. Historic records of teletsunami in the Indian Ocean and insights from numerical modelling. *Natural Hazards*, 42(1): 1-17.
- Dominey-Howes, D. and Papatoma, M., 2007. Validating a Tsunami Vulnerability Assessment Model (the PTVA Model) Using Field Data from the 2004 Indian Ocean Tsunami. *Natural Hazards*, 40(1): 113-136.
- Eisner, R.K., 2001. Designing for Tsunamis: Seven principles for planning and designing for tsunami hazards. *National Tsunami Hazard Mitigation Program*, pp. 60.
- Engdahl, E.R., Villasenor, A., DeShon, H.R. and Thurber, C.H., 2007. Teleseismic relocation and assessment of seismicity (1918-2005) in the region of the 2004 Mw 9.0 Sumatra-Andaman and 2005 Mw 8.6 Nias Island great earthquakes. *Bulletin of the Seismological Society of America*, 97(1 A SUPPL.): S43-S61.
- Farreras, S., Ortiz, M. and Gonzalez, J.I., 2007. Steps towards the implementation of a tsunami detection, warning, mitigation and preparedness program for Southwestern coastal areas of Mexico. *Pure and Applied Geophysics*, 164(2-3): 605-616.
- Fujii, Y. and Satake, K., 2007. Tsunami Source of the 2004 Sumatra-Andaman Earthquake Inferred from Tide Gauge and Satellite Data. *Bulletin of the Seismological Society of America*, 97(1A): S192-207.
- Gahalaut, V.K. and Catherine, J.K., 2006. Rupture characteristics of 28 March 2005 Sumatra earthquake from GPS measurements and its implication for tsunami generation. *Earth and Planetary Science Letters*, 249(1-2): 39-46.
- Geist, E.L., Titov, V.V., Arcas, D., Pollitz, F.F. and Bilek, S.L., 2007. Implications of the 26 December 2004 Sumatra-Andaman Earthquake on Tsunami Forecast and Assessment Models for Great Subduction-Zone Earthquakes. *Bulletin of the Seismological Society of America*, 97(1A): S249-270.
- Geist, E.L., Titov, V.V. and Synolakis, C.E., 2006. Tsunami: WAVE of CHANGE. *Scientific American*, 294(1): 56-63.

- Ghobarah, A., Saatcioglu, M. and Nistor, I., 2006. The impact of the 26 December 2004 earthquake and tsunami on structures and infrastructure. *Engineering Structures*, 28(2): 312-326.
- Giles, J., 2006. India's ban on foreign boats hinders tsunami research. *Nature*, 439(7075): 380-380.
- Grevenmeyer, I. and Tiwari, V.M., 2006. Overriding plate controls spatial distribution of megathrust earthquakes in the Sunda-Andaman subduction zone. *Earth and Planetary Science Letters*, 251(3-4): 199-208.
- Hamouda, A., Z., 2006. Numerical computations of 1303 tsunamigenic propagation towards Alexandria, Egyptian Coast. *Journal of African Earth Sciences*, 44: 37-44.
- Harinarayana, T. and Hirata, N., 2005. Destructive Earthquake and Disastrous Tsunami in the Indian Ocean, What Next? *Gondwana Research*, 8(2): 246-257.
- Harry, Y. et al., 2007. Effects of the 2004 Great Sumatra Tsunami: Southeast Indian Coast. *Journal of Waterway, Port, Coastal, and Ocean Engineering*, 133(6): 382-400.
- Henry, C. and Das, S., 2001. Aftershock zones of large shallow earthquakes: Fault dimensions, aftershock area expansion, and scaling relations. *Geophys. J. Intl.*, 147: 272-293.
- Hirata, K. et al., 2006. The 2004 Indian Ocean tsunami: Tsunami source model from satellite altimetry. *Earth, Planets and Space*, 58(2): 195-201.
- Hori, K. et al., 2007. Horizontal and vertical variation of 2004 Indian tsunami deposits: An example of two transects along the western coast of Thailand. *Marine Geology*, 239(3-4): 163-172.
- Imamura, F., 1996. Review of tsunami simulation with a finite difference method. . In: H. Yeh, P. Liu, C. Synolakis and N.J. Hackensack (Editors), *Long Wave Runup Models*. World Scientific Publishing Co., pp. 25-42.
- Ingram, J.C., Franco, G., Rio, C.R.-d. and Khazai, B., 2006. Post-disaster recovery dilemmas: challenges in balancing short-term and long-term needs for vulnerability reduction. *Environmental Science & Policy*, 9(7-8): 607-613.
- Intergovernmental Oceanographic Commission, 2005. From commitments to actions: Advancements in developing an Indian Ocean tsunami warning and mitigation system., Intergovernmental Oceanographic Commission, Paris.
- Ioualalen, M. et al., 2007. Modeling the 26 December 2004 Indian Ocean tsunami: Case study of impact in Thailand. *J. Geophys. Res.*, 112.
- Ishii, M., Shearer, P.M., Houston, H. and Vidale, J.E., 2005. Extent, duration and speed of the 2004 Sumatra-Andaman earthquake imaged by the Hi-Net array. *Nature*, 435(7044): 933-936.
- Jarusiri, P. and Choowong, M., 2005. Rehabilitation planning for community environment and settlement development in the tsunami disaster area., Chulalongkorn University, Bangkok.
- Ji, C., 2005. Preliminary rupture model tsunami simulations and numerical models. http://neic.usgs.gov/neis/eq_depot/2004/eq_041226/neic_slav_ff.html.
- Johnston, D. et al., 2005. Measuring Tsunami Preparedness in Coastal Washington, United States. *Natural Hazards*, 35(1): 173-184.
- Jonathan, R., Carl, G.-W., Lisa, L. and May, T.-M., 2008. Grounding a natural disaster: Thailand and the 2004 tsunami. *Asia Pacific Viewpoint*, 49(2): 137-154.
- Jonientz-Trisler, C. et al., 2005. Planning for Tsunami-Resilient Communities. *Natural Hazards*, 35(1): 121-139.
- Kanamori, H. and Eeri, M., 2006. Seismological Aspects of the December 2004 Great Sumatra-Andaman Earthquake. *Earthquake Spectra*, 22(S3): S1-S12.
- Karlsruhe, K. et al., 2005. Tsunami risk reduction measures with focus on land use and rehabilitation. 20051267-1, The Norwegian Geotechnical Institute.
- Kelletat, D., Scheffers, S.R. and Scheffers, A., 2007. Field Signatures of the SE-Asian Mega-Tsunami along the West Coast of Thailand Compared to Holocene Paleo-Tsunami from the Atlantic Region. *Pure and Applied Geophysics*, 164(2): 413-431.

- Kowalik, Z., Knight, W., Logan, T. and Whitmore, P., 2007. The Tsunami of 26 December, 2004: Numerical Modeling and Energy Considerations. *Pure and Applied Geophysics*, 164(2): 379-393.
- Kruger, F. and Ohrnberger, M., 2005. Tracking the rupture of the $M_w = 9.3$ Sumatra earthquake over 1,150[km] at teleseismic distance. *Nature*, 435(7044): 937-939.
- Lay, T. et al., 2005. The great Sumatra-Andaman earthquake of 26 December 2004. *Science*, 308(5725): 1127-1133.
- Liu, P.L.F., 2005. Tsunami simulations and numerical models. *The BRIDGE*, 35 (2): 14-20.
- Long, P.V., Bergado, D.T. and Abuel-Naga, H.M., 2007. Geosynthetic reinforcement application for tsunami reconstruction: Evaluation of interface parameters with silty sand and weathered clay. *Geotextiles and Geomembranes*, 25(4-5): 311-323.
- Madsen, P. and Fuhrman, D., 2007. Analytical and numerical models for tsunami run-up. In: A. Kudur (Editor), *Tsunami and Nonlinear Waves*. SpringerLink, Berlin, pp. 209-236.
- Matsutomi, H. et al., 2005. The December 26, 2004 Sumatra earthquake tsunami, Tsunami field survey around Phuket, Thailand.
- McCloskey, J. et al., 2008. Tsunami threat in the Indian Ocean from a future megathrust earthquake west of Sumatra. *Earth and Planetary Science Letters*, 265(1-2): 61-81.
- McCloskey, J., Nalbant, S.S. and Steacy, S., 2005. Earthquake risk from co-seismic stress. *Nature*, 434: 291.
- Menke, W., Abend, H., Bach, D., Newman, K. and Levin, V., 2006. Review of the source characteristics of the Great Sumatra-Andaman Islands earthquake of 2004. *Surveys in Geophysics*, 27(6): 603-613.
- Nalbant, S.S., Steacy, S., Sieh, K., Natawidjaya, D. and McCloskey, J., 2005. Earthquake risk on the Sunda trench. *Nature*, 435: 756-757.
- National Science and Technology Council, 2005. Tsunami risk reduction for the United States: A framework for action, National Science and Technology Council.
- Neetu, S. et al., 2005. Comment on "The Great Sumatra-Andaman Earthquake of 26 December 2004". *Science*, 310(5753): 1431a-.
- Ni, S., Kanamori, H. and Helmberger, D., 2005. Seismology: Energy radiation from the Sumatra earthquake. *Nature*, 434(7033): 582-582.
- Ohta, H., Pipatpongsa, T. and Omori, T., 2005. Public education of tsunami disaster mitigation and rehabilitation performed in Japanese primary schools., *INTERNATIONAL CONFERENCE ON GEOTECHNICAL ENGINEERING FOR DISASTER MITIGATION AND REHABILITATION (GEDMR05)*, Singapore.
- Oregon Emergency Management and Oregon Department of Geology and Mineral Industries, 2001. Tsunami warning systems and procedures. *Nature of the Northwest Information Centre*, pp. 41.
- Ortiz, M. and Bilham, R., 2003. Source area and rupture parameters of the 31 December 1881 $M = 7.9$ Car Nicobar earthquake estimated from tsunamis recorded in the Bay of Bengal. *Journal of Geophysical Research B: Solid Earth*, 108(4): ESE 11-16.
- Peplow, M., 2005. Sea bed reveals earthquake scars. *Naturenews*.
- Piatanesi, A. and Lorito, S., 2007. Rupture Process of the 2004 Sumatra-Andaman Earthquake from Tsunami Waveform Inversion. *BULLETIN OF THE SEISMOLOGICAL SOCIETY OF AMERICA*, 97(1A): S223-231.
- Pietrzak, J. et al., 2007. Defining the source region of the Indian Ocean Tsunami from GPS, altimeters, tide gauges and tsunami models. *Earth and Planetary Science Letters*, 261: 49-64.
- Plafker, G., 1997. Catastrophic tsunami generated by submarine slides and backarc thrusting during the 1992 earthquake on eastern Flores I., Indonesia., 93rd Annual meeting of Geophysical Society of America. Geophysical Society of America

pp. 57.

- Pomeroy, R.S., Ratner, B.D., Hall, S.J., Pimoljinda, J. and Viveknandan, V., 2006. Coping with disaster: Rehabilitation coastal livelihoods and communities. *Marine Policy*, 30: 786-793.
- Purnachandra, R.N., 2007. Characterization of potential tsunamigenic earthquake source zones in the Indian Ocean. In: A. Kunda (Editor), *Tsunami and non linear waves*. SpringerLink, Berlin, pp. 285-312.
- Radha Krishna, M. and Sanu, T.D., 2002. Shallow seismicity, stress distribution and crustal deformation pattern in the Andaman-West Sunda arc and Andaman Sea, northeastern Indian Ocean. *Journal of Seismology*, 6(1): 25-41.
- Rajendran, C.P. et al., 2007. Crustal Deformation and Seismic History Associated with the 2004 Indian Ocean Earthquake: A Perspective from the Andaman-Nicobar Islands. *Bulletin of the Seismological Society of America*, 97(1A): S174-191.
- Rhie, J., Dreger, D., Burgmann, R. and Romanowicz, B., 2007. Slip of the 2004 Sumatra-Andaman Earthquake from Joint Inversion of Long-Period Global Seismic Waveforms and GPS Static Offsets. *Bulletin of the Seismological Society of America*, 97(1A): S115-127.
- Rittichainuwat, B.N., 2006. Tsunami Recovery: A Case Study of Thailand's Tourism. *Cornell Hotel and Restaurant Administration Quarterly*, 47(4): 390-404.
- Sajjakul, V., 2005. Project for creation of spatial development techniques in geohazard zone, Chulalongkorn University, Bangkok.
- Schwartz, S.Y. and Rokosky, J.M., 2007. Slow slip events and seismic tremor at circum-Pacific subduction zones. *Reviews of Geophysics*, 45.
- Segur, H., 2007. Waves in shallow water, with emphasis on the tsunami of 2004. In: A. Kundu (Editor), *Tsunami and nonlinear waves*. SpringerLink, Berlin, pp. 3-30.
- Seno, T. and Hirata, K., 2007. Did the 2004 Sumatra-Andaman Earthquake Involve a Component of Tsunami Earthquakes? *Bulletin of the Seismological Society of America*, 97(1A): S296-306.
- Shapiro, N.M., Ritzwoller, M.H. and Engdahl, E.R., 2008. Structural context of the great Sumatra-Andaman Islands earthquake. *Geophysical Research Letters*, 35(5).
- Silpakorn University, 2006. Rehabilitation of post tsunami affected area of the Andaman Sea coast of Thailand.
- Silva, R., Losada, I.J. and Losada, M.A., 2000. Reflection and transmission of tsunami waves by coastal structures. *Applied Ocean Research*, 22(4): 215-223.
- Sinadinovski, C., 2006. The event of 26th of December 2004-The biggest earthquake in the world in the last 40 years. *Bulletin of Earthquake Engineering*, 4: 131-139.
- Singh, R.K., Sharma, P.K., Ghosh, A.K. and Kushwaha, H.S., 2008. Tsunami Finite Element Simulation with In-House Code Tsusol and Comparison with Tunami-N2 Code for National Warning System., The 12th International Conference of International Association for Computer Methods and Advances in Geomechanics (IACMAG). Goa, India, pp. 3060-3068.
- Sinsakul, S., 1992. Evidence of Quaternary sea level changes in the coastal areas of Thailand. *Journal of Southeast Asian Earth Sciences*, 7(1): 23-37.
- Siripong, A., Sojisuporn, P. and Wichiencharoen, C., 2005. Risk study and assessment of Tsunami for its mitigation, Chulalongkorn University, Bangkok.
- Sonak, S., Pangam, P. and Giriyan, A., Green reconstruction of the tsunami-affected areas in India using the integrated coastal zone management concept. *Journal of Environmental Management*, In Press, Corrected Proof: 190.
- Song, Y.T. et al., 2008. The role of horizontal impulses of the faulting continental slope in generating the 26 December 2004 tsunami. *Ocean Modelling*, 20(4): 362-379.
- Srinivas, H. and Nakagawa, Y., 2008. Environmental implications for disaster preparedness: Lessons Learnt from the Indian Ocean Tsunami. *Journal of Environmental Management*, 89(1): 4-13.

- Srivastava, A. and Babu, G.L.S., 2009. Analysis and design of reinforced earth wall for shore protection system against tsunami. *Science of Tsunami Hazards*, 28(3): 186-204.
- Stein, S. and Okal, E., 2005a. The 2004 Sumatra earthquake and Indian Ocean tsunami: What happened and why? *Visual Geosciences*, 10(1): 21-26.
- Stein, S. and Okal, E.A., 2005b. Seismology: Speed and size of the Sumatra earthquake. *Nature*, 434(7033): 581-582.
- Stein, S. and Okal, E.A., 2007. Ultralong Period Seismic Study of the December 2004 Indian Ocean Earthquake and Implications for Regional Tectonics and the Subduction Process. *Bulletin of the Seismological Society of America*, 97(1A): S279-295.
- Subarya, C. et al., 2006. Plate-boundary deformation associated with the great Sumatra-Andaman earthquake. *Nature*, 440(7080): 46-51.
- Synolakis, C., Okal, E. and Bernard, E., 2005. The Megatsunami of December 26, 2004. *The BRIDGE*, 35(2): 26-35.
- Tadashi, A., Kenji, S., Tsutomu, S., Ken, Y. and Nobuo, S., 2007. Logic-tree Approach for Probabilistic Tsunami Hazard Analysis and its Applications to the Japanese Coasts. *Pure and Applied Geophysics*, 164(2): 577-592.
- Tanaka, N., Sasaki, Y., Mowjood, M., Jinadasa, K. and Homchuen, S., 2007. Coastal vegetation structures and their functions in tsunami protection: experience of the recent Indian Ocean tsunami. *Landscape and Ecological Engineering*, 3(1): 33-45.
- Tanioka, Y. et al., 2006. Rupture process of the 2004 great Sumatra-Andaman earthquake estimated from tsunami waveforms. *Earth, Planets and Space*, 58(2): 203-209.
- Thanawood, C., Yingchalermchai, C. and Densrisereekul, O., 2006. Effects of the December 2004 tsunami and disaster management in southern Thailand. *Science of Tsunami Hazards*, 24 (3): 206-217.
- Titov, V. and Gonzalez, F.I., 1997. Implementation and testing of the Method Of Splitting Tsunami (MOST) model, NOAA Technical Memorandum, pp. 11.
- Titov, V., Rabinovich, A.B., Mofjeld, H.O., Thomson, R.E. and González, F.I., 2005. The Global Reach of the 26 December 2004 Sumatra Tsunami. *Science*, 309(5743): 2045-2048.
- Tsuji, Y. et al., 2006. The 2004 Indian tsunami in Thailand: Surveyed runup heights and tide gauge records. *Earth, Planets and Space*, 58(2): 223-232.
- Umitsu, M., Tanavud, C. and Patanakanog, B., Effects of landforms on tsunami flow in the plains of Banda Aceh, Indonesia, and Nam Khem, Thailand. *Marine Geology*, In Press, Corrected Proof.
- United Nations Environmental Programme, 2005. Maldives post-tsunami environmental assessment., UNEP, Nairobi.
- United States Agency International Development., 2007. Review of policies and institutional capacity for early warning and disaster management in Thailand. U.S. IOTWS Program Document No. 17-IOTWS-06, United States Agency International Development.
- Vallee, M., 2007. Rupture Properties of the Giant Sumatra Earthquake Imaged by Empirical Green's Function Analysis. *Bulletin of the Seismological Society of America*, 97(1A): S103-114.
- Venturato, A.J., Arcas, D. and Kanoglu, U., 2007a. Modelling tsunami inundation from a Cascadia subduction zone earthquake for Long Beach and Ocean Shores, Washington. NOAA Technical Memorandum(OAR PMEK-137): 26.
- Venturato, A.J. et al., 2007b. Tacoma, Washington, Tsunami hazard mapping project: Modelling tsunami inundation from Tacoma and Seattle fault earthquakes. NOAA Technical Memorandum(OAR PMEL-132): 23.
- Venturato, A.J., Titov, V.V., Harold, M. and Frank, G., 2004. NOAA TIME Eastern Strait of Juan de Fuca, Washington, Mapping project: Procedures, data sources and products, NOAA/Pacific Marine Environmental Laboratory, Seattle.

- Vigny, C. et al., 2005. Insight into the 2004 Sumatra-Andaman earthquake from GPS measurements in southeast Asia. *Nature*, 436(7048): 201-206.
- Warnitchai, P., 2005. The 26 December 2004 tsunami disaster in Thailand: Experience and lessons learned, Asian Institute of Technology, Pathumthani.
- Wells, D.L. and Coppersmith, K.J., 1994. New empirical relationships among magnitude, rupture length, rupture width, rupture area, and surface displacement. *Bulletin of the Seismological Society of America*, 84(Aug 1994): 974-1002.
- Williams, N., 2005. Tsunami insight to mangrove value, *Current Biology*, pp. R73.
- Wood, N. and Geological Survey (U.S.), 2007. Variations in city exposure and sensitivity to tsunami hazards in Oregon. U.S. Dept. of the Interior, U.S. Geological Survey, Reston, Va., pp. iv, 37 p.
- Yamada, S. et al., 2006. The Sri Lanka Tsunami Experience. *Disaster Management & Response*, 4(2): 38-48.
- Yanagisawa, H. et al., 2009. The reduction effects of mangrove forest on a tsunami based on field surveys at Pakarang Cape, Thailand and numerical analysis. *Estuarine, Coastal and Shelf Science*, 81(1): 27-37.